APOPTOSIS in Breast Cancer Cells

Ching Wan Chan

A dissertation submitted to the University of Bristol in accordance with the requirements of the degree of Doctor of Philosophy in the Faculty of Medicine, URCN, July 2003.

Final word count: fifty-three thousand, nine hundred and ten words

Abstract

The importance of apoptosis as a means of homeostasis and maintaining genomic integrity, as well as the ability of cancer cells to escape this failsafe mechanism, has long been the subject of intense investigation. To investigate the possibility that prolactin might enable breast cancer cells to survive apoptotic insults, we stimulated T47-D and MCF-7 cells with ceramide (C2) and assessed the ability of prolactin to improve cell survival. Morphological studies and cell survival assays demonstrated a significant survival effect in T47-D cells exposed to prolactin. Because prolactin activates the Jak2-STAT5 pathway, we then proceeded to create a model in which the role of this pathway in apoptosis could be investigated. An initial attempt to inhibit dexamethasone-induced apoptosis in a human leukaemic cell line (CEM-C7) by establishing a stable clone expressing the prolactin receptor (for activating the JAK2-STAT5 pathway) was unsuccessful. Next, we established stable clones of breast cancer cells overexpressing STAT5b. Despite increased STAT5 signalling after prolactin stimulation, no enhancement of survival was demonstrated, implying that STAT5b is not responsible for survival following ceramide exposure. Surprisingly, increased STAT5 activation, following prolactin stimulation, actually increased cell death.

The second half of this project involved investigation and characterization of the newly identified Met protein, which we showed to induce apoptosis in breast cancer cells as well as in other cell lines. Met is structurally related to SAF-B – which attaches to DNA at scaffold / matrix attachment regions and is thought to be involved in DNA transcription or mRNA processing. Met was shown to be confined to the nucleus, and partially co-localized with SAF-B, but not with splicing factor speckles. Signalling assays show that Met downregulates transcriptional activity within cells.

Dedications and Acknowledgements

I would like to take this opportunity to acknowledge and thank Dr. Michael Norman, my supervisor, for all his help, advice, and guidance, without which this thesis would not have been possible. I also want to thank Dr. Andrea Flynn for her help and teaching and my fellow students and postdocs for all their advice and input. Last I want to acknowledge my sponsors, the National Medical Research Council of Singapore, for supporting me financially for this new stage of my career.

AUTHOR'S DECLARATION

I declare that the work in this dissertation was carried out in accordance with the Regulations of the University of Bristol. The work is original except where indicated by special reference in the text and no part of the dissertation has been submitted for any other degree.

Any views expressed in the dissertation are those of the author and in no way represent those of the University of Bristol.

The dissertation has not been presented to any other University for examination either in the United Kingdom or overseas.

SIGNED: 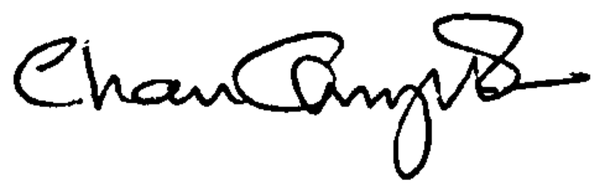 DATE: 25/5/04

Table of Contents:

Table of Figures:

Abbreviations

AP-1 – Apoptosis protein 1

Apaf 1 – Apoptotic Protease Activating Factor 1

Bcl-2 – B cell Lymphoma/leukaemia 2 gene

BH – Bcl-2 homology

C2 – N-acetyl-D-sphingosine, Ceramide, C2 analogue

CARD – Carboxy-terminal caspase Activation and Recruitment Domain

CDK – Cyclin Dependent Kinase

CHO – Chinese Hamster Ovary

CMV – Cytomegalovirus

CO_2 – Carbon Dioxide

CREB - cyclic AMP response element-binding protein

CRPG - Chlorophenol red-β-D-galactopyranoside

CSS – Charcoal Stripped Serum

Cyt c – Cytochrome c

DD – Death Domain

DED – Death Effector Domain

DMEM – Dulbecco's Modified Essential Medium

DNA – deoxyribonucleic acid

DR – Death Receptor

E_2 - 17β- Estradiol

EGFP – Enhanced Green Fluorescent Protein

ELISA – Enzyme Linked Immuno Assay

EPO R – Erythropoietin Receptor

ER – Estrogen Receptor

ERE – Estrogen Response Element

ERK – Extracellular Regulated Kinase

EYFP – Enhanced Yellow Fluorescent Protein

FACS – Flow Activated Cell Sorting

FADD – Fas Associated Death Domain

FAK – Focal Adhesion Kinase

FasL – Ligand for Fas

FITC – Fluoroscein Isothiocyanate

FL1 – Filter 1

FL2 – Filter 2

FLIP - Fas-associated death domain-like interleukin-1-beta-converting enzyme-inhibitory protein

GH – Growth Hormone

GR – Glucocorticoid Receptor

H&E – Haemotoxylin and Eosin

HA – Haemagglutinin

HeLa – Henrietta Lac

HET – Heat shock protein 70-Estrogen response element – TATA box binding protein

hnRNP – heterogenous nuclear ribonuclear proteins

Hsp-27 – Heat Shock Protein 27

IAP – Inhibitor of Apoptosis Protein

Ich-1 – Interleukin-1-β-converting enzyme homologue 1

IGF-1 – Insulin-like Growth Factor 1

IgG – Immunoglobulin G

IL-1 – Interleukin 1

IL-2 – Interleukin 2

ISEL – *In Situ* End Labeling

Jak – Janus Kinase

JNK – Jun amino-terminal Kinase

kDa – kiloDalton

LHRE – Lactogenic Hormone Response Element

MAPK – Mitogen Activated Protein Kinase

MEK – MAP kinase / ERK Kinase

mRNA – messenger ribonucleic acid

MW – Molecular Weight

NF-κB – Nuclear Factor κB

NGF – Nerve Growth Factor

PARP – Poly-(-Adenosine diphosphate-Ribose) Polymerase

PBS – Phosphate Buffered Saline

PCD – Programmed Cell Death

PCR – Polymerase Chain Reaction

PEI – Polyethyleneimine

PI – Propidium Iodide

PI3 – Phophatidylinositol 3

PI-3 kinase – Phosphoinositide – 3 kinase

PKB – Protein Kinase B

PKC – Protein Kinase C

PR – Progesterone Receptor

Prl – Prolactin

PrlR – Prolactin Receptor

PS – Phosphatidylserine

PTEN – Phosphatase and tensin homolog deleted on chromosome ten

PTP – Permeability Transition Pore

R - arginine

Rb – Retinoblastoma

RIP – Receptor-Interacting Protein

RLU – Relative Light Units

RRM - RNA recognition motifs

RSV – Rous Sarcoma Virus

RT-PCR – Reverse Transcription – Polymerase Chain Reaction

S - serine

S/MAR – Scaffold / Matrix Attachment Region

SAF – Scaffold Attachment Factor

SAPK – Stress-Activated Protein Kinase

SD – Standard Deviation

SFM – Serum Free Medium

SLB – Standard Lysis Buffer

SM – Sphingomyelin

Smac - second mitochondria-derived activator of caspase

snRNP - small nuclear ribonucleoproteins

SMases – Sphingomyelinases

SOCS – Suppressor of Cytokine Signalling

SSB – Stock Sample Buffer

STAT – Signal Transducer and Activator of Transcription

TBS – Tris Buffered Saline

TIA-1 – T-cell restricted intracellular antigen

TNF – Tumour Necrosis Factor

TNF-R1 - Tumour Necrosis Factor Receptor 1

TRADD – TNF receptor associated death domain

TRAF 2 – TNF Receptor Associated Factor 2

TUNEL – Terminal deoxynucleotidyl transferase mediated UTP Nick End Labeling

U2AF - U2 auxiliary factor

UV – Ultraviolet light

β-Gal – β-galactosidase

1 INTRODUCTION

1.1 The Development of Cancer

Cancer is a disease that involves multiple changes in the genome. The initial discovery of mutations within the genome associated with cancerous phenotypes led to the identification of oncogenes, whose presence conferred a dominant gain of function, and tumour suppressor genes, associated with recessive loss of function. Study of these genes has rapidly advanced our understanding of the nature of cancer, how it progresses and how it develops[1].

Accumulating evidence indicates that tumourigenesis is a multistep process in humans and reflects the genetic alterations that drive the transformation of normal human cells into malignant derivatives. Most cancers are diagnosed in the human population with an age-dependent incidence[2]. Analysis of various organ sites reveals lesions that may represent the intermediate steps through which cells have to evolve in the transformation from normality to a malignant phenotype[3]. This is further supported by increasing evidence showing that tumour cells invariably have mutated genomes, not just at one site, but multiple sites, from simple point mutations to massive disruptions such as chromosomal translocations[4]. The evidence in cultured cells is just as compelling. Rodent cells require at least two introduced genetic changes before they develop tumourigenic capability, and their human counterparts are even more resistant to transformation[5]. Transgenic tumour models also support the conclusion that tumourigenesis in mice requires multiple rate-limiting steps[6]. When considered together, these observations imply that for cancers to develop, each cell has to go through a series of genetic

alterations, which confer on the cells a growth or survival advantage until the final transformation of normal cells into cancer cells[3,7].

In normal cells, regulatory pathways monitor the extra- and intra- cellular conditions in order to maintain cell proliferation and homeostasis. Thus in order for a cell to transform into a cancer cell, there are several obstacles to overcome before it can achieve immortality and ungoverned proliferation. There appear to be at least six essential alterations in cell physiology before this occurs: self-sufficiency in growth signals, insensitivity to growth-inhibitory signals, evasion of programmed cell death (apoptosis), limitless replicative potential, sustained angiogenesis, and tissue invasion and metastasis[8].

1.2 Apoptosis: Definition and Mechanisms

The term 'apoptosis' was first used in 1972 by Kerr et al[9] to refer to the distinctive morphology of physiological cell death, and is interchangeably used with 'programmed cell death'. Thus apoptosis results from the controlled activation of a death mechanism already encoded within the genome of every cell. This programme is usually directed and executed by the cell itself – an autodestruct mechanism that is aided by neighbouring cells only in the final stages when it is phagocytosed.

Apoptosis was first described by its morphological characteristics, which comprise cell shrinkage, membrane blebbing, and nuclear fragmentation after chromatin condensation[9-11]. This is followed by fragmentation into apoptotic bodies and eventual phagocytosis by surrounding cells[12].

The importance of apoptosis in the development of on organism has become increasingly apparent in recent years. This process is important early in embryonic development for the moulding of body parts – such as digit separation and cavity formation – and also the elimination of vestigial structures[13]. It is also important in tissue homoestasis, balancing cell division and attrition, and maintaining tissue mass. Damaged, diseased or genetically unstable cells are removed by apoptosis[14]. The controlled elimination of autoreactive lymphocytes is also mediated by apoptosis, the lack or disruption of which results in autoimmune diseases[15].

Apoptosis is a programme, initiated and executed by cellular components under stringent control, requiring the coordinated activation of enzymes and the availability of adenosine triphosphate (ATP). In contrast, the other form of cell death – necrosis – does not require energy and is a result of the loss of the cell's ability to maintain ionic homeostasis. Apoptosis only involves one cell – the cell that is executing the programme - and does not lead to inflammation, destruction, or scarring and fibrosis of adjacent tissues.

The apoptotic mechanism can be divided into two broad groups – sensors and effectors. The sensors monitor the extracellular and intracellular environment for conditions that determine whether a cell should live or die. Signals from these sensors regulate the latter group of components, which are responsible for effecting cell death if it is required. Extracellular death signals include Fas ligand (FasL), which signals via its binding to the Fas receptor[16], and tumour necrosis factor(TNF)-α, which binds to the TNFR-1 receptor[17,18]. Intracellular signals that can initiate apoptosis include DNA damage,

signalling imbalance provoked by oncogene action, survival factor insufficiency, and hypoxia[12]. Most cells also depend partly on cell-matrix and cell-cell adherence-based survival signals, the loss of which can elicit apoptosis (sometimes known as anoikis)[19]. Both soluble and immobilized survival signals probably reflect the needs of the tissue to maintain their cells in appropriate architectural configurations.

Many of the apoptotic signals converge eventually on the mitochondria, which respond by releasing cytochrome c when stimulated by pro-apoptotic stimuli. This portion of the apoptotic pathway is influenced in part by the Bcl-2 family of proteins which have both pro-apoptotic (Bax, Bad, Bid, Bim) and anti-apoptotic (Bcl-2, Bcl-xL, Bcl-W) members whose actions determine the release of cytochrome c[20,21].

The final effectors of apoptosis comprise a group of intracellular proteases called caspases[22]. Two 'initiator' caspases, -8 and –9, activated by death receptors such as Fas[23,24] or cytochrome c[25,26] respectively, trigger the activation of a dozen or more effector caspases which are responsible for executing the apoptotic program[27].

1.2.1 Pathways for Apoptosis

1.2.1.1 Caspases – the executors of apoptosis

Caspases are cysteine proteases that specifically cleave after aspartic acid residues in the P1 position of substrates[28], and are present as inactive proenzymes in the cytosol. Caspases are homologous in structure and usually synthesised as inactive zymogens with four distinct domains[12]. Activation of caspases requires proteolytic cleavage, usually by

other caspases, between domains with the removal of a prodomain and a linker region, and rearrangement of large and small subunits into an active tetrameric complex[12]. An additional mechanism of caspase activation involves the recruitment of adaptor proteins that allow procaspases to come into close proximity with each other and enables caspases to activate themselves *in vivo*[29-32].

Caspases can be classified as 'initiators' or 'effectors', where initiator caspases are responsible for activating effector caspases, that are the ultimate effectors of apoptosis[29]. 'Initiator' caspases (namely caspase 8 and 9) have long prodomains with structural motifs (eg death effector domain, DED, or caspase recruitment domain, CARD) that allow enzymes to associate with their activators[33,34]. It is this binding of DEDs in the prodomains of caspases to DEDs on adaptor proteins, such as Fas-associated death domain (FADD), that results in activation of the caspase[23,24]. 'Initiator' caspases are also distinguished by the fact that they are able to activate themselves as well as downstream caspases to generate active enzymes[12]. In contrast, 'effector' caspases, namely caspase-3, -6, -7, and -14, all have short prodomains.

Thus in the caspase cascade activation sequence, apoptotic signals arising extracellularly (e.g. tumour necrosis factor (TNF)-α) or intracellularly (e.g. p53 activation following deoxyribonucleic acid (DNA) damage), result in the activation of either caspase-8, caspase-9, or both. These in turn proceed to activate the effector caspases – principally caspase-3 – which are responsible for many of the morphological changes associated with the apoptotic process[35,36].

Knockout mice deficient in various caspases have been created and have clarified the roles each caspase plays in apoptosis. Functional caspase-3 is required for some typical hallmarks of apoptosis and is essential for the formation of apoptotic bodies, chromatin condensation and DNA fragmentation[37-39]. Cells lacking caspase-8 do not apoptose in response to tumour necrosis factor (TNF) signaling, but are still susceptible to serum deprivation, chemotherapeutic drugs, γ-irradiation and dexamethasone-induced killing[40,41]. Caspase-9 is essential for apoptosis induced by intracellular activators, especially those that cause DNA damage[42]. Moreover, caspase-9 deficient cells do not show activation of caspase-3, implying caspase-3 is downstream of caspase-9, thus they are resistant to dexamethasone and irradiation but retain sensitivity to TNF-α and CD-95 induced cell death[42,43]. This sensitivity can be explained by the presence of caspase-8, the initiator caspase involved in death receptor signaling that can activate caspase-3[42] in caspase-9 deficient cells[43]. From all the evidence, it appears that different death-signalling pathways converge on downstream effector caspases, of which caspase-3 is regarded as a key executioner of apoptosis as activated by extracellular or intracellular stimuli[44].

Activated caspases have two targets: regulatory proteins of apoptosis, whose breakdown enhances apoptotic activity in the cell, and structural and housekeeping proteins, the degradation of which results in cellular disintegration. Regulatory proteins targeted by caspases include p21-activated kinase (PAK), focal adhesion kinase (FAK), inositol-3-phosphate (PI-3) kinase, protein kinase B (PKB/Akt), anti-apoptotic members of the Bcl-2 family and members of the IAP family. Structural components that are degraded by

caspases include nuclear lamins, actin, various regulatory proteins (e.g. fodrin, gelsolin, keratin), and proteins involved in DNA repair (e.g. poly-(-adenosine diphosphate-ribose) polymerase (PARP))[45,46] (Fig. 1.1)

In the mitochondrial pathway, most caspases are activated after the release of cytochrome c, but there is evidence to show that disrupting the action of caspases only delays the onset of apoptosis[47]. However, in other circumstances, loss of caspases results in a pathological increase in cell number[39,42,43]. Very little is known about mutations in caspases in cancers.

1.2.1.2 The Death Receptor Pathway

The death receptor pathway is triggered by 'death receptors' (DR) such as Fas/CD95, tumour necrosis factor receptor (TNFR)-1, DR3, and TNF-related apoptosis-inducing ligand receptors (TRAIL-R) 1 (also called DR4) and 2 (also known as DR5)[17,48] (Fig 1.1). The receptors are characterized by the possession of a conserved extracellular cysteine rich domain, and the presence of a 'death' domain within the cytoplasmic tail.

These receptors initiate apoptosis in a similar fashion. This involves the binding of ligand, the formation of a trimeric or multimeric death-inducing signalling complex (DISC), and the recruitment of adaptor molecules. Each of the adaptor molecules binds procaspase-8, thus bringing the zymogens into close proximity with each other, initiating autoactivation and the release of activated caspase-8, which activates the caspase cascade.

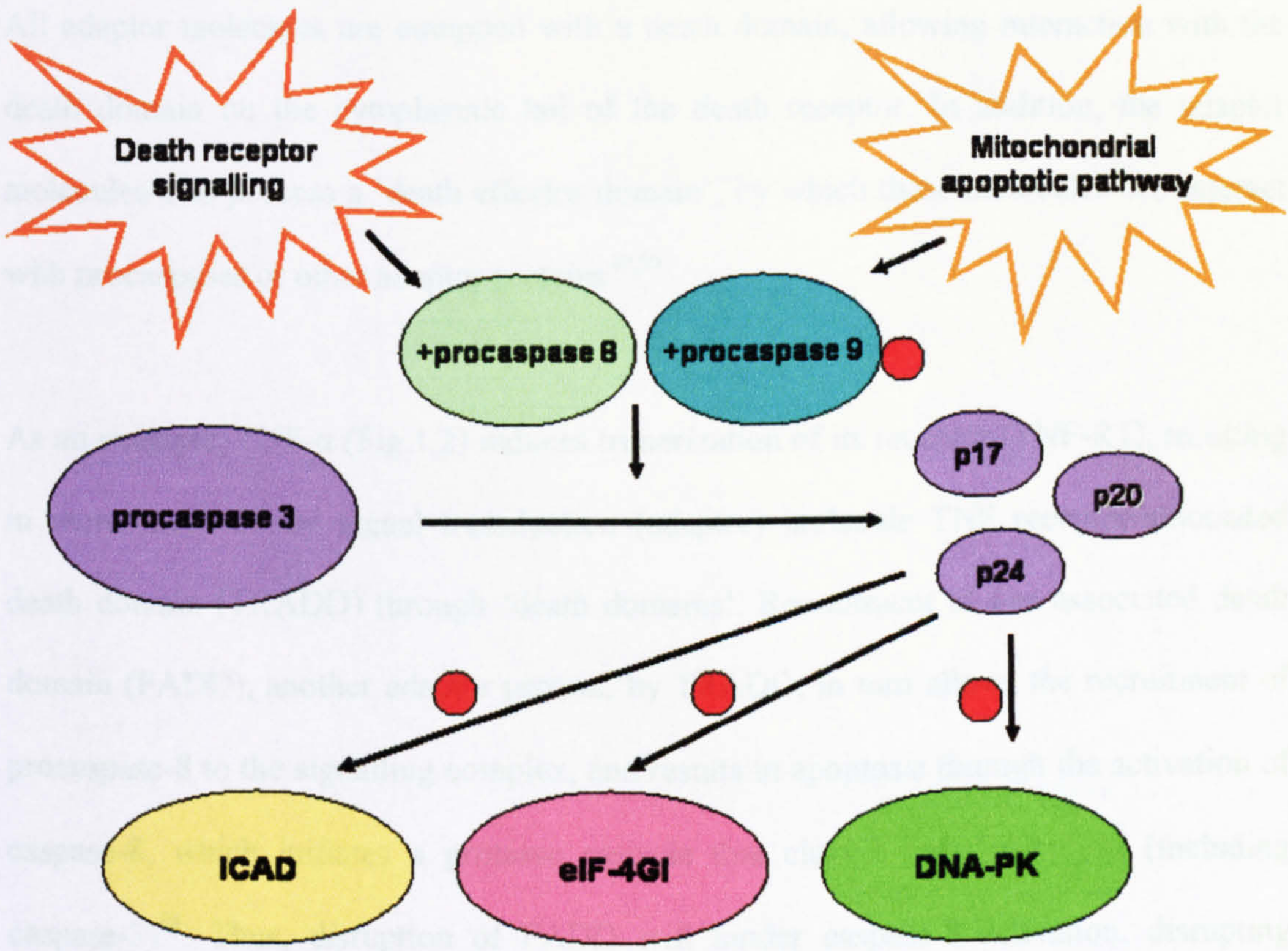

Figure 1.1Role of caspases in apoptosis (based on Wallach *et al* 1997[17] and Ashkenazi *et al* 1998[48]).

Initiator caspases -8 & -9 are activated by the death receptor pathway and the mitochondrial pathway respectively. Both are capable of activating caspase-3, the main effector caspase for apoptosis. Caspase-3, apart from activating other caspases in the caspase cascade, also has specific targets. It cleaves inhibitor of caspase activated deoxyribonuclease (ICAD), and releases the inhibition on caspase activated deoxyribonuclease (CAD), allowing DNA degradation to begin. Caspase-3 also cleaves proteins involved in transcription (eIF-4GI) and DNA repair (DNA protein kinase), thus disrupting protein synthesis and DNA maintenance. These activities, as well as caspase-9 activation, can be inhibited by XIAP (red dots), a member of the inhibitors of apoptosis protein family.

All adaptor molecules are equipped with a death domain, allowing interaction with the death domain on the cytoplasmic tail of the death receptor. In addition, the adaptor molecules also possess a 'death effector domain', by which these molecules can interact with procaspases or other adaptor proteins[49,50].

As an example, TNF-α (Fig.1.2) induces trimerization of its receptor (TNF-R1), resulting in recruitment of the signal transduction (adaptor) molecule TNF receptor-associated death domain (TRADD) through 'death domains'. Recruitment of Fas associated death domain (FADD), another adaptor protein, by TRADD, in turn allows the recruitment of procaspase-8 to the signalling complex, and results in apoptosis through the activation of caspase-8, which initiates a protease cascade that cleaves cellular targets (including caspase-3)[48]. Thus, disruption of FADD will hinder caspase-8 activation, disrupting receptor-mediated cell death[40]. Surprisingly, this pathway is seldom altered in tumours, indeed it is often enhanced[51]. TRADD also recruits receptor-interacting protein (RIP) and TNF receptor-associated factor (TRAF-2), which result in activation of nuclear factor κB (NF-κB), and can suppress TNF-α-induced apoptosis[52]. This pathway itself can be blocked by TRAF-interacting proteins (TRIPs) which bind TRAF and block NF-κB activation[53].

Although TNF-R signalling was described in detail here, there are other members in this group, such as Fas, and TNF-related apoptosis inducing ligand (TRAIL) that signal in a similar fashion, involving the recruitment of death domains and culminating in the activation of caspase-8.

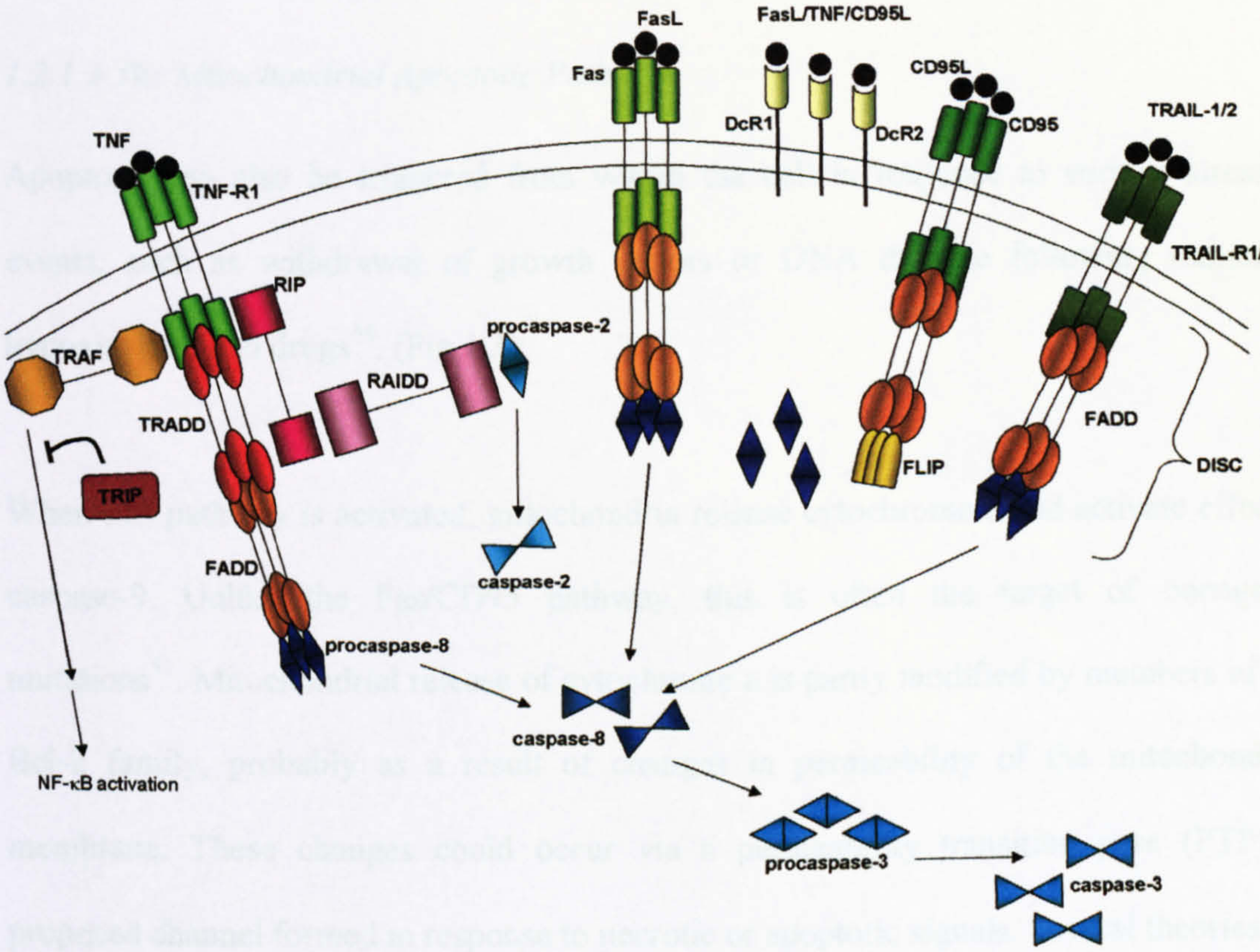

Figure 1.2The TNF Receptor Family (based on Baker *et al* 1998[50], Wallach *et al* 1997[17] and Pimental-Muinos *et al* 1999[54]).

This family includes TNF-R1, CD95, Fas and TRAIL-R1/R2 (green). Activation by ligand (black circles) results in formation of a trimeric/multimeric complex. Adaptor molecules (red, orange, pink) are recruited in various stages, and this comprises the death inducing signalling complex (DISC), which is able thus to recruit procaspases (blue) and activate them. Regulators of this pathway include decoy receptors (DcR1/2) which are able to bind ligand, but lack a death domain and are unable to recruit adaptor molecules required for signal transduction. Another group of inhibitors are the FADD like ICE inhibitory protein (FLIP) family, which bind the DED domain of FADD and prevent recruitment of caspase-8. The TNF-R1 also recruits TNF-R associated factors (TRAFs - 6 members), which links the death receptor pathway to the NF-kB pathway, with ultimate inhibition of cytochrome c release. The action of TRAFs can be inhibited by Traf interacting protein (TRIP) to block NF-kB activation.

1.2.1.3 The Mitochondrial Apoptotic Pathway

Apoptosis can also be triggered from within the cell in response to various stressful events, such as withdrawal of growth factors or DNA damage following radiation, hypoxia, heat and drugs[55]. (Fig.1.3)

When this pathway is activated, mitochondria release cytochrome c and activate effector caspase-9. Unlike the Fas/CD95 pathway, this is often the target of oncogenic mutations[51]. Mitochondrial release of cytochrome c is partly modified by members of the Bcl-2 family, probably as a result of changes in permeability of the mitochondrial membrane. These changes could occur via a permeability transition pore (PTP), a proposed channel formed in response to necrotic or apoptotic signals. Several theories are still under intense investigation regarding the mechanism by which cytochrome c, along with other proteins such as apoptosis-inducing factor (AIF), second mitochondria-derived activator of caspase (Smac)[56]/ direct IAP-binding protein with low pI (DIABLO)[57] (an inhibitor of the inhibitor of apoptosis protein family) and certain caspases, are released into the cytosol following activation of the mitochondria.

The PTP appears to be a contact point between the outer and the inner mitochondrial membrane. From current evidence, the pore in the outer membrane appears to be under the control of voltage-dependent anion channel (VDAC) and possibly Bax (a member of the Bcl-2 family of proteins), while the inner membrane is under the influence of the adenine nucleotide translocator (ANT) and Bax[61,62].

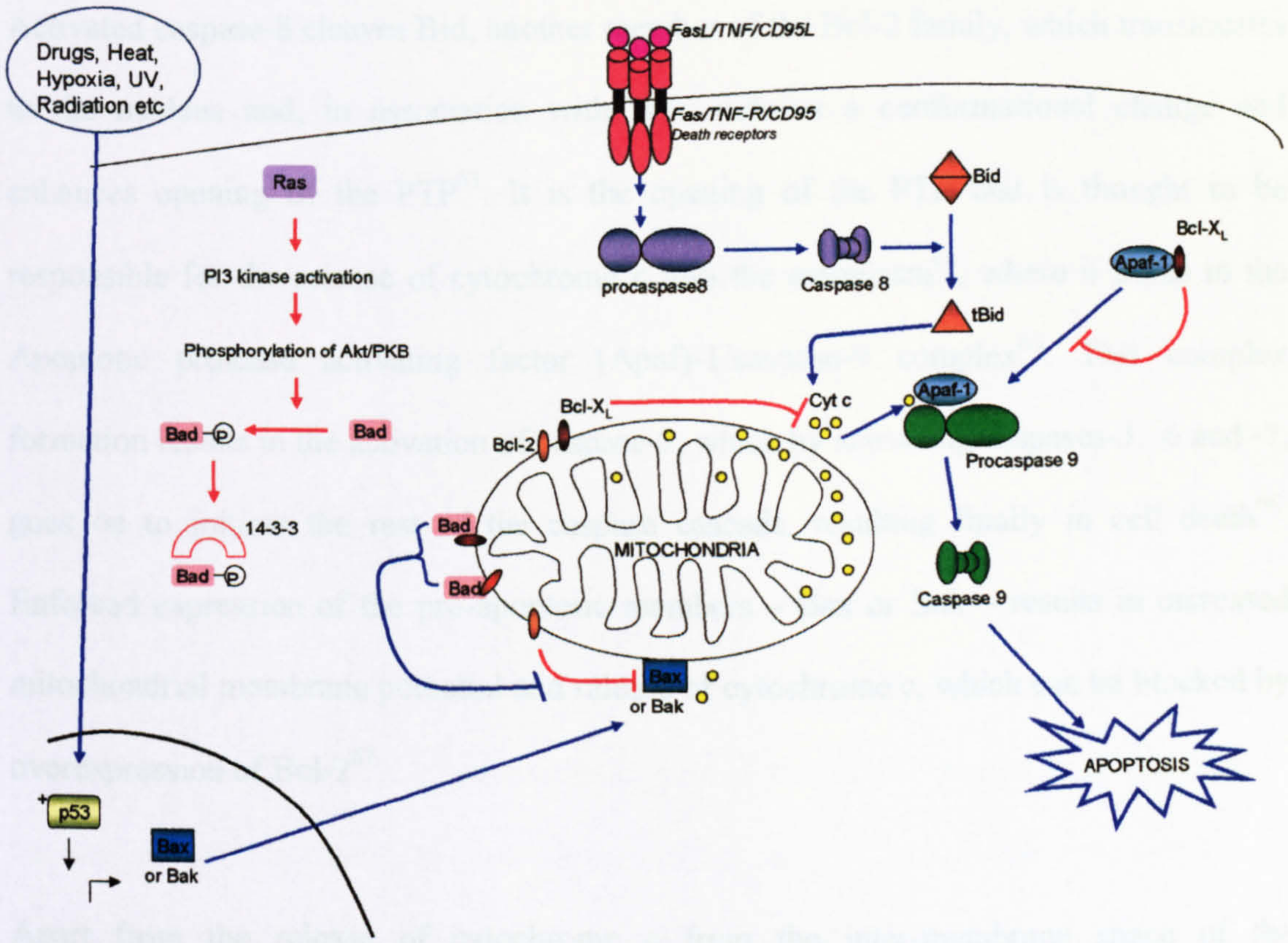

Figure 1.3The mitochondrial Apoptotic pathway, and the role of the Bcl-2 family in the induction or apoptosis (based on Gupta 2003[58], Cai *et al* 1998[59] and Kroemer 1999[60]).

(Red lines: protective mechanisms, blue arrows: apoptotic pathways) Bcl-2 and Bcl-xL both prevent cytochrome c release from mitochondrion. When Bad dimerizes with either of them, Bax is released and initiates cytochrome c release. Truncated Bid (tBid)(formed by caspase-8 processing of Bid) also activates Bax. Bcl-2 and Bcl-xL can prevent the formation of the apoptosome complex that comprises Apaf-1, cytochrome c and procaspase-9, which inhibits the downstream caspase cascade. Bad activity is regulated by phosphorylation by Akt/PKB, which initiates the sequestration of Bad by the 14-3-3 protein, thus inactivating it. Bax and Bak transcription are up-regulated in response to p53 activation.

Activated caspase-8 cleaves Bid, another member of the Bcl-2 family, which translocates to the nucleus and, in association with Bax, induces a conformational change and enhances opening of the PTP[63]. It is the opening of the PTP that is thought to be responsible for the release of cytochrome c into the cytoplasm[64], where it binds to the Apoptotic protease activating factor (Apaf)-1/caspase-9 complex[65]. This complex formation results in the activation of caspase-9, which by activating caspases-3, -6 and -7, goes on to initiate the rest of the caspase cascade, resulting finally in cell death[66]. Enforced expression of the pro-apoptotic members – Bax or Bak – results in increased mitochondrial membrane potential and release of cytochrome c, which can be blocked by overexpression of Bcl-2[67].

Apart from the release of cytochrome c from the inter-membrane space of the mitochondria, apoptosis inducing factor (AIF) is also released. AIF, which also resides in the inter-membrane space of the mitochondria[68] is a 57kDa protein. It was initially thought to be a protease, but has since been found to be homologous to NADPH-oxidoreductase[69] and is thought to be responsible for the various nuclear changes that are characteristic of apoptosis, namely chromatin condensation, prótein proteolysis and DNA fragmentation[68].

Another protein, Smac/DIABLO is released from the mitochondria following apoptotic stimuli. Smac/DIABLO is known to bind IAP proteins, and prevents their inhibition of caspase activities[56].

Ultimately, the final event of both pathways (i.e. TNF/TNFR-1 and activation of mitchondria) is activation of the caspase cascade that is responsible for digesting cellular contents. Cytosolic and nuclear proteins involved in DNA replication and repair, RNA splicing, cell division and cytoskeletal structure are digested, and their loss finally results in the morphological changes associated with apoptosis[12].

1.2.2 Regulators of Apoptosis

Apoptosis being a gene-directed programme, it is not surprising that this pathway is safeguarded by many regulators and checks before it is allowed to proceed. Thus, there are many levels at which this programme may be aborted/prevented. A brief summary of the various proteins and pathways whose function it is to ensure that apoptosis occurs only when it is required, and not before, is outlined below.

1.2.2.1 The Bcl-2 family of proteins

The first member of this family to be identified, Bcl-2, was discovered at the interchromosomal breakpoint of the t(14:18), now known to be the distinguishing feature of follicular B cell lymphoma[70,71]. Oncogenes typically enhanced cell proliferation, however, in contrast, Bcl-2 exerted its effect by enhancing cell survival and defined a new group of oncogenes[20,72,73].

The first pro-apoptotic member of the family to be identified was Bax - Bcl-2 associated protein X[74]. To date 17 members of the family have been identified and they can be

divided into 2 functional groups: those which promote apoptosis, such as Bax, Bad, Bid and those which suppress it, like Bcl-2 and Bcl-xL[20,75].

Mechanism of Action

Anti-apoptotic proteins, such as Bcl-2 and Bcl-xL reside on the outer mitochondrial membrane, where they are thought to prevent the release of cytochrome c (possibly by interacting with the voltage-dependent anion channel (VDAC))[76]. There is some evidence that Bcl-xL, and possibly Bcl-2, can bind apoptotic protease activating factor (Apaf) – 1, preventing the association of procaspase-9 with Apaf-1 and cytochrome c, and hence, inhibits activation of caspase-9[77].

The pro-apoptotic members, Bax, Bad and Bak, on reception of apoptotic signals, translocate to the mitochondria, where they initiate the release of cytochrome c, AIF and Smac/DIABLO[78,79]. In addition, Bad dimerizes with Bcl-xL, relieving its inhibitory effect on cytochrome c release[80,81]. Bad is itself regulated by Akt/protein kinase B (PKB), which phosphorylates Bad, allowing the protein 14-3-3 to bind and inactivate it[82]. Another member of the Bcl-2 family, Bid, is activated, by truncation to tBid, by caspase-8[83]. tBid translocates to the mitochondrion where it stimulates Bax and Bad, and initiates cytochrome c release[84-86] (Fig 1.2).

1.2.2.2 The inhibitor of apoptosis protein (IAP) family

This family of proteins was first discovered in baculoviruses where they are responsible for suppressing the host apoptotic response to viral infection. Members of the IAP family

are characterised by a domain of ~70 aminoacids named the baculoviral IAP repeat (BIR). Members can possess up to three tandem repeats of this sequence which appears to code for a zinc-binding fold[87]. The proteins are conserved between species, and are also found in humans, with all members possessing a BIR domain and the ability to suppress apoptosis, though the latter has still to be proven for many of them.

There are six human IAPs – including c-IAP1, c-IAP2 and XIAP. The mechanism of action of these proteins is still under investigation, but they are known to be expressed in a wide variety of tissues, apart from XIAP, which has a restricted distribution[88]. Overexpression of XIAP, c-IAP1, c-IAP2 and other IAPs protects against apoptosis induced by various factors, including TNF, FasL, staurosporine, etoposide and growth factor withdrawal[88-91]. The three IAP members mentioned have been shown to bind and inhibit the activities of caspases 3, 7 and 9, but not caspases 1, 6, 8 or 10[92-94]. Thus, these proteins are able to block both the death receptor pathway as well as the mitochondrial apoptotic pathway. Consistent with reports that IAPs bind to caspases is the observation that they do not affect the release of cytochrome c from mitochondria[95,96], thus raising the question of whether IAP suppression of apoptosis is complete, or only delays the inevitable[87].

1.2.2.3 Serine/Threonine protein kinases and apoptosis

Apoptosis can be regulated not only intrinsically, but also by extrinsic factors, such as growth factors, hormones, and cellular factors. In this regard, serine/threonine kinases have been implicated in the regulation of apoptosis. Kinases involved include the

mitogen-activated protein kinase (MAPK) family, cyclic AMP dependent protein kinase (PKA), protein kinase B (PKB/Akt) and protein kinase C (PKC)[97].

Mitogen-Activated protein kinases (MAPKs)

The kinases in this family that are involved in apoptosis are the p42/44 extracellular signal-related kinases (ERK) 1 and 2[98], p38 MAPK[99] and c-Jun N-terminal kinase (JNK)[100] specifically. The latter two enzymes appear to be involved in inducing apoptosis, while the former appears to enhance survival.

On growth factor withdrawal, both JNK and p38 MAPK are activated[101], resulting in upregulation of Fas ligand production and release[102], and subsequent activation of caspase-3[103]. Other triggers of JNK activation are hypoxia, TRAIL receptor stimulation, nitric oxide and cellular stress[104-106].

Concurrent with the activation of JNK/p38, inhibition of ERK signalling is also noted[101]. This is probably due, in part, to caspase-3 which has been shown to cleave Raf-1 (an upstream activator of ERK)[107]. In addition, ERK activation has also been proven to suppress apoptosis induced by hypoxia[108], growth factor withdrawal[109] and chemotherapeutic agents[110]. The actual mechanism for ERK inhibition of apoptosis is as yet undefined. However, possible candidate substrates include Bad[111], and caspase-9[112].

Protein Kinase A (PKA)

The PKA enzyme is a complex entity, consisting of two catalytic subunits bound to regulatory subunits. There are three isoforms for the catalytic subunit, and four for the regulatory subunits. Regulatory subunits can be bound to PKA as either homo- or hetero-dimers[113]. Depending on the regulatory subunit in use (RI or RII), PKA is identified as type I or II respectively. PKA type I appears to be anti-apoptotic, and is thought to have a role in phosphorylating Bad[114], whereas the role of type II PKA is still unclear.

Protein kinase B (PKB) / Akt

The importance of PKB/Akt in the suppression of apoptosis is no longer in dispute, and a large body of literature is now devoted to identifying and mapping out the signalling pathways involving this protein kinase, its regulation, and the role it plays in tumourigenesis[115]. PKB/Akt is thought to be the major pathway by which trophic factors are able to inhibit apoptosis, via activation of the phosphoinositide-3 kinase (PI3K), which is the upstream activator of PKB. The targets of this cascade are Bad, caspase-9, transcription factors of the Forkhead family and inhibitor of IκB (inhibitor of nuclear factor kappa-B) kinase (IKK).

Phosphorylation of Bad allows it to bind 14-3-3 proteins and release Bcl-X_L. 14-3-3-bound Bad is thus sequestered from the cytoplasm, unable to inhibit anti-apoptotic proteins further[81,82,111]. Another action of activated PKB is to phosphorylate caspase-9[65], thereby reducing its protease activity[112].

The third substrate of PKB is IKK-α, which it phosphorylates and activates[116]. IKK-α inactivates IκB, and brings about the nuclear translocation and activation of nuclear factor-κB (NF-κB), thus upregulating the transcription of various survival factors[117]. The final substrate of PKB/Akt is the Forkhead transcription factor FKHRL1, which has been shown to induce the transcription of FasL and TNF-α[102,118,119], and the proapoptotic Bcl-2 family member, Bax[120,121].

1.2.2.4 The tumour suppressor gene- p53

p53, the first tumour suppressor gene to be linked to apoptosis, is found mutated in many cancer types and is often associated with an advanced disease stage and poor patient prognosis[122]. It is now known that p53 is a checkpoint protein involved in cell cycle arrest that is responsible for ensuring retention of genomic integrity following DNA damage[51]. Studies in p53 knockout mice show that endogenous p53 is involved in apoptosis: it is required for radiation induced apoptosis in the thymus but not for apoptosis induced by glucocorticoids or other stimuli[123,124]. This implies that p53 is involved in apoptosis resulting from DNA damage and can be stimulation- and tissue-specific. Other stimuli can also induce p53 to promote apoptosis, and mutations of both upstream and downstream components of the pathway can be found in human tumours[122].

The p53 protein has several functions: it can promote apoptosis, induce cell cycle arrest and senescence. Thus loss of p53 function could result in increased viability, chromosomal instability and increased cell lifespan. However, there is evidence to show that it is the apoptotic function of p53 that is crucial to tumour suppression. Disruption of

several p53 effectors (e.g. bax, apaf-1, casp-9) can promote oncogenic transformation and tumour development in mouse model systems[125-127]. Some tumour-derived p53 mutants remain capable of inducing cell cycle arrest but have lost their ability to induce apoptosis [128,129].

Please see Fig. 1.4 for overview of Apoptosis and its regulation.

1.3 The Disruption of Apoptosis in Cancer

The ability of a tumour cell population to expand reflects not only the rate of proliferation, but can also depend on the rate of cell attrition, which can be changed as a result of decreased apoptosis or necrosis. Apoptosis appears to be a major source of cell death[130], and there is increasing evidence that resistance to programmed cell death is characteristic of most, if not all, cancers[48,64,131,132]. That apoptosis may serve as a barrier to carcinogenesis was first suggested in 1972, when Kerr, Wyllie and Currie described massive apoptosis in cells populating rapidly growing, hormone-dependent tumours following withdrawal of the hormone[9].

The discovery that apoptosis was a gene-directed program had a significant impact on the understanding of tissue development and homeostasis, for it meant that cell number was regulated by factors that controlled proliferation and differentiation, as well as survival factors[48,51,133]. More importantly, this genetic basis implied that cell death, like any other metabolic or developmental program, could be affected by mutation with resultant susceptibility or resistance to the process.

It is clear that the apoptotic mechanism exists in all cell types throughout the human body, requiring only activation to be initiated[134]. Upon activation, apoptosis proceeds through distinct stages, ending in the disruption of cellular membranes, dissolution of cyto- and nucleo-skeletal structures, extrusion of the cytosol, degradation of chromosomes and breakup of the nucleus, all this occurring within a 30-120 minute period. All that remains is a shriveled cell body that is engulfed by neighbouring cells and disappears within 24 hours[11].

Several signal transduction pathways promote cell survival when stimulated by growth and/or survival factors and may be important in controlling cell number. One such pathway is the PI-3 kinase pathway, which can be activated by Ras and downregulated by the PTEN tumour suppressor[135]. Many studies using either transgenic or knockout mice have shown that disruption of apoptosis is important in tumour development[136-138].

Identification of apoptotic triggers is important as it provides insight into the forces of tumour development and progression. In skin, excessive exposure to ultraviolet radiation induces apoptosis – which serves to remove heavily damaged cells. When p53 function is lost, these damaged cells survive, paving the way towards future tumour development[142]. Other apoptotic triggers are also important. As tumours increase in size, they outgrow their blood supply, encountering hypoxia, which can activate p53 and trigger apoptosis[143]. A p53 defect allows the cells to survive this hypoxic stress and enables cell proliferation within the tumour[144]. With repeated divisions, telomeres within the cell shorten until they trigger apoptosis, or signal for the cell to become quiescent. As

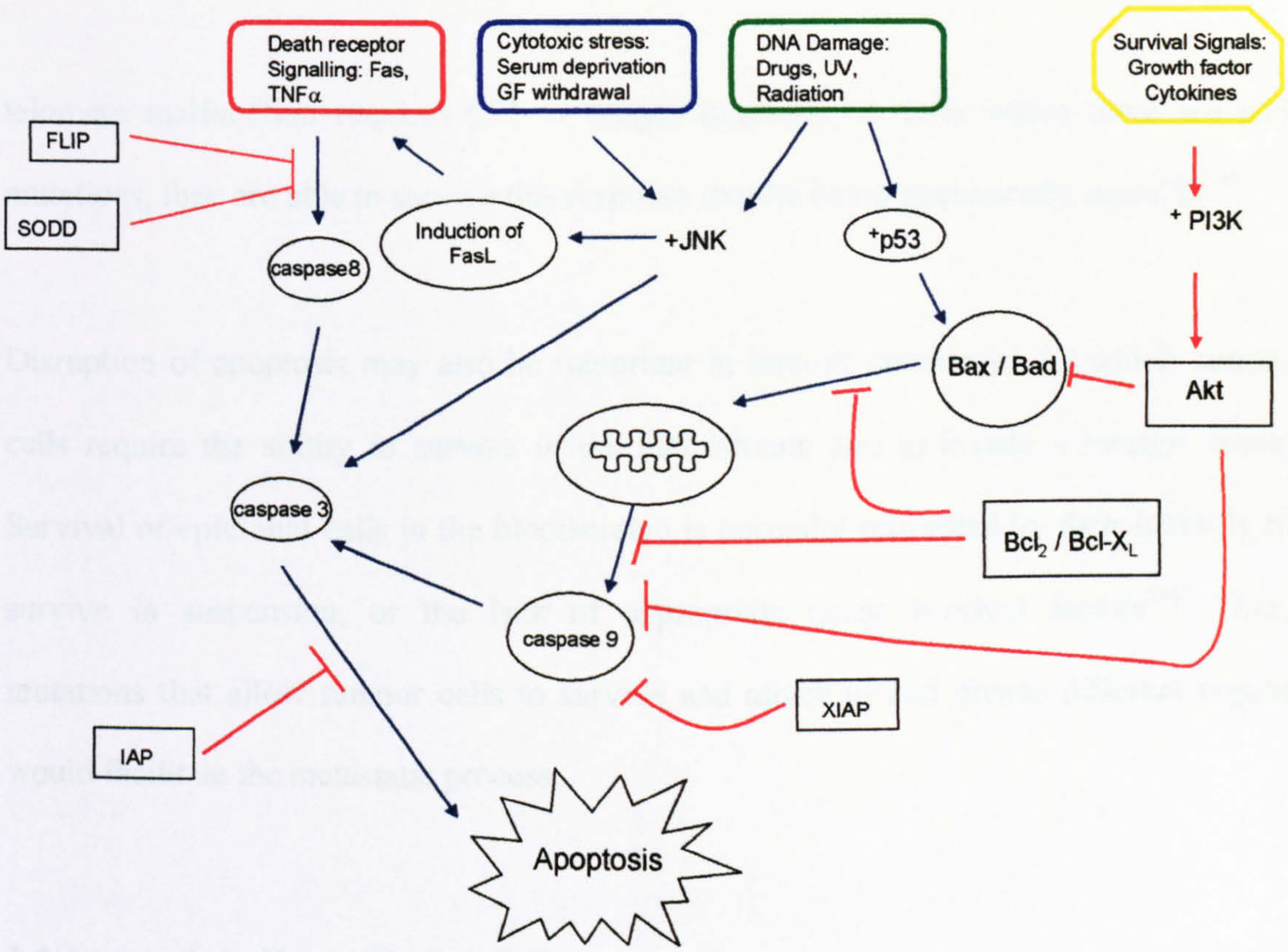

Figure 1.4 Summary of apoptotic (blue) and survival (red) pathways (based on Datta *et al* 1999[115], Mak & Yeh 2002[139], Reed 1999[140] and Reed 1999[141]).

Apoptosis is induced in response to death receptor signalling, cytotoxic stress, such as serum deprivation, hypoxia and growth factor withdrawal, or DNA damage resulting from UV/radiation, heat, and drugs. All pathways activate either caspase 8 or caspase 9, and these in turn activate caspase 3, which is responsible for the morphological changes seen with apoptosis. At various stages of the apoptotic cascade, survival signals are able to intervene and inhibit apoptosis, and these factors include members of the Bcl-2 protein family, Akt/PKB and the IAP family. In addition, the death receptor pathway can be inhibited at the level of the death domain by FLIP or SODD.

telomere malfunction requires p53 to trigger apoptosis, in cells where there are p53 mutations, they are able to survive this response despite being genomically unstable[145].

Disruption of apoptosis may also be important in tumour metastasis, for which tumour cells require the ability to survive in the bloodstream and to invade a foreign tissue. Survival of epithelial cells in the bloodstream is normally prevented by their inability to survive in suspension, or the lack of appropriate tissue survival factors[146]. Thus, mutations that allow tumour cells to survive and attach to and invade different organs would facilitate the metastatic process.

1.4 Apoptosis in Breast Cancer Cells

Cancer of the breast is the most common cancer affecting women in the United Kingdom (18%)[147]. Studies of cancerous breast epithelium shows that the rate of apoptosis is increased in ductal carcinoma *in situ* and invasive cancer[148,149], however, compared to normal breast epithelium, this is still reduced relative to the rate of proliferation[150].

As an indicator of prognosis, increased rates of apoptosis, contrary to expectation, are associated with worse prognosis and survival[149,151,152]. Similarly, in cancers of higher grade, apoptosis is increased, but there is also a concomitant increase in the proliferative rate[149].

1.4.1 Mutations affecting Apoptosis in Breast Cancer Cells

1.4.1.1 The Bcl-2 Oncogene

Oncogenes are genes whose products stimulate cell cycle progression. In normal cells, the activation of oncogenes triggers a failsafe mechanism against malignant transformation by directly inducing apoptosis or 'sensitizing' the cell to apoptotic stimuli. However, when this mechanism is overcome, cell cycle progression can proceed unchecked.

Mutation of Bcl-2 has been observed in at least 80% of breast tumours[153] and, surprisingly, was associated with better prognosis in Bcl-2 positive patients[153]. In addition, there was a positive association between Bcl-2 status and hormone receptor positivity and low histologic grade[154].

Bcl-2 appears to modulate cell division, and its loss is associated with increased tumour grade and proliferation, associated with high apoptotic and necrotic rates within tumours[155]. The presence of Bcl-2 does confer a survival advantage against apoptosis. MCF-7 breast cancer cells, positive for epidermal receptor 2 (HER-2), are more resistant to apoptosis and exhibit an upregulation of Bcl-2 and Bcl-xL expression[156]. Moreover, the ligand heregulin, which activates HER-3 and HER-4 receptors and downregulates Bcl-2 expression, can induce apoptosis in certain breast cancer cell lines[157]. Thus, aside from the influence of Bcl-2 on cell cycle progression, its increased expression in breast cancer cells can suppress apoptosis induced by a number of factors, and is associated with the increased expression of proteins involved in metastatic spread[158].

1.4.1.2 The c-Myc oncogene

In normal cells, ectopic c-myc expression drives proliferation and prevents cell cycle arrest upon serum withdrawal, yet there is no accumulation of cell number as there is a corresponding loss of cells due to apoptosis[159]. Survival factors, such as IGF-1, can suppress c-myc induced cell death without affecting c-myc-induced proliferation[160]. Likewise, c-Myc cooperates with Bcl-2 to transform cells[161,162] because Bcl-2 allows c-myc-induced proliferation to proceed without apoptosis.

1.4.1.3 The p53 tumour suppressor gene

Loss of p53 function *in vivo* results in acceleration of the rate of tumourigenesis induced by mitogenic oncogenes, which is associated with decreased apoptosis *in situ*[163-165]. C-Myc induces apoptosis in a p53-dependent manner[166,167] and cells overexpressing c-Myc are more sensitive to various apoptotic stimuli such as serum-deprivation, hypoxia, Fas and TNF-α[132]. Another target of oncogene-induced sensitization is the mitochondrion, where c-Myc enhances cytochrome c release from mitochondria and cytochrome c is itself sufficient to sensitize cells to diverse agents[168,169]. Oncogenes can facilitate cytochrome c release independent of p53[169], though p53 is capable of inducing Bax and proteins that can affect mitochondrial function[170,171]. Thus, p53 may be responsible for the sensitization to, as well as the active induction of, cell death in oncogene-expressing cells and mutations in the p53 gene would facilitate oncogenesis by allowing cells to evade oncogene-induced apoptosis.

The role of p53 in breast tumourigenesis is well documented. Mutations involving p53 are fairly common[172], with one study estimating a mutation rate of 20-40%[173]. Indeed, in BRCA1-associated tumours, 90% are associated either with mutations in p53, or exhibit increased expression of p53 protein[174]. *In vitro* studies involving the T47-D cultured human breast carcinoma cell line have shown that expression of wild-type p53 protein was able to inhibit proliferation[175] (T47-D cells possess a mutation in the p53 gene[176]). In addition, Patel et al. showed that there was a strong correlation between overexpresion of p53 and breast tumour aggressiveness in patients with node-negative disease[177].

1.4.1.4 The PTEN tumour suppressor gene

The PTEN (phosphatase and tensin homolog deleted on chromosome 10) gene encodes a 55kDa enzyme that possesses phosphatase activity[178,179]. Mutation or loss of PTEN has been implicated in a large number of cancers, including breast cancer[180]. Despite this finding, PTEN does not appear to have a dominant role in the majority of breast cancers. Germline mutations are rare in breast cancer (6% of cancers)[181], while loss of heterozygosity at the PTEN locus is the most frequent lesion observed[182] In breast cancer cells, overexpression of PTEN can induce apoptosis, and cell cycle arrest[183]. Clinically, decreased expression of PTEN has been associated with a more advanced stage of breast cancer[179]. The PTEN enzyme has been shown to negatively control the PI3-kinase survival pathway by dephosphorylating phosphatidylinositol-3,4,5 triphosphate[184,185], thus preventing activation of PKB/Akt[115].

1.4.1.5 Death receptors in breast cancer

The TNF-receptor family in the form of Fas (or CD95) is widely expressed in normal breast epithelia. FasL was found to be markedly higher in breast malignancies compared to normal epithelium and benign breast lesions[186]. Moreover, there was a correlation between FasL and lymph node status, while Fas expression correlated with smaller tumour size and negative node status, which was consistent with another study that showed patients with Fas-positive tumours had longer disease-free survival when compared to Fas-negative patients[187]. In contrast, Fas expression was very low in several different breast tumour cell lines[186].

1.5 Methods for the Detection of Apoptosis

As investigation into the field of apoptosis increased over the last ten years, the number of methods of detecting apoptosis has increased in parallel. Most methods employ techniques that exploit characteristics that are unique to the dying cell.

Evidence acquired over the last decade shows that the apoptotic mechanism is highly conserved, which has made it possible to devise methods for detecting the products at various stages in order to differentiate apoptotic cells. Methods for detecting apoptotic cells can be divided into the following categories: surface morphology and composition, nuclear events and DNA cleavage, cell dissolution, cytoplasmic biochemical activation events, and mitochondrial function and integrity[188].

1.5.1.1 Surface Morphological and Biochemical Changes

The classical features of apoptosis, best observed under electron microscopy, can be detected with light microscopy with the help of dyes e.g. haematoxylin, or propidium iodide[26,189,190]. The first signs of apoptotic cell death are the condensation of nuclear material, with the accumulation of densely staining chromatin at the periphery of the nucleus. This is accompanied by cell shrinkage. Cell surface blebbing then occurs and the cell detaches itself from its neighbors. The nuclear outline becomes much folded before the nucleus disintegrates, dispersing the nuclear fragments throughout the cytoplasm. Eventually the cell fragments, resulting in the formation of several discrete membrane-bound apoptotic bodies. These bodies are then phagocytosed by surrounding cells. Apoptotic bodies are thus a common hallmark of apoptosis and can be found either extracellularly or inside other cells following phagocytosis. Apoptotic bodies can be diverse in appearance, but tend to be round or oval, and contain varying amounts of condensed chromatin. Their size varies considerably[9,10,191].

Externalization of phosphatidylserine (PS) and phosphatidylethanolamine is another hallmark change to the cell surface during apoptosis[192-194]. Annexin V, which binds to these molecules, is a good marker for this process and can be detected using either flow cytometry or fluorescent microscopy[195,196]. These phospholipids are normally found on the inner layer of the plasma membrane bilayer as well as other membranes. The reason why PS appears on the outer membrane is not clear but it has been shown to occur quite early, just after segmentation of nuclei. It has also been found that not all cells exhibit this phenomenon[197,198], and that caspase inhibition can prevent its occurrence[199].

When interpreting Annexin-labeling results, care has to be exercised because towards the terminal stages of apoptosis, or during necrosis when the plasma membrane is leaky, Annexin can diffuse inside the cell and interact with intracellular PS.

Permeability of the plasma membrane is another difference between necrotic and apoptotic cells which can be exploited by the use of large molecular weight DNA binding dyes, e.g. propidium iodide (PI), which are unable to enter intact cells without permeabilization, and thus are unable to label apoptotic cells until the final lytic stage. Conversely, smaller dyes that can attach to DNA can label both apoptotic and normal cells. By the use of flow cytometry, apoptotic cells can be distinguished from necrotic cells as those that show internal labeling with a small dye (e.g. DAPI, Hoechst 33342) without taking up PI[198,200].

1.5.1.2 Nuclear changes and DNA changes

It was observed at an early stage that nonmitotic cells entering apoptosis exhibited characteristic changes in nuclear shape and organization. This change is probably the most accurate indicator of apoptosis, though it does not have to be present for apoptosis to occur. Cells that have been enucleated may still be able to initiate and execute the apoptotic program, which indicates that the effector mechanism for apoptosis lies in the cytoplasm[201]. Despite this, nuclear changes provide an early and relatively unequivocal landmark of apoptosis in nucleated cells, which occurs just after surface blebbing begins[202].

Another characteristic of apoptosis is the loss of DNA integrity where DNA fragmentation occurs with cleavage of DNA between nucleosomes. DNA fragmentation has been exploited by the addition of enzymes that are capable of adding labeled nucleotides to the 3'-OH ends of single-stranded DNA[203,204]. The labeled nucleotides can then be detected by immunological methods. Such assays were originally called TUNEL (terminal deoxynucleotidyl transferase mediated UTP nick end labeling) but may also be called ISEL (*in situ* end-labeling technique).

When nuclei from apoptotic cells are extracted and analyzed by gel electrophoresis, a distinctive internucleosomal 'ladder' of DNA fragments is usually apparent. This remains one of the most widely used methods for the detection of apoptosis, but requires extraction of DNA from a large number of cells. Moreover, apoptosis in these cells must be fairly synchronous for analysis, and this may not always be possible. Another problem with this and other DNA based methods involving electrophoresis is that spatial information as well as quantification of apoptosis is lost.

1.5.1.3 Other Biochemical Changes

Recent discoveries regarding the many steps in the apoptotic program include caspase activation and the cleavage of specific caspase substrates. By incorporating these specific substrates into cells and detecting the cleaved product, new assays have been developed. Other biochemical changes that occur in apoptosis which may be used as a marker include transglutamine activation, the expression of certain surface and intracellular antigens, changes in mitochondrial activity, and cytochrome c release.

1.6 Aims of Project

1) Previous studies have provided some evidence for a protective role of prolactin in breast cancer cells, so one aim of this project was to investigate in greater detail the role of prolactin, and in particular its ability to activate the Jak-STAT pathway, as a survival factor for breast cancer cells.

2) Initial studies with Met (a SAF-B related protein) suggested that its expression had profound changes on gene expression in cultured breast cancer cells. A second aim of this project was therefore to test the hypothesis that this protein might induce apoptosis in breast cancer cells.

2 Materials and Methods

Recombinant human prolactin was kindly provided by V. Goffin of INSERM, Paris. The freeze-dried powder was dissolved in 1.5M Tris (pH 8.0) and the concentration determined by the Micro Protein Determination kit (Sigma). A stock solution of 500µg/ml was made, and stored in aliquots at –80°C. As concentration of a protein does not necessarily reflect the biological potency of the hormone, bioactivity was confirmed using the Nb2 Prolactin Bioassay (see Section 2.3). Unless stated otherwise, this was used in all assays requiring prolactin.

All cell lines, unless stated otherwise, were obtained from the European Collection of Cell Cultures (ECACC, Porton Down). The HeLa cell line, a human cervical carcinoma cell line, was a kind gift from Dr. Craig McArdle (URCN, Bristol), and the SF cell line, a primary human fibroblast cell line, was kindly given by Dr. Andrew Morgan (University of Bristol).

2.1 Micro Protein Determination

The Sigma Micro Protein Determination kit (p.225) was based on the Biuret and Lowry methods for determining protein concentration, with modifications to improve the sensitivity and stability of the reagents. A sample of the protein solution was mixed with the Biuret reagent and later with the Folin and Ciocalteu's phenol reagent. The colour formed was read at 570nm and protein concentration determined from a calibration curve. The Protein Standard solution provided was diluted 1:100 using 0.85% (w/v) NaCl solution. This gave a protein concentration of 100mg/dL, and from this protein solutions of 0, 25, 50 and 75 mg/dL were obtained by diluting with the appropriate amount of

0.85% NaCl solution. 40µl of each protein solution, as well as the test solution, was pipetted into 0.5ml Eppendorf tubes. 440µl of Biuret agent was added to each tube, mixed well and incubated at room temperature for 10 minutes. 20µl of Folin and Ciocalteu's phenol reagent was added to each tube, mixed well and incubated at room temperature for 30 minutes. 200µl of each solution was then transferred to a microtitre plate and absorption at 750nm determined using a microplate reader (Dynex Revelation).

2.2 Cell Culture

All adherent cell lines were maintained in Dulbecco's modified Eagle's medium (DMEM) supplemented with 2mM L-glutamine, 10% fetal calf serum, incubated in a humidified 5% CO_2 atmosphere at 37°C. The CEM-C7 cell line, and its sub-clones, as well as the Nb2 lymphoma cell line, were maintained in RPMI 1640 medium supplemented with 2mM L-glutamine and 10% fetal calf serum. Experiments were performed on cells in serum free medium (SFM): Ham's nutrient DMEM/F12 1:1 mix without phenol red supplemented with sodium bicarbonate (1.2 mg/ml), 0.1% (w/v) bovine serum albumin (BSA) and apo-transferrin (10 µg/ml).

2.3 Nb2 Prolactin Bioassay

The bioactivity of prolactin was assayed using Nb2 rat lymphoma cells. $5x10^4$ cells were plated in 1ml in each well of a 24 well plate in serum free medium and incubated for 24 hours. Following this, varying concentrations of prolactin (final concentration ranging

from 10ng/ml to 10μg/ml) were added to the wells and the cells incubated for a further 4-5 days. Cells were then counted using a Coulter Counter (p.221).

2.4 Cell Counting using the Coulter Counter

On the day of counting, the medium was aspirated, and the cells gently washed with PBS. 100μl of trypsin was added to each well and cells were incubated at 37°C for 5 minutes before 900μl of serum-containing medium was added to the wells. After resuspension, the cells were separated gently using a 21G needle, and 0.2ml of the cell suspension was added to 19.8ml of PBS for counting in the Coulter counter. Cell density in 0.5ml PBS was then assessed by the Coulter Counter. Each suspension was counted in triplicate and the average count taken in order to calculate cell concentration of the original suspension solution (by multiplying cell count obtained by 40).

2.5 Induction of Apoptosis

Apoptosis in breast cancer cells was induced using the ceramide C2 analogue. Cells were seeded onto six well plates ($3x10^5$ per well) in complete medium, incubated for 48-72 hours, and the medium changed to SFM for 24 hours prior to treatment. Cells were dosed with ceramide with or without prolactin and incubated for 24 hours before being collected for analysis of apoptosis.

2.5.1 Assessment of Apoptosis by Light Microscopy

Cells ($2.5x10^4$ per well) were plated into 8-well Labtek Chamber slides in 500µl of medium and incubated overnight. After washing with Dulbecco's PBS (phosphate buffered saline) and starving for 24 hours in serum free medium (SFM), cells were exposed to ceramide in the presence or absence of prolactin for 24 hours before they were fixed and stained. For fixation, cells were first washed twice in PBS and air-dried. This was followed by dipping in acetone for 5 minutes. Slides were then air-dried and placed in the freezer for storage until they were stained. Staining was carried out by washing the slide with water, then dipping each slide 4-5 times in haemotoxylin, and rinsing with water before dipping 4-5 times in eosin. Slides were then dipped in 70% ethanol followed by 100% ethanol to fix the stains and then air-dried. Coverslips were fixed onto the slides with glue and allowed to dry before viewing under the light microscope. In order to assess the apoptotic index, a total of at least 1000 cells were counted, in at least three separate fields per well. Cells that exhibited nuclear shrinkage, chromatin condensation and also fragmented nuclei were all counted as apoptotic.

2.5.2 Assessment of Apoptosis using FACS Flow Analysis

After induction of apoptosis, cells (seeded in 6-well plates as previously stated) were collected as follows: the supernatant was aspirated and centrifuged (2000 rpm, 5 minutes) to collect floating cells. Attached cells were then washed with 0.5ml PBS, which was collected and centrifuged to collect unattached cells. 200µl of trypsin-EDTA was then added to each well and incubated at 37°C for 5 minutes. A further 800µl of complete

medium was then added to the well, and cells transferred to a 1.5ml Eppendorf tube. These cells were centrifuged at 2000 rpm for 5 minutes and the supernatant discarded.

2.5.2.1 Analysis of cell cycle profile by flow cytometry

This experiment relies on the ability of propidium iodide to bind DNA. The amount of propidium iodide bound is proportional to the amount of DNA, thus providing a measure of the quantity of DNA present in each cell.

For analysis of cell cycle profiles, the pelleted cells were fixed in 70% ethanol for at least 24 hours prior to analysis by flow cytometry. The fixed cells were re-pelleted (2000 rpm, 5 min) and washed with PBS. The washed cells were then resuspended in Krishnan's reagent (p.220) and incubated at 4°C in the dark for at least 30 min prior to analysis on a FACSCalibur flow cytometer (Becton Dickinson) (See Fig. 2.1).

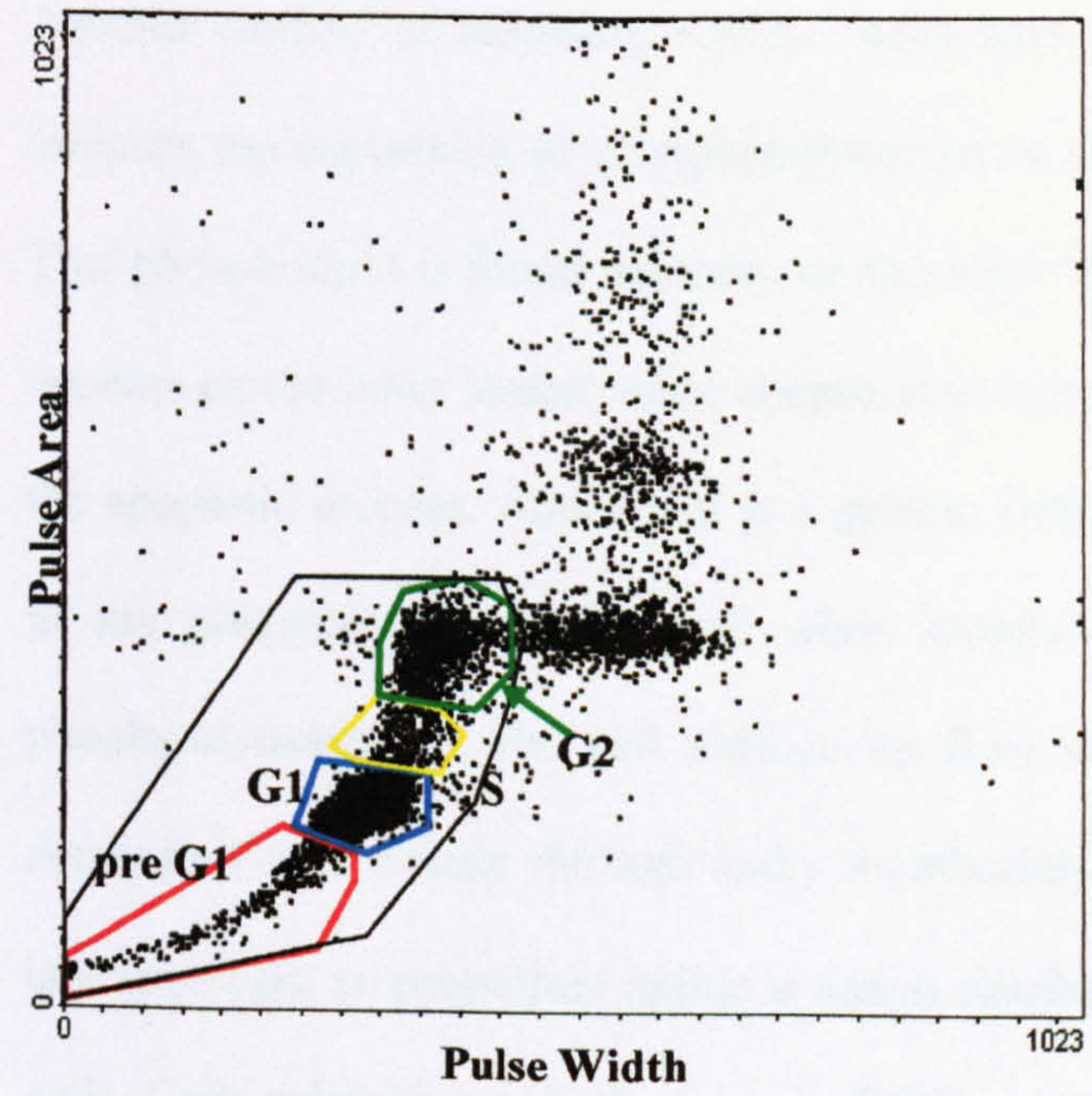

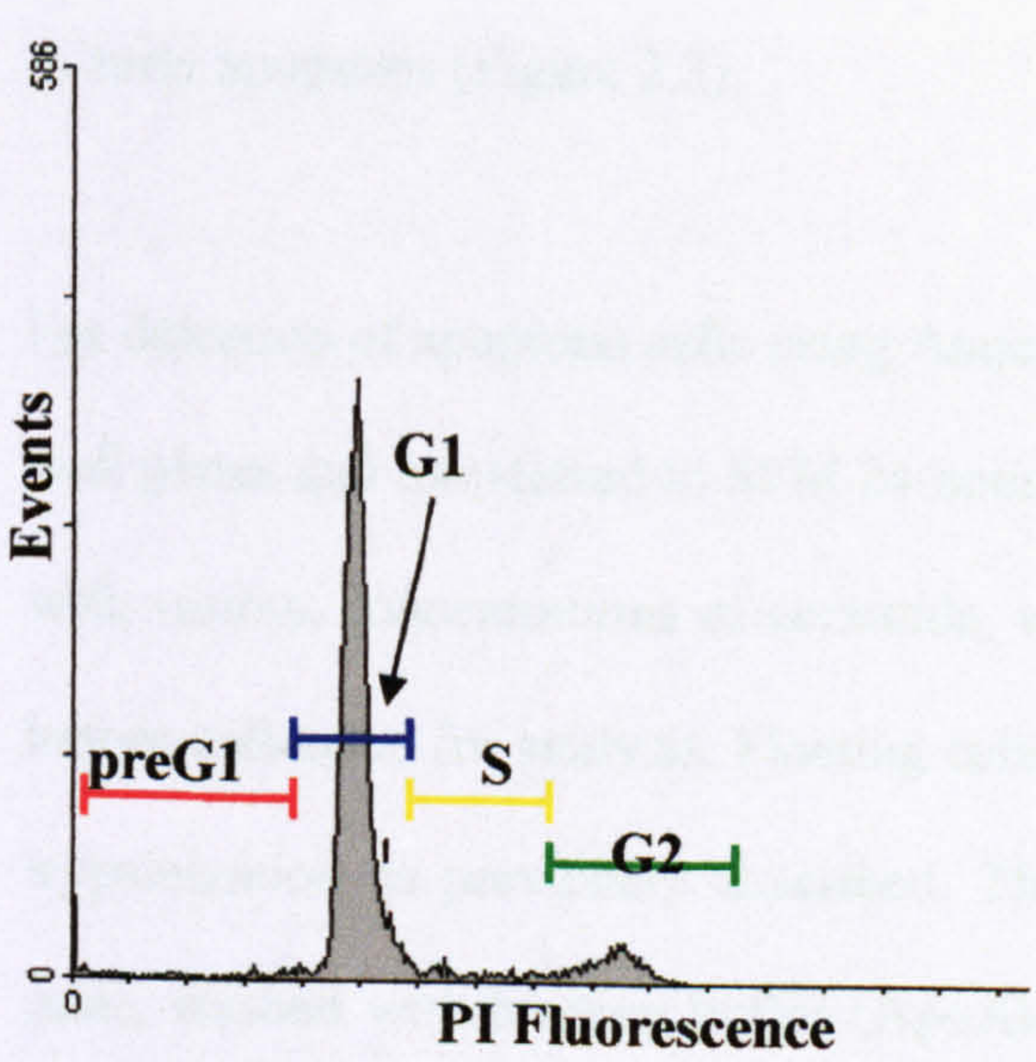

Figure 2.1 Diagrams showing a typical dot plot (top) and histogram (bottom) obtained during FACS analysis of the cell cycle profile.

Cells in G1 contain the normal quantity of DNA, while cells in G2, representing cells that have completed DNA replication, possess double this amount. Cells in S phase represent cells that are in the midst of replicating their DNA, in the synthesis phase, while cells in preG1 contain less than the normal quantity of DNA and are thought to represent cells undergoing apoptosis.

2.5.2.2 Analysis of apoptotic index using Annexin-V

Another method of assessing whether cells have initiated the apoptotic pathway is to measure the expression of phosphotidylserine on the outer leaflet of the cell membrane. This phospholipid is found naturally on the inner leaflets of all cell membranes, but only appears on the outer leaflet when apoptosis is induced. This change occurs quite early in the apoptotic process. Annexin-V is a protein with a high affinity for phosphatidylserine in the presence of calcium, and when coupled to FITC, enables the detection of phophatidylserine on the cell surface by flow cytometry or fluorescent microscopy. Annexin-V can diffuse through leaky membranes in necrotic cells or cells undergoing late apoptosis, so propidium iodide is added simultaneously to identify the latter group of cells. Cells exhibiting only the annexin-FITC complex on their surface are assumed to be in early apoptosis (Figure 2.2).

For detection of apoptotic cells using Annexin-V, cells ($3x10^5$ per well) were seeded in 6-well plates and transferred to SFM 24 hours prior to treatment. Cells were then incubated with various concentrations of ceramide, with or without prolactin at 37°C for 24 hours before collection for analysis. Floating cells were collected and added to cells obtained by trypsinization as previously described. The combined cells were pelleted (2000rpm, 5 min), washed with binding buffer (ApoAlert® Annexin-V-FITC kit, p.225), and stained with Annexin-V and propidium iodide as described in the manufacturer's manual. The labeled cells were taken up in the buffer provided to a final volume of 0.5ml. $1x10^4$ cells were counted and the proportion of apoptotic, necrotic and live cells determined according to the pattern of fluorescence detected (See Fig. 2.2)

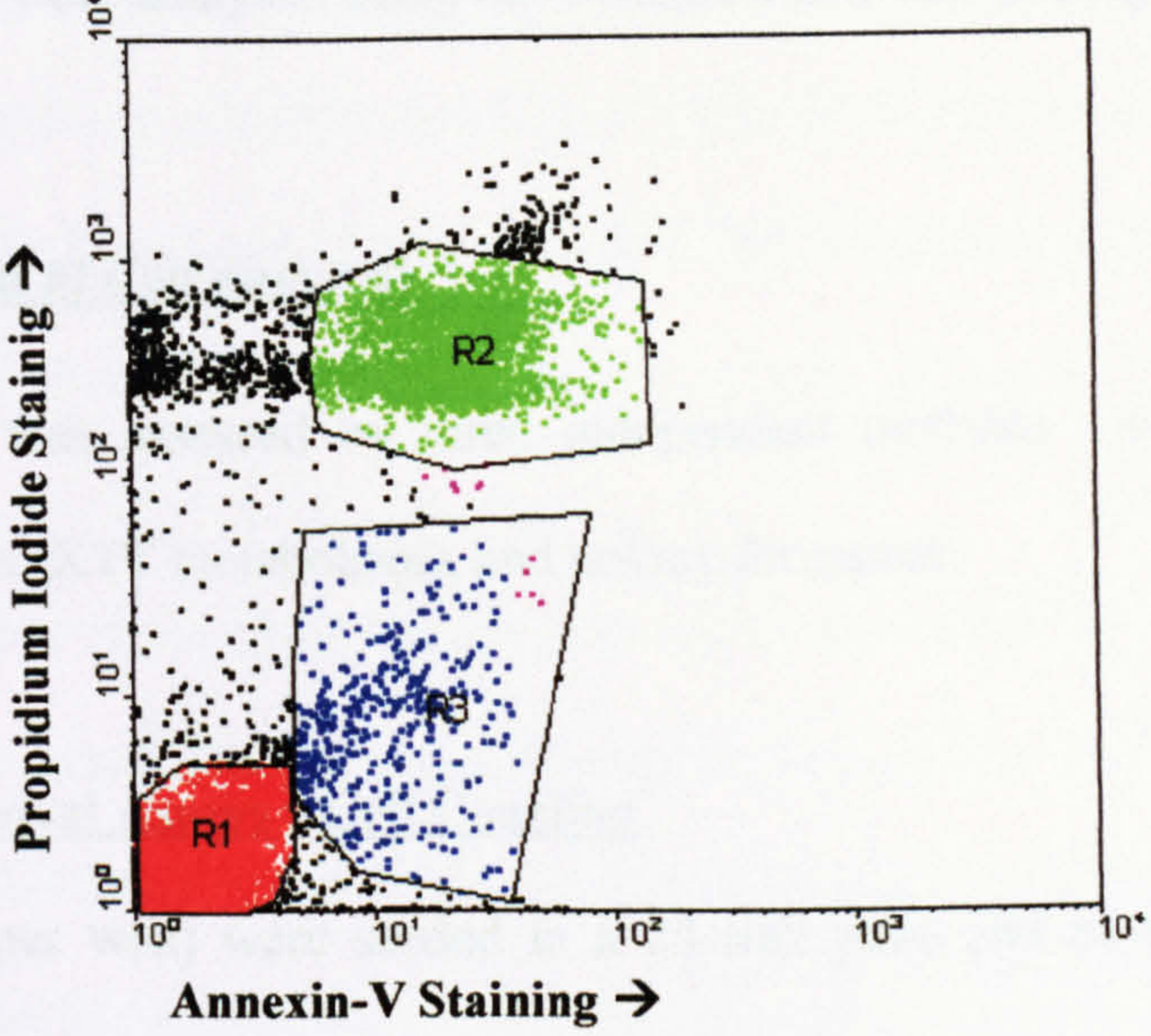

Figure 2.2 Figure to demonstrating the various populations that appear following Annexin-V and propidium iodide staining.

R1 is the population of live cells that excluded both stains. R2 is the cell population that exhibits dual staining, and is consistent with cells in necrosis or late apoptosis. Region R3 represents cells with Annexin-V staining alone, consistent with early apoptosis.

All FACS data were analysed using the CellQuest software package (p.221).

2.6 Assessment of Cell Survival

Cell survival was assessed by three independent methods - cell number, metabolic activity of cells (XTT metabolism), and colony formation.

2.6.1 Cell Survival Assays – Cell Counting

Cells ($5x10^4$ per well) were seeded in a 24-well plate and incubated overnight. After being washed twice with Dulbecco's PBS the cells were starved in SFM for 24 hours. Cells were pretreated with or without prolactin for 30 minutes prior to exposure to ceramide in SFM and incubated for the time specified, after which fetal calf serum was added to a final concentration of 10% (v/v). Following this, cells were incubated for another 4-5 days before being trypsinised and counted using a Coulter counter (Sect 2.4).

2.6.2 Cell Survival Assay – Cell Proliferation Kit II (XTT)

The Cell Proliferation Kit II (XTT) (p.225) was used to ascertain the viability of cells after treatment with ceramide. XTT (sodium 3'-[1-(phenylaminocarbonyl)-3,4-tetrazolium]-bis (4-methoxy-6-nitro) benzene sulfonic acid hydrate) is a yellow tetrazolium salt. It is cleaved into a soluble orange formazan dye by mitochondrial dehydrogenases, found only in metabolically active cells, and the optical density is then spectrophotometrically quantified by spectrophometrical absorbance using a scanning multiwell spectrophotometer. The proportion of cleaved XTT is directly proportional to the number of viable cells left in the population.

The components of the kit are a XTT labeling reagent and an electron coupling reagent. Both components are stored in working aliquots at -20°C. To assay one 96-well plate, 5ml of XTT labeling reagent is mixed with 0.1ml electron coupling reagent and aliquots (50µl) added to each well.

Cells ($1x10^5$ per well) were seeded into a 96-well plate, in 100µl of medium, and incubated overnight. They were washed once with Dulbecco's PBS before being starved in 100µl of SFM for 24 hours. Following serum starvation, cells were pre-incubated with prolactin before the addition of ceramide. Cells were exposed to ceramide for 24-48hrs prior to the addition of fetal calf serum to the final concentration of 10% (v/v). (The time of incubation for each of the cell lines was determined by morphological analysis; MCF-7 cells required 24 hours before developing the morphological characteristics of apoptosis, whilst T47-D cells required a further 24 hours before taking on the apoptotic characteristics.) Cells were then incubated for a further 4-5 days before 50µl of XTT labeling mixture was added to each well. Cells were incubated with the labeling mixture for 18hrs before the spectrophometrical absorbance was measured using a microplate reader at 450nm.

2.6.3 Cell Survival Cloning Assay

T47-D cells ($1x10^6$ per well) were seeded into T25 flasks and incubated overnight. The cells were then washed twice with SFM and incubated in SFM for a further 24 hours. After incubation in the presence or absence of prolactin for 30mins, cells were exposed to varying concentrations of ceramide for 24 hours in the continued presence of prolactin

before they were trypsinized and set in agarose gels. Agarose gels were set up by first laying down a base layer of a 0.6% gel consisting of 1 volume of 1.2% solution of a low gelling agarose and 1 volume of 2x DMEM (p.221), total volume 2.5 ml per 60mm petri dish. This was allowed to gel at room temperature before being incubated at 37°C in 5% CO_2 while the top gel layer was prepared. The top layer consisted of a 0.35% gel prepared by mixing 4.5 volumes of 2xDMEM, 4.5 volumes of 0.7% agarose solution and 1 volume of cells. For each plate, approximately 250 cells were plated. Plates were incubated for 10-14 days before being assessed for colony formation. Prior to staining, Neutral red solution (p.221) was diluted 1 in 25 with PBS and 500µl of the final solution was added to the gels and incubated for at least 30 minutes prior to counting colonies consisting of four or more cells under a dissecting microscope.

2.7 Growth Assays

Cells ($5x10^4$ per well) were seeded in 24-well plates in complete medium and left to attach overnight. They were then washed twice with Dulbecco's PBS and transferred to SFM with or without prolactin before being incubated at 37°C in 5% CO_2 for 4-5 days. Cells were then harvested and counted on a Coulter counter as previously described (Sect 2.4).

2.8 Measurement of Cell Proliferation using Thymidine Incorporation

Cells were seeded into 96-well plates in 100µl DMEM supplemented with 1% serum (that had been charcoal stripped, p.216) and incubated overnight. The cells were then exposed to prolactin for 18 hours before the addition of [^{3}H] thymidine (50nCi/ml) for 6

hours. Medium was then discarded and 100µl of trypsin-EDTA added to each well. The cells were incubated at 37°C for 30 minutes before being frozen at –20°C for at least 3 hours before harvesting. Cells were thawed before they were harvested and the radioactivity captured onto filter mats using a cell harvester (TOMTEC Harvester). Next, the filter mat was impregnated with wax enriched with a radio-scintallant and allowed to dry. Radioactivity was then determined in a Wallac MicroBeta Trilux 1450 liquid scintillation and luminescence counter to assess [^{3}H]thymidine incorporation (software – 1450 MicroBeta Windows Workstation, Version 3.2).

2.9 Preparation of plasmid DNA

2.9.1 Miniprep plasmid DNA preparation

Plasmid minipreps were prepared using a QIAprep Miniprep Kit (p.225). The bacteria were lysed under alkaline conditions, neutralized, and the lysate cleared of cell debris and genomic DNA using a filter. The plasmid DNA was then adsorbed onto the QIAprep membrane under high salt conditions, and released from the filter using a low salt buffer.

E. coli bacteria transformed with the desired plasmid DNA were inoculated into antibiotic-treated LB and incubated for 18-20 hours at 37°C with gentle shaking (300rpm). Bacteria were then pelleted by centrifugation at 3000rpm for 15min at 4°C. The pellet was resuspended in 250µl of buffer P1, which contains RNase A, before addition of 250µl buffer P2 (lysis buffer). The solution was then mixed and incubated at room temperature for 5 min before being neutralized with 350µl of buffer P3. The resulting cloudy solution was centrifuged for 10 min at 13,000rpm.

The supernatant was transferred to a QIAprep spin column and centrifuged at 13,000 for 1min. The membrane was washed using buffers PB and PE, which were added to the column and centrifuged at 13,000 for 1 min. The DNA was then eluted into a clean Eppendorf tube using 50μl of EB buffer amd stored at -20°C until required.

2.9.2 Midi- or Maxi-prep plasmid DNA preparation

Plasmid DNA was extracted from *E. coli* cultures using the HiSpeed Plasmid Purification Kit (p.225). Briefly, transformed *E. coli* containing the desired plasmid DNA were inoculated into 150-250 ml of antibiotic-treated LB medium and incubated at 37°C for 12-16 hours with gentle shaking (37°C, 300rpm). The bacterial cultures were collected by centrifugation (3000rpm, 4°C, 30 minutes) and the supernatant removed completely. The bacterial pellet was suspended in buffer P1, and an equal volume of buffer P2 added. The solutions were gently mixed by inversion before being incubated at room temperature for 5 minutes. Chilled buffer P3 was then added to the mixture, mixed by inversion, and then poured into the prepared QIAfilter Cartridge and incubated at room temperature for 10 minutes.

A HiSpeed tip was prepared by the addition of buffer QBT. The bacterial lysate was passed through the QIAfilter cartridge by inserting the plunger and filtered onto the equilibrated HiSpeed tip. After the lysate had passed through the HiSpeed tip by gravity, the tip was washed with buffer QC. The DNA immobilized on the tip was eluted using buffer QF, and precipitated by adding isopropanol and incubating for 5 minutes at room temperature. A QIAprecipitator was attached to the nozzle of a 20ml syringe and the

DNA solution emptied into the barrel. The plunger was inserted and the mixture filtered through the QIAprecipitator. The collected DNA was finally eluted into a clean Eppendorf tube with TE buffer and DNA concentration determined by spectrophotometry.

2.10 Spectrophotometric Determination of DNA concentration

This was performed using the GeneQuant II. The machine was first programmed to measure the concentration of dsDNA, at a dilution factor of 71. The cuvette was filled with 70µl of Elgastat water, which was used as the reference point. 1µl of the plasmid preparation was then added, pipetted gently to mix, and the dsDNA concentration read at 260Å.

2.11 Horizontal Agarose Gel Electrophoresis

Plasmid DNA was isolated by agarose gel electrophoresis. A 1% TAE gel was formed by dissolving SeaKem Agarose (0.5mg) in 1xTAE buffer (50ml) (p.223). Ethidium bromide was incorporated into the gel by the addition of 1µl ethidium bromide solution (10mg/ml) for every 10ml of the agarose gel. The cooled gel mixture was poured into a horizontal electrophoretic gel tank, the comb inserted, and allowed to set at room temperature for 30-60 minutes. Sufficient 1xTAE buffer was used to cover the gel, before DNA samples were loaded. DNA samples for analysis were prepared by the addition of 2.5µl of loading buffer to 10µl of each sample.

Depending on the molecular weight of the DNA plasmid, the markers (either VII or VIII, p.226) were also loaded onto the gel. Samples were electrophoresed at a constant voltage of 50V for 1-2 hours.

DNA separated in this manner was visualized using a UV transilluminator and photographed. Gel blocks of desired DNA products could be cut out at the same time and plasmid DNA purified using the QIAquick™ Gel Extraction Kit (p.225).

2.12 Purification of DNA from Agarose Gels

DNA was extracted from TAE gels using the Gel Extraction Kit. The DNA band of interest was excised from the gel using a sharp, clean scapel. The gel sample was weighed and placed in a 1.5ml Eppendorf tube. 3 volumes of Buffer QG were added for 1 volume of gel (100mg ~ 100µl). The tube was incubated at 50°C for 10min or until the gel dissolved. Following gel dissolution, the colour of the solution has to be compared with that of Buffer QG. If the colour is orange or purple, 3M sodium acetate can be added to alter the pH, as the QIAquick membrane works best at pH≤7.5. Next, 1 gel volume of isopropanol was added to the mixture and mixed. The solution was then applied to the QIAquick spin column, centrifuged at 13,000rpm for 1min and the flow-through discarded. Next 0.5ml Buffer QG was added to the column, centrifuged as before, and the flow-through discarded. The column was then washed with 0.75ml of Buffer PE by centrifugation as before. The QIAquick column was then placed over a clean Eppendorf tube and the DNA eluted into it with 50µl EB by centrifugation. The eluted DNA was then stored at -20°C until required.

2.13 Restriction Enzyme Digests

Restriction enzyme digests of plasmid DNA were performed to analyse DNA products as well as to isolate plasmid DNA of interest for subsequent reactions. A typical digestion would be performed at 37°C for 4-18hrs and would consist of the following components:

x µl of DNA (containing 5-10µg plasmid DNA)

5 µl restriction enzyme A

5 µl restriction enzyme B

5 µl appropriate restriction enzyme 10x buffer

+ y µl nuclease free water (to bring final reaction volume to 50µl).

Analytical digests were performed on a smaller scale and were typically as follows

x µl of DNA (containing 1-2µg plasmid DNA)

1 µl restriction enzyme A

1 µl appropriate restriction enzyme 10x buffer

+ y µl nuclease free water (to bring final reaction volume to 10µl).

2.14 Ligation Reaction

Following enzymatic digests to create free ends, insert DNA can be ligated to linearized vector DNA to form a circular plasmid. 1µl of T4 DNA Ligase (Roche) was added to reaction mixtures that contained 1µl of T4 DNA Ligase 10x buffer, and various ratios of vector to insert DNA. The final reaction volume was 10µl and any shortfall was made up

with nuclease free water. Vector to insert ratios of 1:1, 1:3, and 1:6 were used, and the mass of DNA required for each reaction was calculated as follows:

$$\frac{\text{ng of vector} \times \text{kb size of insert}}{\text{kb size of vector}} \times \text{molar ratio of } \frac{\text{insert}}{\text{vector}} = \text{ng of insert}$$

Ligation reactions were incubated at 14°C overnight, and products of the reaction were separated and isolated by horizontal agarose gel electrophoresis.

2.15 Transformation of competent E. coli with plasmid DNA

Commercially available competent cells were used for the transformation (Top10, p.225). 2µl of the DNA plasmid was incubated with 50µl of competent cells on ice for 30 min. The cells were then shocked in a 42°C water bath for 30s, re-incubated on ice for 1 min before 250µl of LB was added. The cells were incubated at 37°C for 1 hour, then plated onto antibiotic-treated LB agar plates using an ethanol-flamed glass rod, and incubated at 37°C overnight. Plates were examined the next day for colony formation and colonies were picked at random and inoculated into antibiotic-treated LB of various volumes as required for mini-, midi-, or maxi- DNA preparations.

2.15.1 Storage of Transformed E. coli

0.85ml of the clones of transformed *E. coli* incubated in LB(p.220) overnight was added to 0.15ml of sterile glycerol, and the solution pipetted to ensure thorough mixing before storing at –80°C.

2.16 Methods used in the Transfection of Cells

The various cell lines used were transfected with a variety of methods. The T-47D, MCF-7, COS-7, HepG2, SF and Ros cell lines were all transfected using the Fugene6 transfection reagent. Hela cells were transfected using Lipofectamine Plus, and the CEM-C7 cells were transfected by electroporation.

2.16.1 Transfection of Cells using the FuGENE 6 Transfection Reagent (Roche)

The FuGENE 6 reagent is a lipid based transfection reagent that complexes with and transports the DNA into the cell during transfection. Adherent cells are plated one day before transfection, aiming for a confluency of 50-80% on the day of transfection. Depending on the size of the plate to be transfected, varying amounts of DNA and FuGENE 6 reagent were used to transfect the cells according to the manufacturer's protocol.

Transfection reactions were performed according to the manufacturer's protocol. Briefly, FuGENE 6 reagent was equilibrated to room temperature before use. SFM, enough to bring the total volume of the mixture to 100µl per transfection sample, was added to a small sterile Eppendorf tube. Next, FuGENE 6 was added directly into the SFM and the contents mixed by gentle tapping. DNA solution was then added to the prediluted FuGENE 6 reagent and the solution mixed again. The contents were incubated at room temperatre for 15-45 minutes to allow Fugene6 to complex with the DNA.

The transfection mix was added dropwise to each dish and swirled around to ensure thorough mixing. Cells were returned to the incubator for 24-48 hours depending on the assay performed.

2.16.2 Transfection of cells by Lipofectamine Plus

Lipofectamine Plus (p.226) was used to transfect HeLa cells, as this method provided a higher rate of transfection (~80%) compared to other methods. HeLa cells were plated in 6-well plates the day before transfection so that they were ~40-50% confluent on the day of transfection. The transfection mix was constituted in serum free DMEM (SFDMEM, p.222). The DNA was first added to SFDMEM (100µl per well to be transfected), followed by the Plus reagent. This solution was mixed by tapping and then incubated for 15-20 minutes at room temperature. Lipofectamine reagent was then added to SFDMEM (100µl for every well to be transfected), and this was mixed with the pre-incubated DNA-Plus mixture for another 15-30 minutes. The transfection mixture was then added to each well (200µl of mixture per well), and the cells incubated at 37°C, 5% CO_2 until the cells were required.

2.16.3 Transfection of Cells by Electroporation

CEM-C7 cells were prepared for electroporation by washing twice in PBS, before being resuspended to a final concentration of $10x10^6$ cells per ml in PBS. 500µl of the cell suspension was then electroporated with 40µg of DNA plasmid in a 0.4cm cuvette (BioRad), using a BioRad Gene Pulsar II. Cells were electroporated using 1050µF and 300V, the time constant ranged from 11.6-12.7ms. Cells were immediately transferred to

complete medium and allowed to recover for 48 hours before being placed in RPMI-1640 medium containing selection antibiotic (G418) at 800μg/ml. Cells were kept in this medium for 2 weeks before being transferred to maintenance medium (RPMI-1640 with 350μg/ml G418).

2.17 Methods for Clonal Selection

2.17.1 Clonal selection by serial dilution

Clones of CEM-C7, MCF-7 and T47-D cells were obtained by limiting dilution. Parent cultures were harvested by the usual method and diluted to a final concentration of one cell per ml of complete medium. Cells were then seeded in to a 96-well plate at 200μl per well, so that on average there would be one cell every five wells. Cultures were left to grow over two to three weeks at 37°C in 5% CO_2. Colonies detected after this period were transferred to T25 flasks for subsequent analysis.

2.17.2 Clonal selection by colony formation in agarose gels

The CEM-C7, MCF-7 and T-47D cell lines were also cloned by plating in low gelling agarose gels using a method similar to that described in Section 2.5.3. A feeder layer of human fibroblasts ($5x10^4$ cells/dish) was initially seeded onto 60mm dishes and allowed to attach. The base gel consists of a 0.6% agarose gel, and is formed by mixing equal volumes of 2xDMEM (2xRPMI for CEM-C7 cells) (p.221) and a 1.2% agarose gel solution. This mix is allowed to set at room temperature and then incubated with 5%CO_2 at 37°C till required.

Cells to be cloned are collected by trypsinization where necessary, and diluted down to a concentration of 400 cells per ml. The upper 0.3% gel is then formed by mixing 1 volume of cell suspension with 4.5 volumes of 2xDMEM (or 2xRPMI for CEM-C7 cells) and 4.5 volumes of a 0.6% agarose gel solution. This gel was allowed to set at room temperature before the dishes were placed in a humidified chamber and incubated at 37°C in 5%CO_2 for 10-14 days. Colonies that developed were transferred to T25 in medium containing G418 before subsequent analysis.

2.18 Protein Extraction and Western Blotting

Cells were washed twice with PBS and resuspended in SLB supplemented with aprotinin (12.5μg/ml), leupeptin (12.5μg/ml), PMSF (1mM) and pepstatin A(10μg/ml). The cell lysate was kept on ice for 10 minutes, with occasional vortexing to break up the DNA. The lysate was then centrifuged at 13,000rpm for 10 minutes at 4°C to pellet the genomic DNA. 40μl of crude cell extract was added to an equal volume of loading buffer (containing 5% 2-mercaptoethanol) (p.221) and heated to 95°C for 5 minutes before being cooled to room temperature and loaded onto a vertical polyacrylamide gel (4% stacking gel and 8% separation gel) containing SDS (p.222).

Where appropriate, immunoprecipitation was performed on the crude lysate. In this case, 750μl of crude lysate was incubated with primary antibody for 2 hours at 4°C with gentle rocking. Protein-A agarose beads were washed three times in ice cold SLB (p.222) and suspended to a final volume of 100μl, and suspended beads (90μl) added to the mix and incubated for a further 1 hour at 4°C with mixing. The antibody-agarose-A bead

complexes were collected by centrifugation and washed 3 times in SLB (6000 rpm, 1 minute, 4°C) and the supernatant removed. Loading buffer (containing 5% 2-mercaptoethanol) was added to the protein-A agarose-antibody pellet and the mixture heated to 95°C for 5 minutes. The mixture was centrifuged briefly to pellet the agarose beads, and the supernatant loaded onto the acrylamide gel as above.

Electrophoresis was performed at 55V overnight with molecular weight markers (p.226) run alongside samples.

Separated proteins were transferred to a nitrocellulose membrane by using a semidry transfer blotter (BioRad) at 15V for 30 minutes. The nitrocellulose membrane was then incubated in a blocking solution (5% milk in TBS-Tween, p.223) for 60 minutes at room temperature on a shaker. The membrane was washed twice with TBS-Tween before incubation with the primary antibody for at least one hour at room temperature on a shaker. Excess antibody was removed by washing the membrane in TBS-Tween for 30 min at room temperature on a shaker, the buffer being changed every 5 minutes. The membrane was incubated with the secondary antibody for 1 hour and washed again before incubation with the horseradish peroxidase substrate in the ECL (Enhanced Chemiluminescence) Kit (p.225), and then exposed to photographic film for 1-10 mins.

The following antibody combinations were used (primary antibody; secondary antibody): Flag-PrlR: anti-Flag M2 antibody (Sigma, 1:1000 dilution); sheep anti-mouse, HRP-linked (1:10,000 dilution).

STAT5: anti-STAT5, C-17 (Santa Cruz, 1:2000 dilution); goat anti-rabbit, HRP-linked (1:10,000 dilution).

HA-STAT5b: anti-HA – mouse monoclonal (Sigma, 1:3000 dilution); sheep anti-mouse, HRP-linked (1:10,000 dilution).

HA-Het, or Met-HA: rabbit HA-probe (Santa Cruz, 1:1000 dilution); goat anti-rabbit, HRP-linked (1: 10,000 dilution)

2.19 Lactogenic Hormone Response Element (LHRE) Reporter Assay

Reporter gene assays are widely used to determine the transcriptional activity of cells. A reporter assay consists of a reporter gene linked to a promoter that is transfected into the cells. In the LHRE reporter assay, a luciferase gene is linked to 6 tandem copies of the STAT5 response element. The addition of prolactin to responsive cells results in the formation of STAT5 homodimers that bind to the STAT5 response element. This activates transcription of the luciferase gene with resultant expression of the luciferase enzyme. This enzyme catalyzes a reaction involving D-Luciferin and ATP in the presence of oxygen and Mg^{2+} resulting in light emission. Luciferase activity was quantified using a Dynex luminometer.

Cells ($1x10^5$ per well) were seeded into 24-well plates and incubated overnight before being transfected with the LHRE reporter gene together with other plasmids as specified, using the Fugene 6 reagent as previously described. The cells were incubated overnight, and then transferred to SFM for 6 hours before the addition of prolactin. After incubation for a further 18 hours, cells were lysed in 65µl of lysis buffer A (p.221). 20µl of the lysate

was added to 100µl of luciferase assay reagent (p.220) (20 min, room temperature) and luciferase activity assessed immediately using a Dynex luminometer. The amount of light emitted was integrated over 12s (100µl assay buffer injected per sample, time to read 10s).

2.20 ERE-Tk-Luc Reporter Assay

To assess transcriptional activity of the oestrogen receptor, cells were seeded into 48-well plates and incubated overnight. The cells were then transfected with ERE-Tk-Luc and various plasmids using FuGENE 6 and incubated overnight. The cells were then serum starved in SFM for at least 6 hours before the addition of 10^{-8}M oestrogen (final concentration) for 18 hours. The cells were lysed and luciferase activity measured using the Dynex luminometer as above.

2.21 β-Galalactosidase Reporter Assay

The β-galactosidase enzyme is commonly used as a reporter molecule for many assay systems, primarily to assess transfection efficiency of mammalian cells. The β-galactosidase enzyme encoded by the plasmid is constitutively active (under the control of a SV-40 promoter) so that assessing its activity provides a measure of transfection efficiency.

Cells ($3x10^4$ per well) were seeded into a 48-well plate and incubated overnight before being transfected with a plasmid encoding a constitutively active β-galactosidase enzyme (pSV-βgal 60ng). The cells were then incubated overnight and serum starved for a further

24 hours before lysis in 65µl of lysis buffer A (p.221). 30µl of the lysate was added to 170µl of chlorophenol red-β-D-galactopyranoside (CRPG) reagent (p.219) and incubated at 37°C for sufficient time for the colour chage to develop. The colour intensity was then measured at 570nm using the RLX β-microplate reader (Dynex Technologies).

2.22 Cellular localisation Studies

Cells were grown on 22x22mm cover slips to ~50% confluency before transfection with various plasmids (as indicated in each experiment) and incubated for 24-48 hours to allow for protein expression. The cells were then washed with PBS (pH 7.4) and fixed in 2% PFA in PBS (p.218) for 20min at room temperature. The cells were then washed with PBS before permeabilization with 0.1% Triton X/PBS for 5 mins before being washed again in PBS. Non-specific protein binding was blocked by treating cells with 1% (w/v) BSA/PBS for 20mins before incubation overnight with primary antibody at 4°C (see experiments for antibody and dilutions). The cells were next washed 3 times with 1%BSA/PBS before incubation with secondary antibody for 1-1.5 hrs at room temperature in the dark. Following this, coverslips were washed three times in PBS before they were mounted onto glass slides (BDH) using DAKO fluorescent mounting medium. Slides were stored in the dark at 4°C until confocal microscopy.

2.22.1 Confocal microscopy

Confocal images were obtained using a Leica TCS SP scanning laser microscope equipped with a Kr/Ar laser using a 63x oil immersion objective. EYFP was detected using a filter set with excitation filter of 510nm and an emission filter of 530nm. Cy3 was

visualized with a filter set with an excitation filter of 568nm and an emission filter of 590nm. All images were processed with Leica software for 2D analysis.

2.23 Genomic DNA Extraction

High molecular weight DNA was extracted from cultured cells using the following method.

A maximum of $5x10^6$ cells were collected and washed with PBS. Cells were centrifuged at 1000 rpm for 5 min and the supernatant discarded. 700µl of Lysis Buffer B was added, and the cell pellet re-suspended. 35 µl of proteinase K (10mg/ml) was added to the cell suspension and the mixture placed in a heating block set at 55°C for a minimum of 4 hrs. Next, an equal volume (~750 µl) of phenol was added to the mixture, mixed thoroughly by inversion, and then centrifuged at 13,000rpm for 15 min. The aqueous phase was removed carefully and an equal amount of phenol / chloroform / indoleacetic acid added and the mixture centrifuged for 15 min at 13,000 rpm. Next, 70 µl of 3M NaAc (pH 5.2) and 3 volumes of absolute ethanol (at room temperature) was added to the extracted aqueous phase. The mixture was again centrifuged at 13,000 rpm for 15 min at 4°C. The pellet obtained was washed in 70% ethanol and re-centrifuged. Finally, the pellet was re-suspended in 100-500µl of TE to dissolve the DNA.

2.24 RNA Extraction

RNA extraction from cultured cells was performed using the RNeasy Mini Kit (p.225) according to the manufacturer's instructions. The cells are first collected by gentle

trypsinization using 0.25% trypsin EDTA. Approximately $7x10^6$ cells were then lysed in 600µl buffer RLT (containing 10µl of 2-mercaptoethanol per ml of RLT) and the sample homogenized using a 21 gauge needle and 1ml syringe. 600µl of 70% ethanol was then added to the homogenized sample and mixed thoroughly by inversion. The lysate was then added to the mini-column which was centrifuged at 13,000rpm for 15s. The remainder of the lysate was added to the column, which was centrifuged as before.

Next, 700µl of buffer RW1 was added to the column, which was centrifuged as before and subjected to two washes using buffer RPE. Finally, RNA was eluted with two 50µ aliquots of nuclease-free water. The extracted RNA was then either used immediately or stored at -80°C until required.

2.25 Poly(A^+) RNA Isolation

mRNA was isolated using the PolyATract Isolation System IV (p.225), which utilizes biotinylated oligodT bound to streptavidin-linked magnetic beads as a means of separating mRNA from total RNA. The mRNA was extracted according to manufacturer's protocol as follows.

The volume of total RNA was brought up to 500µl using nuclease-free water, and heated at 65°C for 10 minutes. Following this, 3µl of biotinylated oligodTs and 13µl of 20xSSC (sodium chloride, sodium citrate buffer, as supplied) buffer was added to the RNA solution, which was allowed to cool to room temperature.

Magnetic beads were resuspended in the storage buffer and then collected by using the paramagnetic stand (Promega). The storage buffer was carefully removed and the beads washed 3 times using 300µl 0.5xSSC per wash, each time collecting the beads on the magnetic stand. After the final wash, the beads were re-suspended in 100µl of 0.5xSSC buffer.

The entire RNA solution was then added to the magnetic bead suspension and mixed by inversion. The mix was incubated at room temperature for 10 min, inverting the tube to mix the contents at regular intervals. The beads were then washed 4 times using 300µl of 0.1xSSC buffer. Following the final wash, the beads were resuspended in 100µl of nuclease-free water. The beads were mixed, then collected on the magnetic stand, and the supernatant fraction containing mRNA removed and collected in an RNase free tube. The beads were resuspended in another 100µl of nuclease-free water and additional mRNA collected. The mRNA was then aliquoted and stored at -80°C.

2.26 Polymerase Chain Reaction

The PCR amplification cycle consists of a number of steps: denaturation at 95°C, which causes the intertwined DNA strands to separate, annealing at 55°C, to allow the primers to anneal to the template of interest, and finally the extension phase, usually at 72°C (optimal temperature for *Taq* polymerase function) where Taq synthesises the complementary strand of DNA template. The recommended times for denaturation are between 15s-2min, annealing for 30-60s and extension times are usually 1-2 minutes.

After completion of the amplification cycles, the DNA synthesized can be analysed or used as required.

The following is a typical reaction mix for PCR:

	Vol	Final concentration
10x Buffer	5µl	1x
$MgCl_2$ (50mM)	2.5 µl	1.5mM
dnTP mix (20mM)	0.5 µl	0.2mM each
Primer 1 (50pmoles)	1 µl	1µM
Primer 2 (50pmoles)	1 µl	1µM
Taq pol	0.2 µl	0.025u/µl
Template DNA	x µl	
dH_2O	to bring total reaction volume to 50µl	

Depending on the number of samples to be processed, a master mix is made and the sample DNA added to each reaction mix. The final DNA concentration in the mix should not exceed 10ng/ml. Reactions were carried in thin-walled 0.5ml tubes. For each PCR reaction performed. The conditions were optimized for each primer pair, so amounts and concentrations of each component added may vary from the standard protocol (indicated with each specific experiment performed). All components of the PCR reaction were obtained from Gibco-BRL, except for the primers (Invitrogen).

When using RNA (or mRNA) as a substrate, a combined reverse transcription-PCR (RT-PCR) assay was performed using the Access RT-PCR kit from Promega.

A typical reaction mix consists of the following:

	Volume	Final concentration
Nuclease-free water (to final volume of 50μ)	Xμl	
AMV/*Tfl* 5x reaction buffer	10μl	1x
dNTP mix (10mM each dNTP)	1μl	0.2mM
5'primer	50pmol	1μM
3'primer	50pmol	1μM
25mM $MgSO_4$	2μl	1mM
AMV reverse transcriptase (5u/μl)	1μl	0.1u/μl
Tfl DNA Polymerase (5u/μl)	1μl	0.1u/μl
RNA template	Yμl	

The RT-PCR reaction is started by the addition of the RNA template. All components were added into thin-walled 0.5ml reaction tubes on ice. The tubes were then placed in a TECHNE thermocycler and the RT-PCR programme initiated.

All RT-PCR reactions were optimized by using $[Mg^{2+}]$ between 1mM and 3mM for each primer/template reaction. In addition, several reactions were performed at various annealing temperatures in order to identify the best annealing temperature for each primer pair.

2.27 [^{3}H] Uridine Incorporation as a measure of RNA transcription

2.27.1 [^{3}H] Uridine incorporation to assess total RNA synthesis

To measure uridine incorporation into total RNA, cells were plated in 96 well plates and incubated overnight. They were then transfected with the plasmid of interest and incubated for 48 hrs. Following this, tritiated uridine (1μCi) was added to the wells for 1hr before cells were lysed and the radioactivity transferred to Filter Mat A (Wallac) as follows. The medium was discarded and 100μl of trypsin-EDTA added to each well. The cells were incubated at 37°C for 30 minutes before being frozen at –20°C for at least 3 hours before harvesting as previously described for thymidine incorporation. To measure [^{3}H]uridine incorporation into poly(A^+) RNA, cells were plated into 60mm dishes and incubated overnight. They were transfected on the following day with the plasmid of interest and incubated for 48 hrs. [^{3}H]uridine (20 μCi) was then added to each dish, and incubated at 37°C, 5%CO_2 for 1 hr. Next, the cells were collected by trypsinization, and RNA extracted in the manner described previously. From the resulting RNA solutions, an aliquot was removed, to provide a measure of the total radioactivity of the RNA solution. The remaining solution was then subjected to mRNA extraction as described previously. Each mRNA sample was then placed into 6ml polyethylene vials (Packard Biosciences) and 3mls of scintillant (Optiphase 'HISAFE' 3 liquid Scintillation Cocktail, Perkin Elmer, p.218) added to each sample before the radioactivity was measured in the 1400 DSA Liquid Scintillation Counter (Wallac). Analysis was performed using 1400 DSA version 2.5 (software, Wallac).

3 Does Prolactin Protect Breast Cancer Cells against Apoptosis?

Early studies designed to block the release of pituitary prolactin failed to show a convincing therapeutic effect in the treatment of human breast cancer[205,206] although recent studies have returned to the possibility that prolactin may play a role in breast cancer[207,208]. Prolactin does have an established role in murine mammary tumourigenesis[209,210], however. In humans, we know that not only are breast cancer cells able to synthesize their own prolactin[211-213] but breast cancer tissue has been shown to have higher levels of prolactin receptors compared to normal breast tissue[214]. Moreover, the prolactin receptor can be activated by other lactogenic hormones, such as growth hormone (GH)[215] which may account in part for the lack of efficacy reported for agents such as bromocriptine. Thus it appears that the time has come for a re-evaluation of the role of prolactin in breast tuomourigenesis[216-218]. Many cancer therapies rely on the induction of apoptosis and cell death to bring about a reduction in tumour bulk. Evidence suggesting that use of a prolactin antagonist could inhibit growth of breast cancer cells by inducing apoptosis[219] prompted us to investigate this effect in greater detail. Two cell lines were used to investigate the possible effects of prolactin on survival from apoptosis. The MCF-7 and T47-D immortalized cell lines were derived from patients with disseminated breast cancer. It is known that T47-D cells express a high level of prolactin receptors, while MCF-7 cells express fewer receptors on the cell surface[220,221].

3.1 RESULTS

3.1.1 Induction of Apoptosis using Ceramide

In order to provide a system for identifying the anti-apoptotic effects of prolactin (Prl), initial studies were designed to assess the induction of apoptosis in T47-D cells by the C2

ceramide analogue, N-acetyl-$_D$-sphingosine (C2), which had been shown previously to induce apoptosis in breast cancer cells[222,223].

3.1.1.1 Quantification of Apoptosis by Light Microscopy

First, we used morphological analysis by light microscopy to assess the induction of apoptosis. T47-D cells ($25x10^4$ per well) were seeded into 8-well Labtek chamber slides in complete medium and incubated overnight before being transferred to serum free medium for 24 hours prior to treatment with ceramide. Ceramide was added at the concentrations shown, and cells were incubated for a further 24 hours. The medium was aspirated and slides washed with phosphate-buffered saline (PBS) before cells were fixed with 100% acetone. The slide was stained with haemotoxylin and eosin (H&E) and a cover slip mounted to aid viewing under the microscope. The extent of apoptosis was assessed by counting 1000 cells in three separate fields in the same well, at the same time determining the proportion of apoptotic cells. Fig. 3.1 shows a dose response of the effect of ceramide on T47-D cells. From this graph, it can be seen that apoptosis rises from ~5% in untreated cells to ~13% in T47-D cells treated with 30μM ceramide. The rate of apoptosis appeared to plateau after 20μM and this concentration was used for most studies. Over the course of these studies, the effectiveness of ceramide varied somewhat so that for some experiments it proved necessary to use higher concentrations.

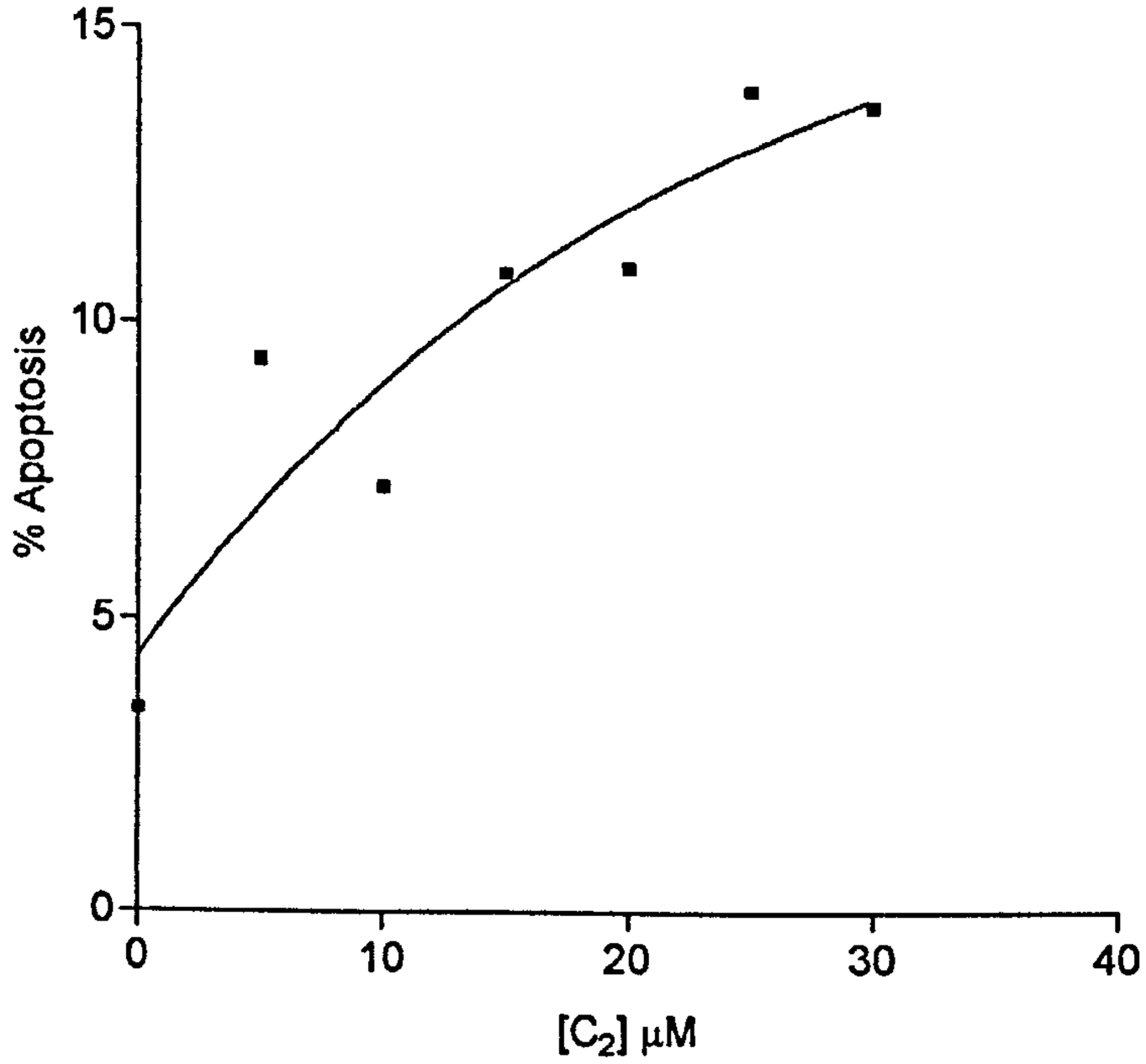

Figure 3.1 Morphological assessment of apoptosis in T47-D cells exposed to ceramide.

Cells in 8-well Labtek chamber slides were incubated with ceramide in serum free medium for 24 hours before being fixed with acetone and stained with H&E for assessment under the light microscope.

T47-D cells were then treated with a single dose of ceramide (20μM) in the presence or absence of prolactin (200ng/ml) after being starved for 24 hours in serum-free medium. Following the addition of ceramide, cells were incubated for a further 24 hours before the slides were washed, fixed and stained for assessment by light microscopy. As seen in Fig. 3.2, there is a clear increase in the number of apoptotic cells to 13%±5 (SD) in cells treated with ceramide, which decreases to 4%±2 (SD) ($p<0.05$) in the presence of prolactin. The results shown are the mean of three experiments.

Although these experiments seemed to demonstrate a clear protective effect of prolactin, there were several inherent difficulties in assessing apoptosis by this method. In particular, reproducibility proved extremely difficult to achieve and it could be argued that assessment by this method is subjective. Therefore we decided to investigate the use of other methods for assessing apoptosis.

3.1.1.2 Quantification of Apoptosis by Analysis of the Cell Cycle Profile

The cell cycle profile of a given cell population allows the observer to assess how various treatments are able to affect population dynamics, as well as allowing the identification of 'pre-G1' cells that are undergoing apoptosis.

As an initial experiment, a dose response to ceramide was performed in T47-D cells (Fig.3.3a), which were then subjected to cell cycle analysis. Surprisingly, there did not appear to be any significant increase in the pre-G1 population after ceramide treatment (1.6% in controls and 2.2% in cells treated with 70μM ceramide).

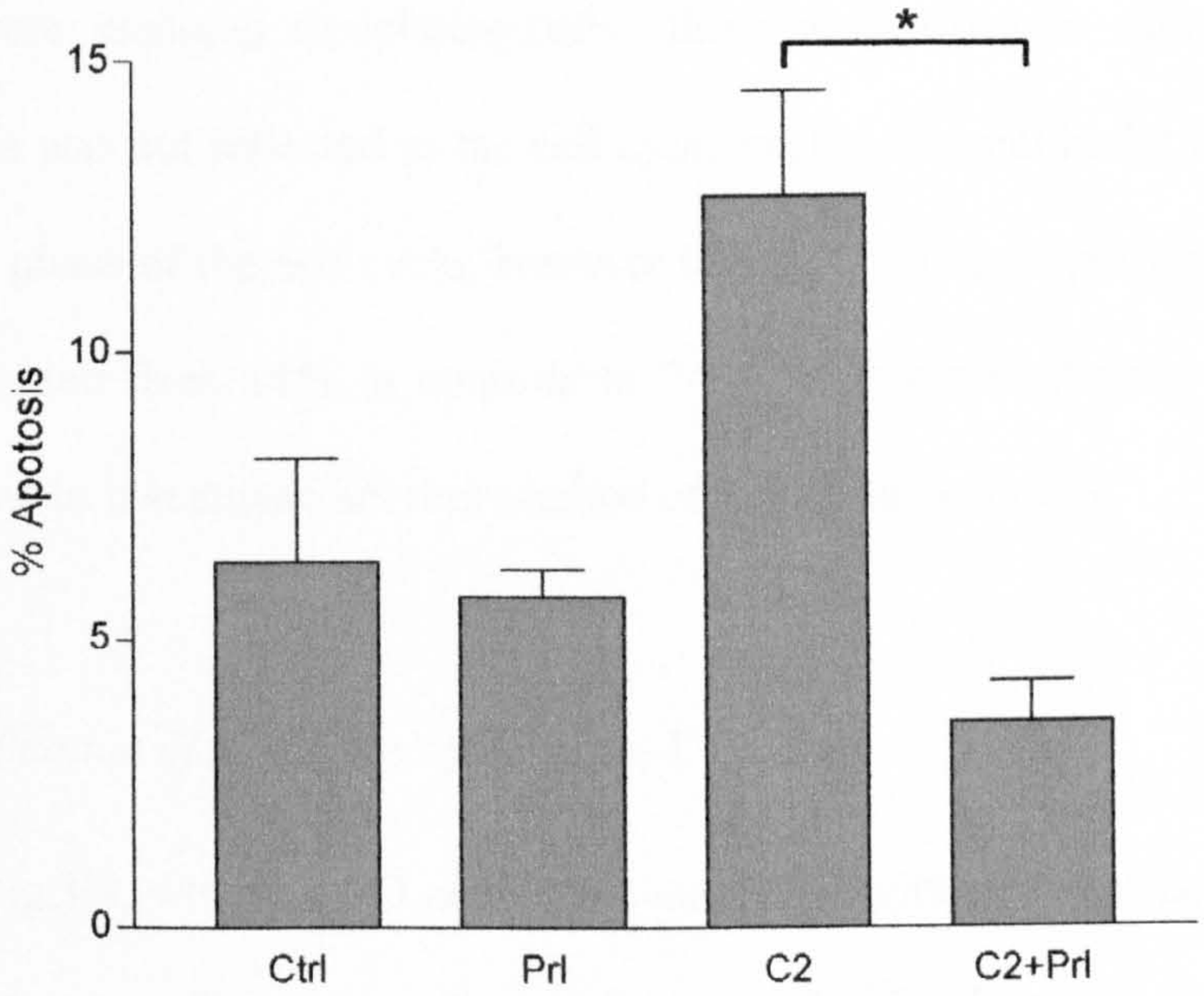

Figure 3.2 Morphological assessment of apoptosis in T47-D cells exposed to ceramide in the presence of prolactin.

*T47-D cells were treated with 20μM ceramide in the absence or presence of prolactin (200ng/ml). Cells were incubated with ceramide for 24 hours before being fixed and stained. The figure is the mean of 3 separate experiments (error bars indicate standard deviation, *=p<0.05) each performed in triplicate.*

From this experiment, it would appear that DNA degradation is minimal in these cells. When cells were assessed morphologically, there were obvious signs of apoptosis present, but this was not reflected in the cell cycle profile. Ceramide did appear to arrest cells in the G2 phase of the cell cycle, however (Fig.3.3b). The proportion of cells in the G2 phase increased from 14% in controls to 24% following treatment with ceramide. Thus we decided to investigate another method of assessing apoptosis.

3.1.1.3 Quantification of Apoptosis by Annexin-V Binding

As shown in Fig.3.4, when T47-D cells were incubated with different concentrations of ceramide for 24 hours, there was a clear decrease in the fraction of live cells (80.6% to 51.2%) and a corresponding increase in the number of necrotic cells (5.5% to 23.3%). The fraction of apoptotic cells, however, showed minimal change (1.3% to 2.7%).

On the basis of this experiment, we were interested to assess whether prolactin would reverse the increase in the 'necrotic'cell population following ceramide treatment after pre-incubation with 250ng/ml prolactin. Therefore, T47-D cells were treated without or with 50μM ceramide for 48 hours before cells were analysed for Annexin-V staining (Fig.3.5).

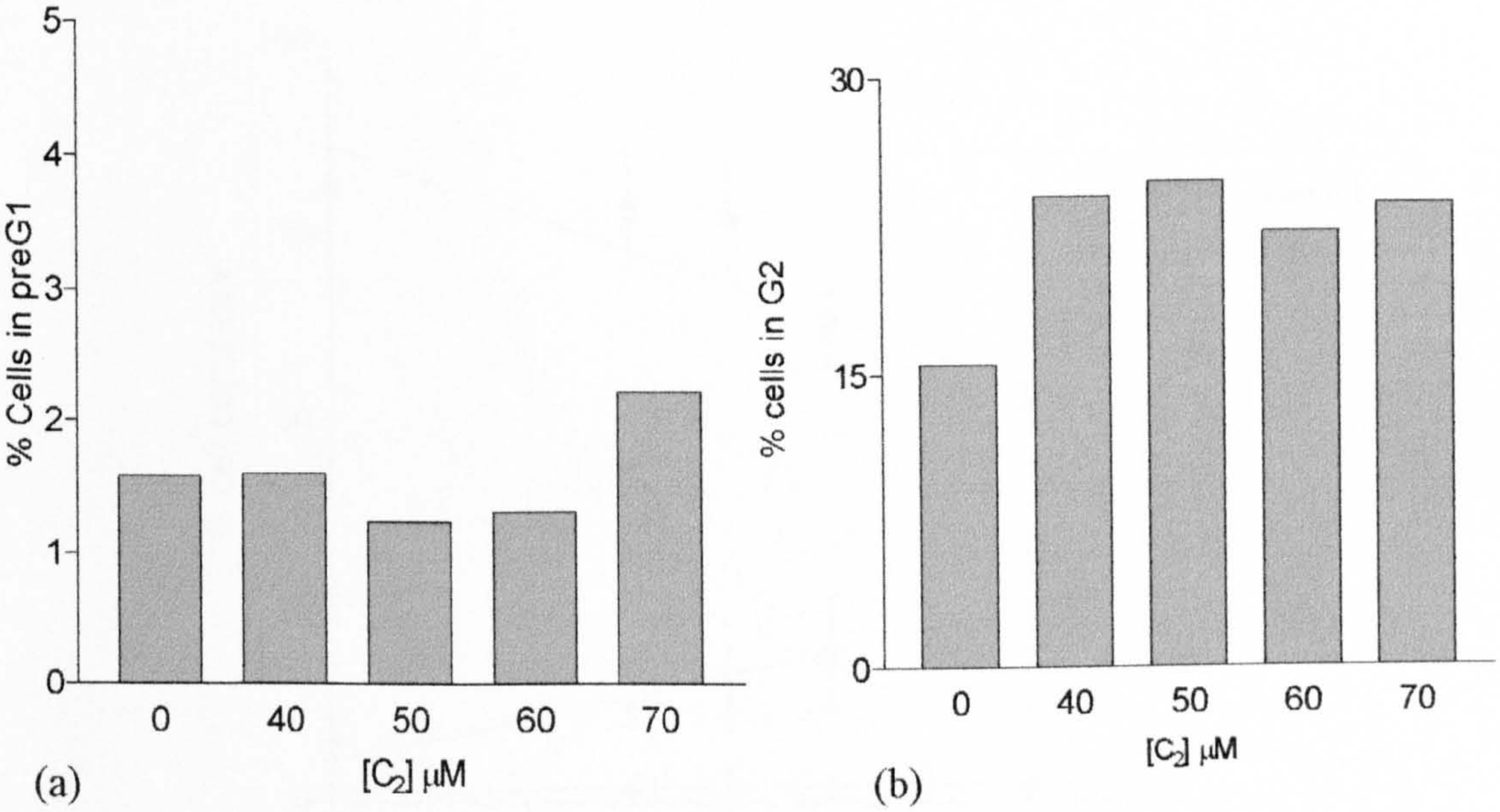

Figure 3.3 PreG1 (a) and G2 (b) populations of T47-D cells after exposure to ceramide as assessed by Cell Cycle Profile analysis.

Cells were serum starved for 24 hours before treatment with ceramide. Cells were then incubated for a further 24 hours before they were collected by trypsinization, washed and fixed with 70% ethanol, and stained with propidium iodide for analysis of the cell cycle profile on the flow cytometer.

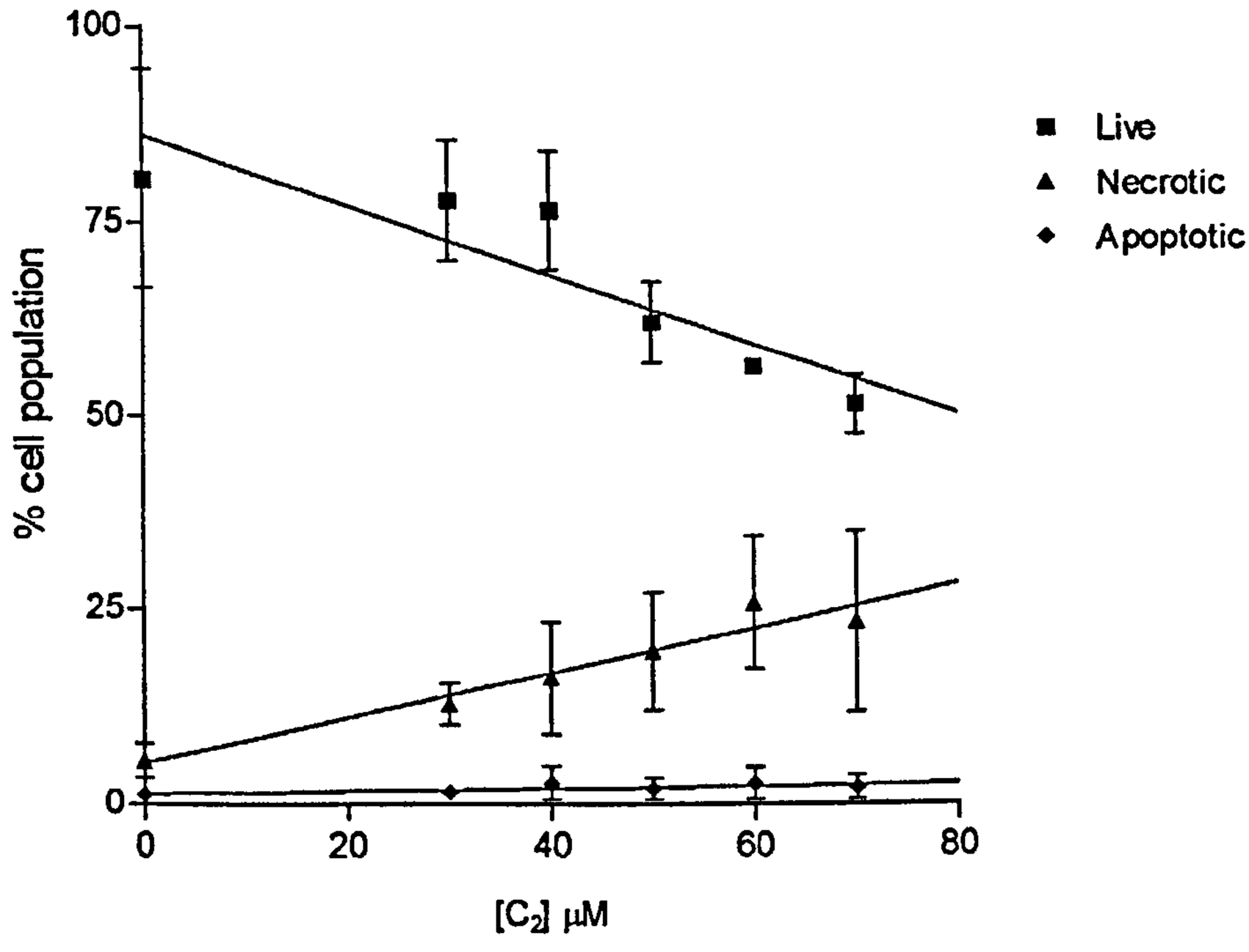

Figure 3.4 Annexin-V staining to assess apoptosis in T47-D cells exposed to ceramide.

T47-D cells were deprived of serum for 24 hours before exposure to ceramide. The cells were collected and stained with Annexin-V and propidium iodide to identify live, necrotic and apoptotic populations.

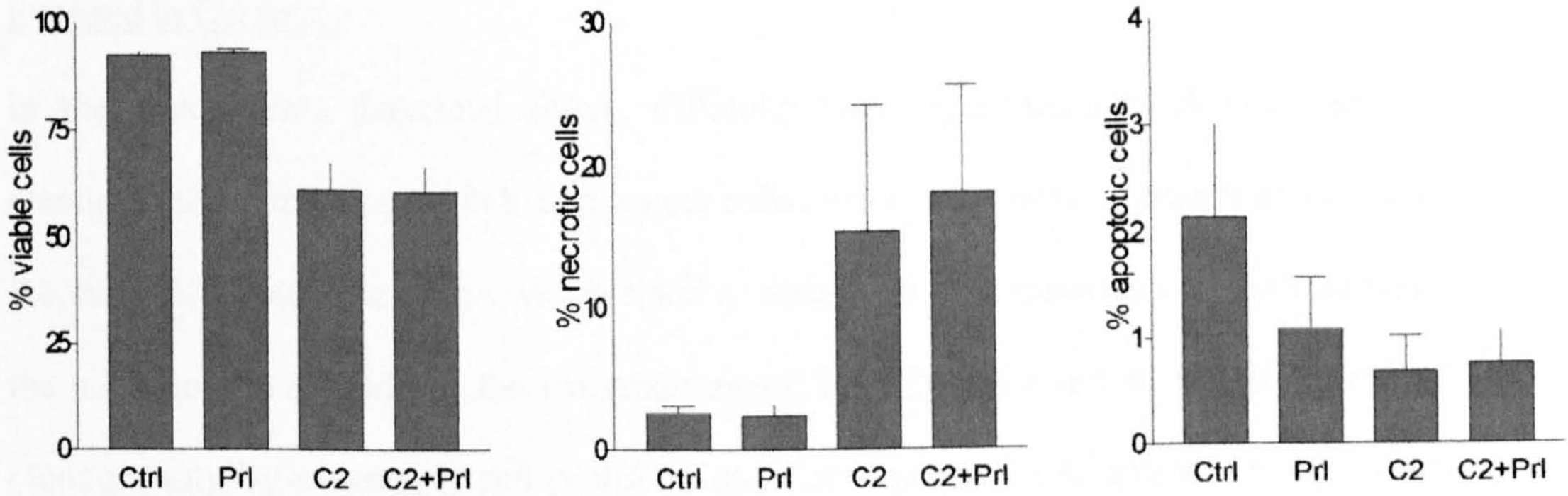

Figure 3.5 Use of annexin staining to assess possible protective effect of prolactin on ceramide-induced cytotoxicity in T47-D cells.

Cells were treated with serum free medium alone (Ctrl), 200ng/ml prolactin (Prl), 50μM ceramide (C2), and 50μM ceramide with 200ng/ml prolactin (C2+Prl) and incubated for 48 hours. They were then collected by trypsinization, washed and stained with Annexin-V and propidium iodide for analysisof the extent of apoptosis by flow cytometry. The results shown represent the mean of 3 experiments (error bars indicate standard deviations).

3.1.2 Ability of Prolactin to Preserve the Proliferative Capacity of Breast Cancer Cells Exposed to Ceramide

In the experiments described above, difficulty was experienced in demonstrating a classical apoptotic response in breast cancer cells. As an alternative approach to assessing the survival effect of prolactin, we decided to assess the clonogenicity of cells following the addition of ceramide as the cytotoxic agent. Initially, we used an indirect assay of clonogenicity by measuring cell proliferation after exposure to ceramide. Owing to the change in approach, we decided to include MCF-7 cells in the investigation as a separate control population, as they have prolactin receptors, but fewer than T47-D cells(~8000 sites and ~26,000 sites per cell respectively)[220].

3.1.2.1 Quantification of Cell Survival using a Growth Assay

For this study, cells were seeded into 24-well plates and left overnight to attach. They were then placed in serum-free medium for 24 hours before the addition of ceramide (40μM ceramide to MCF-7 cells and 50μM ceramide to T47-D cells) in the presence or absence of prolactin (200ng/ml). The cells were incubated further (MCF-7 cells for 24 hours and T47-D cells for 48 hours) before fetal calf serum (10% v/v) was added to the wells. The cells were then allowed to proliferate for 4-5 days before being collected by gentle trypsinization for counting on the Coulter counter.

In MCF-7 cells (Fig.3.6a), the cell count fell from $45\pm16x10^4$(SD) to $16\pm11x10^4$(SD) after treatment with ceramide. After treatment with both prolactin and ceramide, there

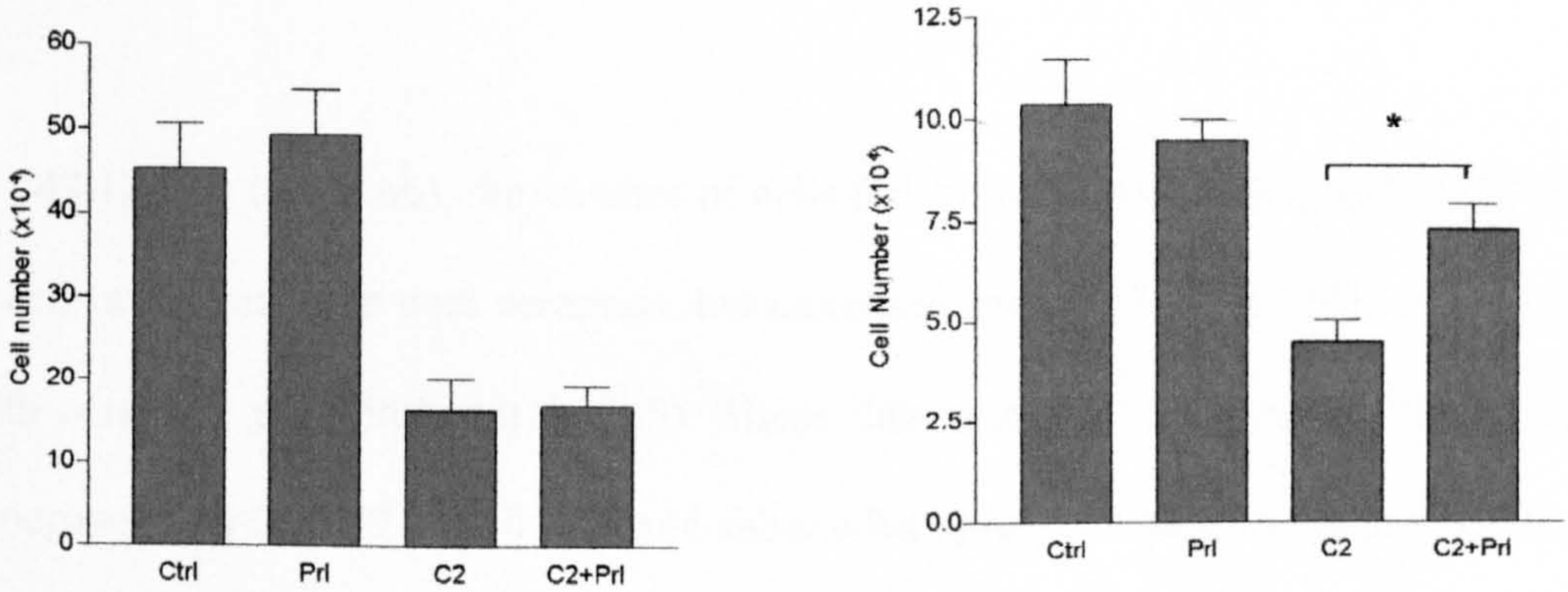

Figure 3.6 Use of cell counting to assess the effect of prolactin on survival of (a) MCF-7 and (b) T47-D cells.

*MCF-7 and T47-D cells were treated in serum free medium alone (Ctrl), with 200ng/ml prolactin (Prl), 40μM ceramide in MCF-7 cells and 50μM ceramide in T47-D cells (C2), or both ceramide and prolactin (C2+Prl). MCF-7 cells were incubated for 24 hours and T47-D cells for 48 hours before 10% (v/v) fetal calf serum was added. The cells were then incubated for a further 5 days before they were collected by trypsinization and counted using a Coulter Counter. Figures represent the mean of three independent experiments (error bars indicate standard deviations, *:$p<0.5$).*

was no significant protective effect of prolactin, the cell count being $17\pm7x10^4$(SD). These data represent the mean of three separate experiments in the MCF-7 cell line.

In T47-D cells (Fig.3.6b), the number of cells fell from $10\pm4x10^4$(SD) to $5\pm2x10^4$(SDM) in cells after treatment with ceramide, but increased again to $7\pm2x10^4$(SD) after treatment with ceramide plus prolactin ($p<0.5$). These data represent the mean of three separate experiments in the T47-D cell line, and show what appears to be a strong protective effect of prolactin. It was also observed that prolactin alone did not induce any significant proliferation in either cell population and confirms observations made by Vonderhaar that fetal calf serum inhibits prolactin-indiced proliferation[224].

3.1.2.2 Quantification of Cell Survival using the XTT Cell Proliferation Kit II

For this assay, we seeded $5x10^4$ cells in complete medium and allowed them to attach in 96-well plates. They were then washed gently with Dulbecco's phosphate buffered saline before they were serum-starved for 24 hours. Following this, ceramide (40μM to MCF-7 cells, and 50μM to T47-D cells) was added in the absence or presence of prolactin (200ng/ml) and cells were incubated for 24 hours (MCF-7 cells) or 48 hours (T47-D cells). The XTT was then added to the wells and incubated for a further 18 hours before the optical density was read at 450nm using a microplate reader. Fig.3.7a shows the mean result from three experiments in MCF-7 cells. The addition of ceramide decreased the optical density from 2.0 ± 0.4(SD) to 0.6 ± 0.1(SD). The addition of prolactin did not give a significant increase in the optical density measured (0.7 ± 0.3(SD)). Fig.3.7b shows the mean data from four separate experiments with T47-D cells. The optical density

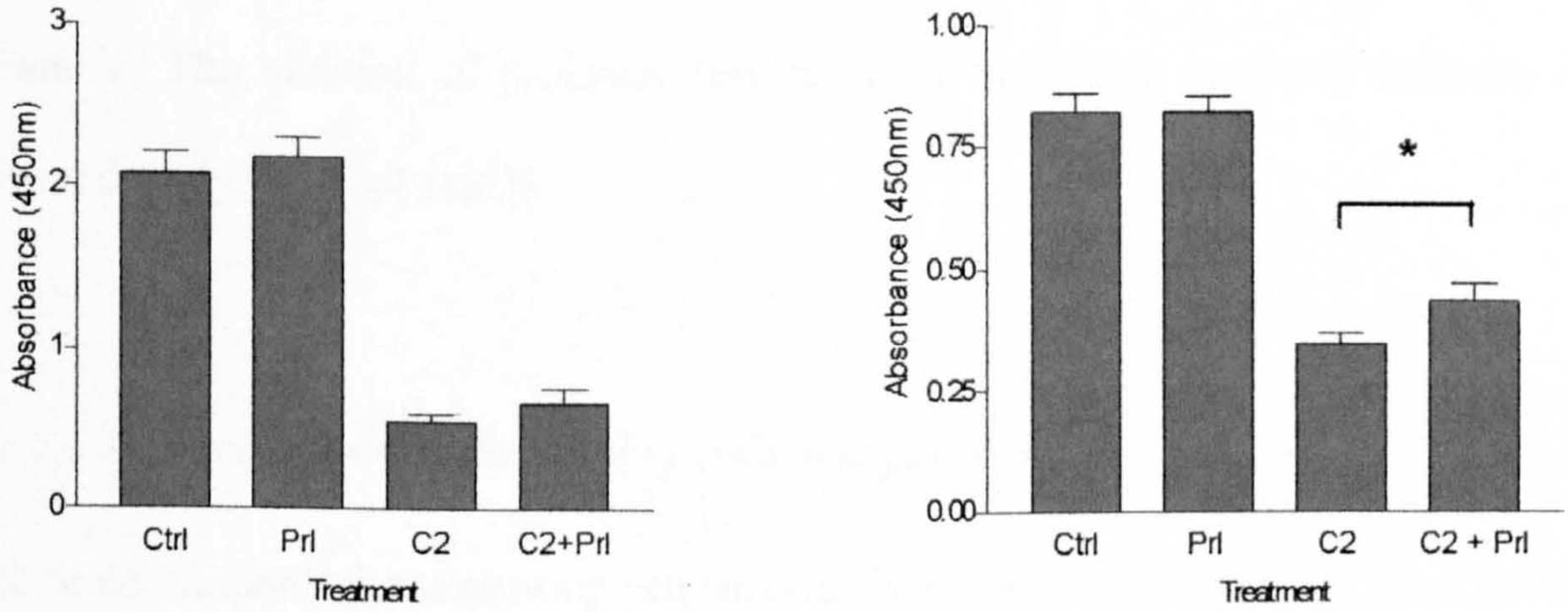

Figure 3.7 Use of the XTT assay to assess the effect of prolactin on survival of (a) MCF-7 and (b) T47-D cells.

Cells were serum starved for 24 hours before treatment with: serum free medium only (Ctrl), 200ng/ml prolactin (Prl), ceramide (C2) (40μM in MCF-7, 50μM in T47-D cells), or both ceramide and prolactin (C2+Prl). MCF-7 cells were incubated for 24 hours, and T47-D cells for 48 hours, before fetal calf serum was added to a final concentration of 10% (v/v). Cells were incubated for a further 5 days before the addition of XTT, and the optical density read 18 hours later. (:p–0.03). The above figures are the mean of 4 experiments, each performed with 6 replicates.*

decreased from 0.8±0.2(SD) in control cells to 0.3±0.1(SD) when cells were exposed to ceramide. The addition of prolactin resulted in a significant ($p<0.05$) increase in the optical density to 0.4±0.1(SD).

3.1.2.3 Assessment of Cell Survival by a Clonogenic Assay

The 'gold standard' for measuring cell survival is to assess clonogenicity. Thus the ability of T47-D cells to form colonies in agar gels following cytotoxic insult by ceramide was assessed. Fig.3.8 shows a dose response curve to ceramide using this assay in T47-D cells, and on this basis a concentration of 20μM was chosen for subsequent experiments.

To determine whether prolactin could exert a protective effect in this assay, $1.5x10^6$ cells were seeded into a T25 flask and allowed to attach. The cells were then serum-starved for 24 hours before they were incubated in the absence or presence of 250ng/ml of prolactin for an hour. Ceramide (20μM) was then added in the continued presence of prolactin and cells were incubated for a further 24 hours. Following this, all the cells, including floaters, were collected by trypsinization and 250 cells were plated onto 60mm dishes in agarose gels and incubated for 14 days. Three replicates for each treatment condition were plated. The gels were then stained with 0.05% Neutral Red Solution for 1 hour before the number of colonies was counted using a dissecting microscope. A typical experiment is shown in Fig.3.9. When results of 3 experiments were combined, treatment with ceramide resulted in a small decrease in the number of colonies formed (from 183±63(SD) to 160±63(SD)), but there was no protective effect when cells were treated with prolactin (140±48(SD). Unfortunately, given the poor reproducibility of these

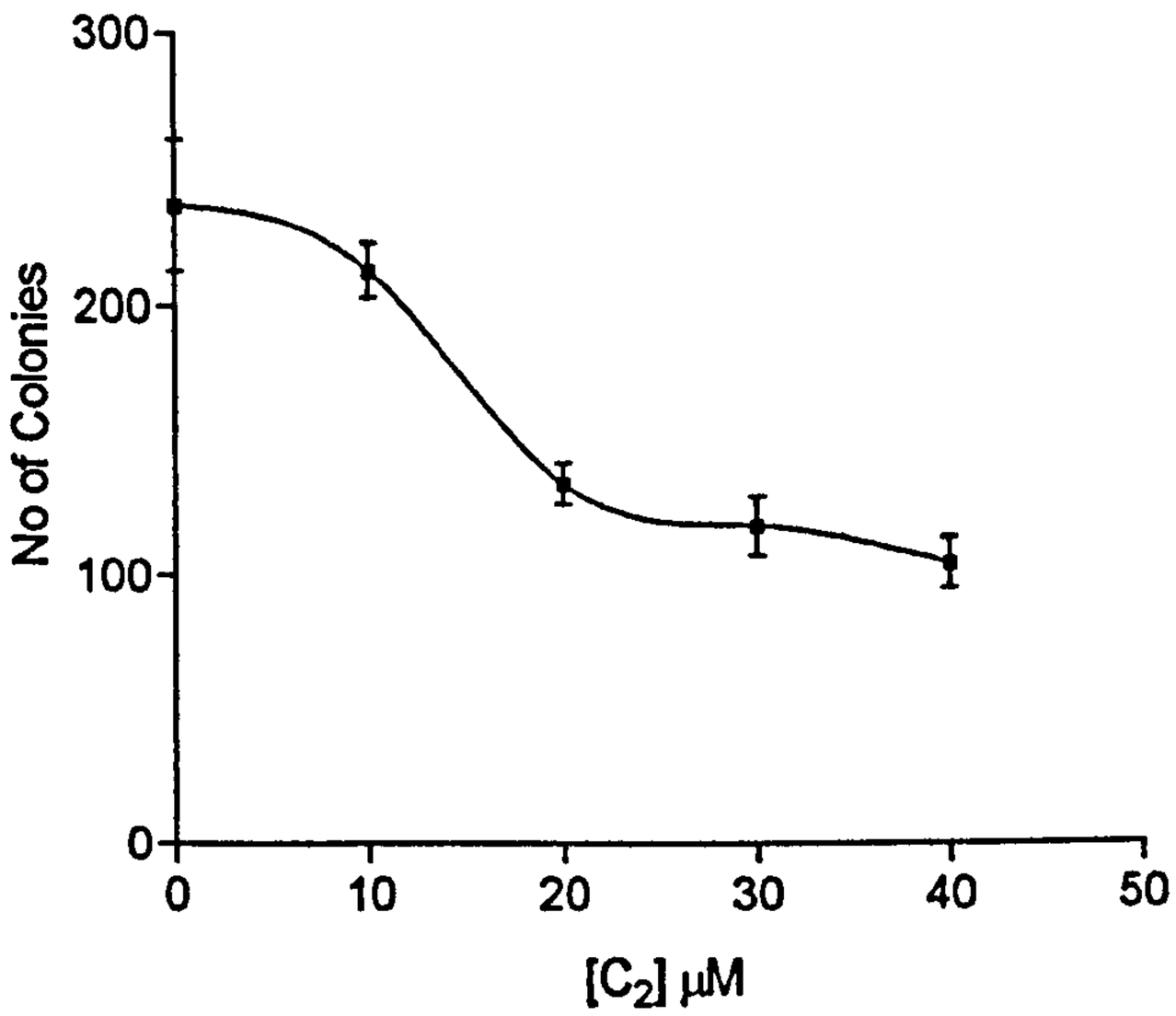

Figure 3.8 T47-D Clonogenic survival assay of T47-D cells exposed to ceramide.

T47-D cells were seeded into T25 flasks and serum starved for 24 hours. The cells were then exposed to various concentrations of ceramide 24 hours before being collected by gentle trypsinization and seeded onto agarose gels at a concentration of 500 cells per gel. The gels were then incubated for 14 days before they were stained with neutral red solution and the number of colonies counted.

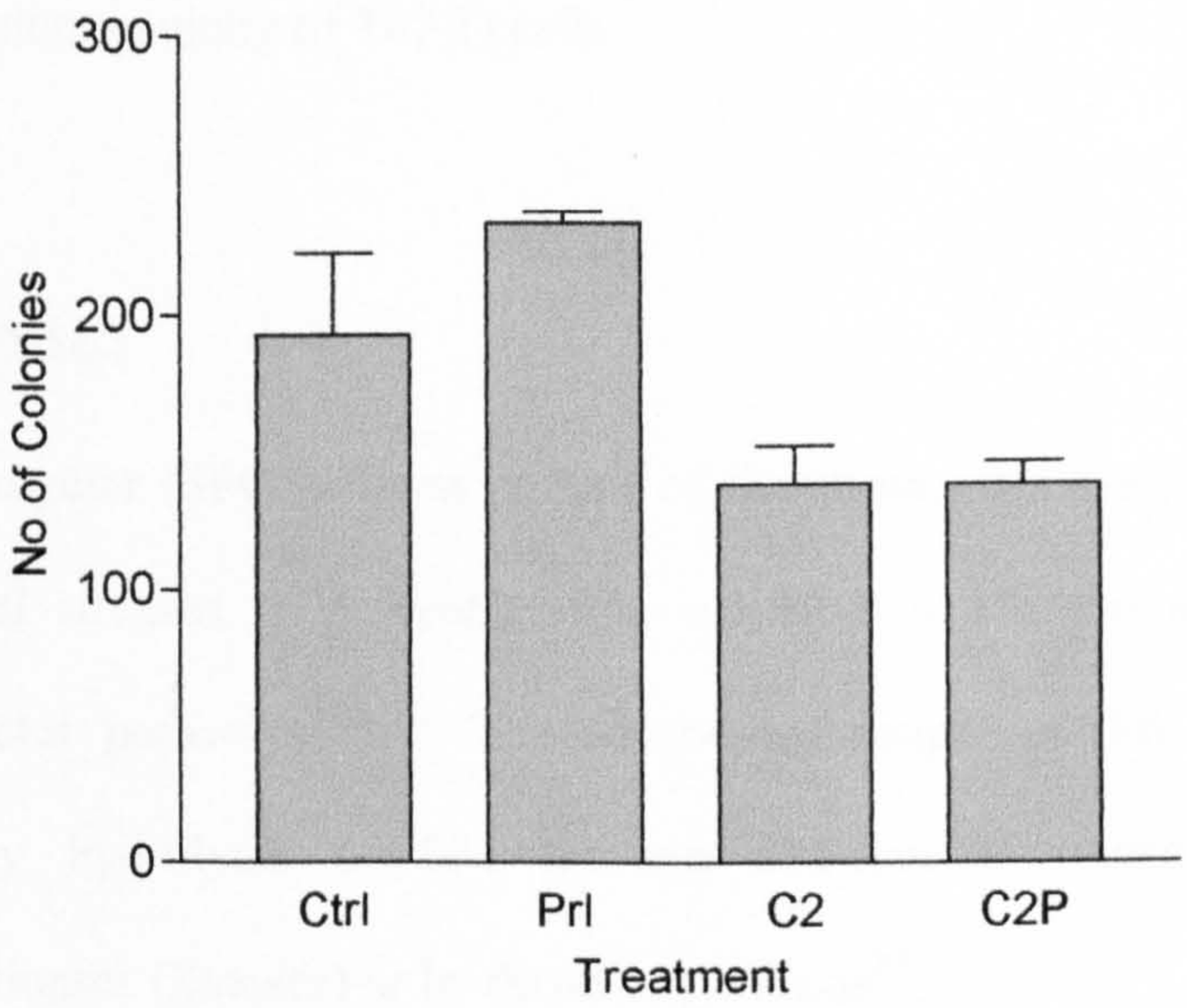

Figure 3.9 Use of clonogenic survival assay to assess the effect of prolactin on survival of T47-D cells.

T47-D cells were seeded into T25 flasks and starved of serum for 24 hours. The cells were then treated without or with 250ng/ml prolactin for 1 hour before addition of 20μM ceramide for 24 hours. The cells were then trypsinized and seeded into agarose gels and incubated for 14 days. The gels were then stained with neutral red and the number of colonies counted. The figure represents a typical experiment. This experiment was performed 3 times in triplicate.

experiments, it is difficult to draw any firm conclusions about the effects of ceramide or prolactin on clonogenicity of T47-D cells.

3.2 DISCUSSION

The sphingomyelin (SM) pathway is part of the stress response system linking diverse environmental stresses (UV, heat shock, oxidative stress and ionizing radiation) to cellular effector pathways[225,226]. The second messenger in this system is ceramide, generated by hydrolysis of SM through SM-specific phospholipases C termed Sphingomyelinases (Smases) or by de novo synthesis[227].

Ceramide generation occurs early and is not dependent on caspase activation[228-231]. Use of exogenous ceramide (either analogs or neutral[222,232,233]) or Smase elevates intracellular ceramide levels and results in apoptosis[225,226].

Extracellular agents and insults (such as TNF, Fas ligands and chemotherapeutic agents) can activate sphingomyelinsases, which act on membrane sphingomyelin resulting in the release of ceramide[225]. Inducers of ceramide generation include 1,25-dihydroxyvitamin D_3, TNF-α, endotoxin, interferon-gamma, interleukin-1 (IL-1), FasL, dexamethasone, ionizing radiation, chemotherapeutic agents, heat and nerve growth factor (NGF)[234].

Breast cancer is the most common cancer affecting women in the world today, making up 18% of all cancers detected in women. In the UK, it is the commonest cause of death in women in the 40-50 age groups. The incidence of breast cancer increases from the onset

of puberty, peaks just before the menopause and then declines thereafter[235]. There also exists a distinct geographical distribution, where incidence rates in the West are greater than in the Far East[235].

All breast cancers arise from the epithelial cells of the terminal duct lobular unit and are classified according to histological appearance. There are seven categories: mucoid, papillary, classical lobular, tubular, cribiform, medullary and NOS (not otherwise specified)[236]. As with all cancers, the aggressiveness of the cancer is classified into grades, which refer to the degree of differentiation of the cells, and stages – which refer to the tumour size, number, presence of spread, whether it affects only lymph nodes or has metastasized to other organs[236].

Prolactin is a pleiotrophic neuroendocrine polypeptide hormone with many actions, the mechanisms of which are still poorly understood[237]. It is synthesized as a 23kD peptide by lactotrophs in the anterior pituitary gland and upon secretion into the blood stream acts as an endocrine factor on its target organs. It is best known for its actions on the mammary gland, being critical for its proper development and maturation[238,239]. Whilst its mitogenic effect has long been accepted, it has only recently become known that prolactin may have a survival effect on certain cell types[240], and possibly in breast cancer cells too[219]. Recent studies have shown that the hormone may be locally produced in tissues (breast epithelial cells and decidual cells of the bone or brain) outside the pituitary gland[237]. The best-characterized action of prolactin is on the mammary gland where it stimulates DNA synthesis, epithelial cell proliferation, and the promotion of milk

production[241,242]. In other mammalian cell lines, STAT5 has been implicated in tumourigenesis [243,244] as well as cell survival[245,246].

The role of prolactin in breast cancer has always been controversial, but recent evidence has shown that it may play a more significant role than was previously believed. Thus, for example, prolactin antagonists have been shown to inhibit proliferation in breast cancer cells[247]. One recent report suggests that this inhibition may actually be due, in part, to the induction of apoptosis by prolactin antagonists[219].

Using morphological analysis, we found that in T47-D cells there was a clear protective effect of prolactin. In these cells (Fig.3.2), the number of apoptotic cells detected decreased after treatment with prolactin (13%$\pm$5 (SD) to 4%$\pm$2 (SD), p value<0.05). Several problems were encountered in using morphological analysis as a method for quantifying apoptosis, however. First, there was some difficulty in identifying the apoptotic cells in ceramide-treated wells, apart from those cells at an advanced stage of apoptosis. The gradual change from viable to apoptotic status made it difficult to identify apoptotic cells with confidence, making assessment somewhat subjective, except where cells displayed the classical features of very densely staining nucleus with a very little cytoplasm. Moreover, if only apoptotic bodies were left, it was difficult to know if they arose from a single cell or from several.

Second, the loss of cells during washing prior to fixation added to the problem as the cells that were lost were likely to be cells that were least viable. This may have led to a

bias during assessment under the microscope when only viable cells were seen and resulted in a contradictory decrease in the amount of apoptosis detected as the ceramide concentration increased. It would have been interesting to have collected these 'floaters' and analysed them by fixing and staining with H&E to assess their morphology.

Due to these difficulties, we investigated the possibility of using other methods to assess apoptosis. Cell cycle analysis of T47-D cells after treatment with ceramide did not result in an increase in the preG1 population. Cells were arrested in the G2 phase, however, which has been reported previously when T47-D cells were exposed to various chemotherapeutic drugs[248].

When assessing the cell cycle profile to estimate the degree of apoptosis that occurs in a given cell population, there is the assumption that the cells undergo DNA degradation resulting in a decrease in the DNA content of the cell. One possible explanation for a lack of change in the pre-G1 population in breast cancer cells could be that either ceramide-induced apoptosis did not result in DNA degradation or laddering during apoptosis, as has been observed by other groups with MCF-7 cells[249,250].

Use of annexin-V binding to determine the extent of apoptosis in breast cancer cells was also rather unsatisfactory. While the number of viable cells was clearly decreased, the apoptotic population (cells stained only with annexin-V-FITC) remained consistently small, with the majority of non-viable cells being stained both by annexin and propidium

iodide. Measurement of live and dead cell populations did not show any protective effect of prolactin on apoptosis / cell death.

The method of Annexin-V staining relies on the expression of phosphatidylserine on the outer leaflet of the cell membrane early in the apoptotic process, but with maintenance of cell membrane integrity, which is responsible for excluding propidium iodide from the cells. In breast cancer cells, either phosphatidylserine exposure does not occur early during apoptosis, or cell membrane integrity is lost early in the apoptotic process as very few cells were labeled with Annexin alone, and the majority of non-viable cells were labelled with both Annexin and propidium iodide. This double staining implies that the cells were necrotic or in late apoptosis.

It is possible that trypsin-EDTA may have affected membrane integrity, allowing diffusion of propidium iodide into the cell, so resulting in the large fraction of apparently necrotic cells detected. Identification of optimal conditions for each experiment was the main obstacle in obtaining consisting results. It was necessary to use various doses of ceramide ranging from 20μM to 70μM during the course of these studies in an attempt to obtain consistent results. Finally, as can be seen in figure 3.5, when all the cell populations were added together, they fail to make up 100% of the cell population. This was because a significant proportion of the propidium iodide stain appeared to detect cell debris, and this population could not be excluded from the total cell count.

Thus, we were unable to detect clear evidence of apoptosis either by cell cycle analysis or by Annexin staining, two methods currently in use to assess the extent of apoptosis. This suggests that T47-D and MCF-7 cells may have an inherent inability to undergo DNA laddering or typical apoptosis. There is increasing evidence to show that different forms of apoptosis or programmed cell death exist[251-253]. Development of the 'classical' features of apoptosis requires the participation of specific caspases as well as other enzymes[83,249]. T47-D cells have a mutated form of the p53 gene[175,254], which may account for their inability to undergo classical apoptosis. High levels of an oncoprotein MDM-2, a negative regulator of p53, have been found in both MCF-7 and T47-D cells lines[248]. MDM-2 functions by binding p53 and antagonizes its transcriptional activity, as well as promoting the degradation and nuclear export of the p53 protein[248], and thus may contribute to the resistance to undergo apoptosis in these cell lines. A literature search revealed very few studies of apoptosis in T47-D cells, although detection of apoptosis in these cells by morphological analysis and flow cytometry using diverse apoptotic agents has been reported[255-257]. The extent of apoptosis induced in T47-D cells ranged from 14%[258], to 43%[255]. This large increase detected using Annexin-V in the latter study, was in response to progesterone treatment. We did not wish to complicate our study by using a hormone to induce apoptosis, as there may be other pathways activated by progesterone which could interact with prolactin. Regarding the efficacy of a prolactin antagonist[219] in inducing apoptosis, the authors reported a 3-to-15 fold induction of apoptosis in the cells by the antagonist, which was dose-dependent. Overall, there is agreement with our observations that the T47-D cell line is relatively resistant to apoptosis induced by a variety of agents[254,259,260].

In addition to ceramide, we tried a variety of other cytotoxic/apoptotic agents (gamma irradiation, progesterone, taxol etc., results not shown), however, we were unable to detect any change in the preG1 population or any increase in Annexin-V binding.

As an alternative approach, we attempted to assess prolactin effects on clonogenic cells. First we used an indirect method of determining numbers of clonogenic cells by allowing cells to proliferate. After a period of proliferation, the number of T47-D cells was reduced from $10\pm4x10^4$(SD) in controls to $5\pm2x10^4$(SD) in cells after treatment with ceramide, but increased again to $7\pm2x10^4$(SD) in cells treated with ceramide and prolactin ($p<0.5$) (Fig. 3.6b).

These results show a clear protective effect of prolactin in T47-D cells. A potential criticism of these experiments could be that prolactin is simply stimulating proliferation. This seems unlikely, however, because there was no proliferative effect of prolactin in this experiment ($10\pm4x10^4$(SD) for control cells, versus $10\pm2x10^4$(SD) for cells treated with prolactin).

Similar results were obtained with the XTT assay (Fig. 3.7b), where there was an increase in optical density from 0.3 ± 0.1(SD) in T47-D cells treated with ceramide alone to 0.4 ± 0.1(SD) ($p<0.05$) when cells were treated with both ceramide and prolactin. Again, this indicates a protective effect conferred by the addition of prolactin.

Next, we assessed clonogenicity of T47-D cells directly by their ability to form colonies. Taking the mean of 4 separate experiments there was no clear protective effect of prolactin on the clonogenicity of T47-D cells (Fig. 3.9). Again, the extremely variable response to ceramide resulted in a much smaller effect of ceramide in these experiments than we predicted from the initial dose response (Fig.3.8), making it difficult to assess any protective effect of prolactin. The apparent lack of protection by prolactin in this assay could result from the distance separating cells when they are suspended in agarose gels. We have recently found (Michael Norman, unpublished results) that the proliferative response to prolactin is strongly dependent on cell density. Thus, as clonogenic assays (Figs. 3.6 and 3.7) abolish cell-to-cell contact, this could account for the lack of survival benefit by the presence of prolactin.

Should prolactin be confirmed as a survival factor, the implications could be far-reaching. Most breast tumours are capable of synthesizing and secreting prolactin[211,261], and the prolactin receptor is found on most breast cancer cells[262,263]. Thus prolactin signalling may provide a mechanism for these cells to evade the apoptotic process. Conversely, antagonizing prolactin receptors in tumour cells, whilst simultaneously exposing the cancer to radio- or chemo-therapy, could increase the effciency of subsequent tumour kill, and thus increase the effectiveness of curent therapies.

The results obtained by morphological assessment and the cell survival assays appear to confirm our hypothesis that prolactin can act as a survival factor in breast cancer cells. Other assays (cell cycle analysis, Annexin-V staining and colony formation in agarose

gels), however, do not support this hypothesis. A likely explanation for this discrepancy would be that the parameters under investigation in each assay were different, and ceramide could have distinct effects in each. The most obvious discrepancy lies between the morphological and growth studies (which show a protective effect of prolactin) and the Annexin-V staining (which does not show any protective effect by prolactin). It is possible that the 'necrotic' population identified in the latter assay (Fig. 3.5) included cells which were still viable, and would have been able to recover subsequently had the assay been allowed to proceed for longer.

Our difficulty in identifying 'classical' signs of apoptosis such as Annexin staining in T47-D cells is not in keeping with available data, though there are very few papers regarding apoptosis in T47-D cells. Evidence from these publications[255,258] suggests that T47-D cells can undergo apoptosis when treated with certain agents. It seems more likely, however, that differences in T47-D cells or other reagents (e.g. fetal calf serum or plastics) used in each laboratory will underlie variations in each response.

One possible reason for the discrepancy in results between the cell survival assays and the clonogenic assay is that in the former, cells are more likely to remain in contact with each other. Thus it is possible that signalling initiated by prolactin is protective, but only under certain circumstances, perhaps requiring the presence of cell-to-cell interactions to be effective. Most of the results in this study only document small increases in cell survival.

4 Attempt to Create a Model for Dissecting the Contribution of the Jak2-STAT5 pathway to Apoptosis

Having obtained some evidence to support the hypothesis that prolactin enables breast cancer cells to survive the apoptotic insult of ceramide, we wished to investigate the signalling pathways underlying this mechanism. One of the major pathways activated by the prolactin receptor is the Jak2-STAT5 pathway[264].

Based on previous work showing that it was possible to inhibit the apoptotic pathway when STAT5 is activated by a variety of cytokines[246,265-268], we postulated that activation of the Jak-STAT pathway mediates the ability of prolactin to confer protection against apoptosis in breast cancer cells.

The results in Chapter 3 showed that the amount of apoptosis detectable in breast cancer cells is both small and variable. Hence, due to the difficulties encountered in analyzing this pathway in breast cancer cells, we decided to create a model of apoptosis in an established cell line that could be used more easily to investigate the role of the Jak-STAT pathway.

The CCRF-CEM cell line was established from a patient with acute lymphoblastic leukaemia. The CEM-C7 sub-clone of these cells could provide a useful test system for the analysis of apoptosis because these cells are particularly sensitive to glucocorticoid-induced apoptosis[269], the extent of which is much greater than that detectable in breast cancer cells. Because no receptor capable of activating the Jak-STAT pathway has been identified in these cells, we decided to create clones stably expressing the prolactin receptor.

One advantage of transfecting CEM-C7 cells with the prolactin receptor would be that transfection of mutated receptors could be performed in the future for further dissection of the signalling pathways involved in any anti-apoptotic effects mediated by the receptor.

4.1 Results

4.1.1 The Presence of Jak2 in CEM-C7 cells

In order for the transfected prolactin receptor to be effective in activating signalling in CEM-C7 cells, the components of the Jak-STAT pathway have to be present. To confirm that Jak2 is expressed in CEM-C7 cells, $5x10^6$ cells were lysed, and crude extract immunoprecipitated with anti-Jak2 antibody (New England Biolabs). After electrophoresis using a 12% acrylamide gel, a Western blot (Fig.4.1) showed that Jak2 (~ 130 kDa) is indeed present in CEM-C7 cells.

4.1.2 The Presence of STAT5 in CEM-C7 cells

Evidence for expression of STAT5 in CEM-C7 cells has been obtained previously (personal communication by E. Brad Thompson). To confirm this finding, $3x10^6$ cells were lysed and a cell extract was electrophoresed using a 12% acrylamide gel. As shown in Fig.4.2, Western blotting with anti-STAT5 (C-17, Santa Cruz) confirmed the presence of STAT5 (~ 92kDa) in these cells.

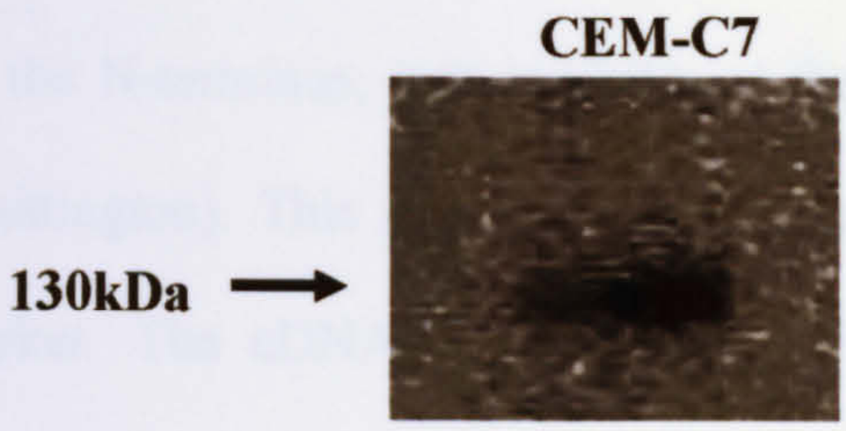

Figure 4.1 Expression of Jak2 tyrosine kinase in CEM-C7 cells.

$5x10^6$ x cells were lysed and the crude extract immunoprecipitated with anti-Jak2 antibody (New England Biolabs). Western blotting was performed on immunoprecipitated extract using anti-Jak2 antibody.

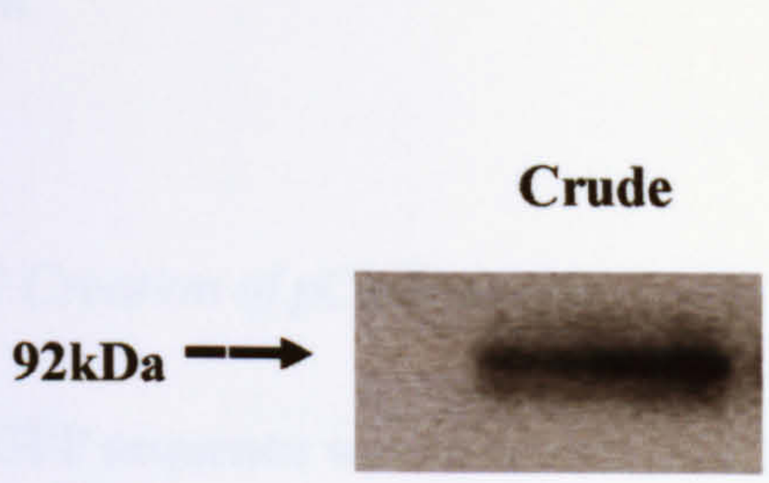

Figure 4.2 Expression of STAT5 in CEM-C7 cells.

$3x10^6$ x cells were lysed and crude extract electrophoresed and transferred to nitrocellulose. The membrane was probed with anti-STAT5b (C-17 antibody, Sigma) as the primary antibody and anti-rabbit IgG as the secondary antibody.

4.1.3 Construction of the pCMV-FlagPrlR plasmid

A plasmid encoding the full-length human prolactin receptor, tagged with a Flag epitope on the N-terminus, was available at the start of this study (constructed by Dr. Hayley Whittington). This sequence was present in a pAdlox vector which lacks a selection marker. The cDNA was therefore first transferred to a vector with an appropriate selection cassette. (See Fig. 4.3)

4.1.3.1 Isolation of Flag-PrlR from Flag-PrlR pAdlox

The Flag-PrlR pAdlox plasmid (10μg) was digested with *Sal*I (50units, at 37°C for 3 hours), and dephosphorylated to prevent re-ligation. The linearized DNA was digested with *Eco*RI (50units, at 37°C for 3 hours), and the resultant Flag-PrlR cDNA fragment isolated.

4.1.3.2 Creation of pCMV vector

The EGFP sequence was removed from the pEGFP-N1 plasmid (Invitrogen, Netherlands) by a 2-stage restriction digest. 10μg of pEGFP-N1 was digested with *Sma*I (50 units, at 25°C for 2.5 hrs) and then with *Not*I (50 units, at 37°C for 2.5 hrs). Blunt ends were created (10 units Klenow enzyme, 15μl Klenow buffer, 1μl 10mM dNTPs and 33μl digested vector DNA, incubated together at 25°C for 1 hour). The resultant DNA was purified and re-ligated (10 units T4 ligase, 14°C overnight).

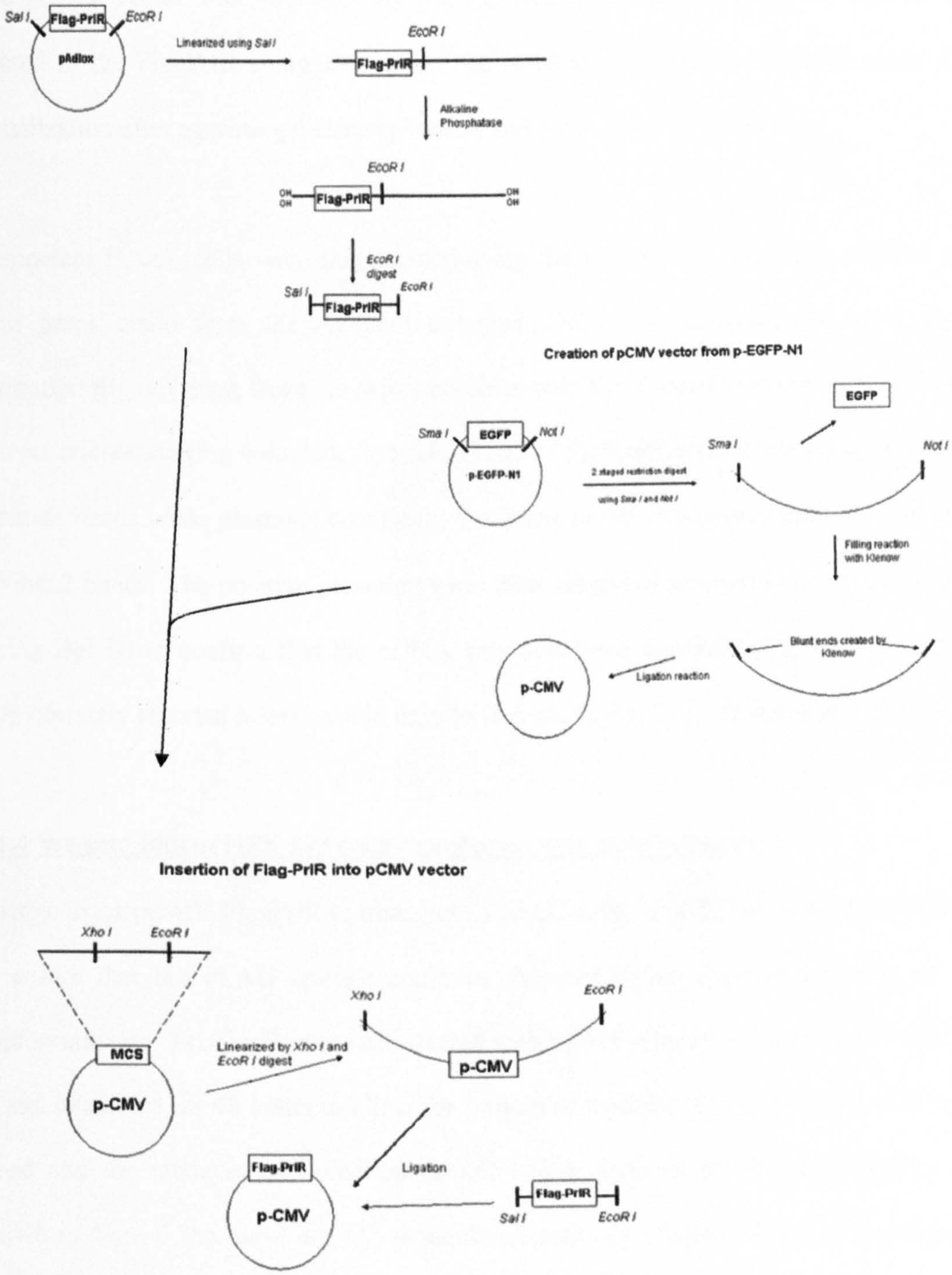

Figure 4.3 Creation of pCMV-FlagPrlR.

4.1.3.3 Insertion of FlagPrlR into pCMV plasmid

The pCMV vector was linearized by *Xho*I (10units) and *Eco*RI (10units) digests and ligated to the FlagPrlR using T4 ligase. The resultant plasmid was isolated under UV visualization after agarose gel electrophoresis and purified by gel extraction.

Competent E. coli cells were transformed using the new pCMV-FlagPrlR plasmid and mini preps made from the resultant colonies. DNA was extracted for an analytic restriction digest (using Dra I) to select colonies with the desired plasmid inserted in the correct orientation (Fig.4.4a, lane 2, 5, 10, 11, and 13). Positive plasmids would exhibit 4 separate bands while plasmids containing the insert in the wrong orientation would only exhibit 2 bands. The positive plasmids were then subjected to another restriction digest (using Bgl II) to confirm that the cDNA was orientated correctly (Fig.4.4b). Plasmids with correctly oriented inserts would only have a single BglII restriction digest site.

4.1.4 Western Blot of HEK 293 cells Transfected with pCMV-FlagPrlR

Prior to using pCMV-FlagPrlR to transfect CEM-C7 cells, Hek 293 cells were transfected to ensure that the FLAG epitope could be detected on an expressed protein of the appropriate size. $3x10^6$ cells were transfected with pCMV-FlagPrlR (5µg) using FuGENE 6, and incubated for 48 hours to allow for protein expression. The transfected cells were lysed and the crude extract electrophoresed before analysis by Western blotting. As shown in Fig.4.5 the anti-Flag M2 monoclonal antibody (Sigma) detected a protein of 90kD, as expected for the prolactin receptor.

(a)

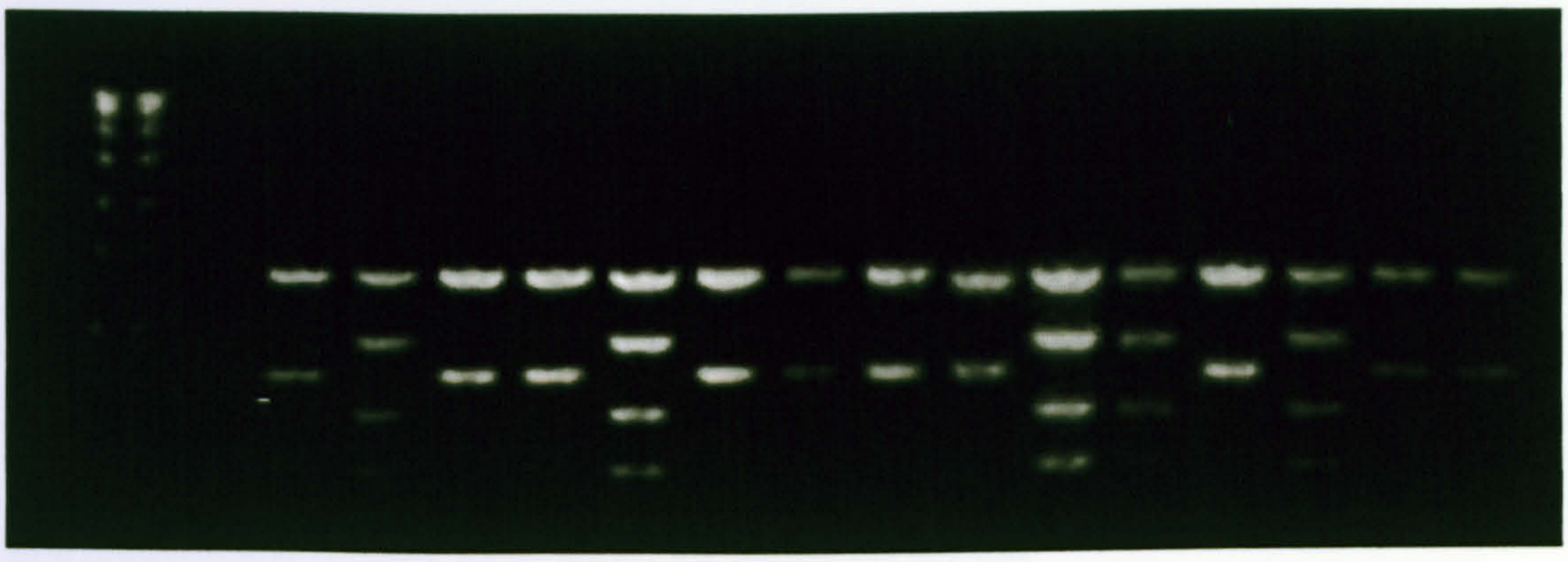

(b)

Figure 4.4 Selection of transformed *E.coli* containing correctly oriented Flag-PrlR plasmid.

(a) Selection of E. coli colonies containing plasmids with the Flag-PrlR in the correct orientation. Colonies of E. coli were chosen at random and mini-preps of DNA made. The resultant plasmids obtained were subjected to diagnostic digest by Dra I.

(b) Confirmatory diagnostic digest of plasmids, previously identified by Dra I, using Bgl II.

4.1.5 The ability of pCMV-FlagPrlR to activate signalling

To confirm that pCMV-FlagPrlR was able to activate STAT5, $3x10^4$ COS7 cells were plated onto 24 well plates and incubated overnight. Each well was then transfected using Fugene 6 with STAT5b (50ng), LHRE reporter (250ng) and one of the following: empty pCMV vector (100ng), pCMV-FlagPrlR (100ng), original vector containing the Flag-tagged receptor pAdlox-FlagPrlR (100ng), or wild type PrlR (100ng). The cells were incubated overnight and then serum starved for at least 6 hours before the addition of growth hormone (250ng/ml) for a further 18 hours. Cells were then lysed in 100µl of Cell Lysis Buffer (Promega), subjected to a freeze-thaw cycle and 50µl of the lysate analysed in a luminometer (Dynex Revelation) for luciferase activity.

Fig. 4.6 shows that whilst the re-constructed plasmid pCMV-FlagPrlR does activate signalling in response to prolactin stimulation, its activity is much less than that of the original pAdlox plasmid. One point to note is the very much higher baseline activity (~3000 RLU) of the both the pAdlox and the wild-type plasmids compared to pCMV-FlagPrlR (~50 RLU). This could be due to an inadvertent mutation introduced into the sequence, resulting in decreased expression.

COS-7 cells ($5x10^6$ in 60mm dishes) were transfected with either 2µg of pCMV-FlagPrlR or pAdloxFlagPrlR. Following a 24 hour incubation, the cells were lysed and the crude extract electrophoresed. Fig. 4.7 shows that the expression of pCMV-FlagPrlR is markedly lower than that of pAdloxFlagPrlR, providing an explanation for the discrepancy in signalling capacity (Fig.4.6).

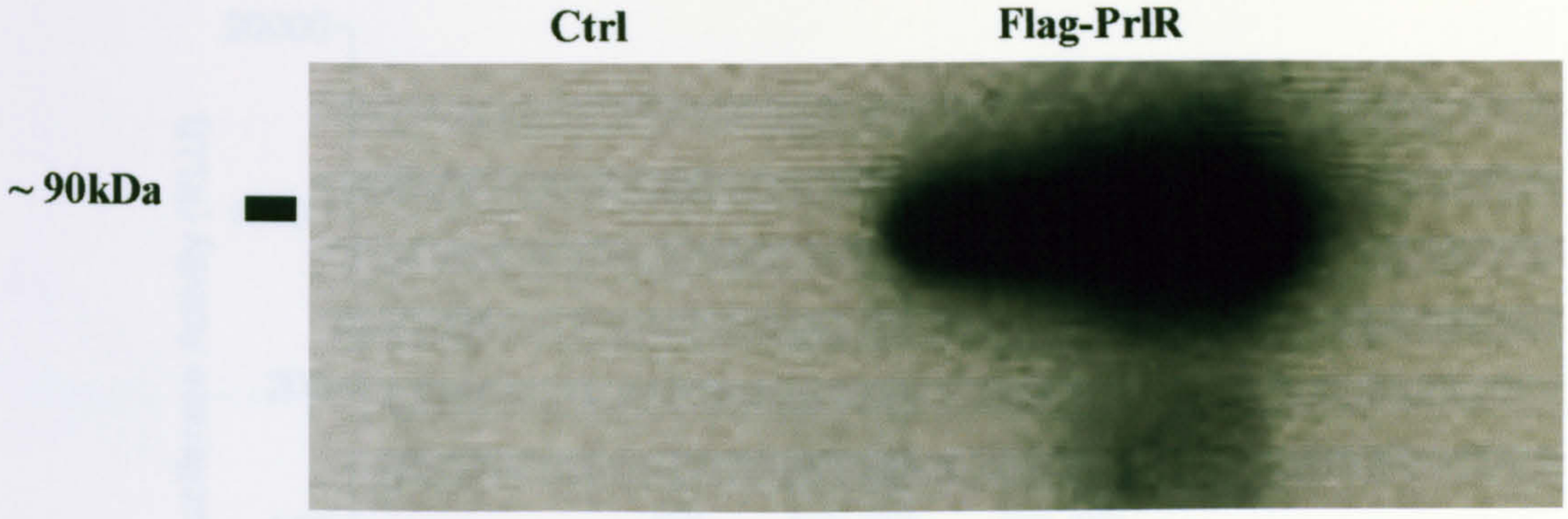

Figure 4.5 Detection of pCMV-FlagPrlR expression in HEK293 cells.

$3x10^6$ cells were lysed. The crude extract was electrophoresed and transferred to a nitrocellulose membrane which was probed with anti-FlagM2 antibody (Sigma) as the primary antibody and anti-rabbit IgG as the secondary antibody (Control lane: untransfected HEK293 cell).

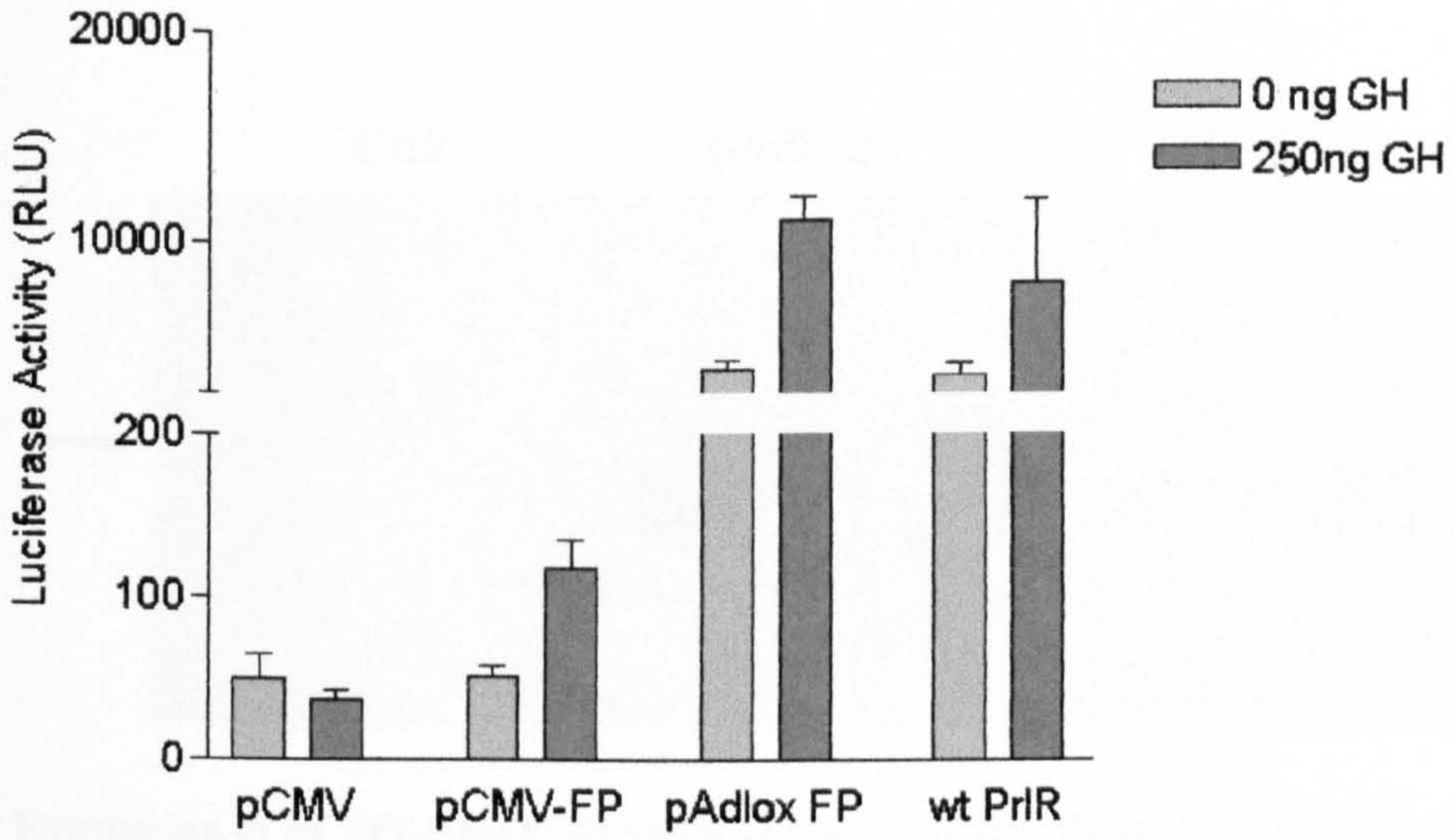

Figure 4.6 Signalling activity of the prolactin receptor expressed by different plasmids in COS-7 cells.

COS-7 cells were transfected with the LHRE reporter and either pCMV (control plasmid), pCMV-FlagPrlR(FP) (test plasmid), pAdlox-FlagPrlR (original Flag-tagged receptor) or wt-PrlR (wild type PrlR plasmid). The cells were serum-starved for 6hrs before exposure to 250ng growth hormone (GH) or vehicle for 18 hours. This experiment was performed using the human growth hormone (GH) as an alternative since prolactin was not available at the time.

Figure 4.7 Expression of pCMV-FlagPrlR and pAdlox-FlagPrlR plasmids in COS-7 cells.

COS-7 cells were transfected with either pCMV-FlagPrlR or pAdlox-FlagPrlR. The cells were lysed and crude extracts were electrophoresed. Western blotting was performed using the anti-FlagM2 antibody.

In view of the discrepancy in both the signalling ability and protein expression of the pCMV-FlagPrlR plasmid compared to the pAdlox- FlagPrlR plasmid, it was decided that co-transfection of the original pAdlox-FlagPrlR with a vector containing a selection cassette was preferable to using the pCMV-FlagPrlR plasmid. The pcDNA3 (Invitrogen) commercial vector was chosen for this purpose as it contains a G418 resistance cassette.

4.1.6 Cloning of CEM-C7 cells

With time in culture, CEM-C7 dexamethasone-resistant cells accumulate[270]. The explanation for this instability is that, having only one functional allele coding for the glucocorticoid receptor, CEM-C7 cells resistant to dexamethasone accumulate rapidly as a result of spontaneous mutations in the remaining allele[271]. Thus, it was imperative to select clones sensitive to both dexamethasone, which induces apoptosis, and G418, - which would be used to select positive clones. Fig.4.8 (top) shows an initial experiment to determine the G418 sensitivity of uncloned cells.

4.1.6.1 Selection of CEM-C7 clones sensitive to dexamethasone

To select glucocorticoid sensitive clones, CEM-C7 cells were cloned by serial dilution and the clones recovered were tested for dexamethasone sensitivity. Fig.4.8 (middle) shows the response of the various clones to incubation with dexamethasone (1μM) for 48 hours. Cell viability was analysed using the XTT assay.

4.1.6.2 Sensitivity of CEM-C7 clones to G418

The CEM-C7 clones obtained by serial dilution were then tested for G418 sensitivity. Fig. 4.8(bottom) shows the effect of exposure to G418 for 72 hours on cell viability, analysed by the XTT assay.

Clones: 21D, 31E, 42G, 59E and 112B were selected for further study as they were sensitive to both dexamethasone and G418.

4.1.6.3 Transfection of CEM-C7.21D cells with pEGFP-N1

The CEM-C7 cell line is difficult to transfect, though most success has been achieved using electroporation[272,273]. In initial experiments designed to establish conditions for effective transfection of CEM cells, a commercial vector expressing the enhanced green fluorescent protein (EGFP), pEGFP-N1 (Clontech), was used. Cells were electroporated with varying amounts of DNA (15-45μg) at 1050μF and 300V. Using this protocol and 40μg of DNA, we were able to transfect about 2% of clone 21D, with the EGFP plasmid (Fig. 4.9) as detected by fluorescent microscopy. With the other concentrations of DNA used (10, 20 and 30μg), however, no fluorescent cells were detected. The other clones (31E, 42G, 59E and 112B) selected for sensitivity to dexamethasone and G418 were also electroporated with pEGFP-N1, but transfection efficiency was very poor (data not shown).

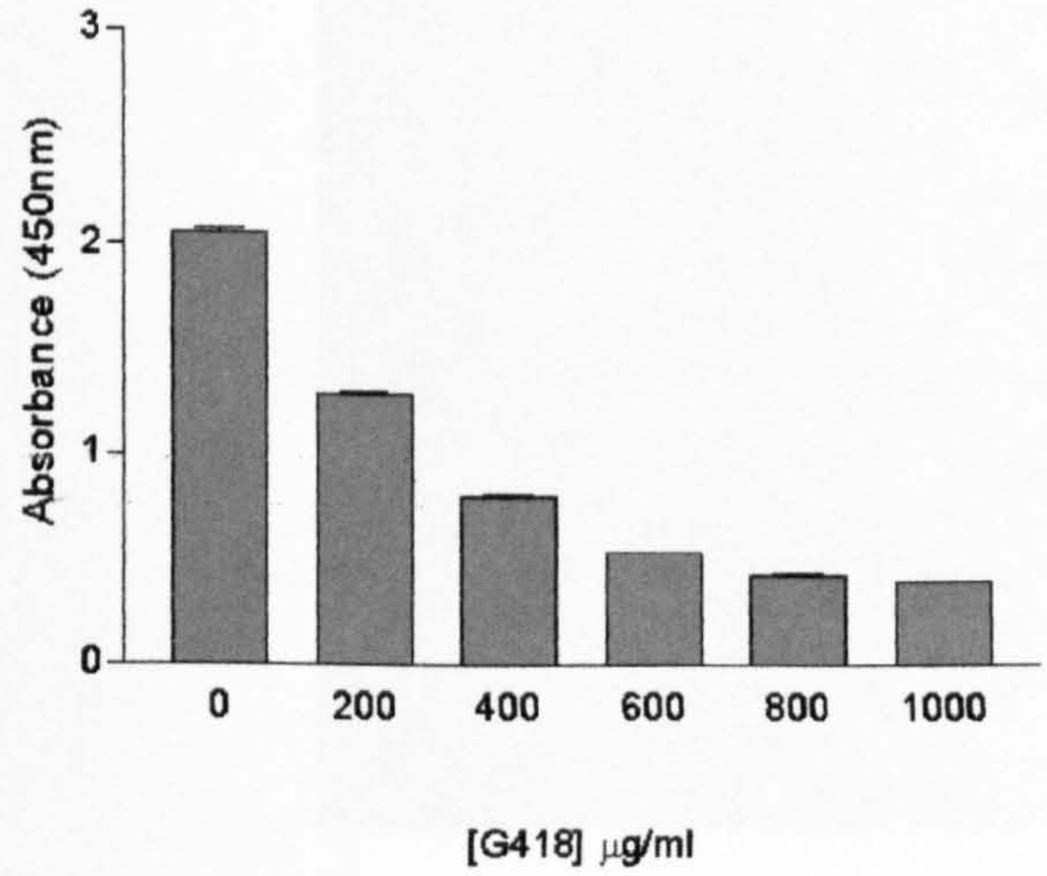

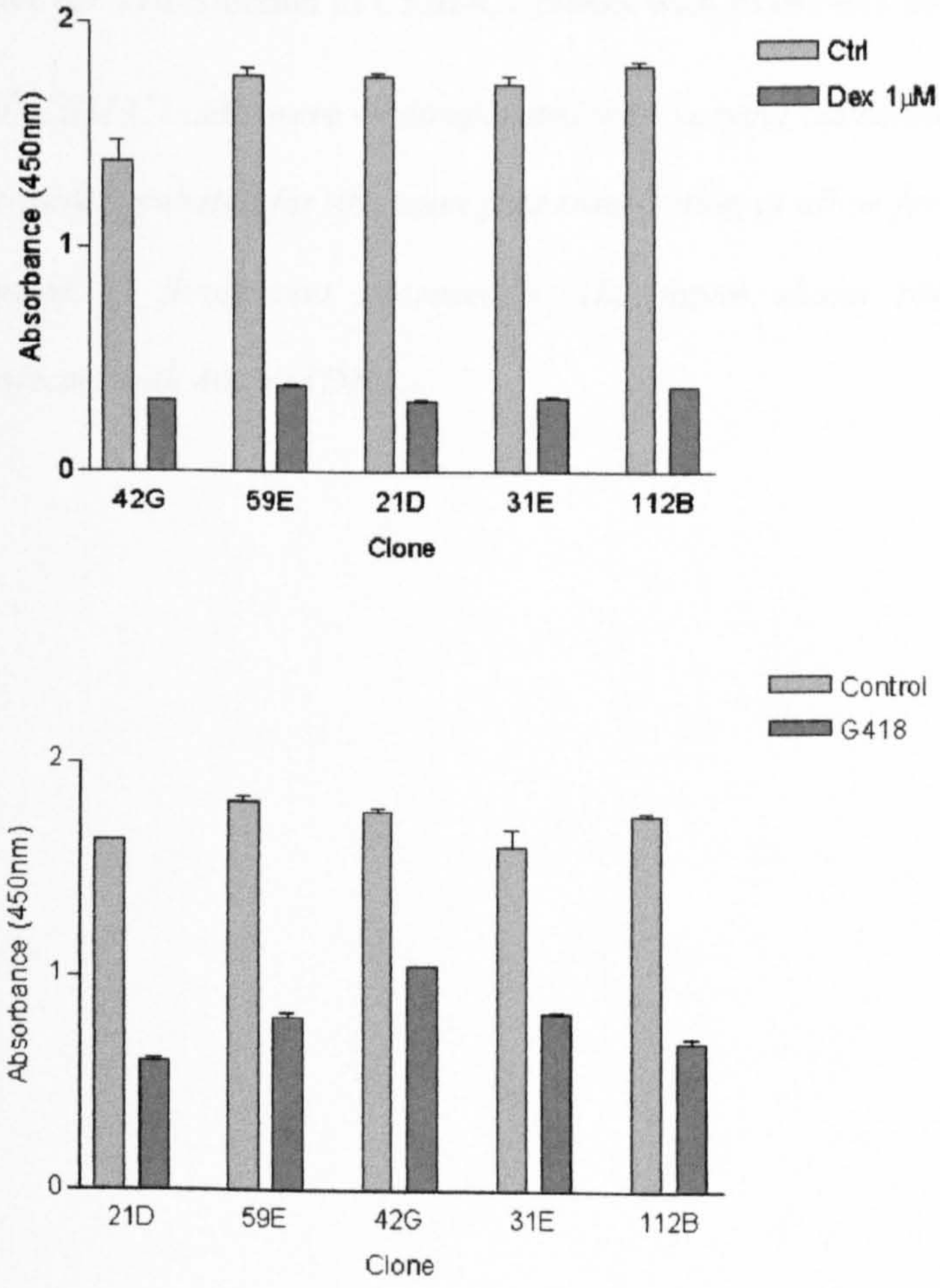

Figure 4.8

(Top) Dose response curve - CEM-C7 cells treated with G418. *Uncloned CEM –C7 cells were incubated with varying concentrations of G418 for 5 days before the addition of XTT.*

(Middle) Sensitivity of CEM-C7 clones to dexamethasone. *Clones of CEM-C7 cells were incubated with 1µM Dexamethasone for 48 hours before the addition of XTT.*

(Bottom) Sensitivity of CEM-C7 clones to G418. *Clones of CEM-C7 cells were incubated with 800µM G418 for 72 hours before the addition of XTT.*

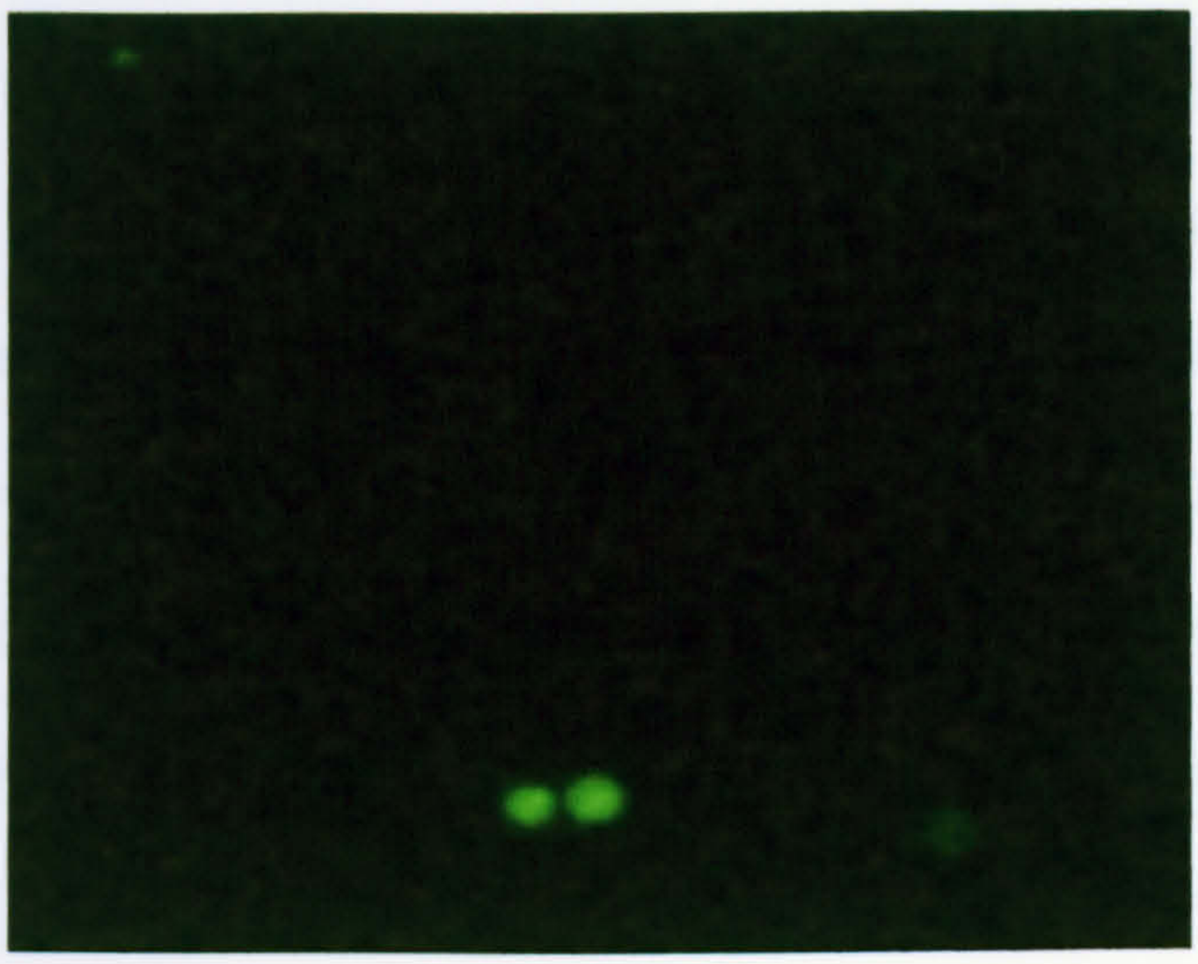

Figure 4.9 Transfection of CEM-C7 clones with EGFP-N1 by electroporation.

$6x10^6$ CEM-C7 cells were electroporated with varying concentrations of EGFP-N1 plasmid. The cells were incubated for 48 hours post transfection to allow for protein expression and the cells screened by fluorescent microscopy. The figure shows results obtained with clone 21D transfected with 40µg of DNA.

4.1.7 Attempt to isolate CEM-C7 cells stably expressing the Prolactin Receptor

CEM-C7.21D cells were initially electroporated with 40μg of pAdlox-FlagPrlR and pcDNA3.1 (80μg DNA in total), but no viable cells were obtained from this transfection. Since the concentration of DNA may have been toxic for the cells, CEM-C7.21D cells were next electroporated with 20μg of pAdlox-FlagPrlR and 20μg of pcDNA3.1 (1050μF, 300V) (40μg of DNA in total). Cells were transferred immediately to RPMI-1640 medium that had previously been placed in a T25 flask, and incubated at 37°C in 5% CO_2.

Following electroporation, cells were allowed to recover over 48 hours before they were placed in medium containing G418 (800μg/ml) to begin the selection process. This selection condition was maintained for 2 weeks, after which the concentration of G418 was decreased to 400μg/ml. Once cell numbers had recovered sufficiently, clones were obtained by serial dilution and then re-cloned in agarose gels.

4.1.8 Attempt to Detect Flag-tagged Prolactin Receptor in CEM-C7 cells

4.1.8.1 Detection of FlagPrlR by Western Blotting

A total of 25 clones were isolated after G418 selection. To test for PrlR expression, $5x10^6$ cells were collected from each clone and lysed. Mouse monoclonal anti-Flag M2 antibody (Sigma) was used for immunoprecipitation and precipitates were electrophoresed on an SDS-Page gel. Separated proteins were then transferred to an Immobilon membrane by semi-dry transfer and the membrane probed using anti-Flag M2 as the primary antibody and an anti-mouse antibody conjugated with horseradish

peroxidase (Amersham Pharmacia) as the secondary antibody. Fig. 4.10 shows a Western blot of the various clones obtained, none of which expressed a detectable Flag-tagged protein.

Our inability to detect Flag-tagged protein could have been due to failure of protein expression, or failure to stably incorporate the prolactin receptor cDNA into genomic DNA. We decided to investigate this further by performing a PCR reaction on genomic DNA extracted from the clones to screen for incorporation of the PrlR cDNA.

4.1.8.2 Detection of Flag-PrlR by Polymerase Chain Reaction

Genomic DNA from $5x10^6$ cells of each clonal population was extracted. Then 1ng of dsDNA was used as a template for a PCR reaction with primers specific for the prolactin receptor. Primers were complementary to different exons, so minimizing the risk of amplifying sequences from the CEM-C7 prolactin receptor gene.

The primers used were:

Forward: CTGTGGATTAAATGGTCTCC

Reverse: TGCAGGTCACCATGCTATA

The forward primer is complementary to a sequence in exon 8 and the reverse primer corresponds to a sequence in exon 10.

The PCR reaction consisted of an initial dissociation period (94°C, 2 min), 40 cycles of dissociation (94°C, 30s), annealing (62°C, 1 min), and extension (68°C, 1 min), and a

final extension period (68°C, 7 min). Positive clones should allow amplification of a 360bp fragment, and Fig. 4.11 shows that a number of clones (1, 3 and 6) had incorporated the Flag-tagged prolactin receptor cDNA into their genome.

4.1.8.3 Detection of Flag-PrlR by STAT5 activation

As we were unable to detect the Flag-PrlR by Western blotting, while PCR demonstrated that the Flag-tagged PrlR cDNA had incorporated into the genomic DNA, we decided to test for PrlR expression by detection of STAT5 activation.

CEM-C7 clones ($1x10^6$) were serum starved for 24 hours, and then exposed to 250ng/ml prolactin for 30 min. The cells were then lysed and the crude extract subjected to electrophoresis. A Western blot was performed using the anti-STAT5b (C-17) antibody (Sigma). Fig. 4.12 shows that no activation of the STAT5 protein by prolactin could be detected (usually detected by a band shift as a result of phosphorylation of the STAT5 protein, thus activated STAT5 runs at a higher molecular weight compared to inactive STAT5), showing that despite incorporation of the Flag-PrlR cDNA into the genome of the CEM-C7 cells, it was not being expressed at a sufficiently high level for detection of activation of signalling pathways. Unfortunately, clones 4 and 5 had a very poor STAT5 yield, hence the faint bands detected in the blot.

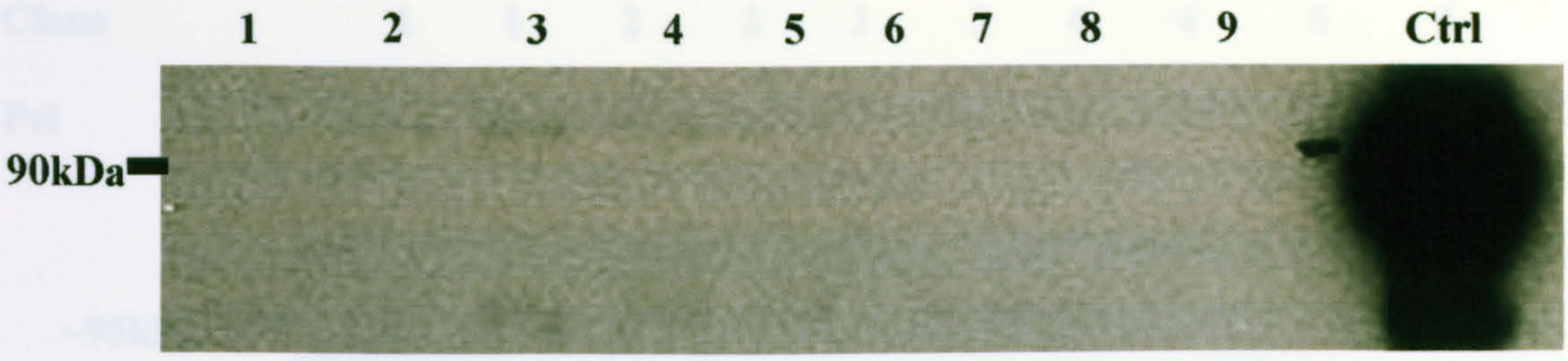

Figure 4.10 Attempt to Detect Flag-PrlR in CEM-C7 clones.

$3x10^6$ cells from each stable CEM-C7 clone were lysed and crude extracts immunoprecipitated with the anti-FlagM2 antibody (Sigma). Western blot was performed with anti-FlagM2 antibody (Sigma). The control lane contains crude extract from COS-7 cells transfected with pAdlox-FlagPrlR.

Figure 4.11 Detection of prolactin receptor cDNA in CEM-C7 clones by polymerase chain reaction.

Genomic DNA was extracted from CEM-C7 clones and subjected to polymerase chain reaction. The PCR products were electrophoresed on an agarose gel and three clones (1, 3 and 6) positive for the prolactin receptor were identified (Positive control (+ve) was the product from PCR of pAdlox- FlagPrlR cDNA, and negative control (-ve) was a water blank).

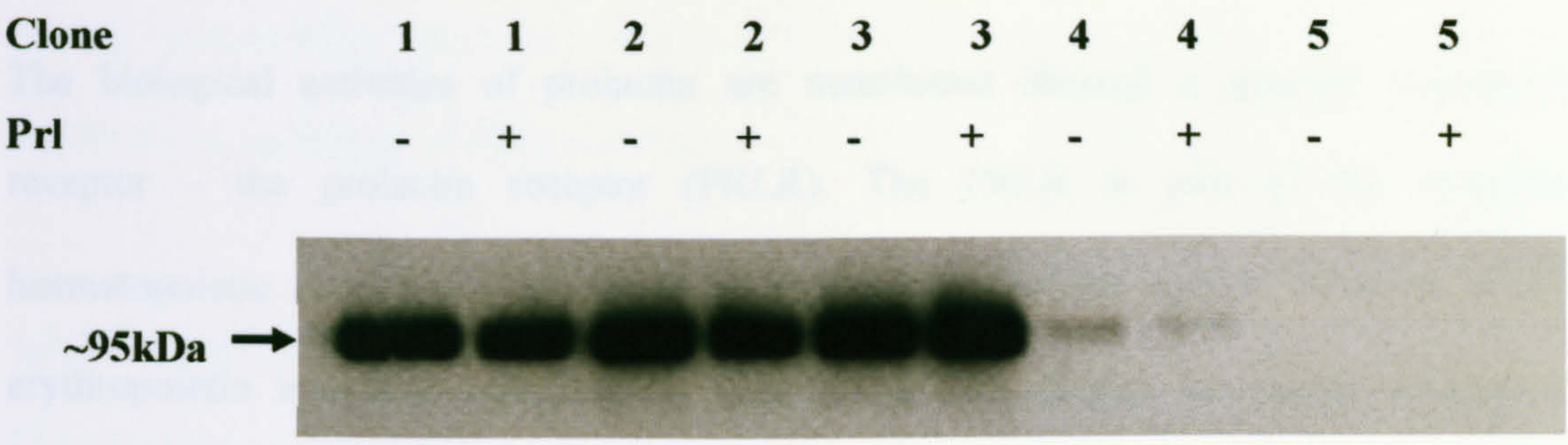

Figure 4.12 Attempt to detect presence of Flag-tagged PrlR by activation of the STAT5 protein.

CEM-C7 cells have no known receptor for the activation of STAT5, thus any activation detected can be attributed to a stably incorporated Flag-PrlR. Clones ($3x10^6$) were serum starved for 24 hours prior to treatment without or with 250ng/ml Prl for 30 min. The cells were then lysed and crude extracts electrophoresed. Western blotting was performed with anti-STAT5b (C-17 antibody).

4.2 DISCUSSION

The biological activities of prolactin are manifested through a specific membrane receptor – the prolactin receptor (PRLR). The PRLR is part of the cytokine haematopoietic superfamily of receptors, which includes the growth hormone (GH), erythropoietin and IL-2 receptors[274]. Members of this family are single membrane spanning receptors organized into three domains: an extracellular ligand binding domain, a hydrophobic transmembrane domain and an intracellular signaling domain containing a proline rich motif[217].

Different forms of the receptor exist. A long (90kDa) and a short (40kDa) form – each generated by differential splicing of a single gene, differing only in the length of the cytoplasmic domain[275]. The intermediate form is a deletion mutant of the long form which in the rat lacks 198 amino acids in its cytoplasmic region. This is the form found in rat Nb2 lymphoma cells and is the most responsive to prolactin[276]. There is also evidence for the presence of this form in some human breast cancers[211]. Both the long and intermediate forms transduce a differentiation signal as measured by induction of milk protein expression[277], and all three promote mitosis[278,279].

4.2.1 Signalling Pathways for Prolactin

When prolactin associates with its receptor, it induces sequential receptor dimerization with the active complex involving one prolactin molecule bound to two receptor molecules[237,264,280], resulting in a cascade of intracellular events. In mammary epithelial cells, prolactin has been shown to activate several signaling pathways (Jak-STAT

pathway[281], Ras-MAP pathway[282], PI-3 kinase pathway, PKC pathway[237] and the FAK-paxillin pathway[283]) which are likely to contribute to the different responses e.g. proliferation, apoptosis or differentiation.

4.2.2 The JAK/STAT Pathway

The prolactin receptor does not have its own kinase activity and thus has to recruit other kinases in order to transduce intracellular signals. Jak2, a member of the Janus family of kinases, is constitutively associated with the prolactin receptor and undergoes phosphorylation when prolactin binds[284]. The Jak2 kinase is transphosphorylated and activated as a result of receptor dimerization[285]. Once activated, Jak2 then phosphorylates tyrosine residues of the PRLR cytoplasmic domain[286]. The phosphorylated tyrosine residues serve as docking sites for the –SH2 domains of STAT5 proteins, bringing STAT5 protein into close proximity with Jak2. STAT5 is then activated by phosphorylation by Jak2, released from the receptor, undergoing homodimerization before translocation to the nucleus where STAT5 dimers regulate transcription of their target genes[287] (Fig. 4.13). Two isoforms of STAT5 have been identified, STAT-5a and STAT-5b[288]. In mouse models, STAT-5a is required for full lobuloalveolar development[289].

We wished to investigate further the possible role of the Jak2/STAT5 pathway in survival signalling that had been studied in the previous chapter using breast cancer cells. The small and variable amount of apoptosis detectable in these cells led us to consider investigating this effect in another cell line where apoptosis could be more readily

induced and detected. The CEM-C7 cell line was selected because these cells apoptose readily when exposed to dexamethasone. We first confirmed that the components of the Jak2/STAT5 pathway were present in these cells (Figs. 4.1 & 4.2). Then, to provide a means for activating the Jak2/STAT5 pathway in these cells, we proceeded to create clones stably expressing the prolactin receptor.

For these studies, a plasmid containing the Flag-tagged prolactin receptor and a selection cassette was first created (Fig.4.3). Luciferase reporter assays showed that while the newly constructed plasmid did respond to prolactin stimulation, it appeared to have decreased signalling ability (Fig. 4.6), and to be expressed at much lower levels compared to the original pAdlox-FlagPrlR plasmid (Fig. 4.7), even though the Flag-tagged receptor was detectable on a Western blot.

Disappointingly, the pCMV-FlagPrlR plasmid created did not appear to be expressed as efficiently as the original pAdlox-FlagPrlR plasmid. When transfected into HEK-293 cells, the protein is detectable by its Flag-tag on western blots, and runs at the correct molecular weight (Fig. 4.5). The pCMV-FlagPrlR, pAdlox-FlagPrlR, and the wild type PrlR all contain the CMV promoter driving transcription, thus transcription rates of these plasmids in the COS-7 cells should be similar. It may be, therefore, that a mutation which affected expression was introduced inadvertently.

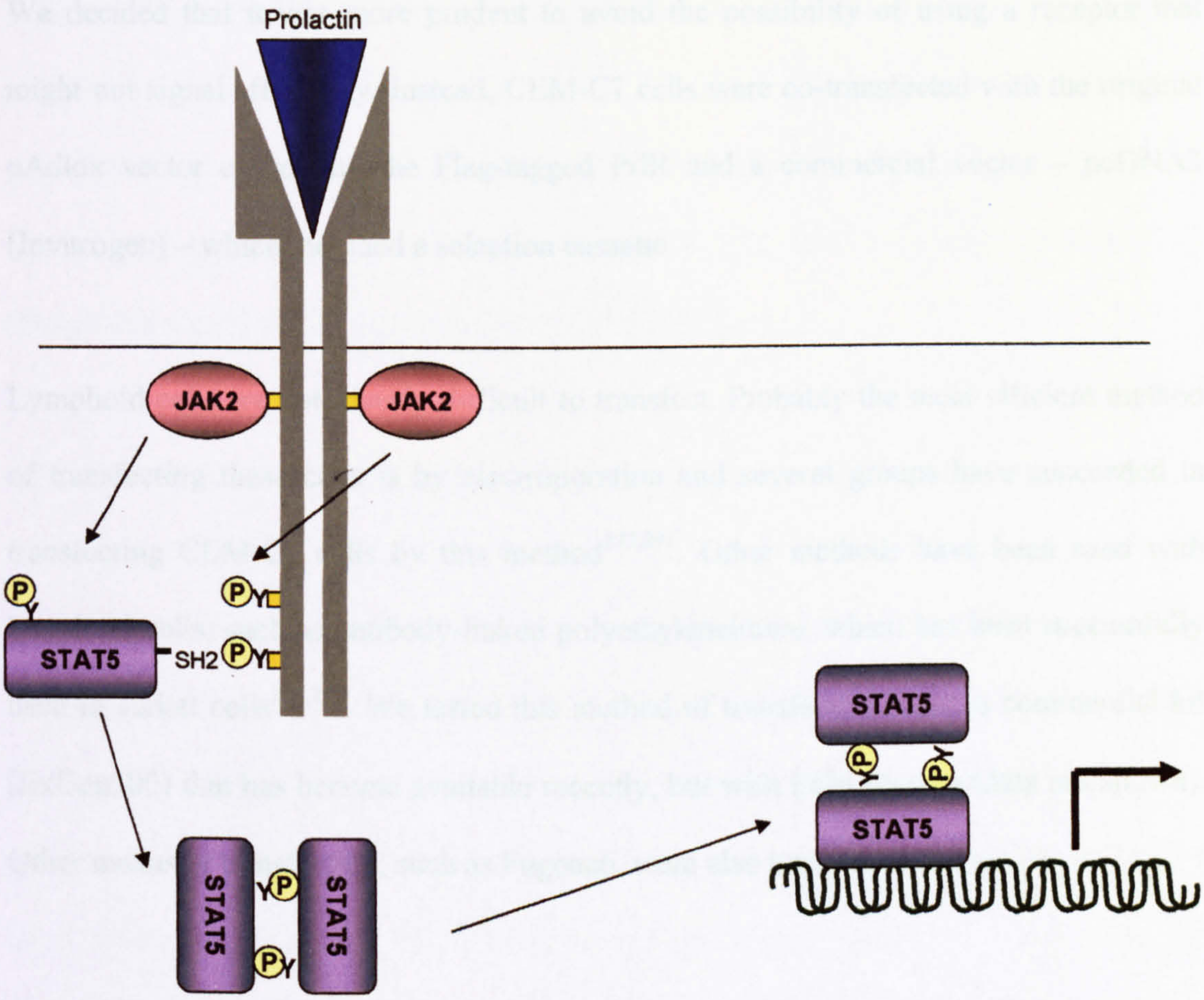

Figure 4.13 The JAK/STAT Signalling Pathway activated by the prolactin receptor (based on Bole-Feysot *et al* 1998[237]).

Binding of prolactin induces dimerization of the receptors. Constitutively associated Jak2 kinases are activated and induce tyrosine phosphorylation of tyrosine residues on the cytoplasmic tail of the receptor, which act as a docking site for STAT5 protein via the SH2 domains. STAT5 then undergoes transphosphorylation by JAK2 and activated STAT5 is released into the cytoplasm. Activated STAT5 homodimerizes, translocates to the nucleus where it binds DNA and regulates target gene trasncription[290].

We decided that it was more prudent to avoid the possibility of using a receptor that might not signal efficiently. Instead, CEM-C7 cells were co-transfected with the original pAdlox vector expressing the Flag-tagged PrlR and a commercial vector – pcDNA3 (Invitrogen) – which included a selection cassette.

Lymphoid cells are notoriously difficult to transfect. Probably the most efficient method of transfecting these cells is by electroporation and several groups have succeeded in transfecting CEM-C7 cells by this method[273,291]. Other methods have been used with lymphoid cells, such as antibody-linked polyethyleneimine, which has been successfully used in Jurkat cells[292,293]. We tested this method of transfection using a commercial kit (ExGen500) that has become available recently, but with little success (data not shown). Other means of transfection, such as Fugene6, were also unsuccessful.

Successful transfection of the CEM-C7 cells was achieved, at low efficiency, using electroporation. Of the G418 sensitive clones tested, clear evidence of transfection was obtained with only one clone (CEM-C7.21D) (Fig. 4.9), and all subsequent transfections were performed with this clone of CEM-C7 cells.

Two separate attempts were made at transfecting the CEM-C7.21D cells with Flag-tagged prolactin receptor, but we were unable to isolate a single clone in which the Flag-tagged protein was detectable on Western blotting. We also attempted to detect cell surface expression using the anti-FlagM2 antibody linked to fluoroscein isothiocynate (FITC) (Sigma), but again no clones were detected using this antibody (data not shown).

Evidence from PCR analysis (Fig. 4.11) showed that 12 clones had incorporated the plasmid into their genome, even though the protein did not appear to be expressed, which was consistent with the failure to activate STAT5 by prolactin (Fig. 4.12). It is possible that receptor number on the cell surface was too low for the Flag-signal to be detected, though this should still have resulted in STAT5 activation.

Failure to detect expression of the Flag-tagged receptor could result from defects in transcription of cDNA into mRNA, translation of the mRNA into the desired protein, or expression of the protein at the cell surface. The CEM-C7 cell line is an immortalized cell line and in the course of its development may have lost certain functions that are present in normal lymphoid cells. Alternatively, it is conceivable that some factor(s) could be present in these cells that block transcription of the gene or destabilize the mRNA. At the level of transcription, the cDNA could have been incorporated into a region of the genome that was 'silent', and thus be unable to recruit the DNA transcription machinery. Another possibility is that by some mischance, all the plasmids that incorporated stably into the host genome were not intact or complete (e.g. linearization of the plasmid could have resulted in cleavage of the cDNA sequence), and thus when transcribed, did not give rise to an intact protein.

Another possible explanation for the failure to detect Flag-tagged prolactin receptor could be that there was insufficient Jak2 in CEM-C7 cells. Lodish et al[294] showed that surface expression of the erythropoietin receptor (EpoR) depends on the presence of Jak2. As the prolactin receptor is closely related to the EpoR, the extent to which it is expressed on the

cell surface may also be dependent on the amount of Jak2, and if other cytokine receptors had sequestered all the available Jak2, this may have affected surface expression of the transfected prolactin receptor. If the time had been available, we would have attempted to co-transfect cells with Jak2 cDNA, together with pAdloxFP and pcDNA3, to determine whether this would enhance expression of the prolactin receptor.

Activation of STATs has been observed in many tumours[295-297], and activation of the Jak/STAT pathway has been shown to promote survival pathways[268,298]. Moreover it has been shown that oncogenic activation of STAT, (e.g c-Src or Abl) is sufficient to induce cells to undergo transformation[299,300]. The creation of a cell line where apoptosis could have been inhibited by activation of the Jak/STAT pathway would have been a very useful model to investigate the role of interactions between signalling pathways and other factors involved in deciding whether cells survive apoptotic insults.

Unfortunately, it appears that either (a) by chance, none of those stable cell lines that incorporated cDNA did so in a manner that allowed protein expression, or (b) CEM-C7 cells possess some property that prevents expression of the prolactin receptor. If (a) is true, it should be possible to derive a clone stably expressing the PRLR by continuing the study. However, due to time constraints, we did not feel that it would be profitable to continue these studies.

5 Creation of Stable Breast Cancer Cell Lines Overexpressing STAT5

5.1 Overexpression of STAT5 in T47-D and MCF-7 breast cancer cell lines

Two closely related transcription factors, STAT5a and STAT5b, mediate signalling by the prolactin receptor. Both are actively involved in organ development and maturation; functions which have been definitively demonstrated by gene knockout studies[301]. STAT5a-knockout mice exhibit defective development of the mammary gland, and impaired lactation when the mice are pregnant[302]. The phenotype displayed is similar to that of prolactin receptor knockouts[303]. Mice that are STAT5b -/- display a phenotype similar to that induced by a defective growth hormone receptor[304]. Mice lacking both STAT5a and STAT5b are infertile, and also have defective immune functions[305].

A role for STAT5 in cell cycle progression and survival has begun to emerge, and a number of target genes have been identified, including cyclin-dependent kinases (cdks), G1 cyclins, and cdk inhibitors[306,307]. Several studies have provided strong evidence that STAT5 is involved in anti-apoptotic signalling in haematopoietic cells[246,268,308], and STAT5 has also been shown to induce Bcl-X_L and Bcl-2 proteins, both of which are anti-apoptotic[268,309-312]. Likewise, constitutive STAT activation has been documented in many malignancies, mostly as a consequence of upstream oncogene activation – e.g. STAT5 in lymphoproliferative disorders activated by BCR-Abl[243,313] and STATs 1, 3, and 5 are activated in mammary / lung tumours[314,315].

Based on the above findings, we hypothesized that activation of STAT5 by the prolactin receptor could also be involved in anti-apoptotic signalling in breast cancer cells. To test

this hypothesis, we decided to overexpress STAT5a and STAT5b in breast cancer cells to determine whether or not the survival effect of prolactin could be enhanced.

5.2 RESULTS

5.2.1 Transient Overexpression of STAT5b in T47-D and MCF-7 Breast Cancer Cells

This experiment was performed to ensure that endogenous STAT5 is not already present in sufficient quantity to provide a maximal signal in T47-D or MCF-7 cells. Thus $3x10^4$ cells (per well) were plated out in 48-well plates and incubated overnight. The cells were transfected with LHRE reporter (200ng) and either 200ng pcDNA (empty plasmid for control) or 200ng STAT5b expression vector using FuGENE 6. The cells were incubated for 24 hours to allow for gene expression, and serum starved for 6 hours before the addition of 250ng/ml prolactin for a further 18 hours. Luciferase activity in cell lysates was then measured using a Dynex luminometer.

From Fig. 5.1, it can be seen that overexpression of STAT5b in T47-D cells results in a marked increase in activation of the LHRE STAT5 reporter gene (from 130±9(SD) to 790±118(SD) arbitrary units, p value<0.05) in the presence of prolactin. In MCF-7 cells, there was also a clear increase (from 216±27(SD) to 749±39(SD), p<0.05), though less than that seen with T47-D cells. Interestingly, in the MCF-7 cells, the basal activity (216±27(SD) without prolactin stimulation) of the LHRE reporter is very much higher than that observed in the T47-D cells (130±9(SD)).

5.2.2 Creation of Breast Cancer Cell Lines Stably Overexpressing STAT5

Since transient transfection with STAT5 increased the signalling activity of the LHRE reporter, we decided to create breast cancer cell lines stably overexpressing either STAT5a or STAT5b to assess the effect of increased levels of activated STAT5 on proliferation and survival in response to prolactin. We initially transfected the breast cancer cells with the HA-STAT5b plasmid as we have had previous experience working with this construct, and have detected it on Western blotting both in crude extracts and by immunoprecipitation.

T47-D and MCF-7 cells ($5x10^5$) were plated onto 6-well plates and incubated overnight. The cells were co-transfected with 1μg HA-tagged STAT5b plasmid and 1μg pcDNA3.1 plasmid, which provided the selection marker, using Fugene 6 as the transfection agent. The cells were incubated for 48 hours to allow for gene expression before the medium was replaced with medium supplemented with G418 (1200μg/ml) to select transfected cells that had stably incorporated the pcDNA3.1 plasmid. The cells were maintained in this medium for 2 weeks, when the G418 concentration was decreased to 400μg/ml.

Following the selection of resistant cells by G418, STAT5b-transfected cells were serially diluted and seeded into 96-well plates to obtain monoclonal populations of cells. Cells were incubated for 2 weeks and colonies transferred to T25 flasks, with 400μg/ml G418 to provide a selection pressure. A total of 13 colonies were derived from the MCF-7 line and 9 colonies from the T47-D line.

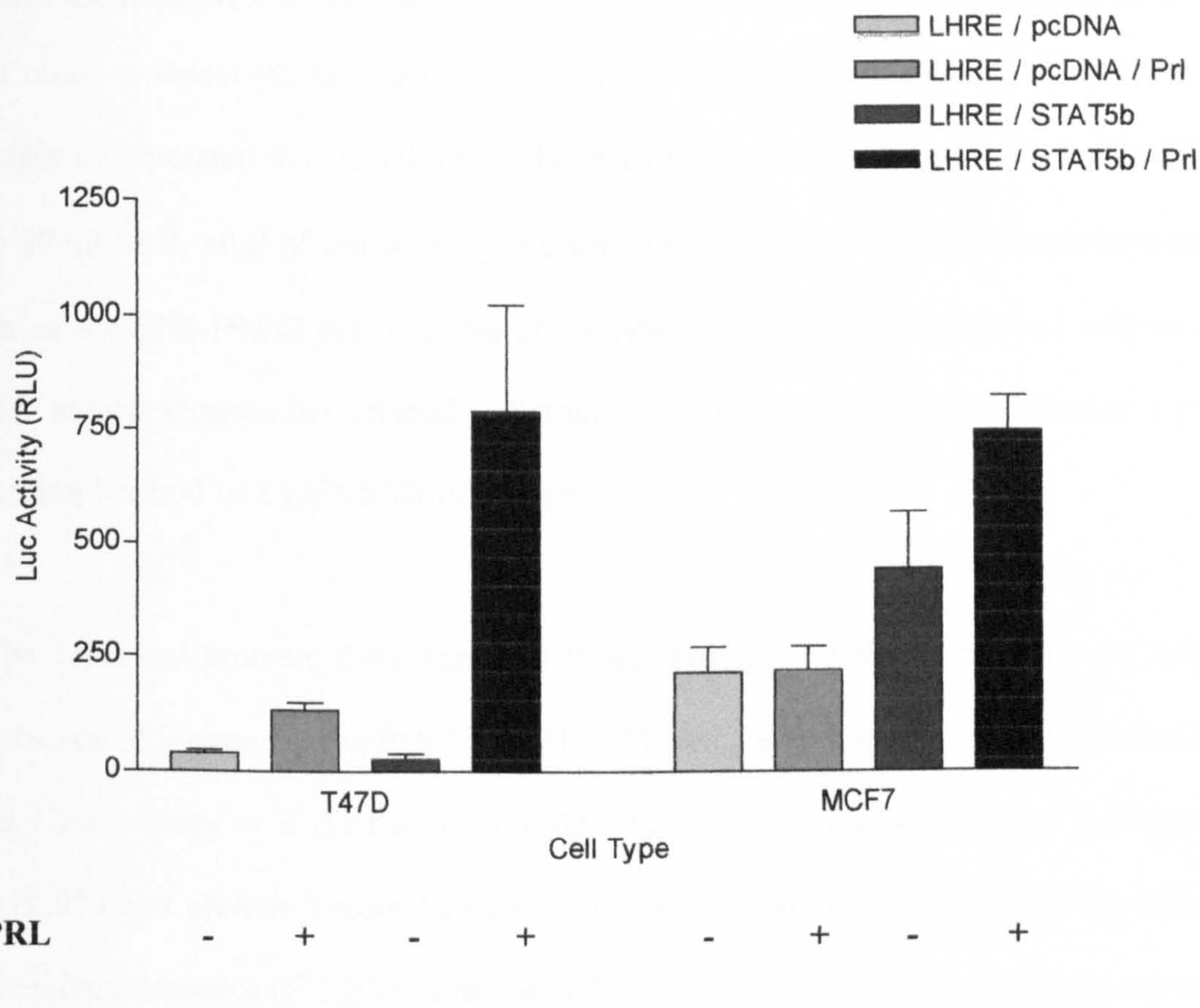

Figure 5.1 Enhanced activation of a STAT5 reporter by prolactin in T-47D and MCF-7 cells transiently overexpressing STAT5b.

T-47D or MCF-7 cells were co-transfected with LHRE reporter plasmid (200ng) and either pcDNA3.1 (control vector, 200ng) or STAT5b plasmid (200ng). 24 hours post transfection, cells were treated without or with prolactin (200ng/ml) for 18 hours before measurement of luciferase activity.

5.2.3 Detection of Transfected STAT5b in Breast Cancer Cells by Western Blotting

In order to detect the presence of the HA tag linked to STAT5b in colonies that had stably incorporated STAT5 cDNA, $5x10^6$ cells from each clone were collected and lysed in 500µl SLB. 40µl of the crude lysate was denatured with 2xSSB and electrophoresed on an 8% SDS-PAGE gel. The rest of the lysate was immunoprecipitated with an anti-HA mouse monoclonal antibody (Sigma) (1:1000) and immunoprecipitated proteins electrophoresed on an 8% SDS-PAGE gel.

The separated proteins were semi-dry transferred to Immobilon-P membrane and the presence of immuno-precipitated HA-STAT5b detected using anti-STAT5b antibody C-17 (Santa Cruz) at a dilution of 1:2000. Goat anti-mouse antibody at a dilution of 1:10,000 was used as a secondary antibody. The blot was developed using the enhanced chemiluminescence (ECL) kit from Amersham. Using this method, two clones expressing the HA tag were detected – one T47-D clone, designated T47-D.st5b1, and one MCF-7 clone, designated MCF-7.st5b1 (see Fig. 5.2). Comparing the two clones, there appears to be a greater expression of STAT5b in the T47-D clone, T.st5b1, compared to the MCF-7 clone, M.st5b1.

5.2.4 Effect of Stable STAT5b Expression on Signalling Activity

To determine whether stable incorporation of STAT5b increased prolactin signalling activity via the STAT5 pathway, activation of transiently expressed LHRE reporter in response to prolactin was assessed.

Each clone was seeded in a 24-well plate ($5x10^4$ cells in 1 ml) and incubated overnight. Cells were transfected with 200ng of LHRE reporter using Fugene 6 and incubated overnight. The cells were then serum-starved for at least 6 hours before treatment with or without 250ng/ml prolactin for 18 hours. The cells were then lysed and luciferase activity measured using the Dynex luminometer.

As shown in Fig. 5.3, both clones with stably incorporated STAT5b cDNA show increased activation of the LHRE STAT5 reporter gene compared to the untransfected parent cell lines. In the parent T47-D cells, luciferase activity increased from 5±3(SD) to 14±3(SD) ($p<0.05$). In clone T.st5b1, luciferase activity increased from 6±3(SD) to 314±71(SD) ($p< 0.05$).

In the MCF-7 untransfected parent line, there was only a very small increase in luciferase activity when cells were stimulated with prolactin (from 552±113(SD) to 680±56(SD), not significant), which was not unexpected due to the low level of prolactin receptor expressed by these cells. The MCF-7 clone stably expressing STAT5b (M.st5b1), on the other hand, showed a small increase in luciferase activity when stimulated with prolactin (423±64(SD) to 743±168(SD), $p<0.05$)), though this effect was largely due to a decrease in basal activity. Again, it should be noted that, compared to T47-D cells, the basal level of STAT5 signalling is much higher in MCF-7 cells, and its STAT5b clone, M.st5b.1.

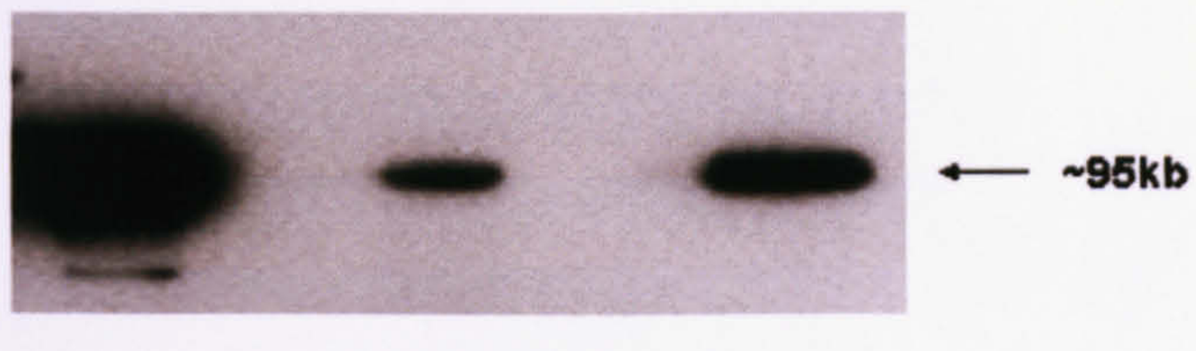

Figure 5.2 Detection of HA-STAT5b in T47-D and MCF-7 clones by Western blotting.

$5x10^6$ cells from each clone were lysed, and the crude extract was immunoprecipitated with the anti-HA antibody, and the proteins separated by electrophoresis. This blot was then probed with anti-STAT5b antibody (C-17, Sigma). Positive (+ve) and negative (-ve) controls are crude extracts from COS-7 cells transfected with and without STAT5b respectively.

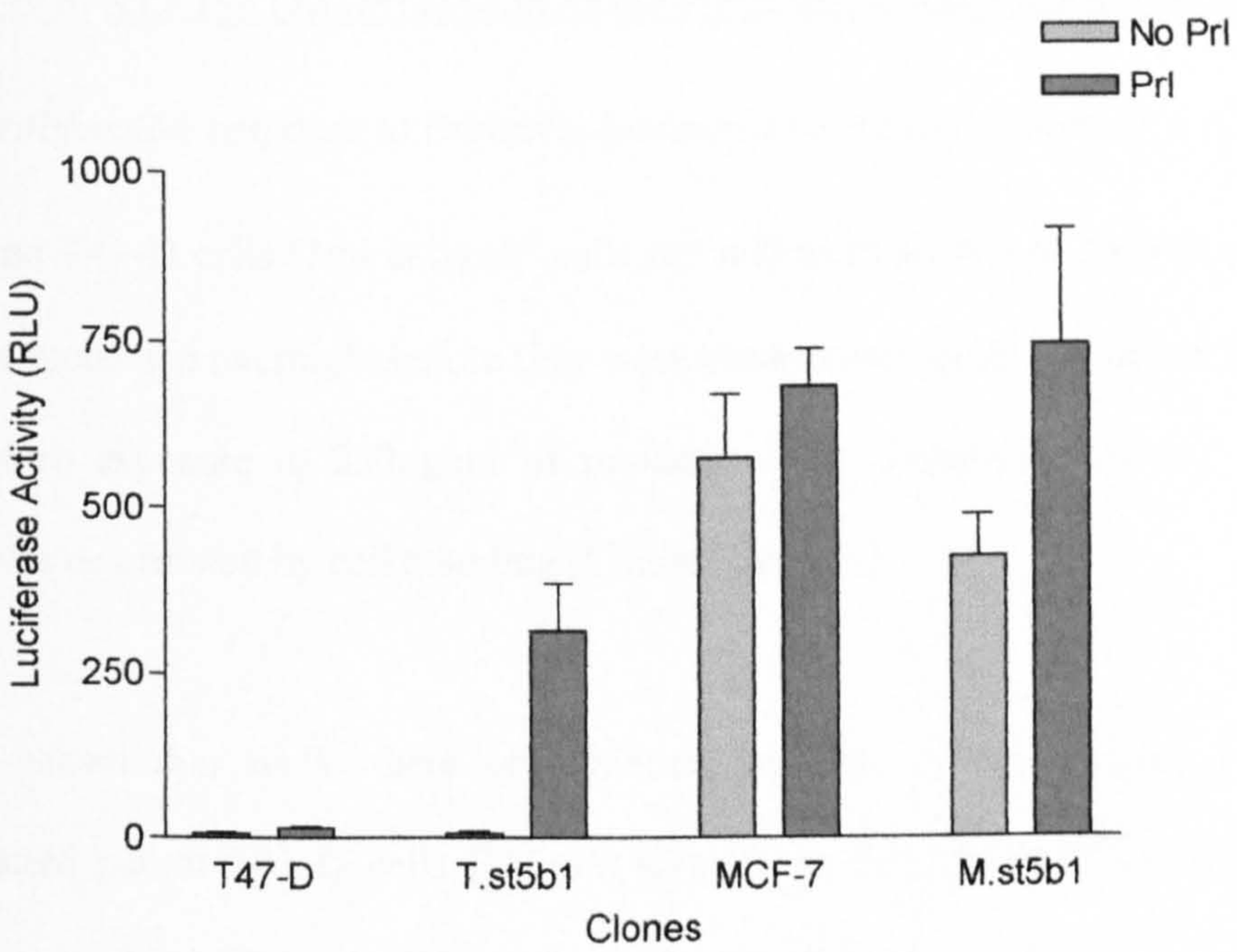

Figure 5.3 Effect of stable overexpression of STAT5b on the ability of prolactin to activate the LHRE reporter.

Parental T47-D and MCF-7 cells, together with clones overexpressing STAT5b, were seeded in complete medium and incubated overnight. The cells were then transfected with the LHRE reporter and incubated for 24 hours before being serum starved for 6 hours. Finally, cells were incubated in the absence or presence of 250ng prolactin for a further 18 hours. The results shown are from a typical experiment, which gave similar results on four separate occasions.

5.2.5 Effect of STAT5b Overexpression on the Proliferative Response to Prolactin

5.2.5.1 Proliferative response to Prolactin Measured Using Cell Counting

MCF-7 and T47-D cells (1ml at $5x10^4$ cells per ml) were seeded in 24-well plates. The cells were incubated overnight before they were washed and serum starved in SFM for 24 hours before exposure to 250ng/ml of prolactin. After incubation for 4-5 days, cell number was determined by cell counting (Coulter Counter).

Fig. 5.4 shows that while there is a modest increase in proliferation rate in the untransfected parent T47-D cells [(43 ± 19(SD)$x10^4$ to 50 ± 2(SD)$x10^4$) cells per well], prolactin actually inhibits proliferation of the T.st5b1 clone. As expected, there is minimal effect of prolactin on the proliferative rate of MCF-7 cells, which may reflect the lower number of prolactin receptors in these cells. Neither was there any proliferative effect of prolactin on the M.st5b1 clone. This experiment was performed 4 times and a typical set of results is shown. From the graph, it can be seen that while the parent T47-D cell line exhibits a mild proliferative effect in response to prolactin, neither the untransfected MCF-7 parent line or either of the STAT5b clones showed any increase in proliferative rate when compared to cells not exposed to prolactin.

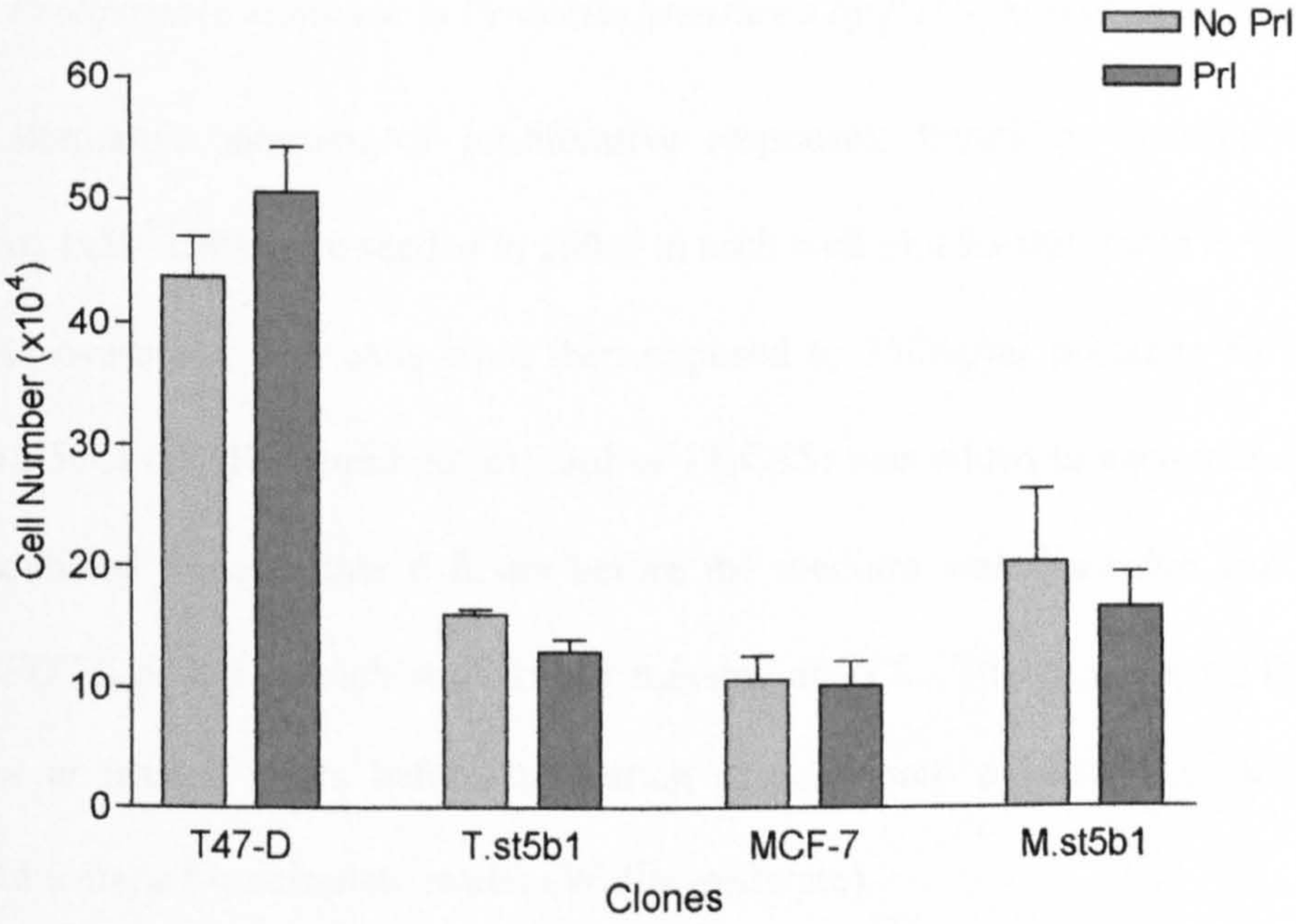

Figure 5.4 Proliferation of clones stably expressing STAT5b as assessed by cell counting.

Cells from the STAT5b clones and both untransfected T47-D and MCF-7 parent lines were serum starved for 24 hrs before exposure to 0ng or 250ng of prolactin for 5 days. Cells were then harvested and counted on the Coulter Counter to assess proliferation. This figure is a typical experiment, which was performed on 4 separate occasions.

5.2.5.2 Proliferative response to Prolactin Measured by [^{3}H]-Thymidine Incorporation.

As an alternative measure of proliferative responses, thymidine incorporation was measured. $1x10^5$ cells were seeded in 100µl in each well of a 96-well plate in 1%CSS and incubated overnight. The cells were then exposed to 250ng/ml prolactin for 18 hours before 12.5nCi of [^{3}H]thymidine (in 20µl of 1%CSS) was added to each well. The cells were incubated for a further 6 hours before the medium was discarded and 100µl of trypsin-EDTA added to each well for 30 minutes at 37°C. The plates were frozen at –20°C for at least 3 hours before harvesting of cells onto a filter mat. Activity was measured using a β-microplate reader (Wallac software).

Fig. 5.5 shows that prolactin increases [^{3}H] thymidine incorporation in the untransfected T47-D cells by ~36% (from 11190±850(SD) to 16640±1330(SD) $p<0.05$). In agreement with results obtained with cell counting, (Fig. 5.4) prolactin did not result in a significant increase in thymidine incorporation in the T.st5b1 clone. Again, no response was detected in the MCF-7 parent line, or in its derivative, M.st5b1.

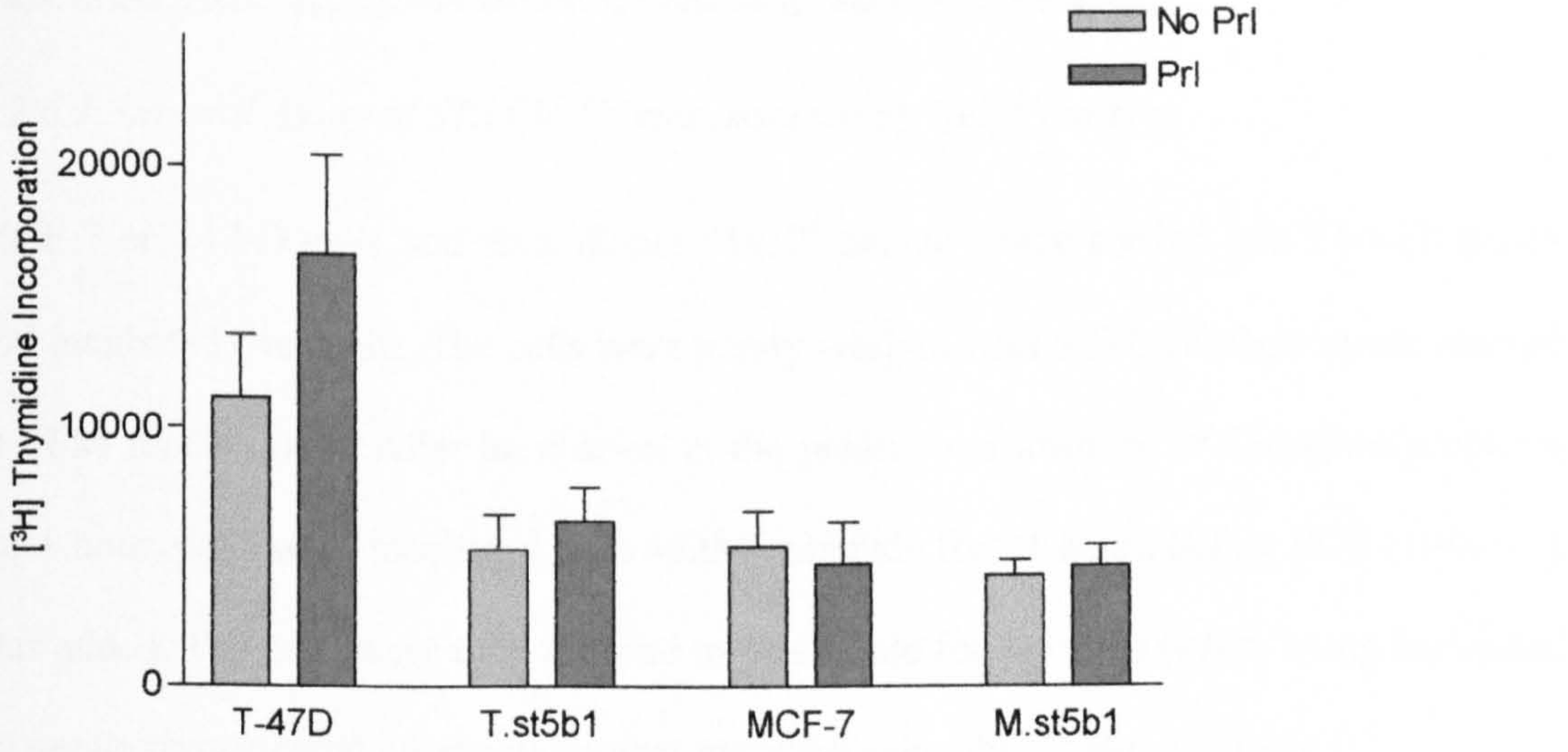

Figure 5.5 Effect of overexpressed STAT5b on [^{3}H] thymidine incorporation in response to prolactin stimulation.

T47-D, MCF-7, T.st5b1 and M.st5b1 cells were seeded in 1%CSS and incubated overnight. They were then exposed to 0ng or 250ng of prolactin for 18hrs before the addition of [3H] thymidine. Thymidine incorporation was allowed to continue for 6 hours, after which cells were lysed, harvested and the radioactivity measured on a β-microplate reader. This experiment was performed 3 times and the figure shows the results from a typical experiment.

5.2.6 Does STAT5b Protect Breast Cancer cells against Apoptosis?

5.2.6.1 Survival Assay of STAT5b Clones assessed by Cell Counting.

MCF-7 or T47-D cells and their clones ($5x10^4$ per ml) were seeded into 24-well plates and incubated overnight. The cells were gently washed with SFM and then serum starved in SFM for 24 hours. After incubation in the presence or absence of 250ng/ml prolactin for 1 hour, cells were incubated with 40μM ceramide for 24 hours before FCS (10% v/v) was added. The cells were then allowed to proliferate for 4-5 days before being harvested by gentle trypsinization and cell number assessed using the Coulter Counter.

From Fig. 5.6, it can be seen that the presence of overexpressed STAT5b in either the T47-D or the MCF-7 cell lines does not confer a survival advantage in ceramide-induced cytotoxicity. In fact, contrary to expectations, there appears to be a survival disadvantage, in the T47-D STAT5b overexpressing clone, T.St5b1. In the untransfected T47-D parent cells, treatment with ceramide decreases the cell population (from $78\pm2(SD)x10^4$ to $17\pm1(SD)x10^4$, ~21% of the untreated population) while in the STAT5b clone, the cell number decreases from $67\pm7(SD)x10^4$ to $7\pm1(SD)x10^4$ (~10% of the untreated population), a greater loss in cell number than that in the untransfected cells ($p<0.005$). Moreover, in the STAT5b over-expressing cells exposed to both ceramide and prolactin, the cell number decreases further to $5\pm1(SD)x10^4$ (~8% of the untreated population).

In MCF-7 cells, and the corresponding STAT5b clone (M.St5b1), prolactin had no effect on survival.

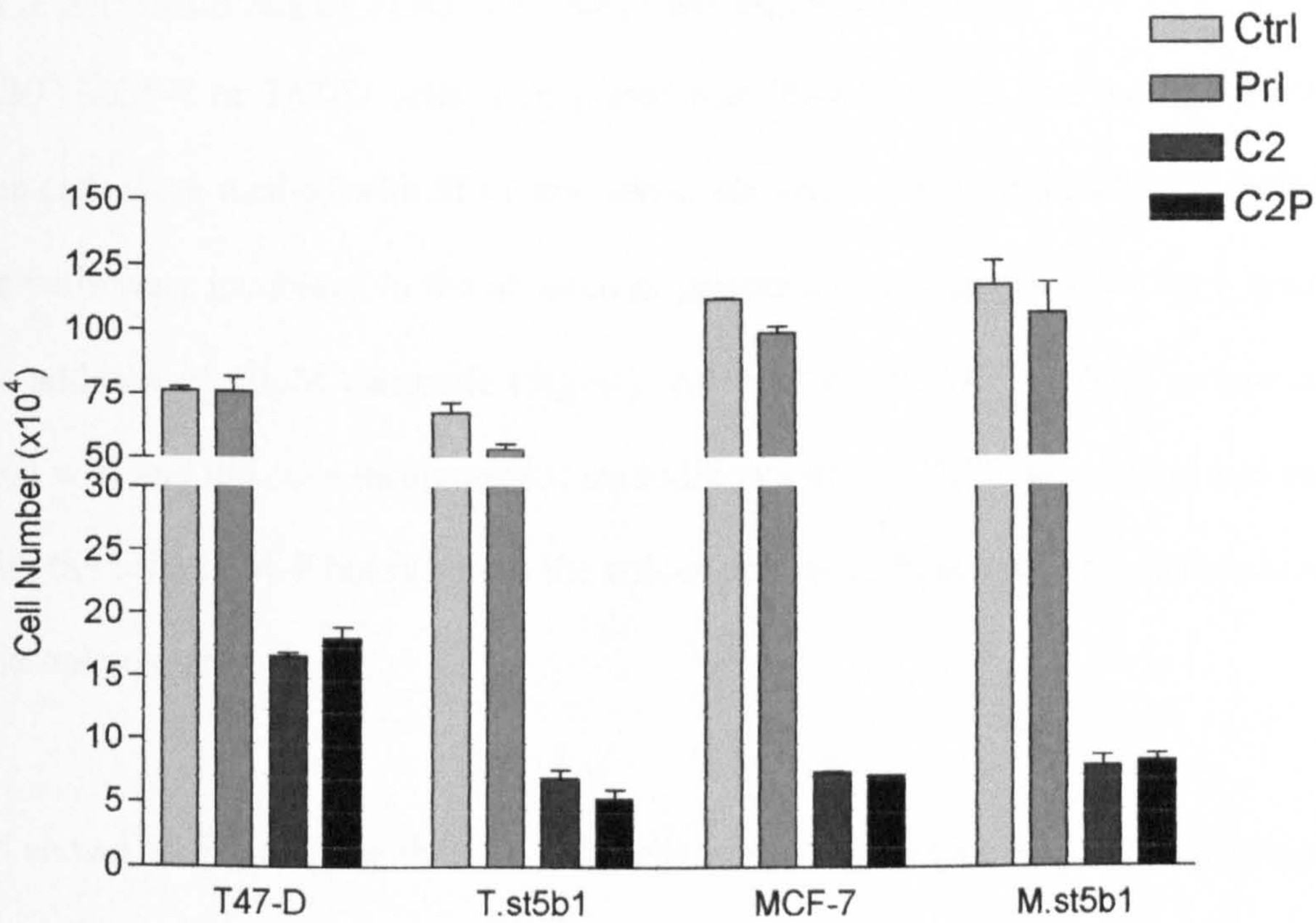

Figure 5.6 Effect of prolactin on survival of STAT5b expressing clones following ceramide exposure, assessed by cell counting.

T-47D, MCF-7, T.st5b1 or M.st5b1 cells were serum starved for 24 hrs before exposure to the absence or presence of 250ng/ml prolactin for 1 hr. The cells were then exposed to 0μM or 30μM ceramide for 24 hrs prior to being 'rescued' by 10%FCS (v/v). The cells were allowed to proliferate for 4-5 days before they were trypsinized and the cell number counted by the Coulter counter. This experiment was performed 3 times, and the results shown are from a typical experiment.

5.2.7 Survival Assay of STAT5b Clones assessed by XTT assay

$1x10^4$ MCF-7 or T47-D cells were plated into 96-well plates and incubated overnight. The cells were washed with SFM, and serum starved in SFM for a further 24 hours. Next, the cells were incubated in the absence or presence of 250ng prolactin for 1 hour before the addition of 40μM ceramide (Sigma). After 24 hours, FCS (10% v/v) was added to each well and the cells incubated for an additional 4 days. XTT was added and incubated with the cells for 4-8 hours before the colour density (570nm) was measured on a Dynex microplate reader.

As shown in Fig. 5.7, neither MCF-7 cells nor the corresponding clone overexpressing STAT5 (M.st5b1) display a response to prolactin treatment. Fig. 5.7 also shows that in T47-D cells ceramide decreases the absorption at 470nm to ~30% of the control. As with the previous assay, ceramide exposure decreases the absorption at 470nm in the STAT5b clone further, to ~11% of control cells ($p<0.05$). Again, a greater decrease than that recorded for the untransfected parent cells. The presence of prolactin, as before, does not appear to contribute to the survival of the STAT5b over-expressing cells.

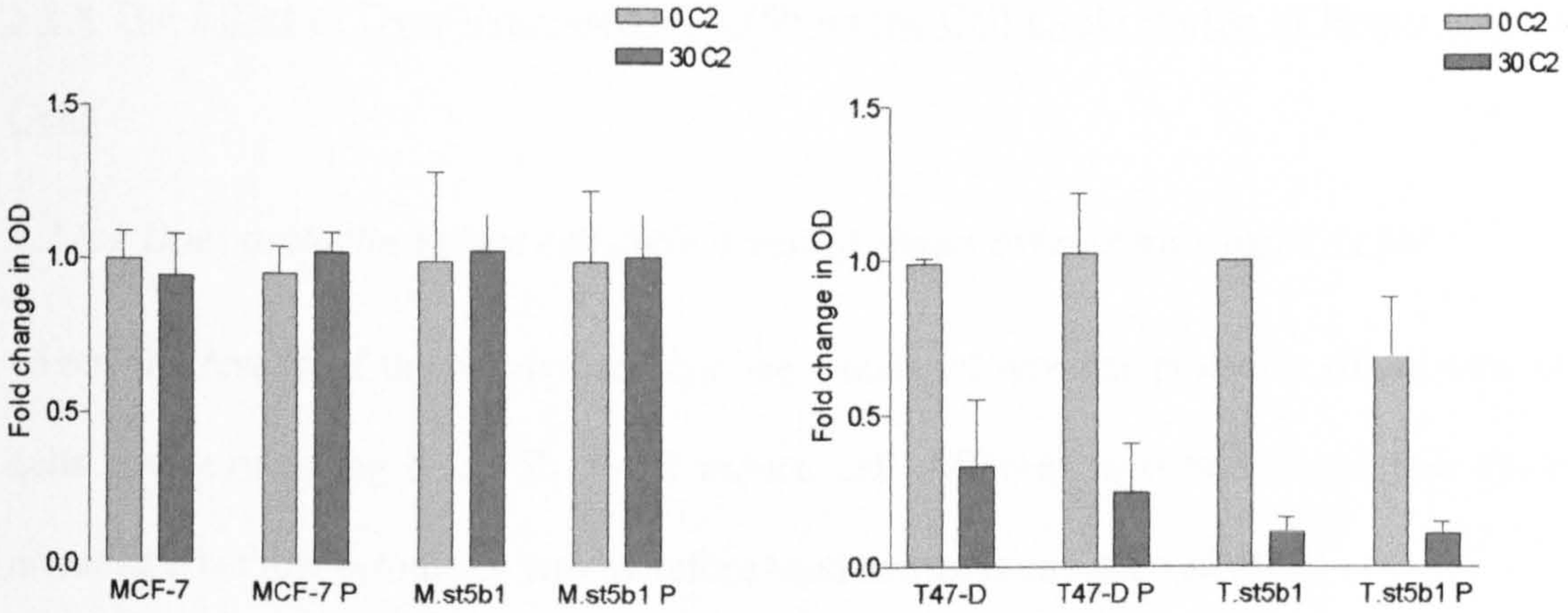

Figure 5.7 Effect of prolactin on survival of STAT5b expressing clones following ceramide exposure, assessed by XTT assay.

T47-D, MCF-7 and their STAT5b clones were plated into 96-well plates and the cells incubated overnight. The cells were serum-starved for 24 hours before exposure to 0ng/ml or 250ng/ml prolactin for 1 hour. The cells were then incubated in 0μM or 40μM for 24hrs and then 'rescued' with 10%FCS (v/v). The cells were allowed to proliferate for 4-5 days before the addition of XTT, and the absorption at 470nm recorded. This was performed 3 times, and the figure shown represents a typical experiment. In each case, parental cells in the absence of ceramide are arbitrarily set at the value of 1.

5.2.8 The Effect of Over-Expressed STAT5b on the Cell Cycle Profile of Breast Cancer Cells

5.2.8.1 Does prolactin induce cell cycle arrest of clones over-expressing STAT5b?

Given the results of the survival assays, we wondered whether prolactin stimulation of cells over-expressing STAT5b could induce cell differentiation and hence cell cycle arrest in G1. Flow cytometry was therefore used to assess any such effect.

$3x10^5$ cells (T47-D, MCF-7 and their STAT5b clones) were each seeded into 6-well plates. The cells were serum starved for 24 hours prior to exposure to vehicle or 250ng/ml prolactin for a further 48 hours. The cells were then collected, stained with propidium iodide, and the cell cycle analysed by flow cytometry.

Fig. 5.8 shows that serum starvation induces a greater G1 arrest in the T.st5b1 clone, with 80±0.4% (SD) of the cells in G1, compared to 60±2% (SD) of the parent T47-D cells ($p<0.0001$). The presence of prolactin does not alter this change. In the MCF-7 cells and the M.st5b1 clone, there is no cell cycle arrest, and prolactin does not alter the cell cycle dynamics.

5.2.9 Attempts to Create Stable Breast Cancer Cell Lines Overexpressing STAT5a

Next, we attempted to create stable cell lines overexpressing the STAT5a protein.

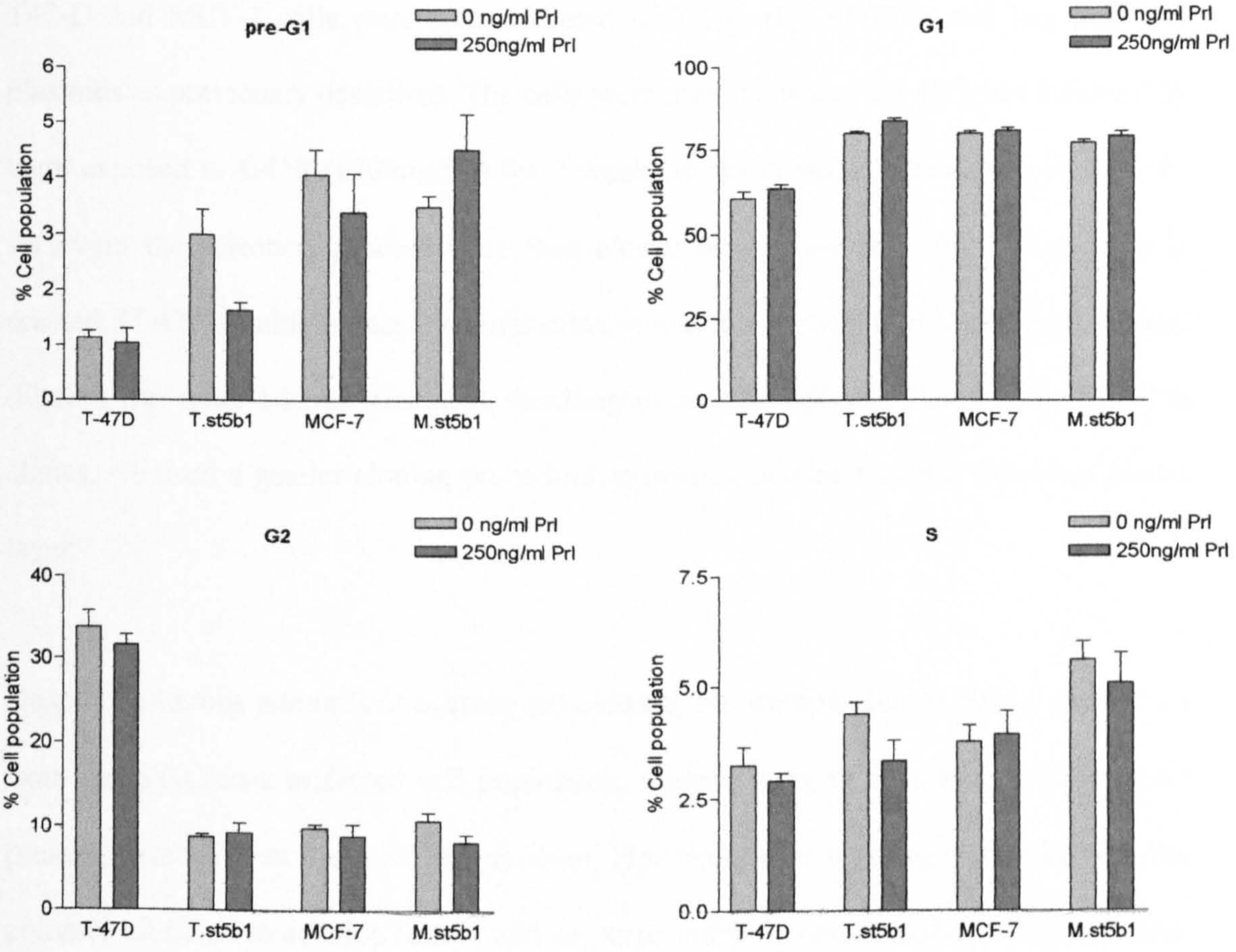

Figure 5.8 Effect of prolactin on the cell cycle profile of STAT5b overexpressing breast cancer clones assessed by flow cytometry.

T47-D, MCF-7, T.st5b1 and M.st5b1 cells were plated onto 6-well plates. The cells were serum starved for 24 hours and then exposed to the absence or presence of 250ng/ml prolactin for a further 24 hours before they were analysed by flow cytometry.

T47-D and MCF-7 cells were co-transfected with 1μg HA-STAT5a and 1μg pcDNA3 plasmids as previously described. The cells were then incubated for 48 hours before they were exposed to G418 (1200μg/ml) for 2 weeks to select stably transfected cells. Cells surviving the selection process were then cloned in agarose gels. We had previously created STAT5b stable clones by serial dilution and it was evident that cloning by serial dilution was quite a harsh treatment, resulting in very few clones. Thus for the STAT5a clones, we used a gentler cloning procedure, providing nutrients with a fibroblast feeder layer.

Despite numerous attempts at agarose gel cloning, we were unable to obtain any clones from the STAT5a-transfected cell population. Observations showed that colonies were present, detectable at the microscopic level. However, after reaching a certain size, the colonies all failed to develop further and we were unable to obtain clones of breast cancer cells stably over-expressing STAT5a.

5.2.10 Detection of STAT5a expression by Western blotting

Concurrent to our attempts to create stable cell lines over-expressing the STAT5a protein, we performed transient transfections using the STAT5a and STAT5b plasmids in COS-7 cells to optimize detection of the proteins in stable clones.

COS-7 cells ($5x10^6$) were seeded into 90mm dishes and incubated overnight. The cells were transfected with 5μg of HA-STAT5a using Fugene6 and then incubated for 24 hours before protein extraction. Crude extracts of the cells were denatured and electrophoresed

in an SDS-Page gel. Western blot analysis was performed using anti-HA antibody (clone H7). HA-tagged STAT5b-transfected COS-7 cell extracts were used as a positive control for both the HA-tag as well as protein expression.

As shown in Fig. 5.9, a faint protein band running at a slightly higher molecular weight than STAT5b was detectable in the crude extracts of cells transfected with the HA-STAT5a plasmid. This is consistent with the documented size of the STAT5a protein (94kDa), compared to the 92kDa molecular weight of STAT5b[316]. Expression of the STAT5a protein was considerably weaker, however. Thus, although the two plasmids are similar constructs and under the control of the same promoter (CMV), for an unknown reason STAT5a expression appeared to be at a much lower level, providing a possible explanation for the difficulty in identifying cells stably expressing the protein. Unfortunately, due to lack of time it was not possible to pursue these studies further.

5.3 Discussion

While STAT5 has been shown to be a growth signal transducer in haematopoietic cells[306] and a survival signal transducer in red cell progenitors where it activates the transduction of Bcl-xL[294], whether it plays a similar role in the survival of mammary cancer cells has yet to be determined. In mammary involution, STAT5 activity decreases, whilst that of STAT3 increases[317].

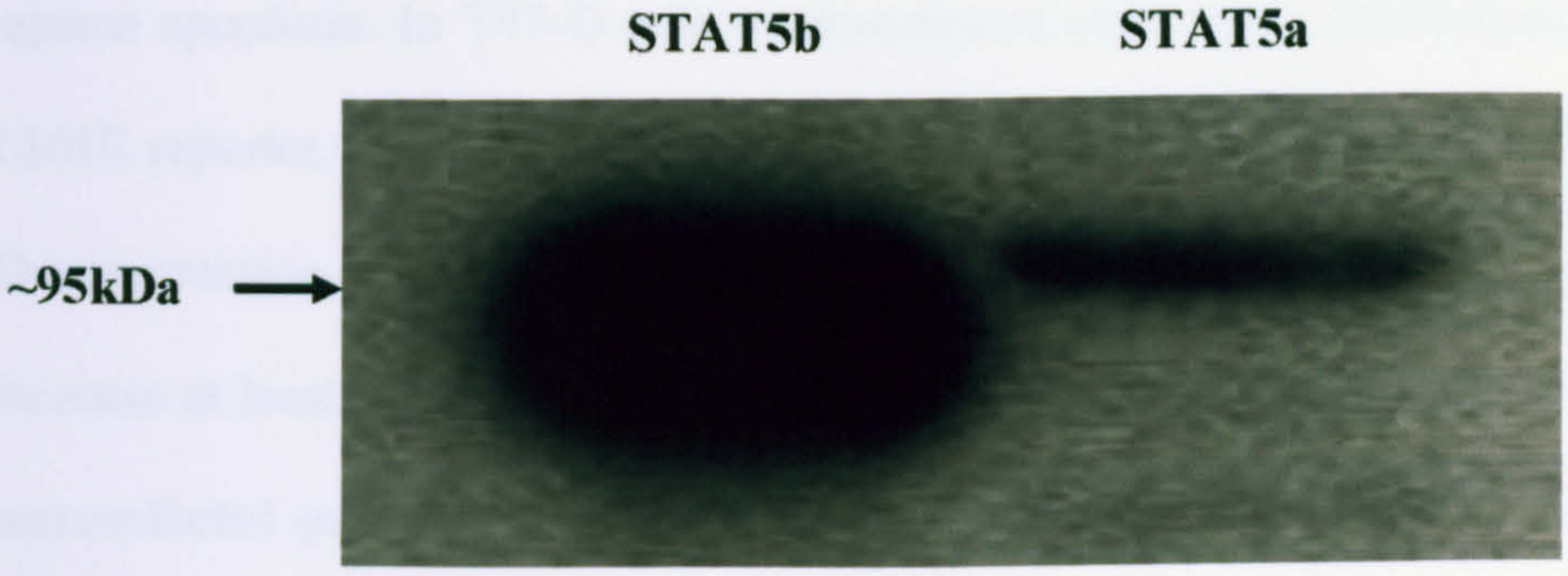

Figure 5.9 Expression of HA-STAT5a and HA-STAT5b in COS-7 cells, assessed by Western blotting.

COS-7 cells were transfected with either HA-STAT5a or HA-STAT5b plasmids. Crude extracts were prepared and electrophoresed. Western blotting was performed using the anti-HA antibody (H7 clone).

The purpose of the work described in this chapter was to determine whether enhancement of the prolactin signalling response could increase the protective effect of prolactin against apoptosis. In T47-D cells co-transfected with empty plasmid (pcDNA) and the LHRE reporter, exposure to prolactin results in a small increase in luciferase activity. Overexpression of STAT5b together with exposure to prolactin causes this activity to increase at least 6-fold. From the results shown in Fig. 5.1, we can conclude that in the untransfected parent cell lines, levels of endogenous STAT5 are a limiting factor for activation of a STAT5 reporter. This increased activation therefore provided an opportunity to investigate the role of STAT5 in prolactin responses of breast cancer cells.

Based on studies in other cell types, we hypothesised that STAT5 is involved in the survival pathway of breast cancer cells. Increasing endogenous levels of STAT5 might therefore be expected to increase signalling along this pathway following prolactin stimulation, and the creation of stable breast cancer cell lines which over-express STAT5 should help to determine whether or not the STAT5 pathway is involved in anti-apoptotic signalling in these cells.

Western blotting (Fig. 5.2) identified clones expressing HA-STAT5b, and LHRE reporter assays confirmed that STAT5b signalling was enhanced compared to that of untransfected parental T47-D cells (Fig. 5.3).

Our original hypothesis was that overexpression of STAT5b would either enhance responsiveness of cells to prolactin (if those responses were mediated by STAT5b), or be

without effect (if signalling pathways other than STAT5 were involved). Contrary to our expectations, the results obtained were not immediately compatible with either of these hypotheses. Figures 5.4 and 5.5 show that while there is a modest increase in proliferation in the untransfected parent T47-D cells, this is not reflected in the T47-D clone overexpressing STAT5b. In fact, the results suggest that the level of STAT5b is not the determining factor in the proliferation of T47-D cells, and instead, its overexpression may actually inhibit the proliferative response to prolactin. As expected from earlier studies[221,283], there is a minimal effect of prolactin on the proliferative rate of MCF-7 cells whether or not they overexpress STAT5b, presumably a reflection of the lower number of prolactin receptors in these cells[221].

Survival assays, whether assessed by cell counting or by the XTT assay, also suggest that, far from conferring protection from ceramide-induced apoptosis, over-expression of STAT5b actually results in increased susceptibility to ceramide-induced cytotoxicity in T47-D cells (Figs. 5.6 and 5.7). In MCF-7 cells prolactin has no significant effect on ceramide-induced cytotoxicity whether or not STAT5b is overexpressed.

Thus, contrary to our expectations, stable over-expression of STAT5b in these breast cancer cell lines did not enhance the proliferative or survival effects of prolactin. Instead, when all the data on proliferation and rate of apoptosis in T.st5b1 are considered, it would appear that by overexpressing STAT5b we have inadvertently created a cell line that could potentially be more susceptible to apoptosis. This goes against the conventional view that STAT5b stimulation results in proliferation[318,319]. Logically, it

should be presumed until proven otherwise that endogenous STAT5b stimulation, in itself, will still result in proliferation of the cell population, however, it would be interesting to investigate how overexpressing STAT5b alters the dynamics of cell metabolism, triggering cell cycle arrest and increasing susceptibility to apoptosis. Perhaps the most likely explanation for this would be that STAT5a mediates the proliferative and protective effects of prolactin in breast cancer cells and overexpression of STAT5b 'squelches' the effects of STAT5a. Although STAT5b appears to be expressed at a higher level than STAT5a in T47-D cells[288], evidence from 'knock-out' animals provides strong evidence for a critical role of STAT5a, but not STAT5b, in mammary development[302,320].

Another possible explanation could be that over-expressed STAT5b induces differentiation of the T47-D cells under conditions of stress (i.e. serum starvation) so that the apparent increase in cell death when prolactin is added to survival assays could be explained by the accumulation of cells in G1 as they differentiate. Cell cycle analysis of the clones following serum starvation (Fig. 5.8) does indeed show the accumulation of cells in G1, but this effect is not enhanced by prolactin, making it unlikely that STAT5b is promoting differentiation. There are several possibilities to consider regarding this unexpected response. One possibility is that STAT5b is not involved in the proliferative or survival pathways in T47-D cells, or if it is involved, it does not have a dominant role in these cells. Another possibility is that even though the basal level of STAT5 signalling has been increased in the STAT5b clones, it is the signalling cascade downstream of this which is the limiting factor, and the increased STAT5 signalling is unable to elicit any further response. However, neither of these possibilities would explain why over-

expressed STAT5b actually reversed the expected responses. It is possible that increased expression of STAT5b interferes with cellular function and diminishes the ability of cells to withstand stress (e.g. when exposed to ceramide or deprived of serum).

It was unfortunate that we were unable to isolate any breast cancer clones stably overexpressing STAT5a. Since over expressed STAT5b does not appear to affect the ability of breast cancer cells to survive apoptosis, this indicates the possibility that STAT5a could be responsible for this effect, which was also suggested in a recent paper[321]. However, in view of the poor expression of the STAT5a plasmid as shown on Western blotting and the lack of time, we were unable to perform further studies to create stable STAT5a cell lines.

In the MCF-7 cell line and its STAT5b clone, M.st5b1, the lack of prolactin response could be explained by the low level of expressed STAT5b (Fig. 5.2) which did not lead to a clear increase in STAT5b signalling (Fig. 5.3). There are several other possibilities to consider regarding the lack of response in MCF-7 cells. One possibility is that STAT5b is not involved in the proliferative or survival pathways in MCF-7 cells and its overexpression interferes with the functioning of whichever protein is responsible. Another possible reason, which would account for the high basal activity of STAT activation in these cells (Figs. 5.1 and 5.3), is that in this cell line STAT5 is constitutively active. This possibility is supported by a recent study showing that both T-47D and MCF-7 cell lines have constitutively active STAT5b[322]. If this is the case, it might explain why the cells did not exhibit any response to further STAT5b expression, as the level of

STAT5b may already be sufficient for maximal response in these cells. Another more interesting possibility would be that the expression of endogenous prolactin by the cells themselves[323,324] may be sufficient for maximal protection against apoptosis. This would also account for the failure to increase STAT5b response to prolactin stimulation. Thus in hindsight, it would have been interesting to measure the level of endogenous prolactin production in these two cell lines whilst they were in serum free conditions, in order to prove or disprove whether they were able to synthesis bioactive hormone despite serum starvation. Moreover, this could be further investigated by using neutralizing antibodies to prolactin to assess if this affected the cell cycle profile and apoptotic response in the MCF-7 cell lines.

Finally, it is possible that the two STAT5b overexpressing clones are not 'typical'. As only one stable clone was isolated from each breast cancer cell line, it would have been difficult to make any definitive conclusions from the results obtained because mutant or variant clones could have been inadvertently selected.

In conclusion, over-expressing STAT5b does not appear to confer a survival advantage in breast cancer cells. In fact, overexpression of STAT5b seems to diminish responsiveness to prolactin. More work needs to be done to confirm this finding, however, as well as to assess what changes are induced by increased STAT5 signalling.

6 Induction of Apoptosis in Breast Cancer Cells by Met, a protein closely related to Het/SAF-B

6.1 Introduction

The Met gene, identified by Dr. Shane Colley, bears a strong similarity to Het (Heat-shock protein 27-Ere-Tata binding protein), also called SAF-B (Scaffold Attachment-Factor B) or HAP (hnRNP A1-associated protein), which was discovered independently by three groups[325-327]. Over a region of 863 amino acids, Met shares 35% identity with Het/SAF-B. Like, SAF-B, Met has a SAF Box, an RNA binding domain and a glutamine/arginine rich region in the carboxyl terminus (Figs 6.1 and 6.2). SAF-B was first identified as one of four novel nuclear proteins that bind to the scaffold/matrix attachment regions (S/MARs) of DNA. S/MARs are thought to be responsible for linking chromatin to the nuclear matrix scaffold, and may be important for transcription of DNA[328]. SAF-B is known to bind RNA polymerase II and is involved in alternative splicing of pre-mRNA[326]. Independently, Oesterreich et al. showed that expression of Het resulted in decreased transcription from the hsp-27 promoter[325] and also caused down-regulation of transcription by the oestrogen receptor[329]. In addition, a third group used yeast two-hybrid screening to isolate a cDNA encoding a protein of 917 amino acids which associated with hnRNP A1 (heterogeneous nuclear ribonucleoprotein A1) and had a sequence identical to Het/SAF-B. In the latter study, this protein was found to co-localize with heat shock factor-1 (HSF-1) following exposure to 42°C for 1 hour[327].

A)

```
MuMET          22   ITELRVIDLRSELKRRNLDINGVKTVLVSRLKQAI
HuMET          22   ITDLRVIDLKSELKRRNLDITGVKTVLISRLKQAI

HET            31   LSDLRVIDLRADVRKRNVDSSGNKSVLMERLKKAI  gi:2828536
SAF-A           8   VKKLKVSELKEELKKRRLSDKGLKAELMERLQAAL  gi:6226894
AcinusL        72   LQALRVTDLKAALEQRGLAKSGQKSALVKRLKGAL  gi:5931959
PIAS           11   VMSLRVSELQVLLGYAGRNKHGRKHELLTKALHLL  gi:3643105
Ku70          571   LGKLTVPTLKDICKAHGLKSGPKKQELLDALIRHL  gi:3241858
DEK           149   LKKFRNAMLKSICEVLDLERSGVNSELVKRILNFL  gi:544150
PARP            2   SARLRVADVRAELQRRGLDVSGTKPALVRRLDAAI  g1:2959360
                    ...hpl.pLb..h..b.h...G.K..L...L....
```

B)

```
                    RNP-2                                                RPN-1

MuMET          386 IWVSGL SSN T KAAD L KNL F GKY   G K   V LSAKVVTNARSPGAKC  YGIVTMSS
HuMET          386 IWVSGL SSN T KAAD L KNL F GKY   G K   V LSAKVVTNARSPGAKC  YGIVTMSS

HET            408 FWVSGL SST T RATD L KNL F SKY   G K   V VGAKVVTNARSPGARC  YGFVTMST gi:282853
ERE-BP         184 IFVGGL SPD T PEEK I REY F GGF   G E   V ESIELPMDNKTNKR    RGFCFITF gi:374705
AcinusL       1013 VHISNL VRP F TLGQ L KEL L GRT   G T   V EEAFWIDKIKS       HCFVTYST gi:593195
CBF-A          161 IFVGGL NPE A TEEK I REY F GQF   G E   I EAIELPIDPKLNKR    RGFVFITF gi:729000
PRC           1544 VFIGKI PGR M TRSE L KQR F SVF   G E   I EECTIHFRVQGDN      YGFVTYRY gi:130218

HnRNP A1       107 IFVGGI KED T EEHH L RDY F EQY   G K   I EVIEIMTDRGSGKK     RGFAFVTF gi:219406
HnRNP C1/C2     18 VFIGNL NTL V VKKSDV EAI F SKY   G K   I VGCSVH             KGFAFVQY gi:133261
HnRNP D        184 IFVGGL SPD T PEEK I REY F GGF   G E   V ESIELPMDNKTNKR    RGFCFITF gi:141104
                   U.U..U[0-6]Z[.]...U ... F ...[.]G.U.[.]Z.6-21              ...U.U.U
```

Figure 6.1 Met SAF Box and RNA binding domains.

A) Mouse and human MET SAF Boxes aligned with corresponding domains in related proteins[330]. Numbers on the left detail position of motifs, and Genbank sequence identifiers are listed for each protein (right). Conserved residues are highlighted in grey; '.': any residue; 'h':YFWLIVMA; 'p':STQNEDRKH; 'b':KREQWFYLMI. B) RNA binding domains of mouse and human Met are based on previously defined sequence consensus[331]. Numbers left refer to initiating residue of motif, and Genbank sequence identifiers are listed for each protein. '.':any residue; 'U':LIVAGFWYMC; 'Z':U+ST. Conserved residues are highlighted in grey. (Data from Dr. S Colley).

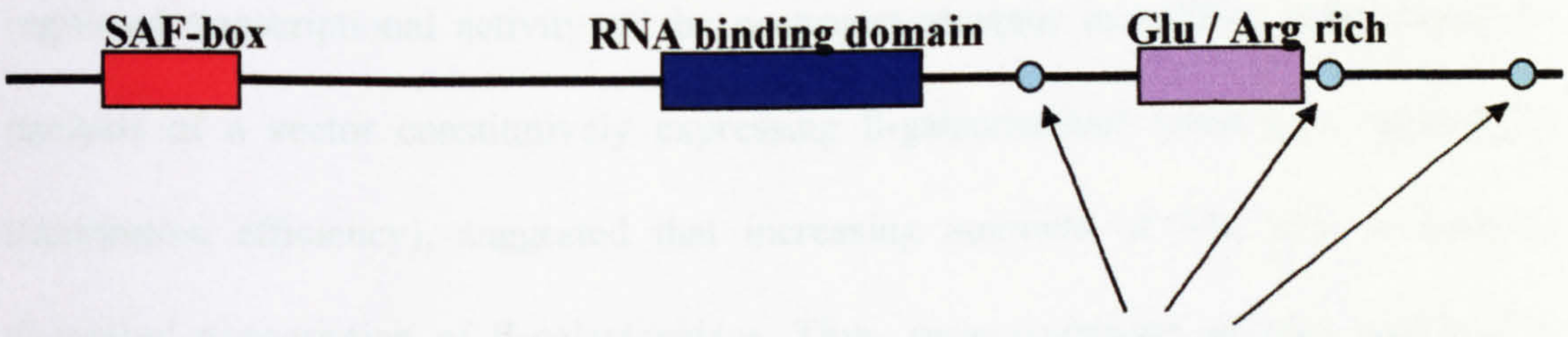

Figure 6.2 Diagramatic representation of the Met protein.

Met is a protein consisting of 1031 amino acids, ~3.7kb. It has three regions which bear strong homology to SAF-B, as indicated above (SAF-box, RNA binding motif and a glutamine/arginine rich region). Also located in the carboxy terminal are 3 nuclear localization sites.

Preliminary studies (performed by Dr. Shane Colley) showed that Met, like Het, down-regulated transcriptional activity of the oestrogen receptor in MCF-7 cells. However, analysis of a vector constitutively expressing β-galactosidase (used as a control for transfection efficiency), suggested that increasing amounts of Met also resulted in decreased transcription of β-galactosidase. Thus, over-expression of Met appeared to cause a generalized inhibition of transcription which might result either in cell toxicity or the induction of apoptosis in MCF-7 cells. The experiments described in this chapter were performed to further analyse the ability of Met to block transcription, and to investigate the possibility that Met might induce apoptosis in breast cancer cells.

6.2 RESULTS

6.2.1 Effect of Met on the activity of reporter genes in MCF-7 cells

All plasmids containing the Het and Met moieties were constructed by Dr. Shane Colley, and all sequences were confirmed by sequencing. Full-length murine Met cDNA (3.7 kb), amplified by RT-PCR from mouse bone marrow, was cloned into pCR3.1 (Invitrogen) (pCR-Met). A BamH I/Eco RV digest of this plasmid was subcloned into Bgl II/Sma I digested pEYFP-C1 (Clontech) resulting in an amino-tagged enhanced yellow fluorescent protein (EYFP)– Met chimera: pEYFP-Met.

pMet-HA was constructed as follows. The 3'end of Met cDNA was amplified with the HA tag using Pfu DNA polymerase (Promega) and specific primers (5'mid Met ATGGAACGCGAACGCTTGGAA and 3'HA-Met : AAAGCGGCCGCTCAAGCGTA

GTCTGGGACGTCGTATGGGTATGCAAATCGCCGTGGAGGTCCACT), resulting in a ~1.1kbp fragment. This fragment was digested with SmaI/NotI and the resultant 397bp fragment isolated, and cloned into similarly digested pCR-Met, to generate pCR-Met-HA (pMet-HA).

pHA-Het was constructed in the following manner. The amino terminus of the IMAGE clone 3611151 (GI 989737) was amplified by PCR using Pfu polymerase (Promega) and specific primers that coded for the haemaglutinin epitope (5'HA Het aaaggatccaaaatggcatacccatacgacgtcccagactacgccatggcggagactctgtcaggcct, 3'mid Het gtcgtaccccttcttagcatca). This resulted in a 1.6kb fragment which was digested using BamH I/Eco RV and subcloned into IMAGE clone 3611151. The latter was then digested with BamH I/Pst I and the insert released was subcloned into a similarly prepared pCR3.1 to generate pHA-Het (with the HA tag at the amino terminus).

Initial experiments by Dr. Colley were performed using the EYFP-Met chimera. Once an HA-tagged Met plasmid had become available, we decided to repeat the initial experiments using the HA-tagged construct, which would be more comparable to the HA-tagged Het and would also avoid the criticism that the chimera might interfere with transcription as a result of toxic effects caused by the EYFP moiety.

6.2.1.1 Expression of Het and Met in MCF-7 cells Assessed by Western Blotting

Fig. 6.3a shows a Western blot of the EYFP-Met chimera, reported to be migrating with an apparent molecular weight of 130kDa (Dr. S. Colley, personal communication). This blot was performed by Dr. Shane Colley.

To confirm that HA-tagged Het and Met constructs of the appropriate size were expressed, a Western blot was performed. COS-7 cells ($5x10^6$) were seeded onto 90mm dishes and incubated overnight. The cells were then transfected with 5μg of HA-tagged Met or Het and incubated for 24 hours before cell lysates were prepared and Western blotting performed. The primary antibody was the anti-HA probe (Santa Cruz) diluted 1:1000, and the secondary antibody was anti-rabbit IgG (diluted 1:10,000).

Fig. 6.3b shows the expression of HA-tagged proteins migrating with an apparent molecular weight of 130kDa. Although the predicted molecular weight of the proteins is approximately 90kDa, Het has previously been shown to migrate at an anomalous rate with an apparent molecular weight of 130kDa[327], probably as result of[325] charged domains on the molecule (basic N- and C- termini, and an acidic central amino acid sequence[326]). It appears that MET migrates in a similarly anomalous manner.

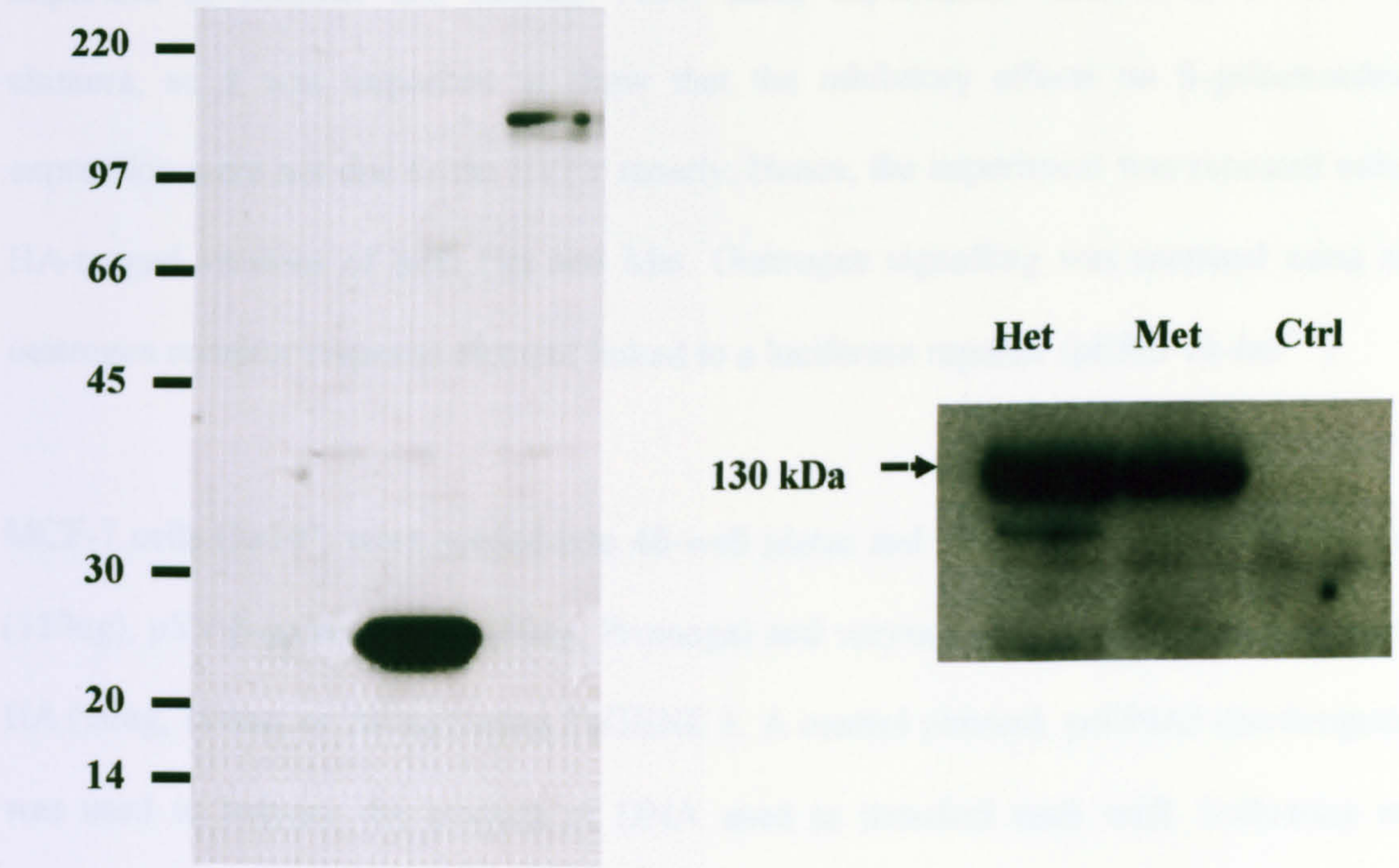

(a) (b)

Figure 6.3 Expression of Het and Met constructs.

(a) Detection by Western blotting of pEYFP-Met expressed in MCF-7 cells (experiment performed by Dr. Shane Colley), (b): Detection by Western blotting of transfected HA-Het and Met-HA expressed in MCF-7 cells. $5x10^6$ MCF-7 cells were transfected with 5μg of HA-Het or Met-HA plasmids. Cells were incubated for 24 hours before being lysed and a Western blot performed on cell extracts using anti-HA probe (Santa Cruz). Control cells were transfected with empty plasmid.

6.2.1.2 Does overexpression of Het and Met regulate oestrogen signalling?

The preliminary experiments performed by Dr. Colley had indicated that both Het and Met down-regulate a constitutively active β-galactosidase reporter, and it was clearly important to confirm this finding. Also, these experiments utilized an EYFP-Met chimera, so it was important to show that the inhibitory effects on β-galactosidase expression were not due to the EYFP moiety. Hence, the experiment was repeated using HA-tagged versions of both Het and Met. Oestrogen signalling was assessed using an oestrogen receptor response element linked to a luciferase reporter (pERE-Tk-luc[332]).

MCF-7 cells ($3x10^4$) were seeded into 48-well plates and transfected with pERE-Tk-luc (150ng), pSV-β-galactosidase (60ng, Promega) and varying amounts of HA-Het or Met-HA (50ng, 100ng, or 200ng) using FuGENE 6. A control plasmid, pcDNA3 (Invitrogen), was used to balance the amount of DNA used to transfect each well. Following an overnight incubation, the cells were serum starved for 6 hours before exposure to 10^{-8}M E2 (17β-oestradiol) for 18hrs. The cells were lysed and luciferase activity of the lysate measured using a Dynex luminometer. Concurrently, a sample of the lysate from each well was also assessed for β-galactosidase activity, which was measured in a Dynex microplate reader.

Fig. 6.4a confirms that both Het and Met decreased the ability of the oestrogen receptor to activate a reporter gene in a dose-dependent fashion (down to 43±13% (SD) of activity

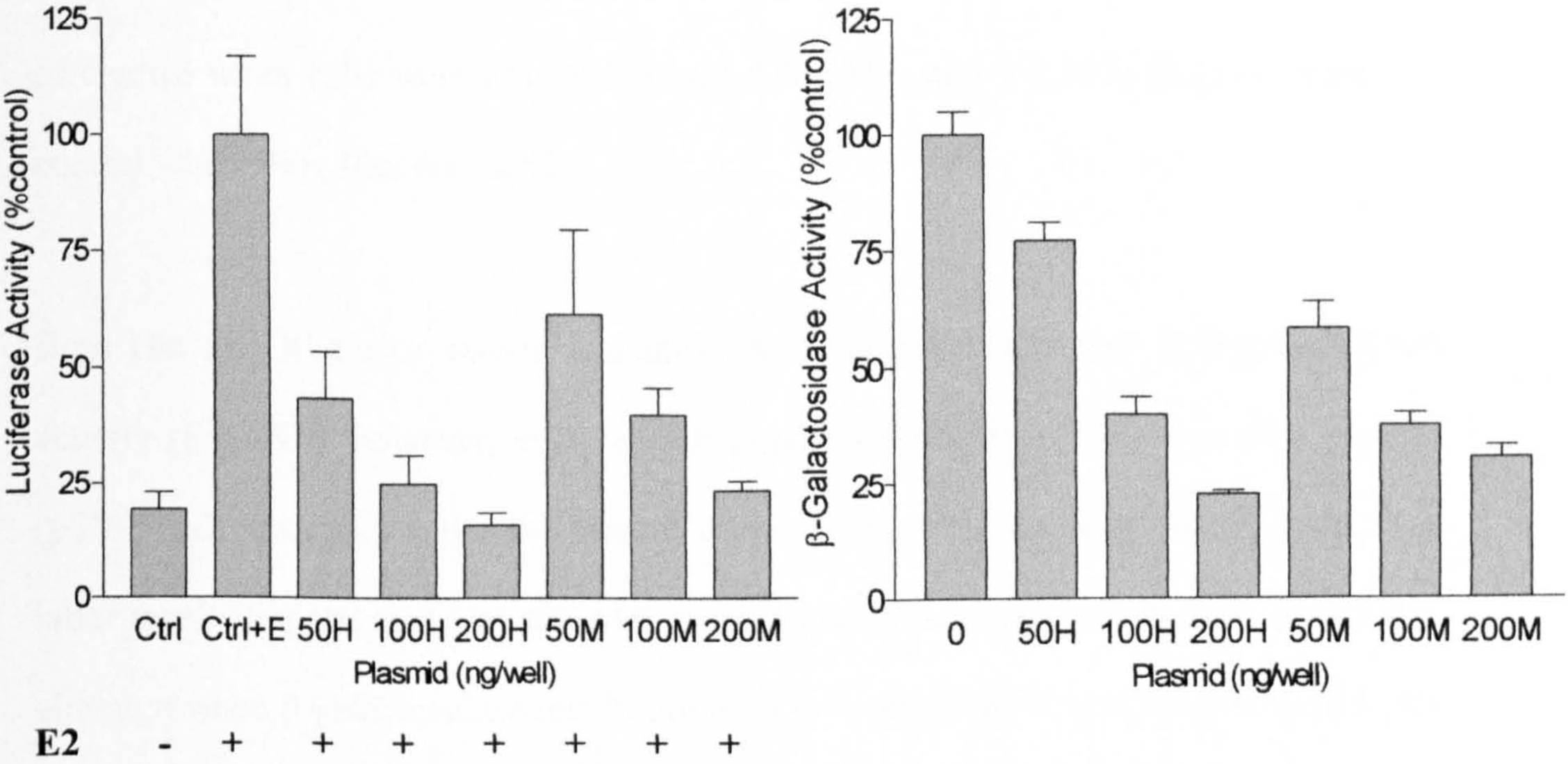

Figure 6.4 Effect of Met and Het on reporter gene activity.

(a): The effect of Met and Het on the activation of the ERE-tk-luc reporter gene by the oestrogen receptor. MCF-7 cells were transfected with pERE-Tk-Luc (150ng) and varying amounts of Met(M), Het(H) or empty plasmid (Ctrl). The cells were incubated overnight and serum-starved for 6 hours before treatment with 10^{-8}M E2 for 18 hours. Next, cells were lysed and luciferase activity measured using the Dynex luminometer. This experiment was repeated on 5 separate occasions, and a typical experiment is shown here (mean $\pm$ SD). Control cells were treated with and without E2 and all cells transfected with Het or Met were treated with E2.

(b): The effect of Het(H) and Met(M) on the activity of a constitutively active β-galactosidase reporter. MCF-7 cells were transfected with pSV-β-galactosidase(100ng) (under the control of a SV40 promoter) and varying amounts of Met or Het, with pcDNA3.1 used to bring total DNA transfected up to 300ng. The cells were incubated overnight and serum-starved for 24 hours, then lysed and β-galactosidase activity measured. The figure is taken from a typical experiment, which was performed 5 times (mean $\pm$ SD).

of control when cells were transfected with 50ng Het, and 47±14% (SD) of activity of control when 50ng Met was used).

Both Het and Met also caused a marked dose-dependent decrease in β-galactosidase activity (Fig.6.4b), however, even though β-galactosidase is expressed from a plasmid (pSV-β-galactosidase) under the control of a constitutively active SV40 promoter. The latter result suggests that Het and Met cause a generalized decrease in gene expression, although when β-galactosidase results are used to 'correct' oestrogen reporter results, the results from 5 separate experiments (Fig.6.5) suggest that there may nevertheless be a specific effect on oestrogen signalling. It is possible that this effect is artefactual, however, resulting from differences in half-life of luciferase (about 3 hrs) and β-galactosidase (over 20 hrs). For this reason, we would predict that if Het and Met block transcription, luciferase activity would be expected to decline more rapidly than β-galactosidase, leading to a false conclusion if the former is 'corrected' by the latter.

6.2.1.3 Effect of overexpressing Met on a constitutively active luciferase reporter.

To confirm our hypothesis that inhibition of oestrogen signalling by Het[329] and Met (Fig.6.5) could be explained by differences in half life of luciferase and β-galactosidase, we went on to investigate the effect of overexpressing Met on the activity of a constitutively active luciferase reporter. MCF-7 cells ($1x10^4$) were seeded into 48-well plates and transfected with 60ng pBR-RSV-Luc plasmid, 60ng pSV-β-galactosidase plasmid, and varying amounts of Met. Following an overnight

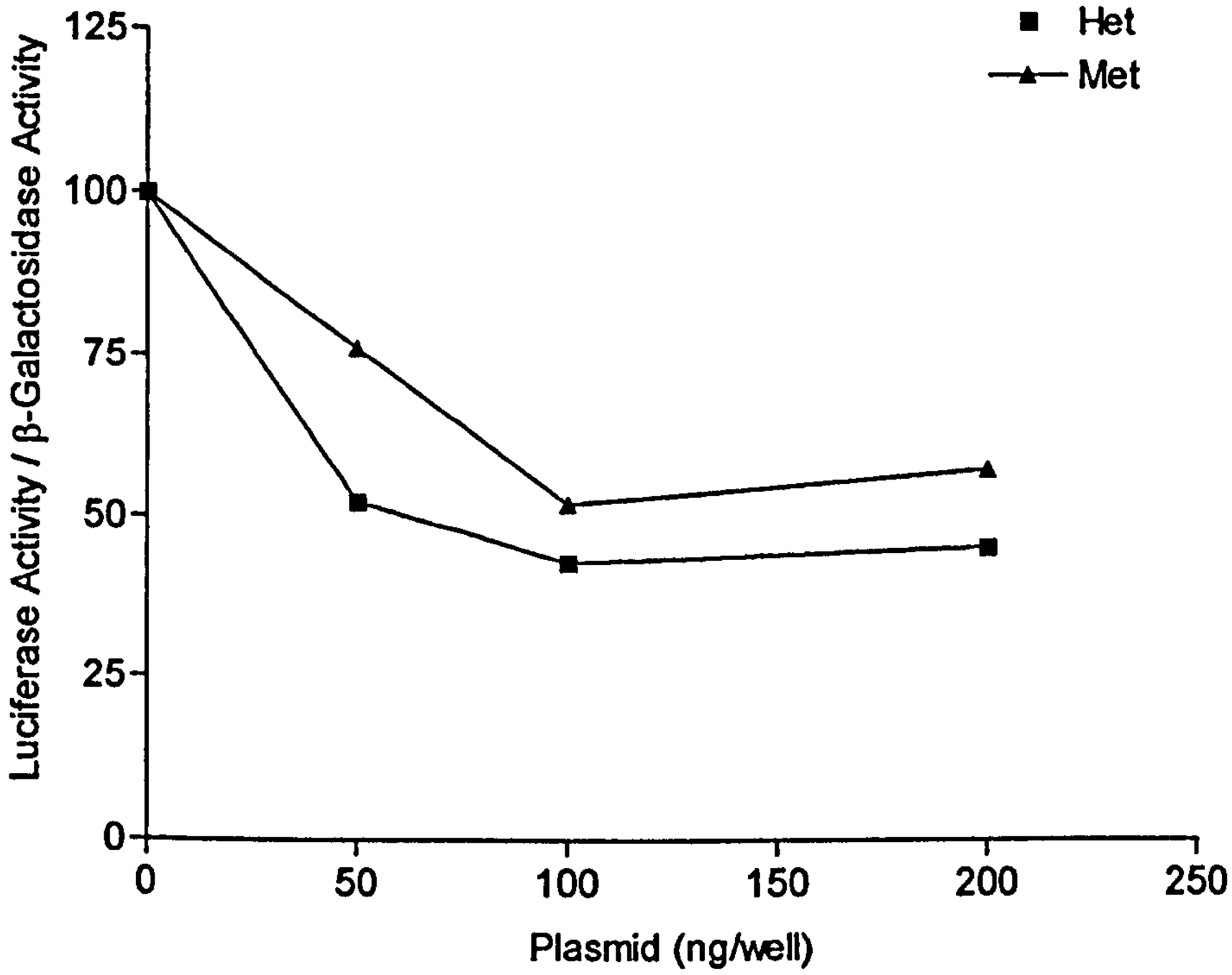

Figure 6.5 Effect of Het and Met on the transcriptional activity of the estrogen reporter after correction of luciferase activity for β-galactosidase activity.

The above figure represents data from the mean of 5 experiments (each point represents percentage of control without Het or Met).

incubation, the cells were serum starved for 24 hours prior to lysis and the luciferase and β-galactosidase activity measured.

Fig. 6.6 shows that Met causes a dose dependent decrease in the activities of both constitutively active reporters. In accordance with our hypothesis, there appears to be a greater inhibition of the luciferase reporter (down to 25±2% (SD) with 50ng Met) activity compared to the decrease in the β-galactosidase reporter activity (down to 38±4% (SD) with 50ng Met) (Student's t test, $p<0.001$), probably reflecting the shorter half-life of the luciferase enzyme.

As a consequence of this discrepancy in the half-lives of both reporters, it is difficult to draw any firm conclusions regarding possible effects of Met on the activity of the oestrogen reporter, but the evidence would suggest that apparent inhibitory effects are primarily artefactual.

6.2.2 Does Over-Expression of Met or Het Induce Apoptosis?

The above experiments suggested that Met (and Het) have generalized inhibitory effects, which could be a result of, or lead to, apoptosis. As the experiments were performed in MCF-7 cells, we first investigated the cell cycle profile of this cell line after transfection with Met to determine whether the effects on reporter gene activity in the cells corresponded to a change in the pre-G1 population of cells.

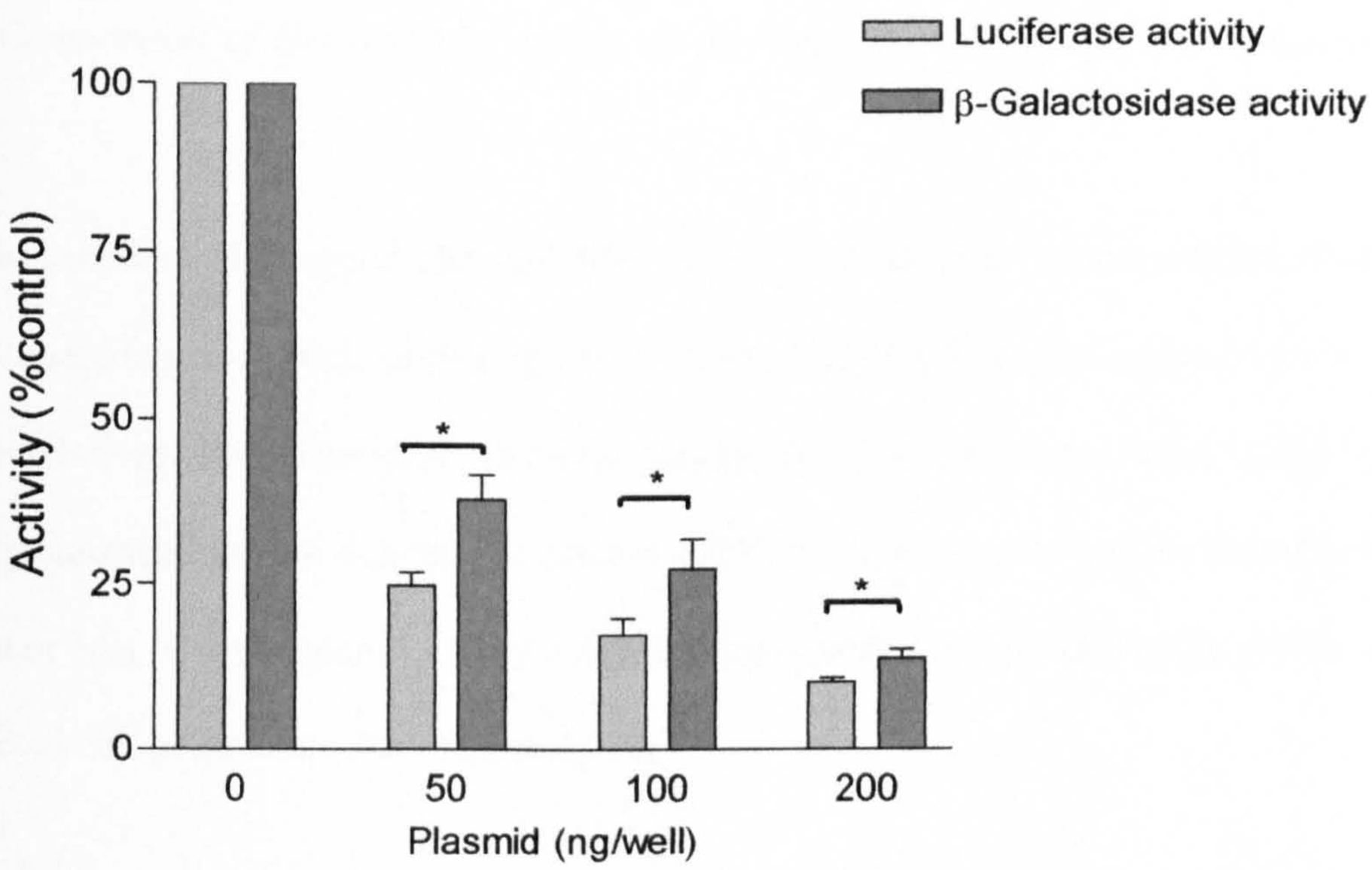

Figure 6.6 Effect of Met on the transcriptional activity of a constitutively active luciferase reporter, compared to its effect on the constitutively active β-galactosidase reporter.

MCF-7 cells were co-transfected with both pBR-RSV-Luc (60ng) (under the control of a Rous sarcoma virus promoter) and pSV-β-galactosidase (60ng), then serum starved for 24 hours prior to assaying for luciferase and β-galactosidase activity (mean ± SD)(: $p<0.01$).*

6.2.2.1 Comparison of Het and Met effects on the Cell Cycle Profile of Breast Cancer cells

Plasmids encoding HA-tagged Het and Met cDNA were used to assess whether these proteins altered the cell cycle profile of MCF-7 cells. Transfection efficiencies of MCF-7 cells are relatively low. Therefore, to allow identification of transfected cells, a plasmid encoding enhanced yellow fluorescent protein (pEYFP-C1, Clontech) was co-transfected with Het or Met. Using a gate that only accepted fluorescent cells, the cell cycle profile of the selected cell population was then analysed.

MCF-7 cells ($3x10^5$) were seeded into each well of a 6-well plate and incubated overnight. The cells were co-transfected with pEYFP-C1 and either pcDNA3.1 (empty plasmid), HA-Het, or Met-HA (1μg of each plasmid). The cells were then incubated overnight before serum starvation in SFM for 24 hours. The cells were collected, fixed in 70% ethanol for 45 min at 4°C, stained with propidium iodide by incubation at 4°C for 1 hour, and the cell cycle profile analysed by flow cytometry. The method of fixation in this instance was modified to a shorter incubation period as EYFP is known to leak out of permeabilized cells.

Fig. 6.7 (top) shows a typical dot plot obtained with MCF-7 cells transfected with EYFP and stained with PI (FL1 and FL2 respectively). The gated region (polygon) shows the boundaries of the gate set to detect cells exhibiting EYFP fluorescence. Fig.6.7 (bottom) is a histogram depicting the cell cycle profile of the EYFP transfected cell population. Regions have been drawn on both figures showing how the cell cycle profile (pre-G1,

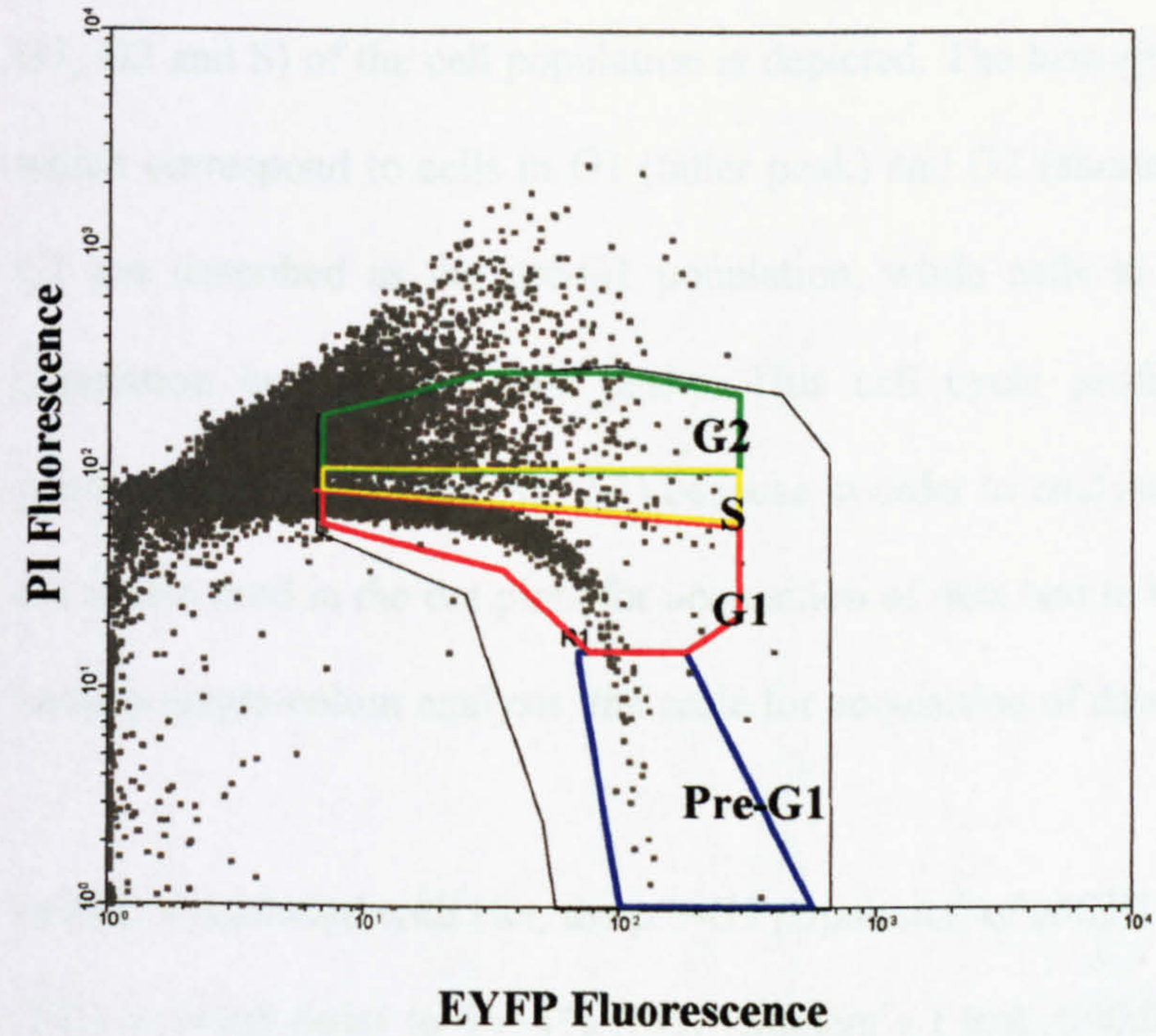

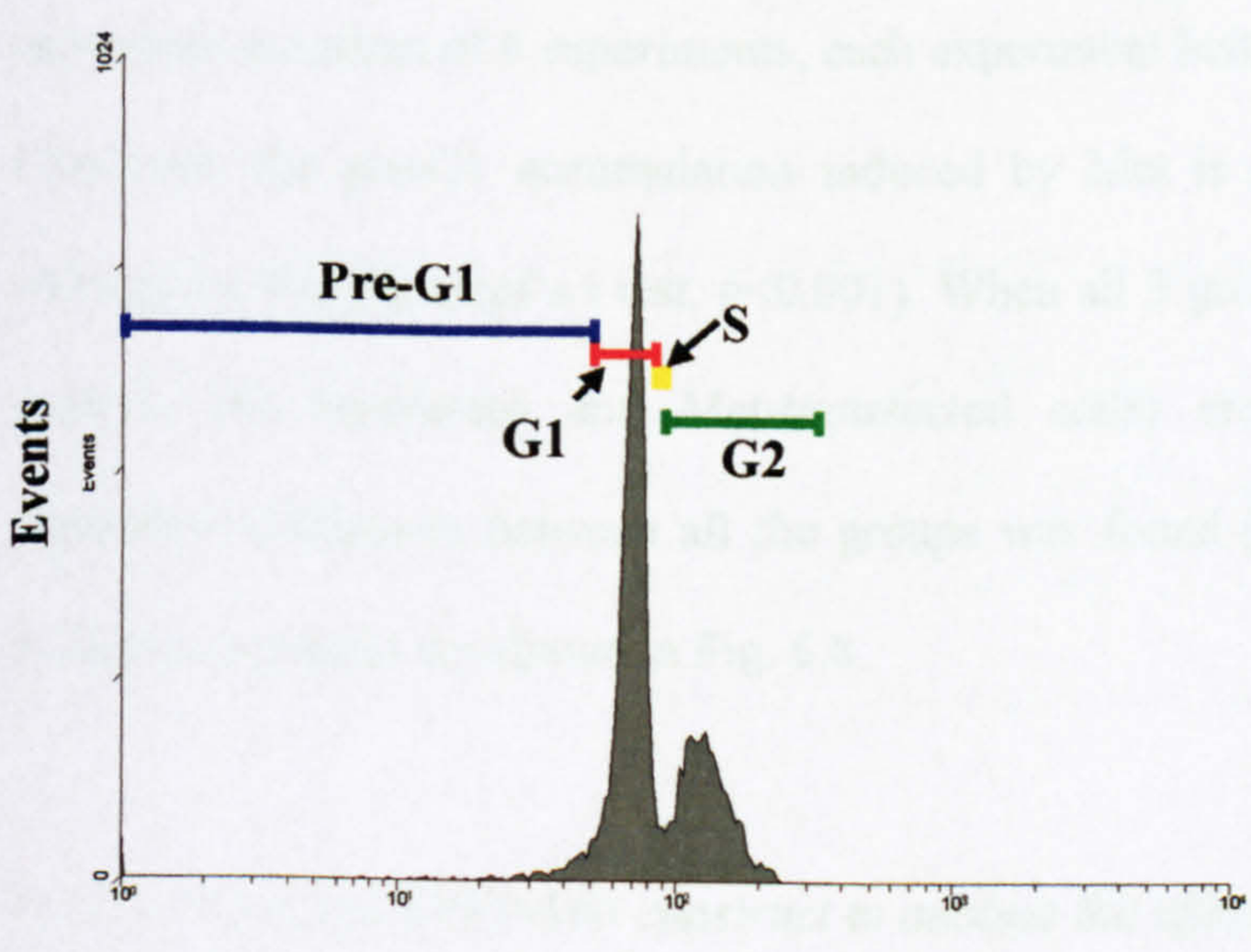

Figure 6.7

(top) Dot plot diagram showing the gate (black polygon) used to isolate the cell population of interest (EYFP-fluorescence) on the flow cytometer, which was analysed for cell cycle distribution on the histogram (bottom). MCF-7 cells were transfected with pEYFP-C1, incubated overnight and then subjected to serum starvation for 24 hours, before being collected and stained with PI. Cells exhibiting EYFP fluorescence are selected, and the cell cycle profile of the fluorescent cells analysed. On the 2 diagrams, the various phases of the cell cycle (preG1, G1, G2 and S) are shown.

G1, G2 and S) of the cell population is depicted. The histogram shown displays 2 peaks, which correspond to cells in G1 (taller peak) and G2 (shorter peak). Cells to the left of G1 are described as the pre-G1 population, while cells in S phase correspond to the population between the two peaks. This cell cycle profile is different from those previously obtained (See Fig. 2.1) because in order to analyse dual-coloured populations, the scales used in the dot plots for acquisition of data had to be on a log scale. In Fig.2.1, being a single-colour analysis, the scale for acquisition of data was linear.

In cells transfected with Het, the pre-G1 population of MCF7 cells increases from 12±3% (SD) (control cells) to 16±4% (SD) (Student's t test, $p<0.05$), and in cells transfected with Met, the preG1 population increases to 23±6% (SD) (Student's t test, $p<0.05$). This represents the mean of 6 experiments, each experiment being performed in quadruplicate. Moreover, the pre-G1 accumulation induced by Met is significantly higher than that induced by Het (Student's t test, $p<0.001$). When all 3 groups (pre-G1 populations from control, Het-transfected and Met-transfected cells) are compared by ANOVA, a significant difference between all the groups was found ($p<0.001$). The results from a typical experiment are shown in Fig. 6.8.

6.2.2.2 Use of the EYFP-Met construct to analyse the effect of Met overexpression on the Cell Cycle Profile of MCF-7 Breast Cancer cells

The pEYFP-tagged Met plasmid was used to investigate ability of Met to induce apoptosis in greater detail. This construct provided a simple method for analysing the

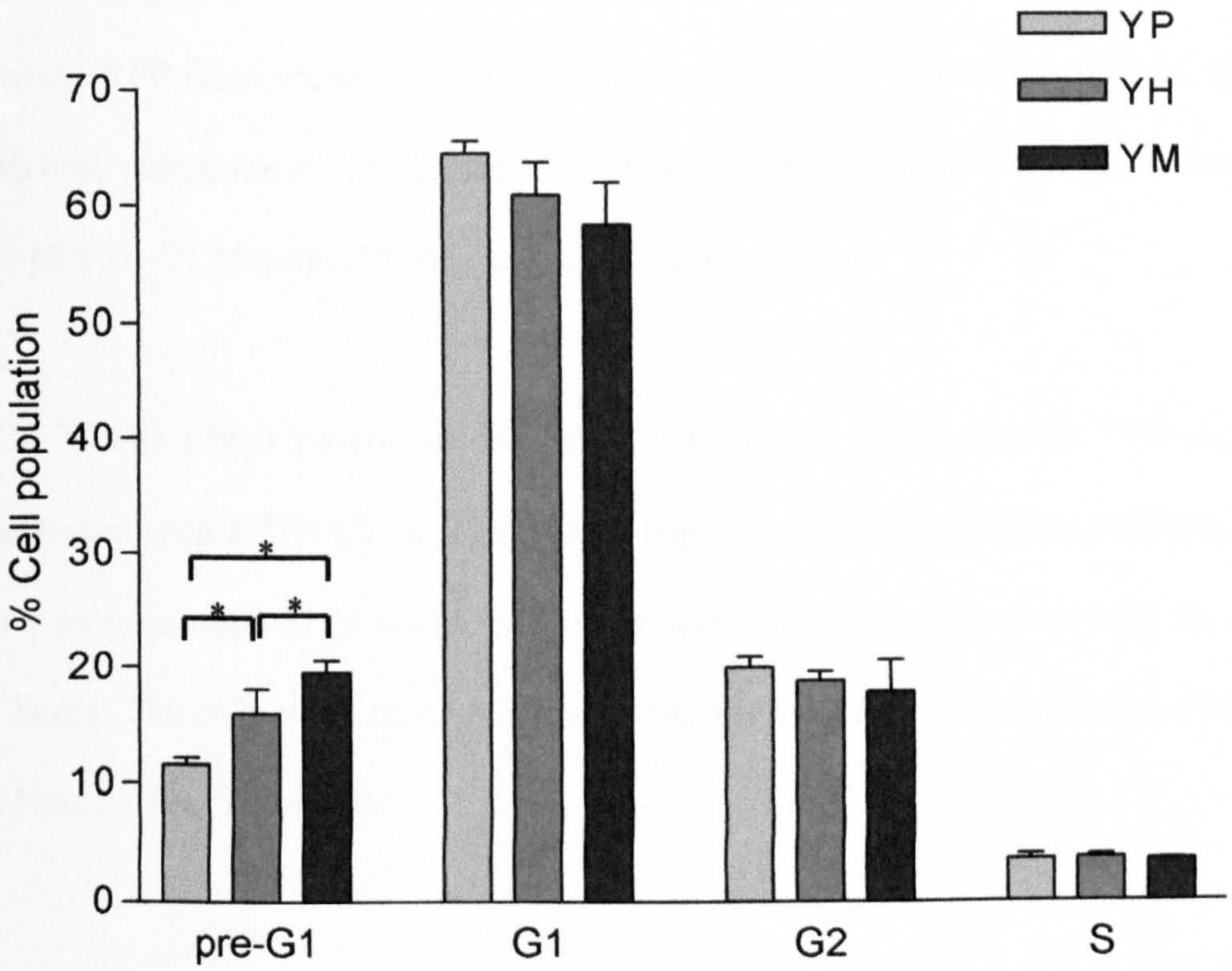

Figure 6.8 Comparison of the effects of Het and Met on the cell cycle profile of MCF-7 cells.

Cells were co-transfected with pEYFP-C1 (1μg) and either pcDNA3 (YP) (empty plasmid, 1μg) Het-HA (YH) (1μg) or HA-Met (YM) (1μg). After an overnight incubation, cells were serum starved for 24 hours before they were collected and stained with PI for cell cycle analysis. This figure represents a typical experiment, of which 5 were performed in quadruplicate(mean ± SD) (= $p<0.05$).*

transfected population on the flow cytometer, because only transfected cells would exhibit EYFP fluorescence, enabling detection by the flow cytometer. Such an analysis is otherwise compromised by the fact that only a small proportion of cells are transfected. The pEYFP-C1 plasmid (Invitrogen) was used as a control.

MCF-7 cells ($3x10^5$) were seeded into each well of a 6-well plate. The cells were transfected with EYFP-C1 or EYFP-Met (1μg of each plasmid) using FuGENE 6 (3μl). After an incubation of 24 hours, cells were washed and transferred to SFM for a further 24 hours. The cells were then collected, fixed and stained with propidium iodide before analysis by flow cytometry.

Fig. 6.9 shows that the pre-G1 population of MCF-7 cells increases markedly when cells were transfected with Met. From the mean of 4 separate experiments, each experiment performed in quadruplicate, the increase was from 10±5% (SD) in control cells transfected with pEYFP to 37±10% (SD) in cells transfected with the pEYFP-Met ($p<0.05$). Importantly, the previous experiment (Fig. 6.8) using the HA-tagged proteins show that apoptosis induced by EYFP-Met is not due to the EYFP-moiety.

6.2.2.3 Effect of Met on the Cell Cycle Profile of the mouse fibroblast cell line, MC3TC

The Met gene was identified by screening a cDNA library of the bone marrow of an oestrogen-treated mouse. Thus, before proceeding any further with experiments in human cell lines, we wished to confirm that the effect of Met was reproducible in murine cells.

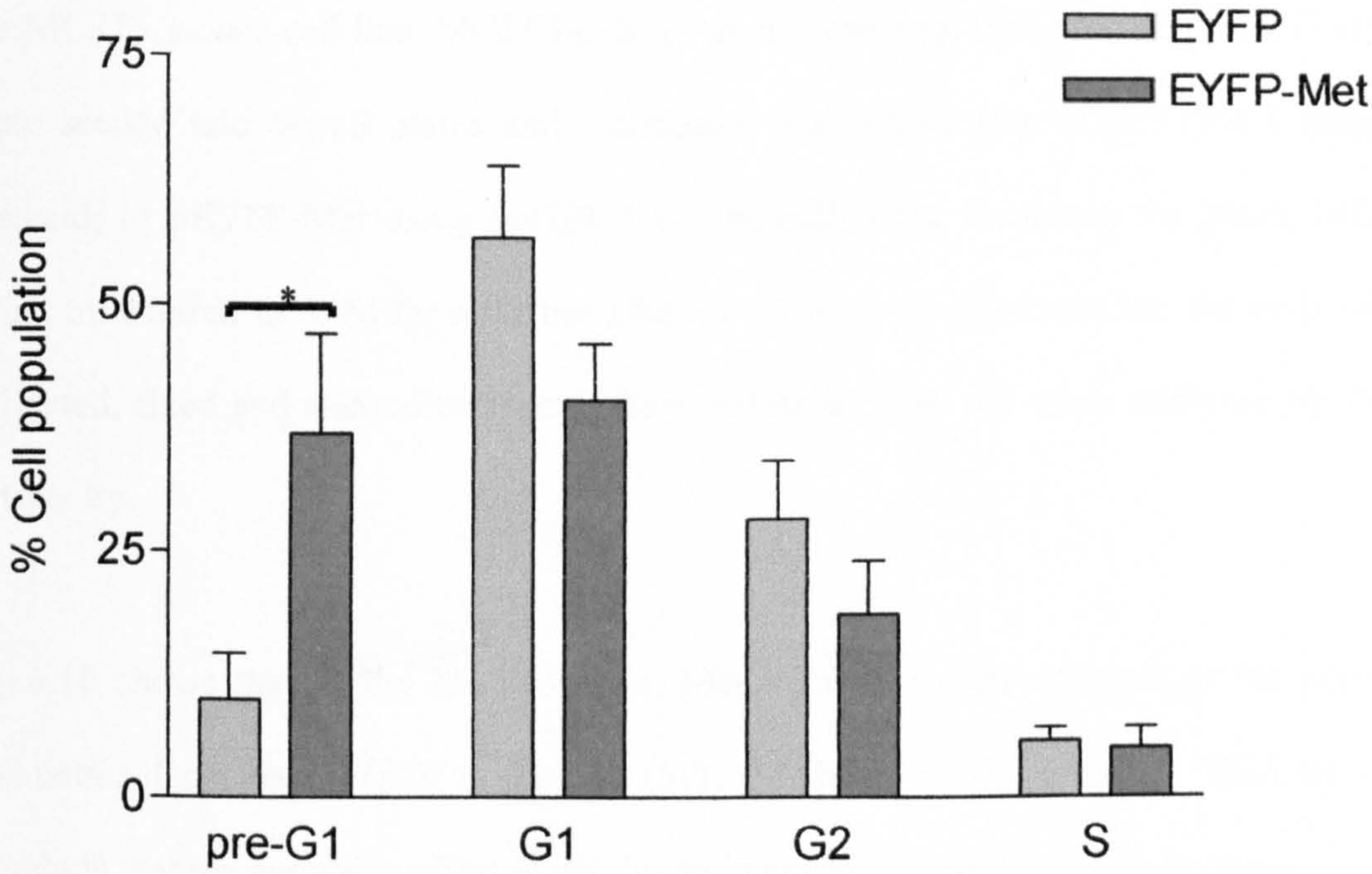

Figure 6.9 Effect of EYFP-Met on the cell cycle profile of MCF-7 cells.

MCF-7 cells were transfected with pEYFP-C1 (1μg) or pEYFP-Met (1μg). Cells were serum starved for 24 hours before they were collected and stained with PI for cell cycle analysis. This experiment was performed 4 times, and a typical experiment is shown (mean ± SD) (= $p<0.05$).*

We therefore decided to investigate the effect of over-expressing Met on the cell cycle of the MC3T3 mouse cell line. MC3T3 cells (a mouse calvarial fibroblast cell line) ($3x10^5$) were seeded into 6-well plates and transfected with either 1μg of pEYFP-C1 (empty plasmid) or pEYFP-Met using FuGENE 6. The cells were incubated for 24hrs, before being transferred to SFM for a further 24hrs. Following serum-starvation, the cells were collected, fixed and stained with propidium iodide and the cell cycle analysed by flow cytometry.

Fig.6.10 shows that in the MC3T3 cells, Met induces a clear increase in the pre-G1 population from 6±3% (SD) to 21±7% (SD) (Student's t test, p value). Thus we can conclude that the apoptotic effect is not due to inter-species differences in proteins.

6.2.2.4 Effect of Met overexpression on the cell cycle profile of different cell lines

To ascertain whether the effect of Met on the cell cycle was limited to specific cancer cells, or if it was a universal effect and would affect all cell lines in the same way, we used Ros (rat osteosarcoma), HepG2 (human hepatocarcinoma), HeLa (human cervical adenocarcinoma) and SF (human fibroblast, primary culture) cell lines. For these experiments, $3x10^5$ cells from each line, seeded in 6-well plates, were transfected with 1μg of pEYFP-C1 or pEYFP-Met as described before.

From Fig. 6.11, it can be seen that Met induces apoptosis in all of these cell lines, albeit to different extents. In Ros cells, the pre-G1 population increases from 9±4% (SD) to 18±6% (SD) ($p<0.001$). In HepG2 cells the increase is from 4±1% (SD) to 17±3% (SD)

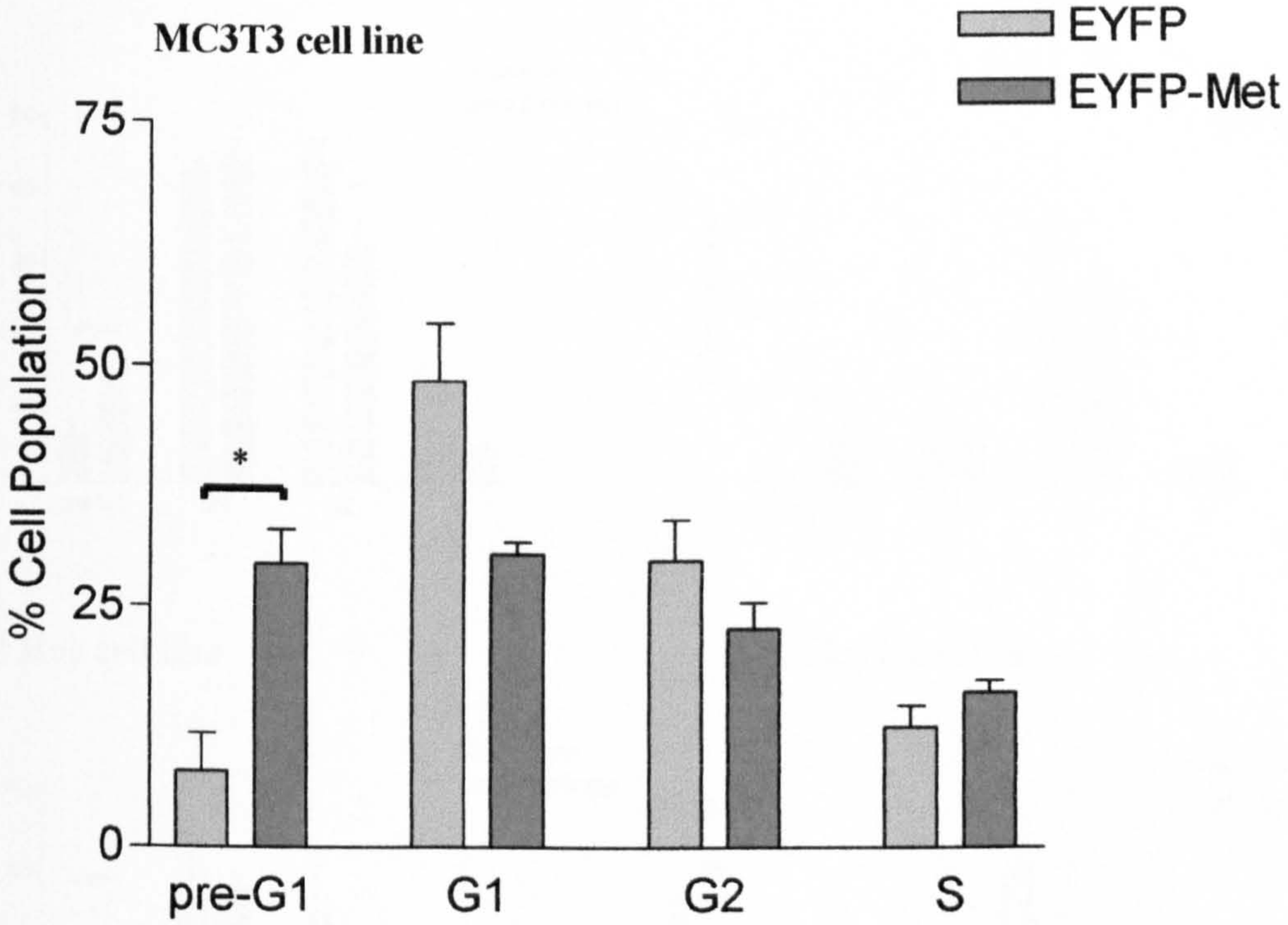

Figure 6.10 Change in cell cycle profile of mouse MC3T3 cells following transfection with Met.

MC3T3 cells were transfected with either pEYFP (control plasmid) or pEYFP-Met. After an overnight incubation, the cells were serum starved for 24 hrs before they were collected, fixed and stained with PI, for analysis of the cell cycle profile by flow cytometry. This experiment was performed 3 times, and a typical experiment is shown (mean $\pm$ SD) (= $p<0.05$).*

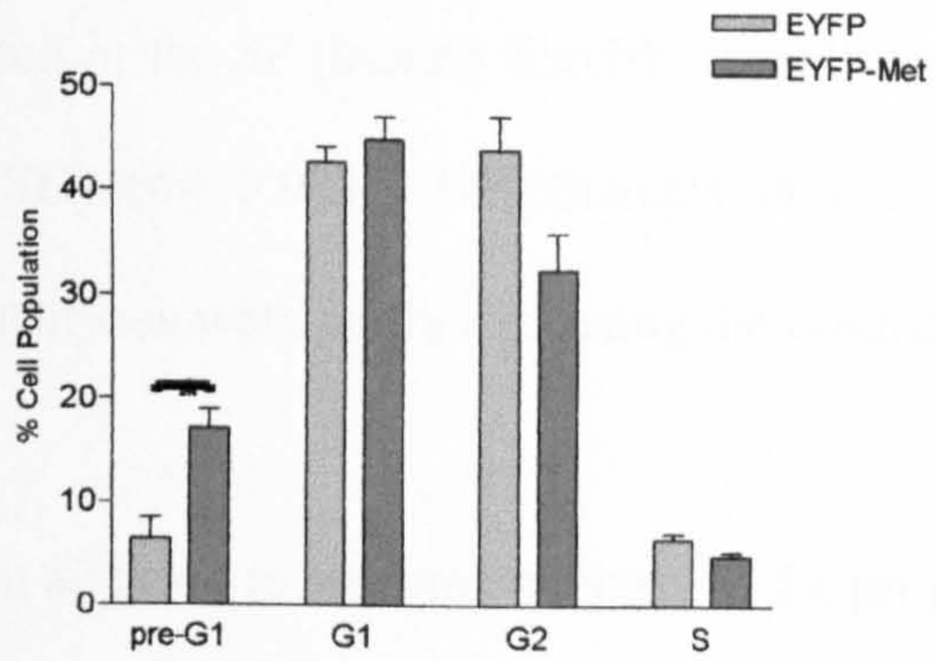

(A) **Ros cell line**

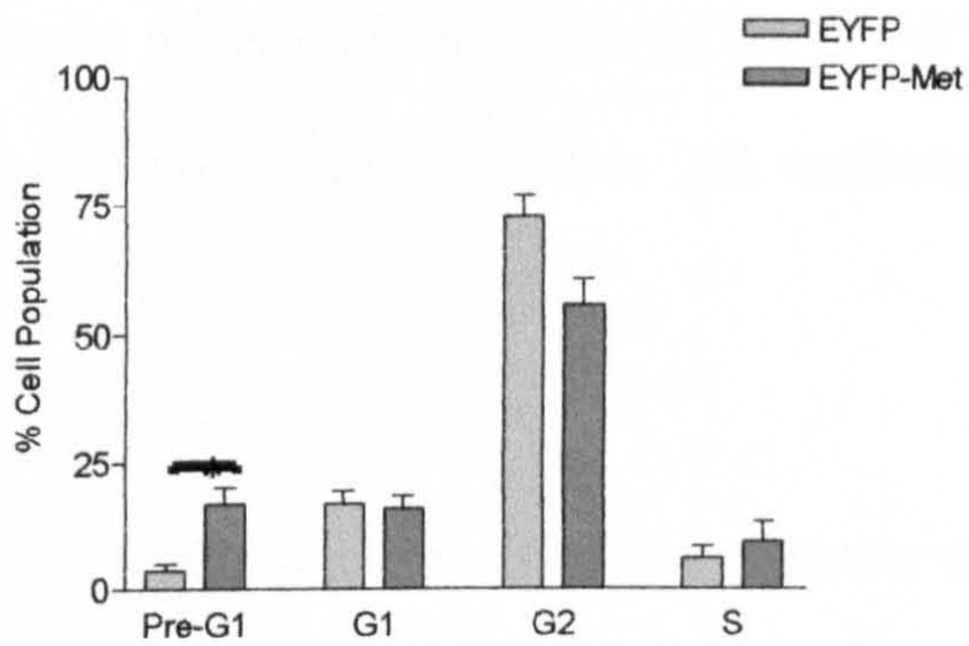

(B) **HepG2 cell line**

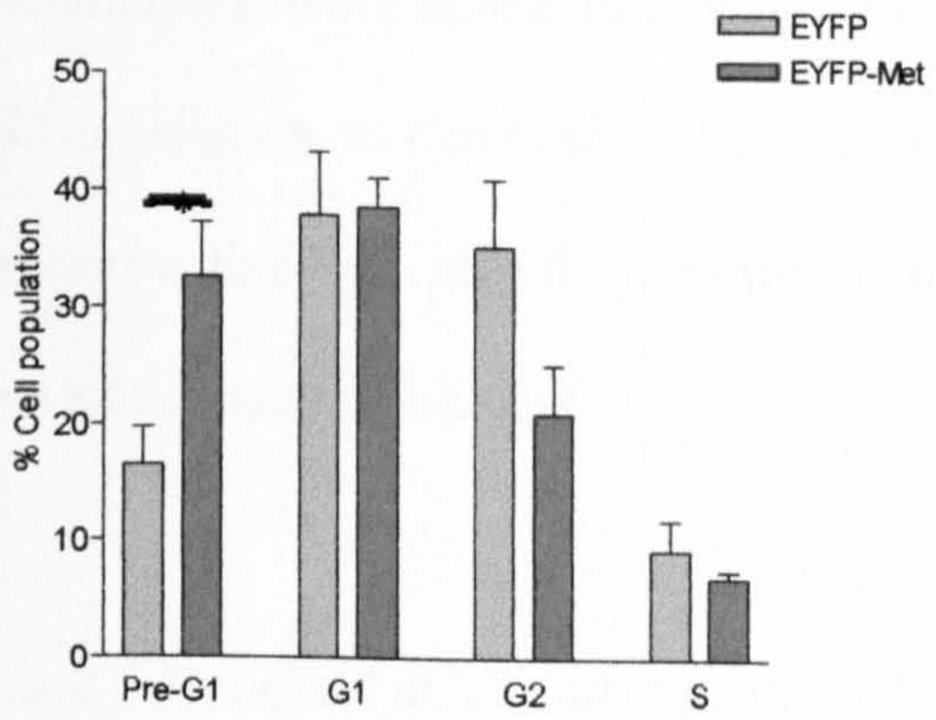

(C) **HeLa cell line**

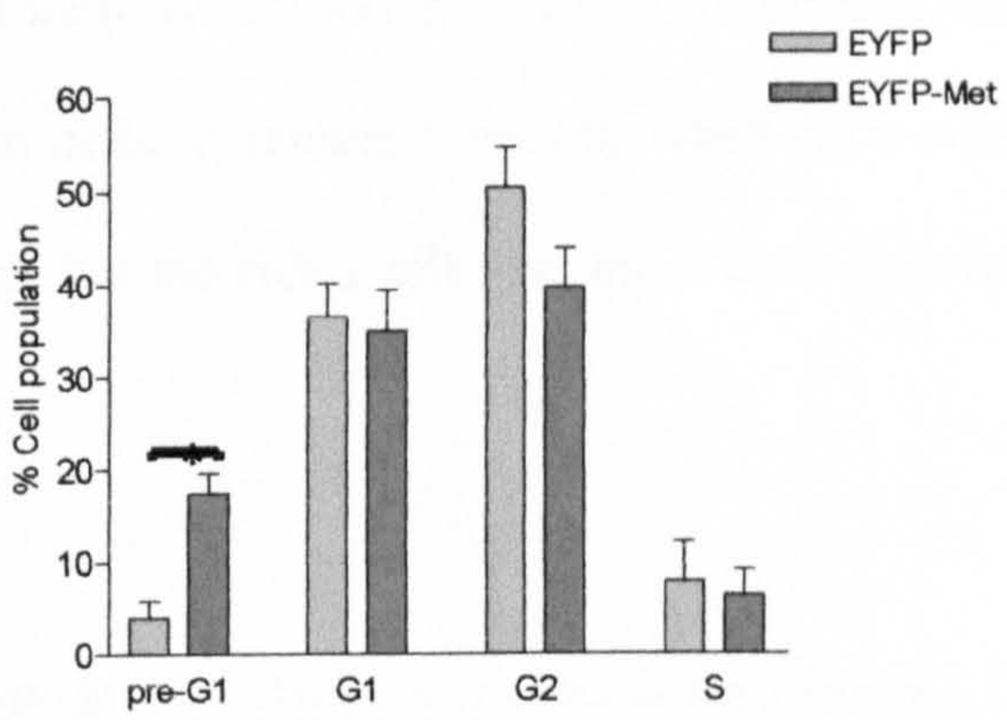

(D) **SF cell line**

Figure 6.11 Effect of EYFP-Met on the cell cycle profile of various cell lines.

$3x10^5$ cells from each of the cell lines shown above were plated out and transfected with pEYFP-C1 (1μg) or pEYFP-Met (1μg). Cells were incubated overnight, followed by serum-starvation for 24 hours before they were collected and stained with PI for cell cycle analysis. (A) = Ros cells, (B) = HepG2 cells, (C) = Hela cells and (D) = SF cells. Figures shown are representative of a typical experiment, experiments were performed in quadruplicate and each was repeated 3 separate times (mean ± SD).

($p<0.001$). In the HeLa cell line, it increases from 17±4% (SD) to 33±5% (SD) ($p<0.001$) and in the SF (human fibroblasts) cell line, pre-G1 increases from 4±2% (SD) to 17±2% (SD) ($p< 0.001$). The changes in pre-G1 are tabulated in Table 6-1. All statistical analyses were performed using the Student's t test.

In addition to studying changes in the proportion of cells in the pre-G1 phase, we went on to analyse the data from all cell lines to assess changes in cell cycle profile of the viable/intact cell population (i.e. cells in G1, G2 or S phase of the cell cycle). From our calculations, there appeared to be a general trend for the G1 population to increase, the G2 population to decrease and the S phase cells to remain constant, when cells were treated with Met (Table 6-2). However, in all but the HeLa cell line, these changes were not statistically significant.

6.2.2.5 The effect of Met on the cell cycle profile of breast cancer cells in the presence of serum.

Because the initial aim of these studies was to assess the effect of Met on oestrogen signalling, all studies were carried out in serum-free conditions. To determine whether Met induced apoptosis only under conditions of stress (i.e. serum starvation) or whether it was a more generalized effect, MCF-7 cells ($3x10^5$) were seeded onto 6-well plates and incubated overnight. The cells were transfected with either 1μg of pEYFP-C1 or pEYFP-Met and incubated overnight. The next day, half of the cells from each group of transfected cells were washed and subjected to serum-starvation as in previous

Cell Line	% EYFP-transfected cell population in pre-G1	% EYFP-Met-transfected cell population in pre-G1	Student t-test
	Mean ± SD (No. of samples)	Mean ± SD (No. of samples)	
MCF-7	10 ± 5 (15)	37 ± 10 (16)	p<0.05
HeLa	17 ± 3 (11)	33 ± 5 (12)	p<0.05
HepG2	5 ± 3 (16)	24 ± 15 (16)	p<0.05
MC3T3	6 ± 3 (12)	21 ± 7 (12)	p<0.05
Ros	9 ± 4 (12)	18 ± 6 (12)	p<0.05
SF	4 ± 2 (15)	17 ± 2 (14)	p<0.05

Table 6.1 Change in the proportion of cells in the pre-G1 population without (EYFP) or with (EYFP-Met) the expression of Met.

Cell line (transfected plasmid)	% Viable population in G1	% Viable population in G2	% Viable population in S
	Mean ± SD	Mean ± SD	Mean ± SD
HepG2 (YFP)	20 ± 5	74 ± 5	6 ± 2
HepG2 (YFP-Met)	22 ±4	68 ± 5	11 ± 4
HeLa (YFP)	45 ± 6*	44 ± 9	11 ± 3
HeLa (YFP-Met)	58 ± 4*	31 ± 5	11 ± 1
MCF-7 (YFP)	58 ± 11	34 ± 8	8 ± 3
MCF-7 (YFP-Met)	63 ± 7	29 ±6	8 ± 2
MC3T3 (YFP)	40 ± 12	49 ± 14	11 ± 3
MC3T3 (YFP–Met)	42 ± 3	42 ± 8	16 ± 6
Ros (YFP)	52 ± 15	41 ± 15	6.4 ± 1
Ros (YFP-Met)	63 ± 10	30 ± 11	6 ± 2
SF (YFP)	40 ± 4	52 ± 4	8 ± 4
SF (YFP-Met)	42 ± 4	50 ± 4	9 ± 4

Table 6.2 Tabulation of the changes in the cell cycle profile of the viable cell population after treatment with Met.

The difference between the preG1 populations of YFP-transfected HeLa cells is significantly different to that of the YFP-Met transfected cells (= $p<0.05$, Student's t test).*

experiments. The other half of the transfected cells were left in normal medium containing 10%FCS until they were collected and stained with PI for cell cycle analysis.

Fig. 6.12 shows that in the absence of serum, the proportion of cells transfected with Met in the pre-G1 phase is 39±4% (SD), while in the presence of serum, 47±7% (SD) of the cells are in the pre-G1 phase. This is in comparison to a pre-G1 population of 9±3% (SD) in the control cells transfected with EYFP alone. Thus the ability of Met to induce apoptosis in MCF-7 cells is independent of whether or not the cells are stressed by serum deprivation.

6.2.2.6 Does Met cause apoptosis as assessed by Hoechst staining?

We next proceeded to verify that the increase in pre-G1 population detected by flow cytometry is due to 'classical' apoptosis. HeLa cells have been documented to undergo apoptosis under various conditions, which is detectable by Hoechst staining[333,334]. Thus we examined pEYFP-Met transfected Hela cells by Hoechst staining to confirm that apoptosis is induced by Met.

HeLa cells ($2x10^5$) were seeded into 60mm dishes and incubated overnight. The cells were transfected, with either 1μg of pEYFP-C1 or pEYFP-Met, and incubated for a further 24 hours. The cells were then serum starved for 24 hours before being fixed (2%PFA/PBS, 20 min at room temperature) and stained with Hoechst (10μg/ml, 15min at room temperature in the dark). Fluorescent microscopy was performed and 300 fluorescent cells per dish were counted. From the pictures taken, it can be seen that the

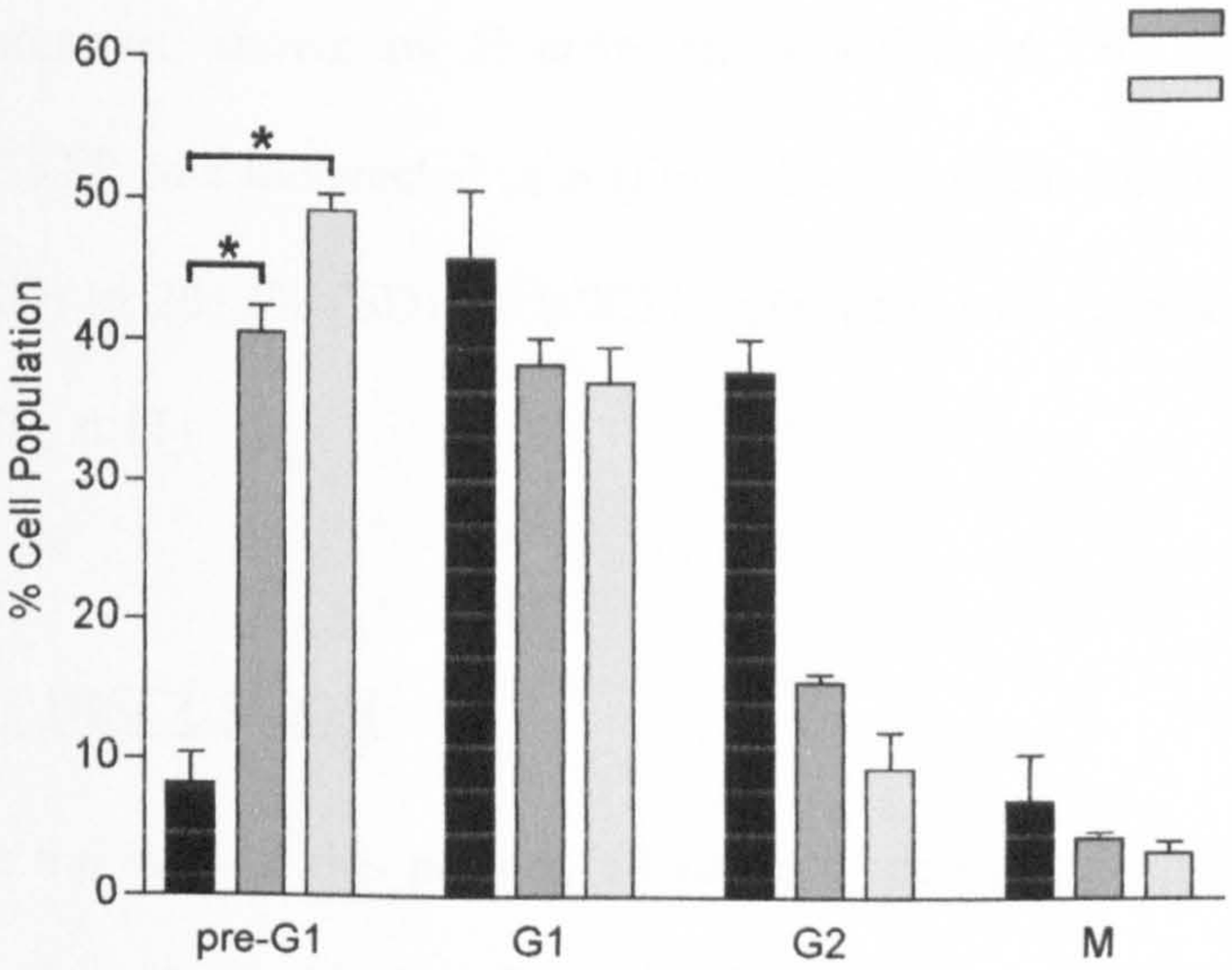

Figure 6.12 The effect of serum on the activity of Met.

MCF-7 cells were transfected with pEYFP-C1 or pEYFP-Met (1μg each) and incubated overnight. The following day, cells were eitherwashed and serum-starved for 24 hours (SFM) or left in normal medium for 24 hours (DMEM). The cells were collected as usual, stained with PI and the cell cycle profile analysed by flow cytometry. This experiment was performed in quadruplicate, and repeated 3 times. The figure shows a typical experiment (mean ± SD) ($p<0.01$, Student's t test).

pEYFP-Met transfected cells (Fig. 6.13a) correspond to cells with the classical features of apoptosis, shown by Hoechst staining (Fig. 6.13b). Cell counts of the pEYFP and pEYFP-Met transfected cells (Fig. 6.13c) show an increase in apoptotic index from 3±1% (SD) to 20±2% (SD) ($p<0.001$), consistent with results obtained by cell cycle analysis (Fig. 6.11).

6.3 DISCUSSION

At the start of this project, all current knowledge regarding the Met protein was from work performed by Dr. Shane Colley. A fragment of the Met gene was isolated from the bone marrow of oestrogen-treated mice by PCR based subtractive hybridization. A full-length virtual cDNA sequence coding for a protein of 1031 amino acids was then generated based on this fragment and using homologous EST sequences. A 3.7kb product was then amplified and cloned from mouse bone marrow cDNA by RT-PCR, using primers designed on the basis of the virtual cDNA sequence. A corresponding virtual human Met sequence (91% homologous to the mouse sequence, 98% if conserved substitutions are taken into account) was generated using human ESTs[335] and consisted of 1034 amino acids.

Met was found to share 35% homology with Het over 863 amino acids, with the greatest homology occurring in three distinct regions of the peptide (Fig.6.1). The first of these conserved regions is a SAF box, which is located between amino acids 22-56 of the Met sequence. The SAF box proteins are known to bind to scaffold/matrix attachment regions

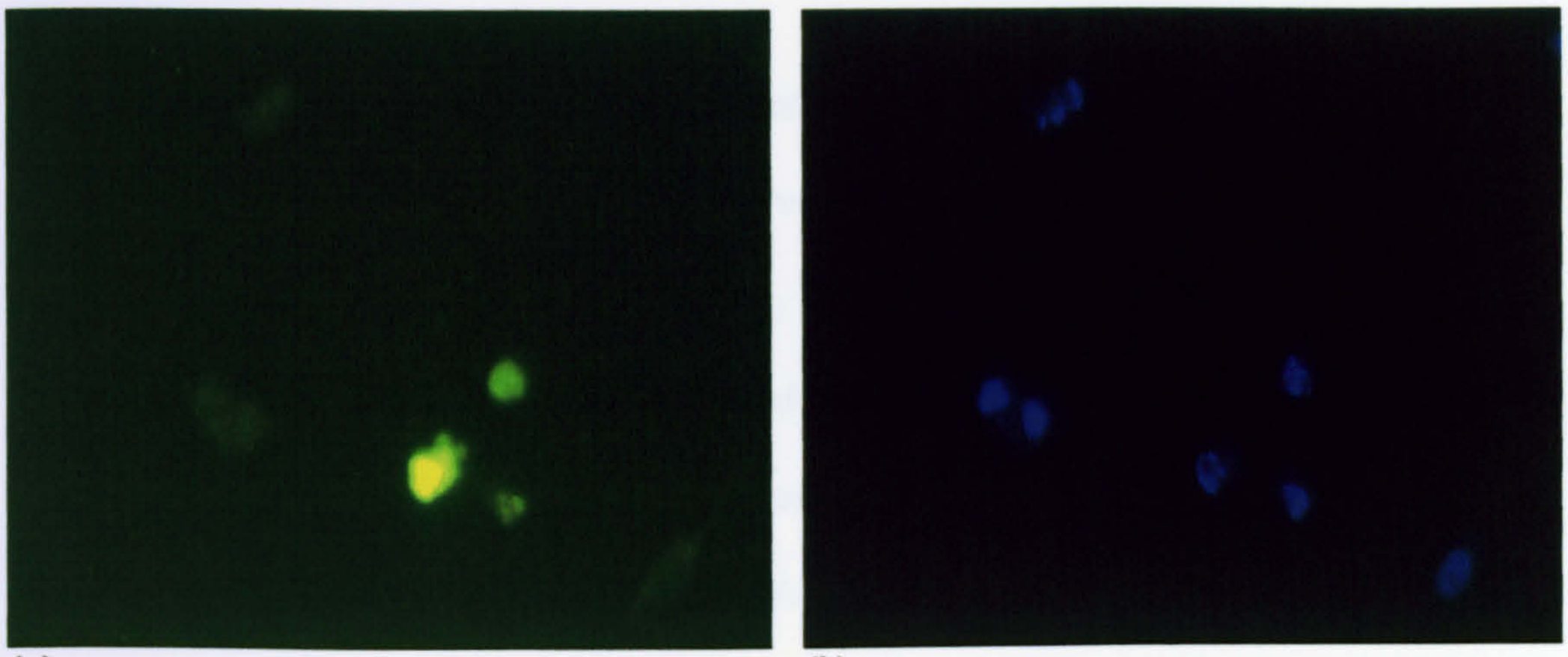

(a) (b)

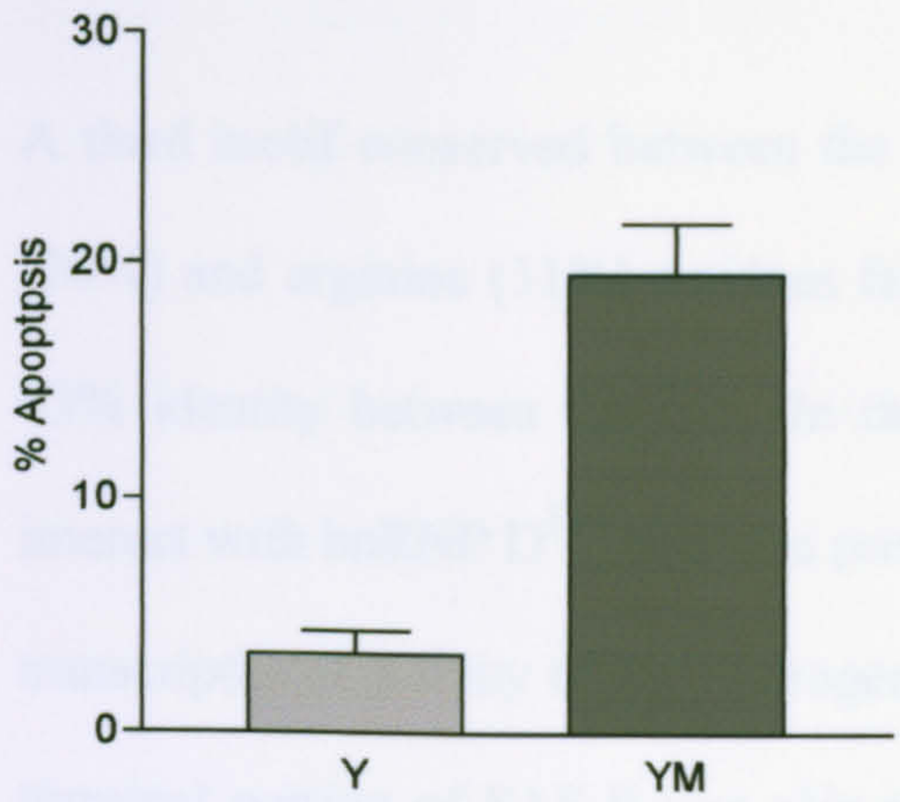

(c): Hoechst staining in HeLa cells, cell counting

Figure 6.13(a, b & c) The induction of apoptosis in HeLa cells by Met, assessed by Hoechst staining.

HeLa cells were transfected with 1μg of pEYFP-C1 or pEYFP-Met. The cells were incubated overnight and then transferred to SFM for 24 hours. Next, cells were fixed and stained with Hoechst and assessed by fluorescent microscopy. Fig.6.13(a):EYFP-Met-transfected cells seen through filter for EYFP(scale bars:5μm), (b):EYFP-Met-transfected cells seen under filter for Hoechst staining. Fig. 6.13(c) shows the change in apoptotic index of HeLa cells after expression of Met, assessed by cell counting. This experiment was performed in triplicate, and repeated 3 times (mean ± SD). The results shown are those of a typical experiment.

(S/MARs) which are believed to be involved in the regulation of chromatin expression and gene expression[328,336]. The next conserved domain in Met corresponds to an RNA binding domain (beginning at residue 382). Such domains are usually about 80 amino acids long and contain two well-conserved sub-motifs RPN-1 (octamer) and RPN-2 (hexamer)[331]. A similar sequence is also found in Het[327], and similar sequences on other proteins have been shown to alter pre-mRNA splicing, and hence cellular responses such as growth, differentiation and apoptosis[337].

A third motif conserved between the Met and Het proteins which is rich in glutamine (26%) and arginine (31%) residues falls between residues 652-740 of Met, and there is 73% identity between the two. In the Het protein, this sequence has been shown to interact with hnRNP D[338], and was proposed to be responsible for the effect of Het on the transcriptional activity of the oestrogen receptor. Nayler et al.[339] demonstrated that the C-terminal portion of SAF-B was able to bind the C-terminal domain (CTD) of the large subunit of RNA polymerase II.

The Met sequence has also been shown to contain 3 separate nuclear localization signals, beginning at residues 593, 726 and 800, all of which are found at the carboxyl end of the protein.Using Northen blot analysis, Met has been shown to be present in most tissues of the mouse (analysis performed by Dr. Shane Colley in this lab) (Fig.6.14).

Like Het, Met appeared in initial experiments to downregulate the transcriptional activity of the estrogen receptor. More careful analysis, however, showed that it also causes a

down-regulation of the constitutively active β-galactosidase reporter (Fig.6.4b). Although 'correction' of luciferase activity by β-galactosidase appears to leave a residual inhibitory effect of Het and Met on oestrogen signalling, it seems likely that differences in half-life of these two proteins are responsible for these changes, raising doubts about the earlier reports describing Het as a regulator of oestrogen signalling[329]. Similar arguments may apply to the ability of Het to downregulate Hsp27 transcriptional activity in various cell lines[325]. Experiments described in this thesis clearly show the potential for misinterpretation of reporter assays when a constitutively expressed reporter is used to control for transfection efficiency of a regulatable reporter[340].

That Met behaves in a similar manner to Het is not entirely unexpected. Het has been shown to bind RNA polymerase II (Pol II)[326], so the ability of Met to interfere with reporter gene activity could be due to its effect on RNA polymerase II activity. If Met does indeed function at the level of the polymerase, it would explain why it has a generalized effect on cellular activity, rather than exerting effects on specific gene sequences.

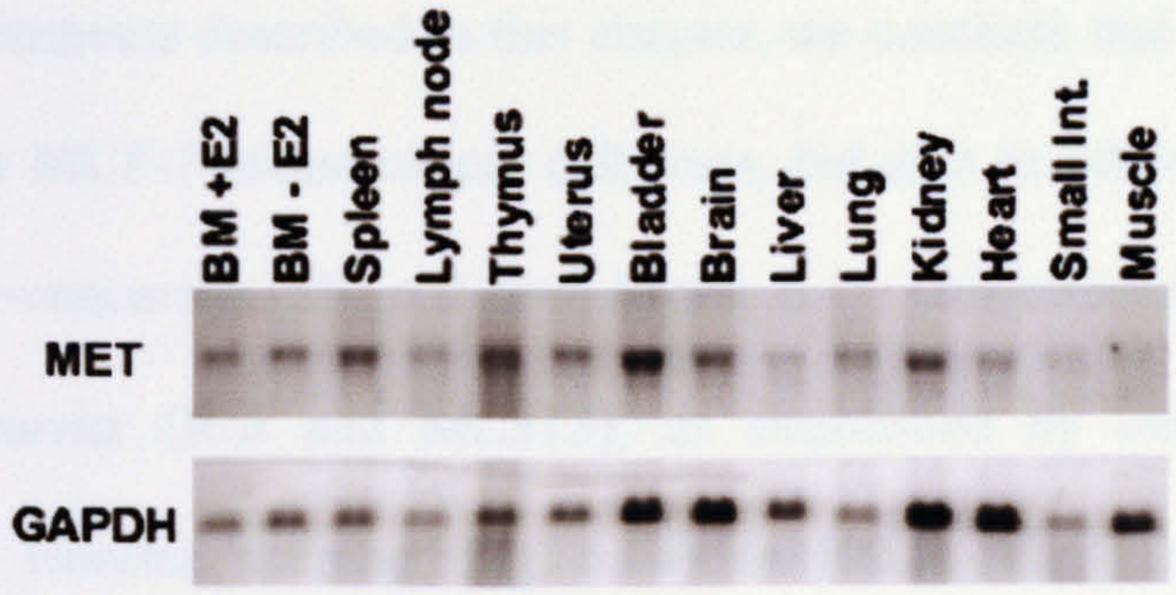

Figure 6.14 Northern Blot showing expression of Met mRNA in various tissues (BM= bone marrow. Experiment performed by Dr. S. Colley).

From the experiments described in this chapter, we conclude that Met induces apoptosis, not just in the MCF-7 breast cancer cell lines, but also in other cancer (HepG2, HeLa cells) and non-cancerous (SF) cell lines (Table 6.1). This effect is also preserved across the species barrier (Ros and MC3T3), as established by cell cycle profiling, and confirmed by Hoechst staining (Fig. 6.14). In HeLa cells, the remaining viable cell population appears to be arrested primarily in the G1 phase, with a corresponding decrease in the G2 population. The proportion of cells in the S phase remained unchanged (Fig 6.12). Similar changes were noted in the other cell lines, but these were not statistically significant (Table 6.2).

From results shown in Figs. 6.9 and 6.8, apoptosis induced using the EYFP-Met chimera (37±10% (SD)) appears to be greater than that detected when HA-tagged Met is used (23±6% (SD)). This discrepancy may be due to preferential leakage of EYFP from cells (co-transfected with pEYFP and HA-Met) in late apoptosis owing to leaky membranes. Leakage of enhanced green fluorescent protein (EGFH) from permeabilized cells is known to occur (infomation from Invitrogen website). EYFP is very similar to EGFP (created by performing 4 amino acid substitutions to EGFP) in structure and size, and it can be expected to behave in a similar manner. In contrast, when cells are transfected with the EYFP-Met chimera, owing to the larger size of the product, there is less likely to be loss of EYFP.

Similarly, the extent of apoptosis induced by Met varies depending on the cell line in question (Table 6.1). In Ros and HeLa cell lines, Met induces a twofold increase in the

amount of apoptosis detected, whereas in the MCF-7 and MC3T3 cell lines, this increase is threefold. In the HepG2 and SF cell lines, the increase is fourfold. The difference does not appear to be due to interspecies differences as Ros and MC3T3 cell lines are derived from rat mouse respectively. The difference in apoptosis detected could be attributed to several factors, the first being differences in transfection efficiency. A difference in the response of each cell line to serum starvation, leading to changes in cell cycle progression, survival signalling, and how these affect the response of the cell to apoptois could also be responsible. Another factor that has to be considered is the effect of transformation/immortalization on susceptibility to apoptosis. SF fibroblast cells were found to be particularly prone to apoptosis. These are primary untransformed cells and their reaction to Met is consistent with the hypothesis that the further along the transformation pathway a cell has gone, the more resistant it is to apoptosis. This leads on to the third possibility that the amount of apoptosis induced is affected by the presence or absence of mutations affecting the apoptotic programme, which will vary from cell line to cell line.

Most probably, decreased expression of reporter plasmids is linked to the induction of apoptosis by Met and could, for example, result from decreased gene expression or mRNA translation, or increased mRNA or protein turnover. Given the similarity between Met and Het, together with evidence that Het interacts with RNA polymerase II, it seems likely that one consequence of overexpressing Met might be inhibition of mRNA synthesis. Whether or not effects on reporter genes are linked to the ability of Met to induce apoptosis is unclear. One possible path by which Met could induce apoptosis

would be by affecting alternative splicing, since Het has been shown to regulate alternative splicing[339]. Thus, Met may favour the splicing of or induce the transcription of pro-apoptotic proteins which result in apoptosis.

Alternative splicing is a rapidly advancing field despite its relative infancy. The discovery that various cell proteins and enzymes exist in various isoforms, each possessing a unique function, has opened up another avenue by which cells can regulate their activities and response to extracellular stimuli[341]. Studies on key apoptotic components confirm that one mechanism of regulation could well be via alternative splicing. The best known example of alternative splicing in apoptosis is that of the Bcl-X protein. This exists as two isoforms, a long form (Bcl-X_L), well known for its anti-apoptotic effect, and a short form (Bcl-X_S) which has been shown to be pro-apoptotic[342]. In the same study, caspase-9 was also shown to have both pro-and anti-apoptotic isoforms. One of the earliest caspases to be discovered, caspase-2 (or Ich-1), has a pro-apoptotic long form and a short anti-apoptotic form[343,344]. In addition, alternative splice forms for Apaf-1[345] and caspase-8[346] have also been identified and their apoptotic activities investigated.

In view of these findings, we decided to characterize the Met protein further, by investigating its cellular localization, its co-localization with sites of transcription, and whether it alters transcription and mRNA processing.

7 Met Expression and Function

7.1 Characterization of Met

Because of its similarity to Het/SAF-B, in the previous chapter we investigated the involvement of Met in oestrogen signalling. In this chapter, we investigate other possible similarities between the two proteins, such as cellular localization. Also, because Het/SAF-B has been shown to be involved in pre-mRNA processing[339], we hypothesized that induction of apoptosis by Met might result from altered RNA processing. All confocal images were acquired using a Leica TCS-NT confocal laser scanning microscope attached to a Leica DM RBE upright epifluorescence microscope with phase-contrast. Leica software was used to process the images acquired.

7.1.1 The cellular distribution of Met

HeLa cells ($1x10^5$) were grown on coverslips in 6-well plates and incubated overnight. The cells were transfected with 1μg of either pEYFP-C1 (control plasmid) or pEYFP-Met using Fugene6 and incubated for 48 hours to allow for protein expression. The coverslips were fixed (2% PFA/PBS, 20min at room temperature) and mounted onto glass slides (BDH) and viewed by confocal microscopy to determine the cellular distribution of Met. From Fig. 7.1, it can be seen that Met is confined entirely to the nucleus, in a speckled distribution similar to that reported for Het/SAF-B. In addition, as with Het/SAF-B[325], it is clear that Met is also excluded from the nucleolus.

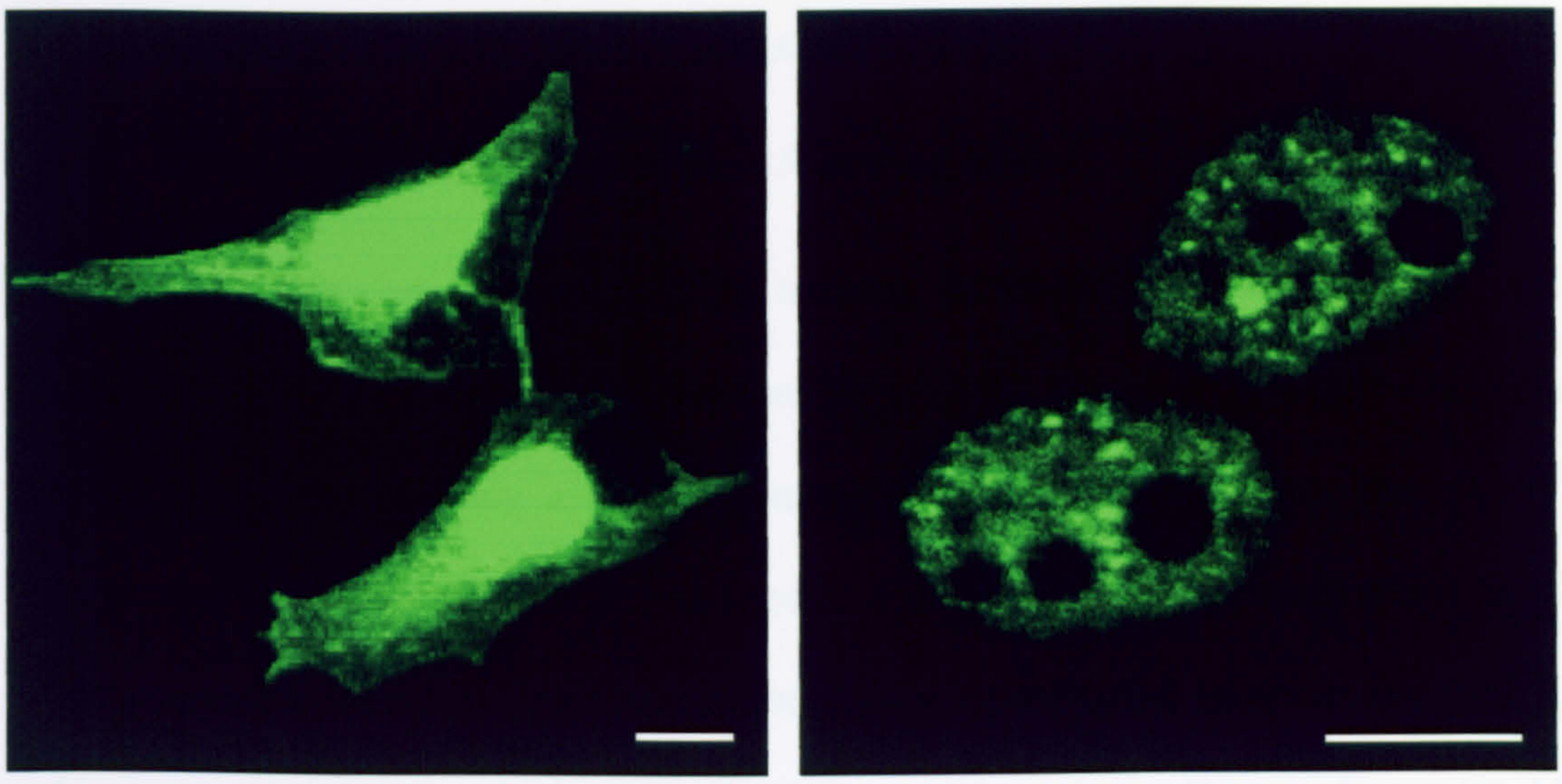

(a) (b)

Figure 7.1 Cellular distribution of Met assessed by confocal microscopy.

HeLa cells were grown on coverslips and transfected with either pEYFP(a) or pEYFP-Met(b). The cells were fixed and mounted onto glass slides and viewed by confocal microscopy. (Scale: white bar: 5μm)

7.1.2 Comparison of Met localization with other proteins

7.1.2.1 Does Met co-localize with the SC-35 splicing factor?

As Met has a speckled distribution in the nucleus, we investigated the possibility that it might co-localize with a nuclear protein that displays the 'classical' speckled distribution within the nucleus, namely a serine/arginine-rich (SR) splicing factor. The SC-35[347] splicing factor is one such protein localized to nuclear speckles. Although initial studies with a partial Het/SAF-B sequence did suggest co-localization between the two[339], a subsequent study showed that Het/SAF-B speckles were distinct from speckles containing SC-35[327].

$1x10^5$ HeLa cells were grown on coverslips in 6-well plates and incubated overnight. The cells were transfected with 1μg pEYFP-Met using Lipofectamine Plus and incubated for 48 hours to allow for protein expression. The coverslips were fixed (2% PFA/PBS, 20min at room temperature) and permeabilized (0.1% Triton X/PBS, 5min, room temperature). The cells were then blocked with 1%BSA/PBS for 20min at room temperature. Next, the cells were incubated with mouse anti-SC-35 primary antibody (Sigma, 1:1000 dilution in 1%BSA/PBS) overnight at 4°C. Following 3 washes with 1%BSA/PBS, the cells were incubated with Cy3-conjugated donkey anti-mouse secondary antibody (Jackson Immunology) (1:800 dilution in 1%BSA/PBS) for 1-1.5 hrs at room temperature in the dark. After 3 washes with PBS, the coverslips were mounted onto glass slides using DAKO fluorescent mounting medium and the slides analysed by confocal microscopy. Fig. 7.2 shows that Met does not co-localise with the splicing factor SC-35, but forms distinct speckles.

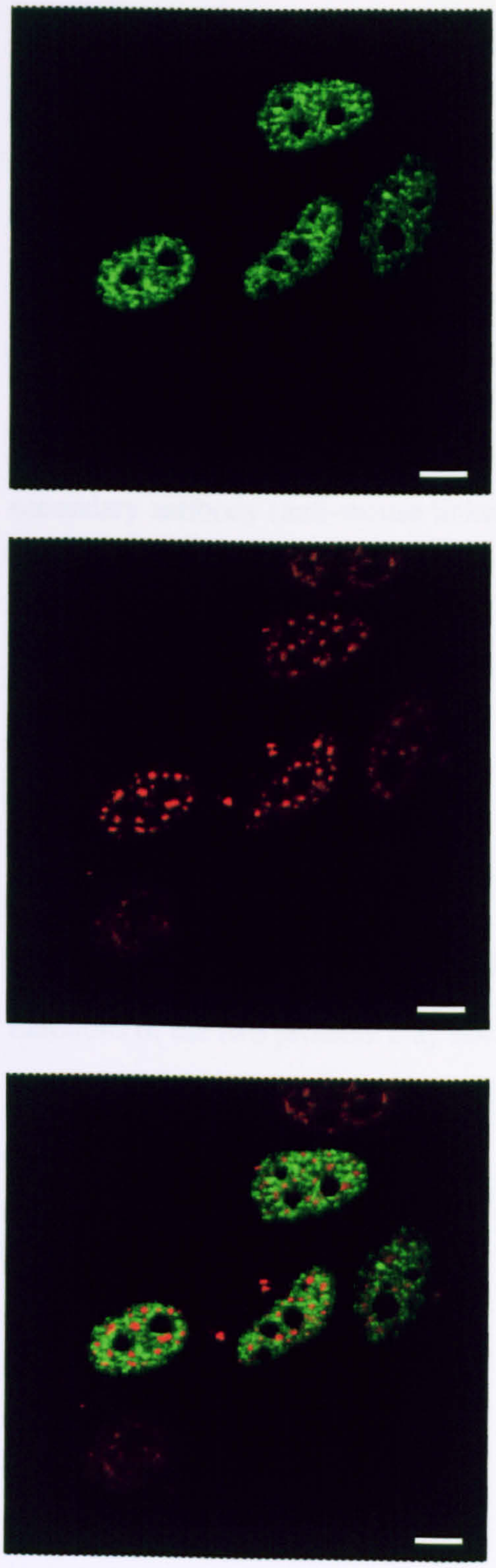

Figure 7.2 Distribution of Met compared with that of SC-35, an SR protein, assessed by confocal microscopy.

HeLa cells were grown on coverslips and transfected with EYFP-Met. The cells were fixed, permeabilized and then stained for SC-35. Following detection of the primary antibody using a donkey anti-mouse secondary antibody, the coverslips were mounted onto glass slides and viewed by confocal microscopy. Cells transfected with YFP-Met(top), distribution of SC-35(middle), and overlay showing different distributions of Met and SC-35(bottom). (Scale: white bar: 5μm)

7.1.2.2 Co-localization of Met with Het

We next studied the distribution of Met in comparison to Het. HeLa cells were plated out as before and co-transfected with 1μg of both pEYFP-Met and pHA-Het. Following a 48 hour incubation, the cells were fixed, permeabilized, and blocked before staining for the Het protein using an anti-HA mouse monoclonal antibody (Sigma, 1:5000 dilution) (4°C, overnight). The cells were washed 3 times with 1%BSA/PBS and then incubated with the secondary antibody (anti-mouse linked to Cy3, Jackson Immunology) (room temperature, 1-1.5 hrs in the dark). The cells were then washed 3 times in PBS and then mounted onto glass slides.

Fig. 7.3 shows that Met partially co-localizes with Het (white arrows). The co-localization is not complete, however, as shown by the presence of some green (Met) speckles in locations where Het appears to be absent (broad arrows) suggesting that functions of the two proteins may not be identical.

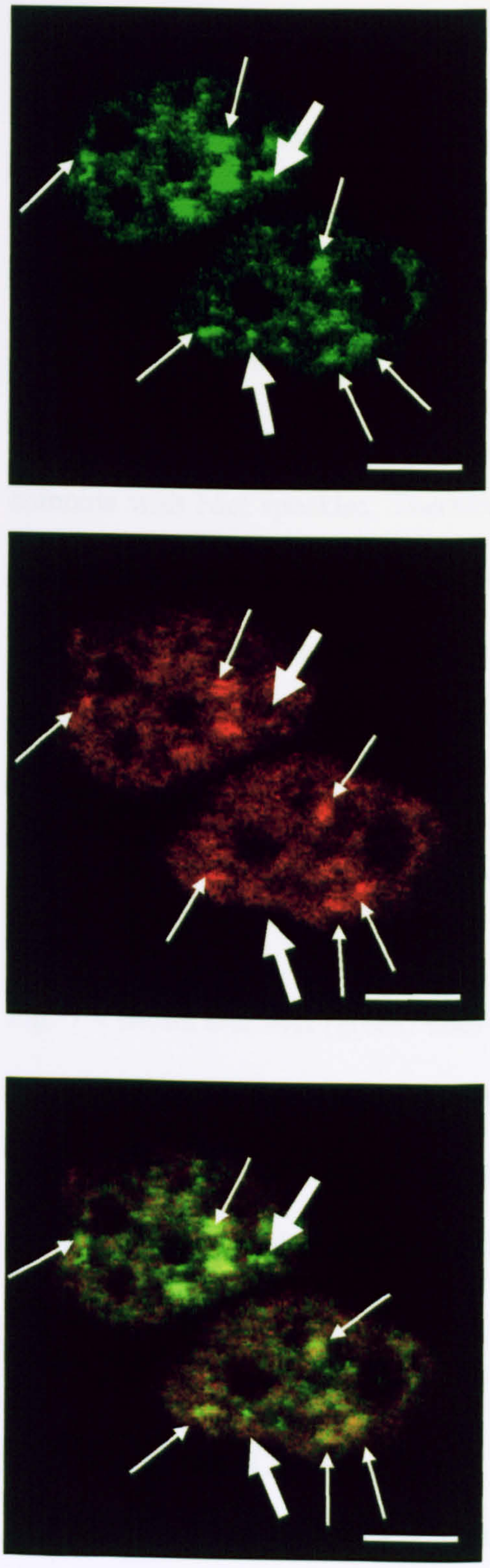

Figure 7.3 Co-localization of EYFP-Met with HA-Het.

Hela cells were transfected with pEYFP-Met and HA-Het. The cells were fixed and stained with anti-HA antibody before viewing under the confocal microscope. The pictures show the distribution of Met (top), Het (middle) and an overlay of both images (bottom) showing co-localization of Het with Met. (co-localization: narrow arrow; lack of co-localisation: broad arrows.). (Scale: white bar: 5μm)

7.1.2.3 Does Met co-localize with the oestrogen receptor (ER)?

Although our initial experiments did not provide evidence in favour of a role for Met in the regulation of oestrogen receptor activity, we could not completely rule out such an interaction. In addition, several studies have shown that members of the nuclear hormone receptor family form discrete foci within the nucleus after activation by ligand[348,349]. The question then arises whether these foci, which probably represent sites of gene regulation, coincide with Met speckles. Therefore, we decided to compare the distribution of Met with the ER. As it is quite difficult to detect endogenous ER, we used a red fluorescent protein tagged ER chimera (pRFP-ERα, provided by Donald McDonald). HeLa cells were co-transfected with 1μg of both pEYFP-Met and pRFP-ERα. After a 48 hour incubation, the cells were exposed to 10^{-8}M E2 for 1 hour, then fixed and mounted onto glass slides before viewing under the confocal microscope.

Fig. 7.4 shows that Met (green) does not co-localise at all with ERα (red) in the absence of E2. Although it has been reported that E2 results in nuclear relocalisation of ER[349], we found that the images were unchanged for cells that had been exposed to E2 (Fig. 7.4d) showing that ERα either does not undergo nuclear localization on ligand binding, or else this change was very transient.

7.1.3 Mechanism of Action of Met

Met and Het induce apoptosis when overexpressed in cells while Het has been shown to alter splicing. Since changes in splicing have been linked with the induction of apoptosis[342,350], we decided to investigate the possibility that the mechanism of Met

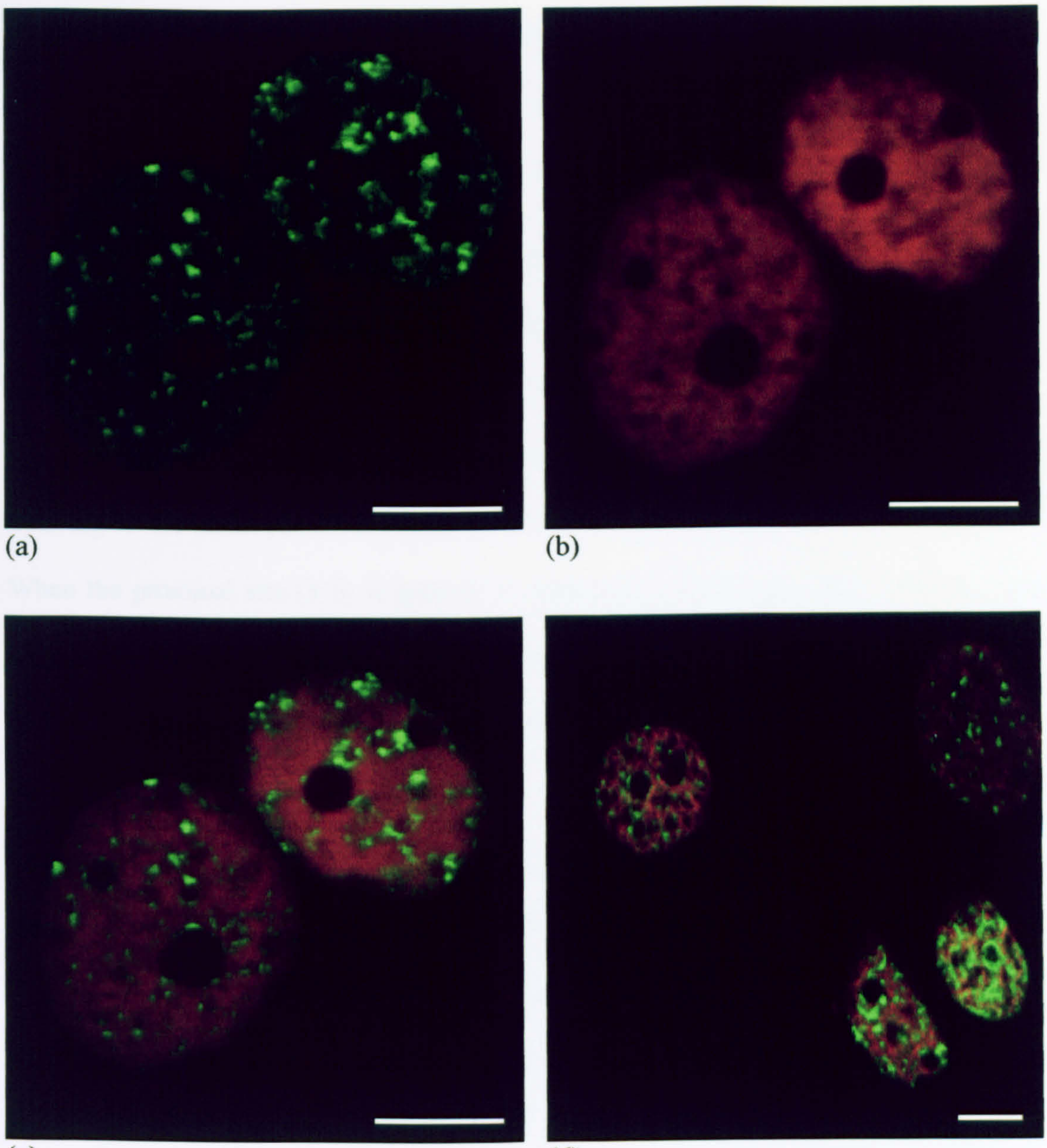

(a) (b)

(c) (d)

Figure 7.4 Distributuion of Met compared with the Oestrogen receptor (ER).

MCF-7 cells were transfected with pEYFP-Met and pRFP-ERα, incubated for 48hrs with or without exposure to 10^{-8}M E2 for 1 hr, prior to fixing and analysis under the confocal microscope. (a) shows the distribution of EYFP-Met in MCF-7 cells, (b) shows the distribution of ERα, and (c) shows an overlay of the two images, with different distributions of Met and the ER. (d) shows an overlay of Met and ER following treatment with E2. (Scale: white bar: 5μm)

action might involve altered splicing of caspases.

7.1.3.1 The presence of Ich-1L and Ich-1S in HeLa cells

Caspase 2 has been shown to have two isoforms which result from alternative splicing[343]. The full-length caspase, called Ich-1_L, is a 435 amino acid product, while the truncated form, Ich-1_S, is only 312 amino acids long. Figure 7.5 shows the isoforms of caspase-2, and how they arise following splicing from the two 5' donor splice sites (blue arrows). Splicing of the distal site (5'a) results in an mRNA encoding the full-length caspase-2. When the proximal site (5'b) is spliced, 61 base pairs of the intron (blue rectangle) are included in the mRNA sequence, resulting in the inclusion of an early Stop codon (red arrow), and hence translation of a shortened protein.

The primers used in the reverse transcription – polymerase chain reaction (RT-PCR) are those described by Wang et al[343]. The purple triangles indicate the approximate positions of the primers. RT-PCR of mRNA is expected to result in two products, corresponding to the long and short forms of caspase-2. Owing to inclusion of the additional 61bp of the intron, following splicing at the proximal 5'site (5'b) for Ich-1_S, the resulting PCR product is longer (~295bp) than the PCR product for Ich-1_L (the full caspase-2) which does not include the additional 61 bases (~234bp). Thus when the products are electrophoresed on an agarose gel, the larger product corresponds to Ich-1_S, while the smaller product corresponds to Ich-1_L.

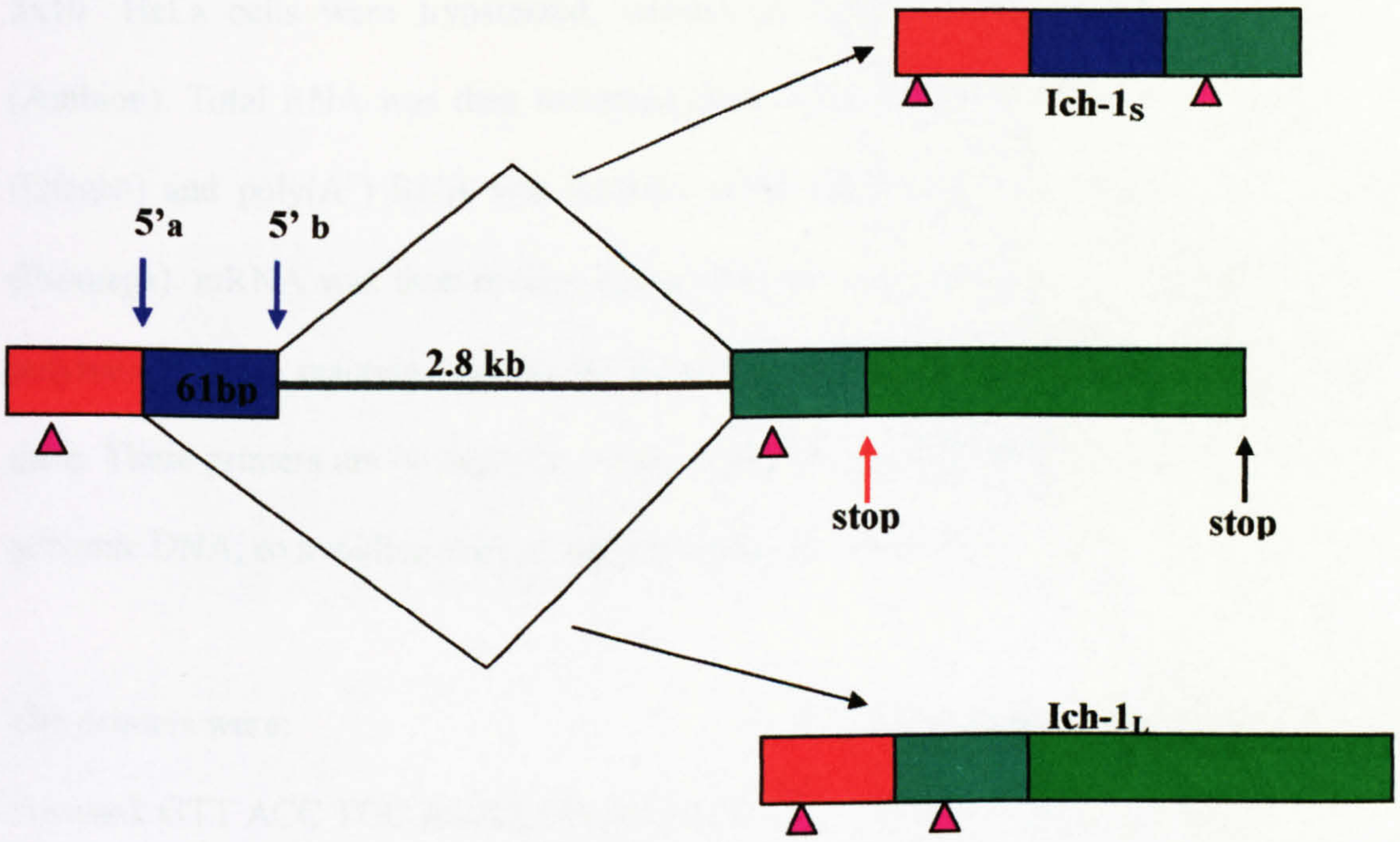

Figure 7.5 Alternatively spliced forms of Caspase – 2 (Ich-1).

Caspase 2 has two isoforms that arise due to alternative splicing of the 5'splice site. Splicing of the proximal site (5' b) results in the inclusion of a 61bp sequence, and places in frame a translational stop codon 21 amino acids downstream of the insertion site. This early stop codon results in the translation of a shortened protein, the truncated caspase 2 (Ich-1S). Splicing of the distal 5'splice site excludes the 61bp sequence and the early termination codon, resulting in the full length caspase 2 protein (Ich-1L) (Purple triangles: position of primers, showing how the PCR product from Ich-1L is shorter than the product from Ich-1S)[343].

$3x10^7$ HeLa cells were trypsinized, washed in PBS and resuspended in RNAlater (Ambion). Total RNA was then extracted from the cells using the RNAeasy Midi Kit (Qiagen) and poly(A^+) RNA was isolated using the PolyATract Isolation System IV (Promega). mRNA was then reverse transcribed and the cDNA obtained subjected to a polymerase chain reaction (Access RT-PCR Kit, Promega), using primers for the Ich-1 gene. These primers are on separate exons, separated by an intronic sequence of 2.8kb in genomic DNA, so avoiding the risk of amplifying genomic DNA.

The primers were:

Forward: GTT ACC TGC ACA CCG AGT CAC G

Reverse: GCG TGG TTC TTT CCA TCT TGT TGG TCA

The following PCR conditions were used: 1mM magnesium sulphate, 50pmol of each primer, and 20mM dNTPs. Reverse transcription was performed at 48°C, for 45 min, followed by a 2 min denaturation at 94°C. The following PCR cycle was used: 40 cycles of 94°C for 1 min, 57°C for 1 min and 68°C for 2 min, and a final extension at 68°C for 10 min.

The products of the PCR reaction were electrophoresed on a 2% TAE agarose gel. Fig. 7.6 shows a band migrating at ~295bp and a weaker band at ~234bp, corresponding to Ich-1_S and Ich-1_L respectively.

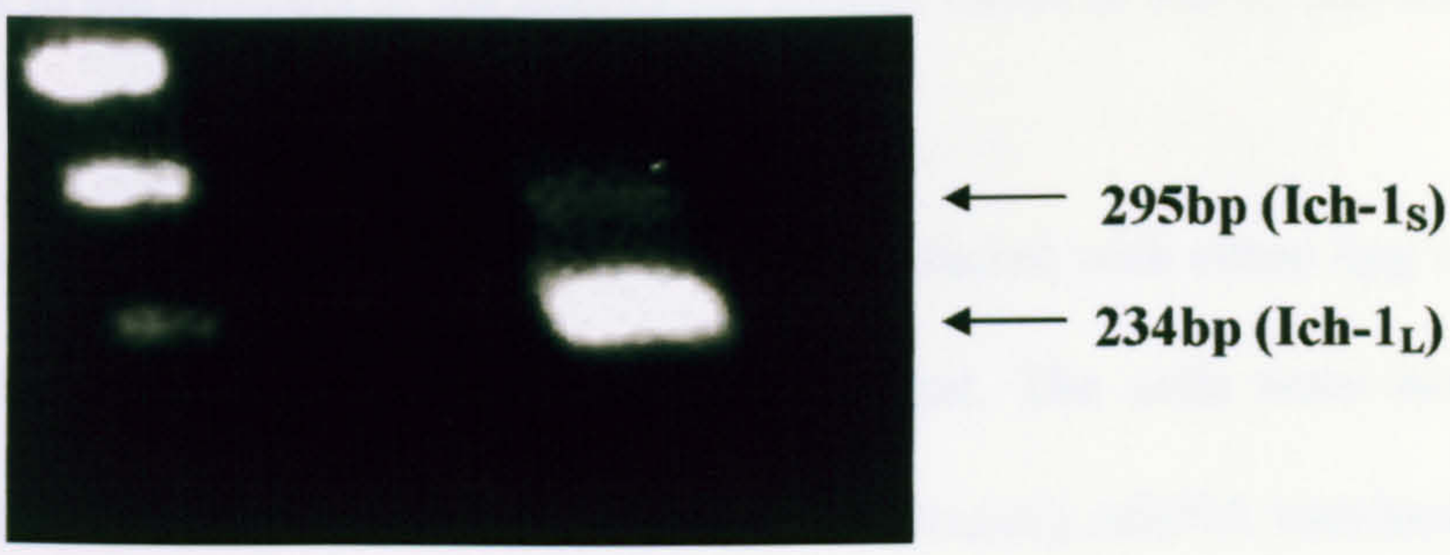

Figure 7.6 RT-PCR of HeLa mRNA to demonstrate presence of the mRNA for Ich-1_S (295bp) and Ich-1_L (234bp).

mRNA from HeLa cells was extracted and RT-PCR using primers specific for Ich-1 was performed (The control (Ctrl) was performed using a water blank).

7.1.3.2 Effect of Met on alternative splicing of pro-caspase2

We next investigated the possibility that overexpression of Met in HeLa cells might result in a change in the amounts of the alternative spliced forms of Ich-1_L and Ich-1_S.

$3x10^6$ cells were seeded in 100mm dishes and transfected with either 4μg of pcDNA3 (P) or pMet-HA (M) using Lipofectamine Plus reagent. The cells were incubated for 48 hours and RNA extracted with the RNAeasy Kit (Qiagen). mRNA was isolated as before. The mRNA was then reverse transcribed and PCR performed using the Access RT-PCR kit (Promega), with the same conditions as described previously.

Fig. 7.7 shows the cDNA products from RT-PCR of mRNA extracted from HeLa cells transfected with either pcDNA3 (P) or pMet-HA (M). In cells transfected with Met, the amount of PCR product for both the long and short forms of caspase-2 appears to be increased compared to the cells transfected with the empty plasmid. RT-PCR for glyceraldehyde-3-phosphate dehydrogenase (GAPDH) from the mRNA samples was subsequently performed as a control to assess consistency of mRNA extraction between the 6 samples. The primers used for PCR of GAPDH were as follows:

Forward primer: AAGGCTGAGAACGGGAAGCTTGTCATCAAT (exon 3, bp241-270)

Reverse primer: TTCCCGTCTAGCTCAGGGATGACCTTGCCC (exon 7, bp 740-711)

The results in Fig. 7.8 show an increase in GAPDH amplification with mRNA extracted

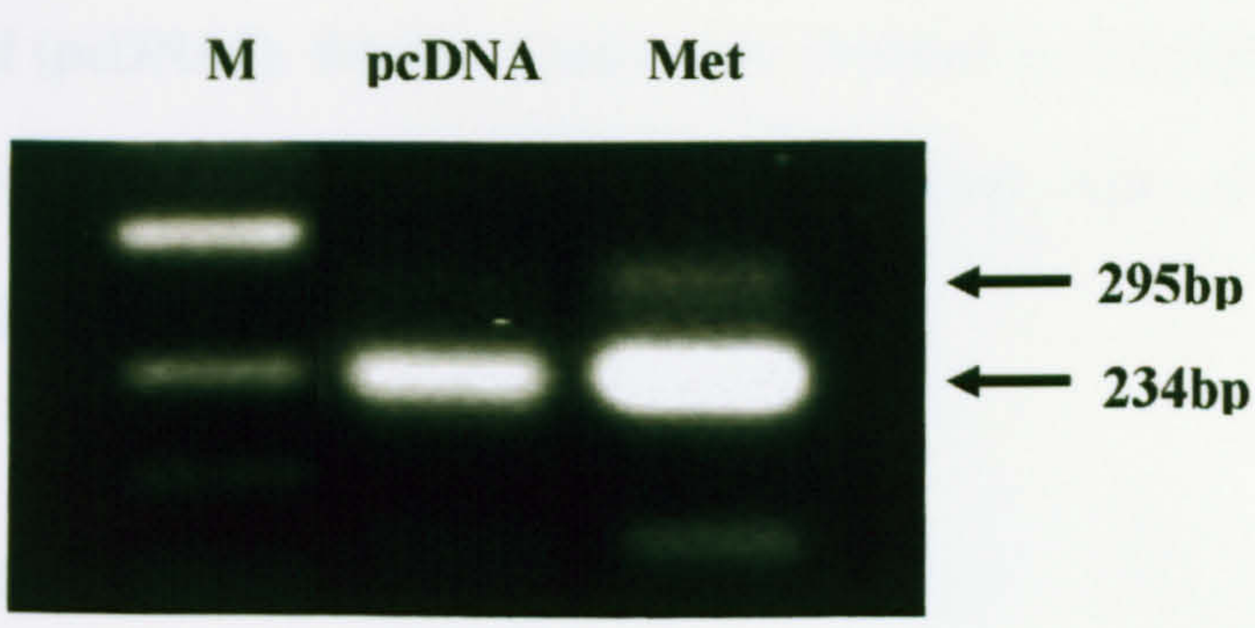

Figure 7.7 cDNA products from RT-PCR assessing the effect of overexpressing Met on the relative abundance of the alternatively spliced forms of the Ich-1 (caspase 2) gene.

HeLa cells were transfected with pcDNA3 (empty plasmid, pcDNA) or pMet-HA plasmid (Met) and incubated for 48hrs. 3 separate transfections with each plasmid were performed and the RNA extracted separately. mRNA was then isolated and RT-PCR using specific primers was performed. The product from the Ich-1S is 295bp, and the product from the Ich-1L isoform is 234bp. (M: markers)

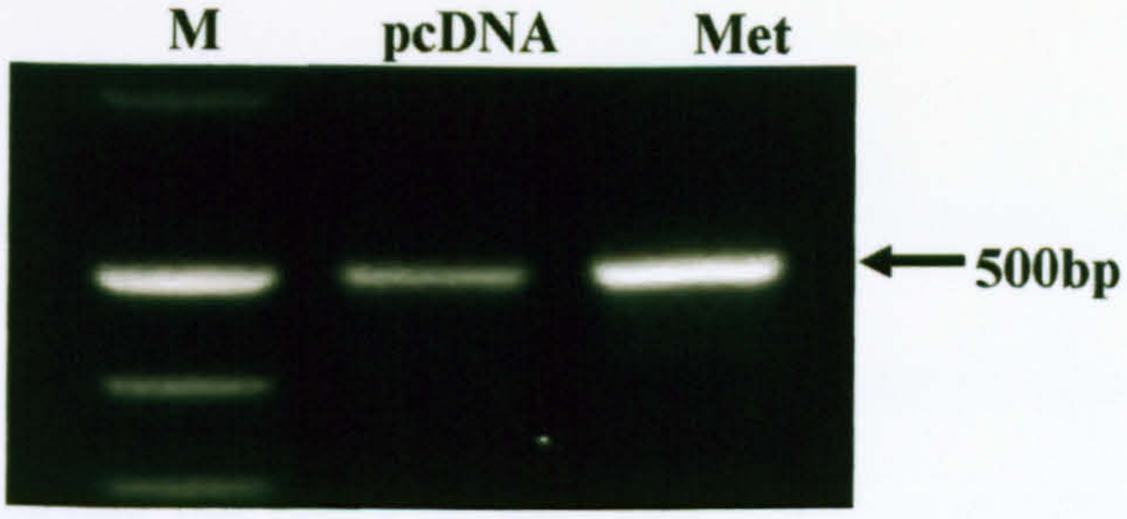

Figure 7.8 cDNA products from RT-PCR of GAPDH mRNA in the above samples.

mRNA from the above samples was subjected to RT-PCR using primers specific to GAPDH. The fragment from GAPDH PCR is about 500bp in size. (M: markers)

from Met transfected cells in comparison to that from the control cells transfected with empty plasmid (pcDNA3). Similar results were obtained in two additional experiments (not shown) implying that total mRNA was extracted more efficiently from Met transfected cells.

The results shown in Fig. 7.7 do not show an obvious change in the ratio of Ich-1_L to Ich-1_S, but it is difficult to quantify bands visually. To obtain a quantitative measure of the ratio of long to short isoforms of Ich-1, the above PCR assay was repeated using a fluorescent moiety on the 5'end of the forward primer, and the fluorescence of the products of the PCR reaction was measured using an ABI Prism 310 Genetic Analyzer (analysis performed by Ms Sarah Groves, Dept of Pathology and Microbiology, University of Bristol).

As shown in Fig. 7.9, there is no change in the ratio of the long to short forms of the caspase-2 PCR products in cells transfected with Met.

7.1.3.3 Measurement of mRNA synthesis using [3H] uridine incorporation.

Given that Met had an inhibitory effect on reporter gene activity, we decided to investigate whether this could be due to an inhibition of mRNA transcription. Therefore, we measured incorporation of uridine into RNA.

HeLa cells ($1.5x10^5$) were seeded into 60mm dishes, and transfected with either 2μg of pcDNA3 (empty plasmid) or HA-Met. After a 48 hr incubation, cells were exposed to

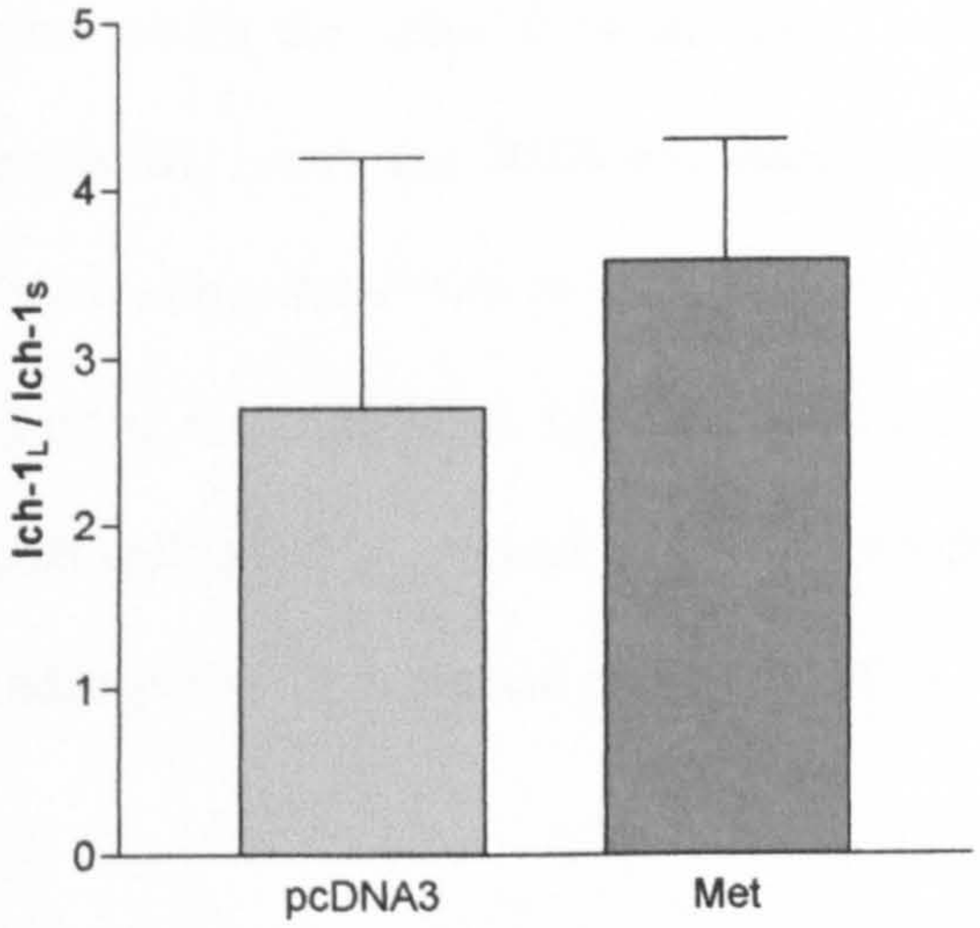

Figure 7.9 Ratio of the PCR products of Ich-1_L to Ich-1_S following transfection with Met.

HeLa cells were transfected with either pcDNA3 (empty plasmid) or pMet-HA (1μg each). Following a 48 hr incubation, cells were lysed and mRNA extracted. RT-PCR of the mRNA, using fluorescent labeled primers, was performed and the products of the reaction analysed on an ABI Prism 310 Genetic Analyser (analysis performed by Dr. S. Groves). This figure is the mean of three separate experiments (showing the mean and standard deviation).

20μCi/dish for 1hr, after which the cells (from medium, 1xPBS wash and following trypsinization) were collected, lysed and RNA extracted using the RNeasy Mini Kit. mRNA was then isolated using the Promega PolyTract A^+ mRNA Isolation Kit and radioactivity measured using the 1400 DSA Liquid Scintillation Counter. As shown in Fig.7.10, Met-transfected cells show a marked inhibition of mRNA synthesis (down to 47%±14(SD)) compared to pcDNA transfected cells, ($p<0.005$).

7.1.3.4 Measurement of total RNA transcription using [3H] uridine incorporation.

To determine whether overall RNA synthesis was affected by Met, HeLa cells ($3x10^4$) were seeded in 96-well plates and incubated overnight. The cells were transfected with 0.1μg of either pcDNA3 (empty plasmid) or pMet-HA using Lipofectamine Plus (Invitrogen), and incubated for a further 48 hours. Following this, cells were exposed to $[^3H]$ uridine (1μCi/well) for 1 hour. The cells were then lysed and transferred to Printed Filtermat A (Wallac), for determination of radioactivity.

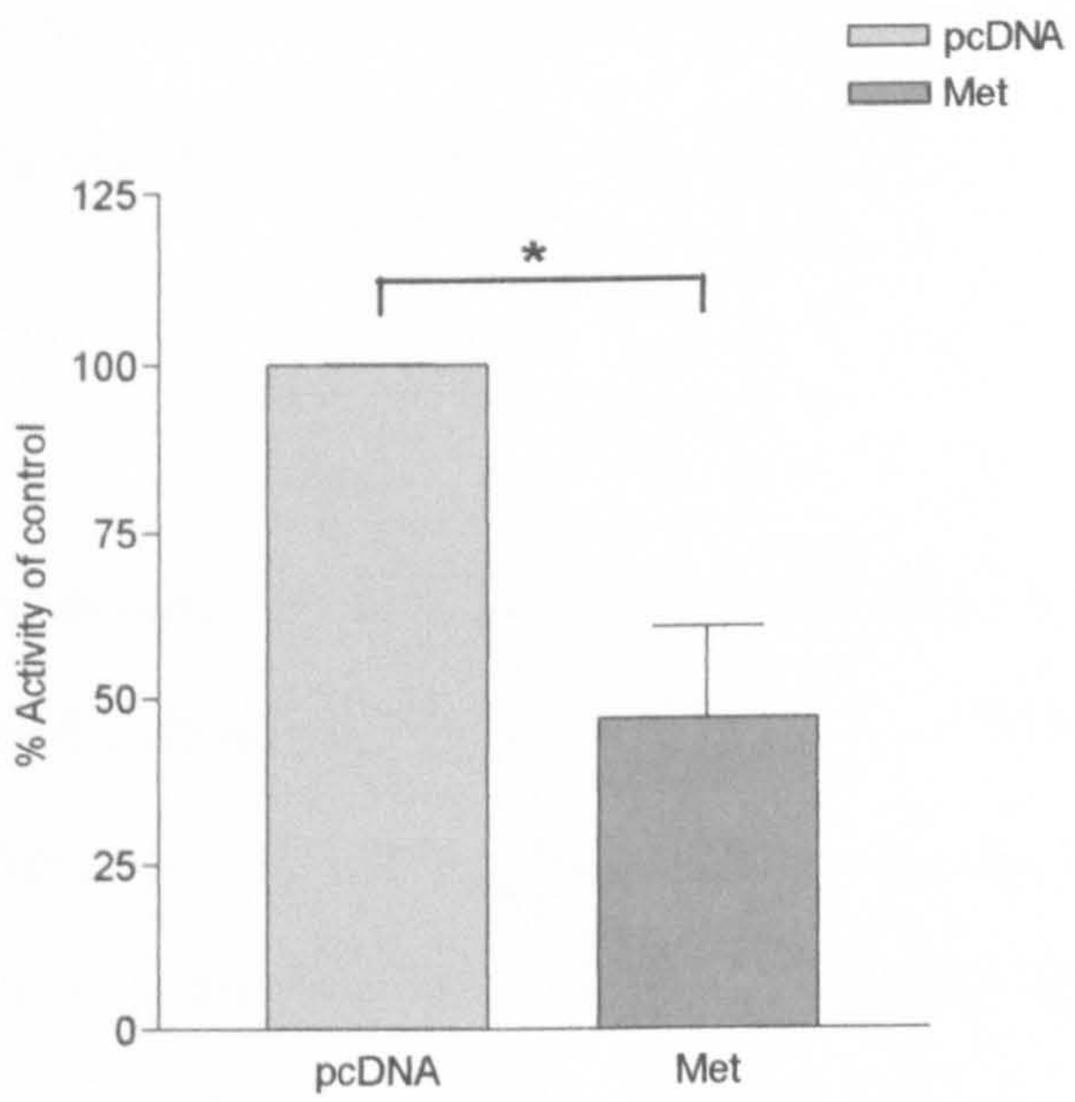

Figure 7.10 Effect of Met on mRNA synthesis in HeLa cells, assessed by uridine incorporation.

HeLa cells were transfected with 2μg of either pcDNA3 (empty plasmid) or pMet-HA, and incubated for 48hrs. The cells were exposed to [3H] uridine (20μCi/dish) for 1hr, before cells were collected and RNA extracted. The mRNA fraction was isolated from this, and the radioactivity measured in the 1400 DSA Liquid Scintillation Counter (Wallac). This figure is the mean of three separate experiments (showing the mean and standard deviation).

Fig. 7.11 shows that there is no significant difference ($p= 0.67$) in the overall rate of RNA synthesis following overexpression of Met in HeLa cells.

7.2 DISCUSSION

Using confocal microscopy, we were able to ascertain that Met was confined to the nucleus in a speckled fashion (Fig. 7.1), in a distribution that was similar, but not identical to that of Het (Fig. 7.3). This implies that while Met may be involved in some of the same processes as Het, this is not the sum of its actions, and thus Met is likely to have some unique functions. Methodological considerations, however, meant that we cannot be entirely sure that the small differences in location reflect true differences in the distribution of these proteins. It is possible that differences in expression result from the use of different vectors (Het in PCR 3.1 and Met in pEYFP-C1), though both are driven by the same promoter (CMV). It is also possible that the EFYP moiety itself affects distribution, perhaps resulting in some degradation of the chimera at specific sites. Finally, incomplete co-localization could arise due to a difference in fluorescent intensities of EYFP and Cy3 since a certain degree of photo-bleaching was observed with Cy3. It was also noted that Met was excluded from the nucleoli of the cell, the main site of ribosomal RNA synthesis, processing and maturation[351], which leads us to infer that Met does not have any direct activity on ribosomal RNA synthesis, a view that was strengthened by our results from [^{3}H] incorporation showing that Met inhibited mRNA transcription without significantly affecting overall RNA transcription rates (Figs. 7.10 and 7.11).

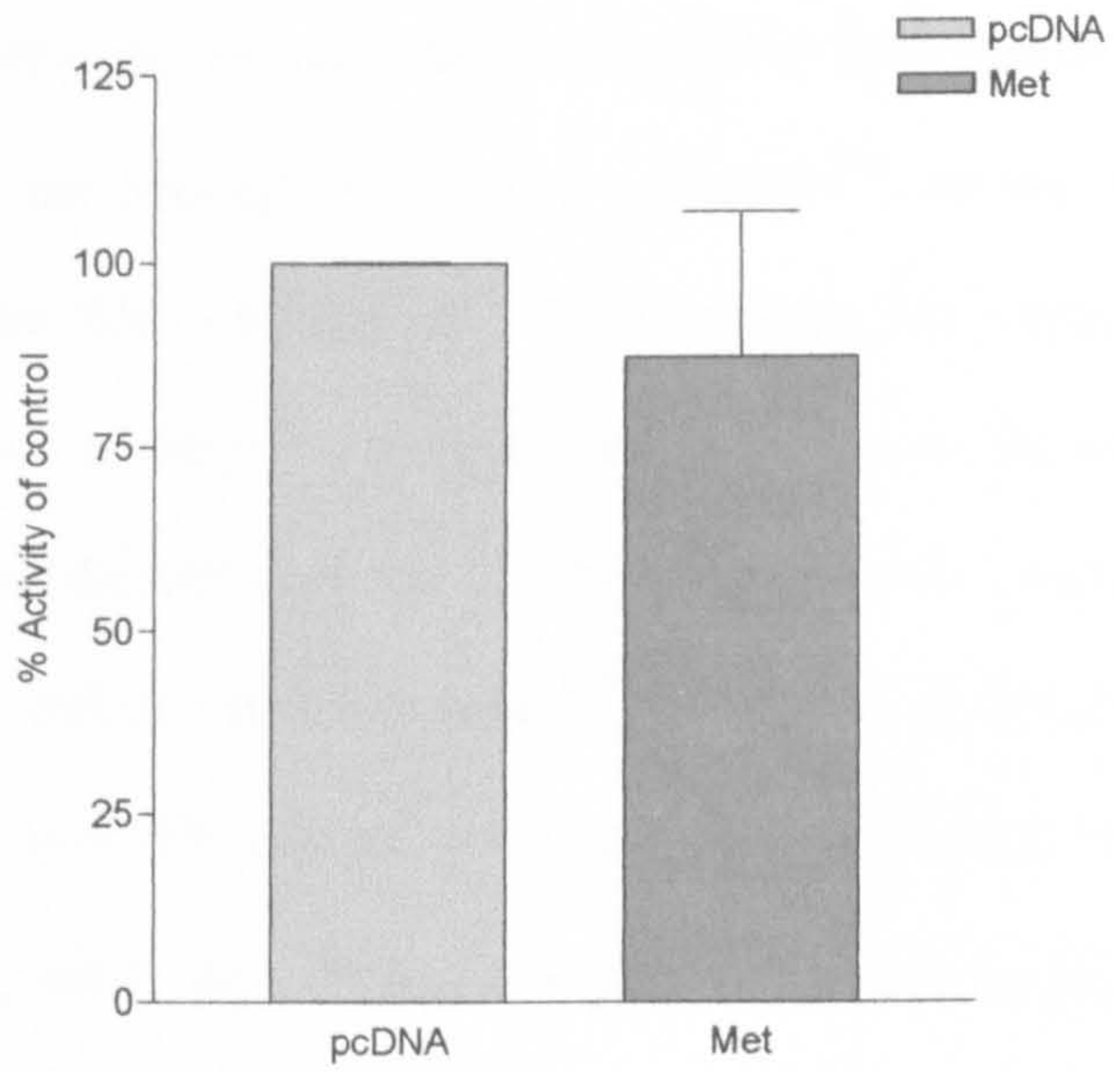

Figure 7.11 Effect of Met on transcription of total RNA in HeLa cells, assessed by uridine incorporation.

HeLa cells were transfected with 0.1μg of either pcDNA3 (empty plasmid) or pMet-HA, and incubated for 48hrs. The cells were exposed to [3H]uridine (1μCi/well) for 1hr before cells lysed, harvested, and radioactivity measured. This figure is the mean of three separate experiments (showing the mean and standard deviation.

The studies described in the previous chapter did not support a role for Met in regulation of ER signalling, but had not completely ruled out such a function. Moreover, earlier studies on nuclear hormone receptors demonstrated that ER could be induced to assume a speckled pattern in the nucleus after ligand activation[349], so we decided to determine whether Met and the ERα co-localised in the nucleus. The complete absence of any overlap in distribution of the two proteins is compatible with our earlier conclusion that Met does not interact directly with the ER, but does not rule out an indirect interaction (Fig. 7.4). However, unlike a previous study[349], we did not observe E2-induced speckling of ERα. The most probable reason was that we were looking at the distribution of overexpressed ERα, while the previous study had analysed distribution of endogenous ERα using labelled autoantibodies.

In recent years, it has been accepted that the nucleus is organized into distinct structural components, called 'nuclear bodies'. These include nucleoli, Cajal (coiled) bodies, promyelocytic leukaemia bodies and speckles[352,353]. Most of these structures have been implicated in RNA metabolism[354]. Nuclear speckles have been found to contain high concentrations of pre-mRNA splicing factors, such as SC-35, and correspond to interchromatin granules originally observed via the electron microscope[355]. Whilst the function of these speckles is still undefined, it is clear from the available evidence that they are involved with the storage and/or assembly of components of the splicing machinery[356-358]. The speckled nuclear distribution of Met therefore suggested that Met may be involved in mRNA transcription or processing and we were interested to compare its distribution with other proteins localized to speckles that are known to be involved in

mRNA splicing. One of these is SC-35, a splicing factor that is involved in mRNA processing[359]. From our studies, it is apparent that Met does not co-localize with SC-35 at all (Fig 7.2). Weighardt *et al.*[327] made a similar observation when studying possible co-localization of SC-35 and Het/SAF-B/HAP. In this initial study, Weighardt *et al.* had described a 917 amino acid protein that was a member of the hnRNP family, as co-immunoprecipitation studies using the anti-HAP antibodies also brought down ribonucleoprotein complexes[327]. In this and a later paper, they also demonstrated the re-localization of HAP/SAF-B into a distinctive punctate pattern that did not coincide with coiled bodies or speckles following heat shock. Incidentally, they had performed co-localisation studies of HAP/SAF-B with splicing factor SC-35 in HeLa cells without heat shock, and also found no co-localisation between the two proteins[327,360]. As Met appears to have a similar distribution, we propose that Met, together with Het/SAF-B, may reside in a previously unidentified nuclear domain, but this will require further investigation.

Studies on uridine incorporation show that Met must exert a profound effect on mRNA synthesis. These experiments were performed on cells transfected with a plasmid expressing Met, so that inhibition of mRNA by ~50% when cells are transfected with an efficiency of about 80% suggests an almost complete cessation of mRNA synthesis in cells overexpressing Met. Given that Met down-regulates both cellular transcriptional activity and induces apoptosis, we wished to identify the initiating event for these processes. It is possible that either Met induces apoptosis which then results in decreased transcriptional activity or that Met inhibits transcriptional activity which then results in apoptosis. The former seems more likely because apoptosis has been associated with

decreased mRNA levels[361-363], probably due to degradation of RNA polymerase II, required for transcription of mRNA, by caspases[364]. The latter posibility seems less likely because generalized inhibition of transcription by itself does not invariably result in apoptosis[365]. The presence of a SAF box and RNA binding domains within Met suggest that Met is involved in mRNA processing, and one way it could induce apoptosis at this level would be to alter splicing of proteins involved in apoptosis.

Several studies have shown that various pro-apoptotic proteins, particularly caspases, have alternative splice forms[342,346,366,367], and the expression of one over the other can tip the cell into apoptosis, or favour cell survival[344,345,368]. Moreover, Valcarcel et al have recently shown that the apoptosis-promoting factor T-cell restricted intracellular antigen (TIA)-1[369] is able to regulate splicing of the human Fas mRNA by strengthening the recognition signal of a particular splice site in the gene[370], thus promoting apoptosis, and we speculated that Met may promote apoptosis via a similar mechanism.

Thus, we decided to investigate the possibility that Met may affect the splicing and hence, change the ratio of caspase-2 (Ich-1) isoforms, which have been shown to have opposite functions[343]. The long form (Ich-1_L) induces apoptosis, while the shorter form (Ich-1_S) blocks apoptosis. Various studies have shown, and we also confirmed (Fig. 7.6), that HeLa cells express both isoforms of Ich-1[343,367]. This, together with the fact that HeLa cells transfect relatively efficiently, made them the cell line of choice to assess whether overexpression of Met affected the ratio at which the long form of Ich-1 was expressed compared to the shorter form.

If our hypothesis were true, we would expect a relative increase in the amount of the long form of Ich-1, associated with either a decrease, or no change, in the amount of Ich-1_S expressed. Unexpectedly, RT-PCR appeared to show an increased amount of mRNA for both Ich-1_L and Ich-1_S (Fig. 7.7). A similar change was observed using primers for GAPDH (Fig. 7.8) as an internal control, however. Similar results were obtained in three separate assays, suggesting that mRNA from Met transfected cells is more efficiently recovered, perhaps due to physical interaction between Met and mRNA preventing degradation, or increased efficiency of mRNA extraction from cells undergoing apoptosis. This was reflected in the results of the RT-PCR reactions using fluorescent primers (Fig. 7.9) which allowed us to quantify the relative amounts of Ich-1_L and Ich-1_S. Thus, regardless of the apparent increase in the amount of mRNA extracted from Met transfected cells, the proportion of Ich-1_L to Ich-1_S remains unchanged, and is not affected by Met. The question arises whether Met is involved in alternative splicing at all. The factors that point to a possible role are the presence of a serine/arginine (SR) rich domain (characteristic of a group of splicing factors called SR proteins, such as SC-35)[347,371], and the RNA recognition motifs that are found in proteins known to affect alternative splicing (e.g. hnRNP A1 and hnRNP D (Fig. 6.1)). Splicing of pre-mRNA occurs in a large ribonucleoprotein complex, termed the spliceosome. This consists of 5 small nuclear ribonucleoproteins (snRNPs) and between fifty to a hundred polypeptides, some of which are splicing factors. The complex functions not only to identify splice sites, but also to position the pre-mRNA transcript into a configuration suitable for efficient excision of introns and ligation of remaining exons, to produce mature mRNA[372]. Whilst the 'core' members of the spliceosome are the snRNPs, they are

facilitated in their function by various SR proteins, such as SC-35 and U2 auxiliary factor (U2AF)[372]. Indeed, it is the RNA recognition motifs (RRMs) of SR proteins that are responsible for binding of RNA and substrate specificity[372,373]. Thus it is possible that the RNA binding sites on Met do not recognize the splice sites of caspase-2 and thus, Met is unable to affect splicing of this protein. A construct that has been used by many groups to assess the ability of a protein to affect alternative splicing is the E1A minigene[374-379]. A partial sequence of Het/SAF-B (corresponding to the C-terminal portion of human SAF-B) has been shown to affect splicing of the E1A minigene[339], but the properties of this fragment differ from those of the full length protein because Nayler et al found that the Het/SAF-B fragment co-localized with the splicing factor SC-35 whereas later studies with the full length protein found that SAF-B did not co-localize with SC-35[327]. Nevertheless, it would clearly be interesting to test the ability of Met to affect splicing of the E1A minigene.

There are a number of questions raised. Is Met a specific trigger for apoptosis in cells, and is there a mechanism by which cells could be stimulated to produce Met? If so, can Met production be initiated by known death ligands / stimuli? Alternatively, is the cellular concentration of Met so critical that a small change disrupts cellular metabolism so severely as to result in apoptosis?

Thus, it would be interesting to assess the effect of Met on caspase activation, cytochrome c release, as well ratios of the bcl-2 protein family. At the same time, it would be interesting to assess gene activation and repression using microarrays, targeted

initially at genes that are important in cell survival and in apoptosis. Another avenue to pursue would be to assess whether Met affects the splicing of other proteins involved in apoptosis that are known to have alternative splice forms such as caspase-9[342], caspase-8[346] and Bcl-x[380].

In summary, the Met protein is located entirely within the nucleus, but is excluded from the nucleoli, which are concerned mainly with the synthesis, processing and maturation of ribosomal components[351,381]. Functionally, this is corroborated by the results of uridine incorporation, where Met overexpression profoundly inhibits mRNA synthesis but has very little effect on overall RNA transcription rate (Fig.7.11), which represents primarily ribosomal RNA synthesis. Within the nucleus, Met is distributed in a punctate fashion, reminiscent of, but distinct from, other nuclear bodies such as speckles, although it has a very similar distribution to Het/SAF-B. Overexpression of Met has been shown to induce apoptosis, but the mechanism is still unclear. We investigated the possibility that Met may alter the alternative splicing of proteins involved in apoptosis, but analysis of alternatively spliced forms of caspase-2 did not show any relative change in the amounts of each transcript.

8 Final Conclusion

The development of tumours is due to the immortalization of cells, linked to various adaptations they undergo in order to bypass normal cellular mechanisms that would otherwise implement programmed cell death in response to DNA damage or lack of growth factors.

We proposed that, in breast cancer cells, one possible survival pathway is provided by activation of the Jak2-STAT5 pathway, by factors such as prolactin[382]. In other mammalian cell lines, STAT5 has been implicated in tumourigenesis[243,244] as well as cell survival[245,246]. In addition, in recent years, there has been increasing evidence to support the idea that prolactin may have a role in breast cancer to an extent that was not previously appreciated[217,219,383,384].

In Chapter 3, we showed that[247,385] prolactin did exert a protective effect in T47-D cells exposed to ceramide. This conclusion is complicated by two factors, however: (a) a protective effect was found using some assays, but not others, and (b) we failed to detect certain apoptotic markers such as annexin staining and accumulation of preG1 cells. In addition to ceramide, we tried a variety of other cytotoxic/apoptotic agents (gamma irradiation, progesterone, taxol etc., results not shown), but were unable to detect any change in the preG1 population or any increase in Annexin V binding, suggesting that these cells are unusually resistant to apoptosis, perhaps because they lack functional p53[176]. Further experiments involving the T47-D cells were also complicated by the limited degree of protection afforded by prolactin, making any assessment of changes / decreases in the protective effect difficult to quantify.

We decided, therefore, to use alternative approaches to dissect out the pathways that may be involved in the protective effects of prolactin. First we attempted to create a model of apoptosis in which the role of the Jak/STAT pathway could be investigated more readily. To this end, we attempted to create a stable cell line from human leukaemic CEM-C7 cells. We chose these cells because they apoptose readily when exposed to glucocorticoids. Also, prolactin had already been established as a survival factor in glucocorticoid-induced apoptosis of the Nb2 rat lymphoma cell line[386,387]. Thus, we wished to translate this model into a human cell line in which we could more precisely assess the role of STAT5 in regulating apoptosis.

CEM-C7 cells were shown to possess the components of the Jak2-STAT5 pathway, but we were unable to establish a stable line expressing the prolactin receptor, despite the fact that clones were isolated that appeared to have incorporated the prolactin receptor cDNA into their genome. Although this project may have provided some insight into the role of the Jak/STAT pathway in mediating the protective effects of prolactin, in retrospect, the information it may have provided might have been of limited value for understanding breast cancer.

Next we attempted to create stable breast cell lines in which the survival effect of prolactin might be augmented. A clone of MCF-7 cells with stably incorporated STAT5b showed no obvious change in response to prolactin, but a clone of T47-D cells overexpressing STAT5b provided quite unexpected results. Rather than the enhanced protective response to prolactin we predicted, these cells exhibited a decreased

proliferative response to prolactin stimulation, and enhanced susceptibility to ceramide cytotoxicity following prolactin exposure. Had additional time been available, it would have been interesting to create stable cell lines expressing the STAT5a transcription factor, which could be responsible for the protective effects of prolactin.

The last part of the study focused on work that had begun in our laboratory on a newly identified gene, which was originally thought to be involved in down-regulation of oestrogen signalling. Preliminary experiments by Dr. Colley appeared to support this finding, but subsequent studies raised doubts because it appeared that Met might be acting as a general inhibitor of transcription. We confirmed that Met exerts generalized inhibitory effects, and showed that constitutively active reporter genes used to control for transfection efficiency may lead to incorrect conclusions when they are used inappropriately. We then went on to show that Met has a punctuate distribution in the nucleus which is distinct from nuclear speckles, and overexpression of Met in a variety of cell types results in apoptosis.

The results raise a number of questions. Is Met a specific trigger for apoptosis in cells, and is there a mechanism by which cells could be stimulated to produce Met? If so, can Met production be initiated by known death ligands/stimuli? Alternatively, is the cellular concentration of Met so critical that a small change disrupts cellular metabolism so severely that apoptosis ensues? Thus, it would be interesting to assess caspase activation, cytochrome c release, and changes in ratios of the bcl-2 protein family in response to overexpression of this protein. At the same time, it would be interesting to assess gene

activation and repression using microarrays, targeted initially at genes that are important in cell survival and in apoptosis. Another avenue to pursue would be to assess whether Met affects the splicing of other proteins involved in apoptosis that are known to have alternative splice forms such as caspase-9[342], caspase-8[346] and bcl-x[380].

Appendix

Ovine prolactin was purchased from Sigma. All tissue culture reagents and media were purchased from Sigma Corp., and tissue culture plastics (Nunc) were purchased from Fisher Scientific. Recombinant human prolactin was a kind gift from Vincent Goffin. All chemicals were purchased from Sigma Corp., unless otherwise stated.

The HA-tagged Stat5a and Stat5b plasmids were a kind gift from Corinne M. Silva (University of Virginia). The pRK5-Jak-2 plasmid was kindly provided by Dr. J. Ihle (St Jude's Children's Hospital). pEYFP-Met, HA-Met plasmids were all constructed by Dr. Shane Colley.

All primers were purchased from Invitrogen.

Chemicals and Reagents

1. Acrylamide/bisacrylamide solution (37.5:1)	Biochemistry Stores, University of Bristol
2. N-acetyl-D-sphingosine (C2- ceramide)	Sigma, Poole, Dorset, UK
3. 17β-Estradiol	Sigma, Poole, Dorset, UK
4. Adenosine 5'-triphospate, sodium salt (ATP)	Sigma, Poole, Dorset, UK
5. Agarose, Type VII: Low Gelling Temperature	Sigma, Poole, Dorset, UK
6. Bovine Serum Albumin, Fraction V	Sigma, Poole, Dorset, UK
7. Charcoal / Dextran stripped Fetal Bovine Serum	Perbio

8. Chlorophenol red-β-D-galactopyranoside (CRPG)	Sigma, Poole, Dorset, UK
9. Co-enzyme A, sodium salt	Sigma, Poole, Dorset, UK
10. Dexamethasone (9α-fluoro-16α-methylprednisolone)	Sigma, Poole, Dorset, UK
11. *DL-Dithiothreitol (DTT)*	Sigma, Poole, Dorset, UK
12. Fetal Bovine Serum	First Link, UK
13. Geneticin, G418 sulphate	Gibco-BRL, Paisley, UK
14. Hoechst 33258	Sigma, Poole, Dorset, UK
15. Kanamycin	Sigma, Poole, Dorset, UK
16. LE Agarose, Seakem	FMC Bioproducts
17. L-glutamine	Sigma, Poole, Dorset, UK
18. Luciferin, sodium salt	Promega, UK
19. Neutral Red	Sigma, Poole, Dorset, UK
20. Optiphase 'HISAFE' 3	Wallac
21. Protein A-agarose beads.	CN Biosciences, UK
22. RNase A	Sigma, Poole, Dorset, UK
23. RNasesZap	Ambion, Uk

Solutions and Buffers

1. 4% paraformaldehyde (PFA): Solution made by dissolving PFA in PBS - heating to 70°C, with stirring. 1M NaOH solution added slowly till PFA has dissolved completely. Stored in working aliquots at -20°C. Solutions can be stored at 4°C for 2 weeks.

2. Antibiotic Stock solutions: All stored in aliquots at -20°C after filter sterilization.

Ampicillin: 100mg/ml in dH_20

Kanamycin: 30mg/ml in dH_20

3. apo-Transferrin: 5mg/ml stored at -20°C *in 1ml aliquots.*

4. ATP solution: 200mM ATP, stored in working aliquots, -20°C.

5. Bovine serum albumin (BSA): 100mg/ml, stored at -20°C in 1ml aliquots.

6. Cell freezing solution: 10% DMSO, 20% FCS in the medium of growth. Mixture is made up just before use, filtered and chilled before cells are resuspended in it.

7. Ceramide stock solution: 20mM in ethanol, Stored at -20°C.

8. CPRG Assay Reagent: To be prepared just before use.

	4 plates	5 plates	6 plates
CPRG Buffer	21ml	21ml	26ml
β-Mercaptoethanol	74µl	74µl	92µl
CPRG Solution	2.8ml	2.8ml	3.5ml

9. CPRG Buffer: 60mM $Na_2HPO_4.7H_2O$, 40mM NaH_2PO_4, 10mM KCl, 1mM $MgSO_4.7H_2O$. pH to 7.3, filter and store at room temperature. Before use, add 50mM β-Mercaptoethanol.

10. CPRG solution: 62.5ml H_2O with 250mg CPRG. Aliquot into light-tight tubes and store at -20°C

11. CoEnzyme A solution: 135mM solution in dH_2O, stored in working aliquots at -20°C.

12. DMEM: supplemented with 10% FCS, 2mM L-glutamine.

13. DNA loading buffer: 30% glycerol, 0.25% bromophenol blue.

14. DTT solution: 1M solution, stored in working aliquots, -20°C, in the dark.

15. G418 solution: 200mg/ml in dH_2O, filter sterilized and stored in aliquots at -20°C.

16. Hoechst Dye: 100μg/ml, stored in working aliquots at -20°C.

17. Krishnan's reagent: 0.05mg/ml PI, 0.1% sodium citrate, 0.02mg/ml ribonuclease A, 0.3% NP-40 (Igepal), pH 8.3. The solution is made up in 100ml of dH_2O, and stored at 4°C.

18. L-glutamine solution: 200mM stock, stored at -20°C, in 5 ml aliquots.

19. Luciferin Solution: 10mM, dissolve in Luciferase Assay Reagent and store in working aliquots at -80°C, in the dark.

20. Luciferase Assay Buffer (1x): 20 mM tricine, 0.1 mM EDTA, 1.07 mM $(MgCO_3)_4Mg(OH)_2.5H_2O$, 2.67 mM $MgSO_4.7H_2O$, pH to 7.8, filter and store at room temperature.

21. Luciferase Assay Reagent: Prepare just before use, protect from light.

for:	10ml	20ml	50ml
1X Luciferase assay buffer	9.5ml	19ml	47.5ml
200mM ATP	26.6μl	53.2μl	133μl
1M DTT	333μl	666μl	1.665ml
135mM CoA	20μl	40μl	100μl
10mM luciferin	500μl	1ml	2.5ml

22. Luria Bertani (LB) Broth: Yeast extract 5g/L, Bacto-tryptone 10g/L, NaCl 10g/L. Aliquoted and autoclaved immediately. For LB agar, 15g/L of bacteriological agar added to LB broth before autoclaving.

23. Lysis Buffer A (1x) for Luciferase Assay and β-Gal Assay: 25mM Tris Phosphate, 2mM CDTA, 10% Glycerol, 0.5% Triton X-100, made up as a 5x solution and stored at room temperature. 2nM DTT added just before use.

24. Lysis Buffer B: 0.05M Tris HCl, pH 8.0; 0.1M EDTA; 0.5% SDS

25. Neutral red solution: 3.3g/l in PBS, stored at 4°C in the dark

26. PMSF solution: 200mM in methanol, stored at 4°C.

27. Prolactin stock: Lyophilized solid is suspended in 10mM Tris HCl (pH 8), allowed to rehydrate for 10min on ice. Solution then centrifuged at 10,000rpm for 10 min at 4°C, and supernatant aliquoted and stored at -80°C.

28. Propidium iodide stock solution: 1mg/ml in dH_20; 0.1% sodium azide, stored at 4°C in the dark.

29. Protein Loading Buffer (SSB): 4.8ml dH_20, 1.2ml 0.5M Tris HCl (pH 6.8), 1ml glycerol, 2ml 10%(w/v) SDS, 0.5ml 0.1%(w/v) *bromophenol blue*. Stored at room temperature. Just before use, add β-mercapthoenthanol (final concentration 5% (v/v)).

30. Recipe for 2xDMEM / 2xRPMI:

	2x DMEM (10mls)	2x RPMI (10mls)
7.5% $NaHCO_3$	0.986ml	0.534ml
L-glutamine (200mM)	0.2ml	0.2ml
Fetal Calf Serum	2ml	2ml
10x DMEM/RPMI	2ml	2ml

dH_20	4.814ml	5.066ml

31. Recipe for SDS-Page Gel:

	8% Separating Gel	4% Stacking Gel
Acrylamide/Bis (30% protogel)	21.4 mls	5.4 mls
Tris HCl, 1.5M, pH 8.8	20 mls	--
Tris HCl, 0.5M, pH 6.8	--	10 mls
10% (w/v) SDS	0.8 mls	0.4 mls
Water	37.8 mls	24 mls
10% Ammonium persulphate	0.8 mls	0.4 mls
TEMED	27µl	20µl

32. RNase A solution : 10mg/ml, stored in working aliquots at -20°C.

33. Running Buffer (5x): 15g Tris Base, 72g Glycine and 5g SDS in 1L dH_20. Stored at room temperature.

34. Serum free DMEM: DMEM, 2mM L-glutamine. Stored at 4°C.

35. Serum Free Medium (SFM): DMEM/F12, 10µg/ml apo-Transferrin, 0.01%BSA and 2mM L-glutamine.

36. Standard Lysis Buffer (SLB): 10mM Tris HCl, pH 7.6; 5mM EDTA (disodium salt);. 50mM NaCl; 30mM Na pyrophosphate; 50mM NaF; 100µM sodium orthovanadate, 1% Triton X-100. Store at 4°C. On day of lysis, the buffer is supplemented with 1mM PMSF, 2.5µg/ml aprotinin, 2.5µg/ml leupeptin and 50µg/ml Pepstatin A.

37. TAE (50x): 242g Tris HCl, 57.1 ml glacial acetic acid and 100ml 0.5M EDTA (pH 8), in 1L of dH_20. Stored at room temperature.

38. TBS-Tween (10x): 100mM Tris HCl, pH 8.0; 1.5M NaCl; 0.5% Tween. Stored at room temperature.

39. TE buffer: 10mM Tris-Cl, pH 8.0; 1mM EDTA. Stored at room temperature.

40. Transfer Buffer: 3g SDS, 87g glycine, 17.4g Tris Base; dissolved in dH_20, with the addition of 600ml methanol, before bringing final volume to 3L with dH_20. Stored at room temperature.

Laboratory Equipment

1. Avanti 30 centrifuge	Beckman, Fullerton, CA
2. Capacitance Extender Plus	BioRad, Hemel Hempstead, UK
3. CellQuest software	Becton Dickinson, Oxford, UK
4. Clifton heating block and stirrer	Jencons-PLS, Leighton Buzzard, UK
5. Cell Counter Model Dn	Coulter, UK
6. Consort E844 electrophoresis powerpack	Jencons-PLS, Leighton Buzzard, UK
7. Coverslips (22mmx22mm)	BDH
8. EPS 600 electrophoresis powerpack	Pharmacia, Little Chalfont, UK
9. FACS Calibur	Becton Dickinson, Oxford, UK
10. Gene Pulser II	BioRad, Hemel Hempstead, UK
11. Gene quant spectrophotometer	Pharmacia, Little Chalfont, UK
12. *Glass Slides*	BDH
13. Grant heating block	Jencons-PLS, Leighton Buzzard, UK

14. Grant waterbath — Jencons-PLS, Leighton Buzzard, UK

15. GraphPad Prism Software — GraphPad Prism CA

16. Hettich zentrifugen Rotanta 46R — Jencons-PLS, Leighton Buzzard, UK

17. Leica TCS-NT confocal laser scanning microscope — Leica

18. Leica DM RBE upright epifluorescence microscope — Leica

19. Leica Confocal Software — Leica

20. LKB EPS 500/400 electrophoresis powerpack — Pharmacia, Little Chalfont, UK

21. Meltilex A (melt-on scintillator sheets, 73x109mm) Wallac

22. Microcentaur tabletop microcentrifuge — Jencons-PLS, Leighton Buzzard, UK

23. Microcentrifuge tubes — Appleton Woods, Selly Oak, UK

24. Microfluor-Microtitre Plates — Dynex Technologies, UK

25. Micromax RF — Thermo Life Sciences, Basingstoke, UK

26. Microsoft Word Software — Microsoft

27. Midi horizontal electrophoresis unit — Jencons-PLS, Leighton Buzzard, UK

28. Mini-plus horizontal electrophoresis unit — Jencons-PLS, Leighton Buzzard, UK

29. MLX microtiter plate luminometer — Dynex Technologies, Ashford, UK

30. Plasticware — Fisher, Loughborough, UK

31. Plugged 20µl, 200µl and 1000µl tips — Anachem, UK

32. Printed Filtermat A(glass fibre filter 90x120mm) Wallac

33. Protean II xi cell Western Blot tank — BioRad, Hemel Hempstead, UK

34. RLX β-microplate reader — Dynex Technologies, Ashford, UK

35. Stuart Scientific Platform Shaker STR6 — Prior Lab Supplies, UK

36. Trans-blot SD, semidry transfer cell — BioRad, Hemel Hempstead, UK

37. Techne Genius Thermocycler	Jencons-PLS, Leighton Buzzard, UK
38. TOMTEC Harvester 96 Mach 3	Receptor Technologies, Ltd. Banbury, UK
39. Ultracentrifuge	Beckman, Fullerton, CA
40. 1450 MicroBeta Liquid Scintillation and Luminescence Counter	Wallac
41. 1450 MicroBeta Windows Workstation Version 3.2	Wallac
42. 1400 DSA Liquid Scintillation Counter	Wallac
43. 1400 DSA version 2.5 (software)	Wallac

Kits:

1. Access RT-PCR System	Promega,
2. ApoAlert® Annexin-V-FITC Kit	Clontech Laboratories, Basingstoke, UK
3. Enhanced Chemiluminescence Kit	Amersham
4. HiSpeed Plasmid Purification Kits	Qiagen
5. PolyA$^+$Tract (mRNA) Isolation System IV	Promega
6. Protein Microdetermination Kit	Sigma, Poole, Dorset
7. QIAprep Miniprep Kit	Qiagen
8. QIAquick Gel Extraction Kit	Qiagen
9. RNAeasy Midi/Maxi Kit	Qiagen
10. Top10 Competant E.Coli	Invitrogen
11. XTT Cell Proliferation Kit II	Roche

Enzymes, Vectors and Antibodies:

1. ANTI-FLAG® M2 monoclonal antibody, FITC-conjugate	Sigma
2. ANTI-FLAG® M2 monoclonal antibody	Sigma
3. EZview™ red ANTI-FLAG® M2 affinity gel	Sigma
4. Monoclonal Anti-HA, clone HA 7	Sigma
5. Anti-HA probe, rabbit polyclonal	Autogen BioClear
6. Monoclonal anti-splicing factor, SC-35	Sigma
7. Anti-Stat5b, C-17, rabbit polyclonal	Autogen Bioclear
8. Donkey anti-mouse, Cy3-linked	Jackson Immunology (Stratech Scientific, Soham, Cambs, UK)
9. FuGENE 6	Roche
10. Goat anti-rabbit, HRP-linked	Amersham
11. Lipofectamine™ reagent	Invitrogen
12. Plus™ reagent	Invitrogen
13. pEGFP-N1 vector	Clontech, Basingstoke, UK
14. pEYFP-C1 vector	Clontech, Basingstoke, UK
15. Sheep anti-mouse, HRP-linked	Amersham
16. Taq polymerase	Gibco
17. Molecular Weight Markers VII / VIII	Roche
18. Full range RAINBOW (molecular weight markers)	Amersham

References

1. *Molecular Oncology*. New York: Scientific American, Inc. 2003.

2. Renan MJ. How many mutations are required for tumorigenesis? Implications from human cancer data. *Mol.Carcinog.* 1993; **7:** 139-146.

3. Rubin H. Experimental control of neoplastic progression in cell populations: Foulds' rules revisited. *Proc.Natl.Acad.Sci.U.S.A* 1994; **91:** 6619-6623.

4. Kinzler KW, Vogelstein B. Lessons from hereditary colorectal cancer. *Cell 1996; 87: 159-170.*

5. Hahn WC, Counter CM, Lundberg AS, Beijersbergen RL, Brooks MW, Weinberg RA. Creation of human tumour cells with defined genetic elements. *Nature* 1999; **400:** 464-468.

6. Bergers G, Hanahan D, Coussens LM. Angiogenesis and apoptosis are cellular parameters of neoplastic progression in transgenic mouse models of tumorigenesis. *Int.J.Dev.Biol.* 1998; **42:** 995-1002.

7. Nowell PC. The clonal evolution of tumor cell populations. *Science* 1976; **194:** 23-28.

8. Hanahan D, Weinberg RA. The hallmarks of cancer. *Cell* 2000; **100:** 57-70.

9. Kerr JF, Wyllie AH, Currie AR. Apoptosis: a basic biological phenomenon with wide-ranging implications in tissue kinetics. *Br.J.Cancer* 1972; **26:** 239-257.

10. Wyllie AH, Kerr JF, Currie AR. Cell death: the significance of apoptosis. *Int.Rev.Cytol.* 1980; **68:** 251-306.

11. Schwartzman RA, Cidlowski JA. Apoptosis: the biochemistry and molecular biology of programmed cell death. *Endocr.Rev.* 1993; **14:** 133-151.

12. Saikumar P, Dong Z, Mikhailov V, Denton M, Weinberg JM, Venkatachalam MA. Apoptosis: definition, mechanisms, and relevance to disease. *Am.J.Med.* 1999; **107:** 489-506.

13. Novack DV, Korsmeyer SJ. Bcl-2 protein expression during murine development. *Am.J Pathol* 1994; **145:** 61-73.

14. Bishop CJ, Whiting VA. The role of natural killer cells in the intravascular death of intravenously injected murine tumour cells. *Br.J Cancer* 1983; **48:** 441-444.

15. Cohen JJ. Programmed cell death in the immune system. *Adv Immunol* 1991; **50:** 55-85.

16. Chinnaiyan AM, O'Rourke K, Tewari M, Dixit VM. FADD, a novel death domain-containing protein, interacts with the death domain of Fas and initiates apoptosis. *Cell* 1995; **81:** 505-512.

17. Wallach D, Boldin M, Varfolomeev E, Beyaert R, Vandenabeele P, Fiers W. Cell death induction by receptors of the TNF family: towards a molecular understanding. *FEBS Lett.* 1997; **410:** 96-106.

18. Magnusson C, Vaux DL. Signalling by CD95 and TNF receptors: not only life and death. *Immunol.Cell Biol.* 1999; **77:** 41-46.

19. Ruoslahti E, Reed JC. Anchorage dependence, integrins, and apoptosis. *Cell* 1994; **77:** 477-478.

20. Reed JC. Bcl-2 family proteins. *Oncogene* 1998; **17:** 3225-3236.

21. Kroemer G. The proto-oncogene Bcl-2 and its role in regulating apoptosis. *Nat.Med.* 1997; **3:** 614-620.

22. Alnemri ES. Mammalian cell death proteases: a family of highly conserved aspartate specific cysteine proteases. *J.Cell Biochem.* 1997; **64:** 33-42.

23. Boldin MP, Goncharov TM, Goltsev YV, Wallach D. Involvement of MACH, a novel MORT1/FADD-interacting protease, in Fas/APO-1- and TNF receptor-induced cell death. *Cell* 1996; **85:** 803-815.

24. Muzio M, Chinnaiyan AM, Kischkel FC *et al.* FLICE, a novel FADD-homologous ICE/CED-3-like protease, is recruited to the CD95 (Fas/APO-1) death--inducing signaling complex. *Cell* 1996; **85:** 817-827.

25. Slee EA, Harte MT, Kluck RM *et al.* Ordering the cytochrome c-initiated caspase cascade: hierarchical activation of caspases-2, -3, -6, -7, -8, and -10 in a caspase-9-dependent manner. *J Cell Biol* 1999; **144:** 281-292.

26. Saleh A, Srinivasula SM, Acharya S, Fishel R, Alnemri ES. Cytochrome c and dATP-mediated oligomerization of Apaf-1 is a prerequisite for procaspase-9 activation. *J Biol Chem* 1999; **274:** 17941-17945.

27. Nicholson DW, Thornberry NA. Caspases: killer proteases. *Trends Biochem.Sci.* 1997; **22:** 299-306.

28. Alnemri ES, Livingston DJ, Nicholson DW *et al.* Human ICE/CED-3 protease nomenclature. *Cell* 1996; **87:** 171.

29. Thornberry NA, Lazebnik Y. Caspases: enemies within. *Science* 1998; **281:** 1312-1316.

30. Hu Y, Ding L, Spencer DM, Nunez G. WD-40 Repeat Region Regulates Apaf-1 Self-association and Procaspase-9 Activation. *Journal of Biological Chemistry* 1998; **273:** 33489.

31. Muzio M, Stockwell BR, Stennicke HR, Salvesen GS, Dixit VM. An induced proximity model for caspase-8 activation. *J Biol Chem* 1998; **273:** 2926-2930.

32. Yang X, Chang HY, Baltimore D. Essential role of CED-4 oligomerization in CED-3 activation and apoptosis. *Science* 1998; **281:** 1355-1357.

33. Hofmann K, Tschopp J. The death domain motif found in Fas (Apo-1) and TNF receptor is present in proteins involved in apoptosis and axonal guidance. *FEBS Lett.* 1995; **371:** 321-323.

34. Hofmann K, Bucher P, Tschopp J. The CARD domain: a new apoptotic signalling motif. *Trends Biochem.Sci.* 1997; **22:** 155-156.

35. Budihardjo I, Oliver H, Lutter M, Luo X, Wang X. Biochemical pathways of caspase activation during apoptosis. *Annu.Rev Cell Dev Biol* 1999; **15:** 269-290.

36. Cohen GM. Caspases: the executioners of apoptosis. *Biochem J* 1997; **326 (Pt 1):** 1-16.

37. Kuida K, Zheng TS, Na S *et al.* Decreased apoptosis in the brain and premature lethality in CPP32-deficient mice. *Nature* 1996; **384:** 368-372.

38. Janicke RU, Sprengart ML, Wati MR, Porter AG. Caspase-3 is required for DNA fragmentation and morphological changes associated with apoptosis. *J.Biol.Chem.* 1998; **273:** 9357-9360.

39. Woo M, Hakem R, Soengas MS *et al.* Essential contribution of caspase 3/CPP32 to apoptosis and its associated nuclear changes. *Genes Dev.* 1998; **12:** 806-819.

40. Yeh JH, Hsu SC, Han SH, Lai MZ. Mitogen-activated protein kinase kinase antagonized fas-associated death domain protein-mediated apoptosis by induced FLICE-inhibitory protein expression. *J.Exp.Med.* 1998; **188:** 1795-1802.

41. Zhang J, Cado D, Chen A, Kabra NH, Winoto A. Fas-mediated apoptosis and activation-induced T-cell proliferation are defective in mice lacking FADD/Mort1. *Nature* 1998; **392:** 296-300.

42. Hakem R, Hakem A, Duncan GS *et al.* Differential requirement for caspase 9 in apoptotic pathways in vivo. *Cell* 1998; **94:** 339-352.

43. Kuida K, Haydar TF, Kuan CY *et al. Reduced apoptosis and cytochrome* c-mediated caspase activation in mice lacking caspase 9. *Cell* 1998; **94:** 325-337.

44. Sun XM, MacFarlane M, Zhuang J, Wolf BB, Green DR, Cohen GM. Distinct caspase cascades are initiated in receptor-mediated and chemical-induced apoptosis. *Journal of Biological Chemistry* 1999; **274:** 5053-5060.

45. Sanghavi DM, Thelen M, Thornberry NA, Casciola-Rosen L, Rosen A. Caspase-mediated proteolysis during apoptosis: insights from apoptotic neutrophils. *FEBS Lett* 1998; **422:** 179-184.

46. Schwab BL, Leist M, Knippers R, Nicotera P. Selective proteolysis of the nuclear replication factor MCM3 in apoptosis. *Exp Cell Res* 1998; **238:** 415-421.

47. McCarthy NJ, Whyte MK, Gilbert CS, Evan GI. Inhibition of Ced-3/ICE-related proteases does not prevent cell death induced by oncogenes, DNA damage, or the Bcl-2 homologue Bak. *J.Cell Biol.* 1997; **136:** 215-227.

48. Ashkenazi A, Dixit VM. Death receptors: signaling and modulation. *Science* 1998; **281:** 1305-1308.

49. Darnay BG, Aggarwal BB. Early events in TNF signaling: a story of associations and dissociations. *J Leukoc Biol* 1997; **61:** 559-566.

50. Baker SJ, Reddy EP. Modulation of life and death by the TNF receptor superfamily. *Oncogene* 1998; **17:** 3261-3270.

51. Lowe SW, Lin AW. Apoptosis in cancer. *Carcinogenesis* 2000; **21:** 485-495.

52. Takeuchi M, Rothe M, Goeddel DV. Anatomy of TRAF2. Distinct domains for nuclear factor-kappaB activation and association with tumor necrosis factor signaling proteins. *Journal of Biological Chemistry* 1996; **271:** 19935-19942.

53. Zornig M, Hueber A, Baum W, Evan G. Apoptosis regulators and their role in tumorigenesis. *Biochim Biophys Acta* 2001; **1551:** F1-37.

54. Pimentel-Muinos FX, Seed B. Regulated commitment of TNF receptor signaling: a molecular switch for death or activation. *Immunity* 1999; **11:** 783-793.

55. Schuler M, Green DR. Mechanisms of p53-dependent apoptosis. *Biochem Soc Trans.* 2001; **29:** 684-688.

56. Du C, Fang M, Li Y, Li L, Wang X. Smac, a mitochondrial protein that promotes cytochrome c-dependent caspase activation by eliminating IAP inhibition. *Cell* 2000; **102:** 33-42.

57. Verhagen AM, Ekert PG, Pakusch M *et al.* Identification of DIABLO, a mammalian protein that promotes apoptosis by binding to and antagonizing IAP proteins. *Cell* 2000; **102:** 43-53.

58. Gupta S. Molecular signaling in death receptor and mitochondrial pathways of apoptosis (Review). *Int J Oncol* 2003; **22:** 15-20.

59. Cai J, Yang J, Jones DP. Mitochondrial control of apoptosis: the role of cytochrome c. *Biochim.Biophys.Acta* 1998; **1366:** 139-149.

60. Kroemer G. Mitochondrial control of apoptosis: an overview. *Biochem.Soc.Symp.* 1999; **66:** 1-15.

61. Crompton M, Virji S, Ward JM. Cyclophilin-D binds strongly to complexes of the voltage-dependent anion channel and the adenine nucleotide translocase to form the permeability transition pore. *Eur J Biochem* 1998; **258:** 729-735.

62. Woodfield K, Ruck A, Brdiczka D, Halestrap AP. Direct demonstration of a specific interaction between cyclophilin-D and the adenine nucleotide translocase confirms their role in the mitochondrial permeability transition. *Biochem J* 1998; **336 (Pt 2):** 287-290.

63. Desagher S, Osen-Sand A, Nichols A *et al.* Bid-induced conformational change of Bax is responsible for mitochondrial cytochrome c release during apoptosis. *J.Cell Biol.* 1999; **144:** 891-901.

64. Green DR, Reed JC. Mitochondria and apoptosis. *Science* 1998; **281:** 1309-1312.

65. Li P, Nijhawan D, Budihardjo I *et al.* Cytochrome c and dATP-dependent formation of Apaf-1/caspase-9 complex initiates an apoptotic protease cascade. *Cell* 1997; **91:** 479-489.

66. Zou H, Henzel WJ, Liu X, Lutschg A, Wang X. Apaf-1, a human protein homologous to C. elegans CED-4, participates in cytochrome c-dependent activation of caspase-3. *Cell* 1997; **90:** 405-413.

67. Tsujimoto Y. Role of Bcl-2 family proteins in apoptosis: apoptosomes or mitochondria? *Genes Cells* 1998; **3:** 697-707.

68. Susin SA, Lorenzo HK, Zamzami N *et al.* Molecular characterization of mitochondrial apoptosis-inducing factor. *Nature* 1999; **397:** 441-446.

69. Susin SA, Zamzami N, Castedo M *et al.* Bcl-2 inhibits the mitochondrial release of an apoptogenic protease. *J Exp Med* 1996; **184:** 1331-1341.

70. Tsujimoto Y, Finger LR, Yunis J, Nowell PC, Croce CM. Cloning of the chromosome breakpoint of neoplastic B cells with the t(14;18) chromosome translocation. *Science* 1984; **226:** 1097-1099.

71. Tsujimoto Y, Cossman J, Jaffe E, Croce CM. Involvement of the bcl-2 gene in human follicular lymphoma. *Science* 1985; **228:** 1440-1443.

72. Vaux DL, Cory S, Adams JM. Bcl-2 gene promotes haemopoietic cell survival and cooperates with c-myc to immortalize pre-B cells. *Nature* 1988; **335:** 440-442.

73. McDonnell TJ, Deane N, Platt FM *et al.* bcl-2-immunoglobulin transgenic mice demonstrate extended B cell survival and follicular lymphoproliferation. *Cell* 1989; **57:** 79-88.

74. Schendel SL, Montal M, Reed JC. Bcl-2 family proteins as ion-channels. *Cell Death.Differ.* 1998; **5:** 372-380.

75. Cory S. Regulation of lymphocyte survival by the bcl-2 gene family. *Annu.Rev.Immunol.* 1995; **13:** 513-543.

76. Shimizu S, Narita M, Tsujimoto Y. Bcl-2 family proteins regulate the release of apoptogenic cytochrome c by the mitochondrial channel VDAC. *Nature* 1999; **399:** 483-487.

77. Hu Y, Benedict MA, Wu D, Inohara N, Nunez G. Bcl-XL interacts with Apaf-1 and inhibits Apaf-1-dependent caspase-9 activation. *Proc Natl Acad Sci U S A* 1998; **95:** 4386-4391.

78. Gross A, Jockel J, Wei MC, Korsmeyer SJ. Enforced dimerization of BAX results in its translocation, mitochondrial dysfunction and apoptosis. *EMBO J* 1998; **17:** 3878-3885.

79. Wang HG, Pathan N, Ethell IM *et al.* Ca2+-induced apoptosis through calcineurin dephosphorylation of BAD. *Science* 1999; **284:** 339-343.

80. Blume-Jensen P, Janknecht R, Hunter T. The kit receptor promotes cell survival via activation of PI 3-kinase and subsequent Akt-mediated phosphorylation of Bad on Ser136. *Curr Biol* 1998; **8:** 779-782.

81. Datta SR, Dudek H, Tao X *et al.* Akt phosphorylation of BAD couples survival signals to the cell-intrinsic death machinery. *Cell* 1997; **91:** 231-241.

82. del Peso L, Gonzalez-Garcia M, Page C, Herrera R, Nunez G. Interleukin-3-induced phosphorylation of BAD through the protein kinase Akt. *Science* 1997; **278:** 687-689.

83. Salvesen GS, Dixit VM. Caspases: intracellular signaling by proteolysis. *Cell* 1997; **91:** 443-446.

84. Eskes R, Desagher S, Antonsson B, Martinou JC. Bid induces the oligomerization and insertion of Bax into the outer mitochondrial membrane. *Mol Cell Biol* 2000; **20:** 929-935.

85. Wei MC, Lindsten T, Mootha VK *et al.* tBID, a membrane-targeted death ligand, oligomerizes BAK to release cytochrome c. *Genes Dev* 2000; **14:** 2060-2071.

86. Wang K, Yin XM, Chao DT, Milliman CL, Korsmeyer SJ. BID: a novel BH3 domain-only death agonist. *Genes Dev* 1996; **10:** 2859-2869.

87. Deveraux QL, Reed JC. IAP family proteins--suppressors of apoptosis. *Genes Dev* 1999; **13:** 239-252.

88. Liston P, Roy N, Tamai K *et al.* Suppression of apoptosis in mammalian cells by NAIP and a related family of IAP genes. *Nature* 1996; **379:** 349-353.

89. Duckett CS, Nava VE, Gedrich RW *et al.* A conserved family of cellular genes related to the baculovirus iap gene and encoding apoptosis inhibitors. *EMBO J* 1996; **15:** 2685-2694.

90. Ambrosini G, Adida C, Altieri DC. A novel anti-apoptosis gene, survivin, expressed in cancer and lymphoma. *Nat Med* 1997; **3:** 917-921.

91. Li J, Kim JM, Liston P *et al.* Expression of inhibitor of apoptosis proteins (IAPs) in rat granulosa cells during ovarian follicular development and atresia. *Endocrinology* 1998; **139:** 1321-1328.

92. Deveraux QL, Takahashi R, Salvesen GS, Reed JC. X-linked IAP is a direct inhibitor of cell-death proteases. *Nature* 1997; **388:** 300-304.

93. Deveraux QL, Roy N, Stennicke HR *et al.* IAPs block apoptotic events induced by caspase-8 and cytochrome c by direct inhibition of distinct caspases. *EMBO J* 1998; **17:** 2215-2223.

94. Roy N, Deveraux QL, Takahashi R, Salvesen GS, Reed JC. The c-IAP-1 and c-IAP-2 proteins are direct inhibitors of specific caspases. *EMBO J* 1997; **16:** 6914-6925.

95. Finucane DM, Bossy-Wetzel E, Waterhouse NJ, Cotter TG, Green DR. Bax-induced caspase activation and apoptosis via cytochrome c release from mitochondria is inhibitable by Bcl-xL. *J Biol Chem* 1999; **274:** 2225-2233.

96. Jurgensmeier JM, Xie Z, Deveraux Q, Ellerby L, Bredesen D, Reed JC. Bax directly induces release of cytochrome c from isolated mitochondria. *Proc.Natl.Acad.Sci.U.S.A* 1998; **95:** 4997-5002.

97. Cross TG, Scheel-Toellner D, Henriquez NV, Deacon E, Salmon M, Lord JM. Serine/threonine protein kinases and apoptosis. *Exp Cell Res* 2000; **256:** 34-41.

98. Boulton TG, Nye SH, Robbins DJ *et al.* ERKs: a family of protein-serine/threonine kinases that are activated and tyrosine phosphorylated in response to insulin and NGF. *Cell* 1991; **65:** 663-675.

99. Han J, Lee JD, Bibbs L, Ulevitch RJ. A MAP kinase targeted by endotoxin and hyperosmolarity in mammalian cells. *Science* 1994; **265:** 808-811.

100. Kyriakis JM, Banerjee P, Nikolakaki E *et al.* The stress-activated protein kinase subfamily of c-Jun kinases. *Nature* 1994; **369:** 156-160.

101. Xia Z, Dickens M, Raingeaud J, Davis RJ, Greenberg ME. Opposing effects of ERK and JNK-p38 MAP kinases on apoptosis. *Science* 1995; **270:** 1326-1331.

102. Le Niculescu H, Bonfoco E, Kasuya Y, Claret FX, Green DR, Karin M. Withdrawal of survival factors results in activation of the JNK pathway in neuronal cells leading to Fas ligand induction and cell death. *Mol Cell Biol* 1999; **19:** 751-763.

103. Chaudhary PM, Eby MT, Jasmin A, Hood L. Activation of the c-Jun N-terminal kinase/stress-activated protein kinase pathway by overexpression of caspase-8 and its homologs. *J Biol Chem* 1999; **274:** 19211-19219.

104. Herr I, Wilhelm D, Meyer E, Jeremias I, Angel P, Debatin KM. JNK/SAPK activity contributes to TRAIL-induced apoptosis. *Cell Death.Differ* 1999; **6:** 130-135.

105. Jun CD, Pae HO, Kwak HJ *et al.* Modulation of nitric oxide-induced apoptotic death of HL-60 cells by protein kinase C and protein kinase A through mitogen-activated protein kinases and CPP32-like protease pathways. *Cell Immunol* 1999; **194:** 36-46.

106. Nagata Y, Todokoro K. Requirement of activation of JNK and p38 for environmental stress-induced erythroid differentiation and apoptosis and of inhibition of ERK for apoptosis. *Blood* 1999; **94:** 853-863.

107. Widmann C, Gibson S, Johnson GL. Caspase-dependent cleavage of signaling proteins during apoptosis. A turn-off mechanism for anti-apoptotic signals. *J Biol Chem* 1998; **273:** 7141-7147.

108. Buckley S, Driscoll B, Barsky L, Weinberg K, Anderson K, Warburton D. ERK activation protects against DNA damage and apoptosis in hyperoxic rat AEC2. *Am.J Physiol* 1999; **277:** L159-L166.

109. Erhardt P, Schremser EJ, Cooper GM. B-Raf inhibits programmed cell death downstream of cytochrome c release from mitochondria by activating the MEK/Erk pathway. *Mol Cell Biol* 1999; **19:** 5308-5315.

110. Anderson CN, Tolkovsky AM. A role for MAPK/ERK in sympathetic neuron survival: protection against a p53-dependent, JNK-independent induction of apoptosis by cytosine arabinoside. *J Neurosci* 1999; **19:** 664-673.

111. Zha J, Harada H, Yang E, Jockel J, Korsmeyer SJ. Serine phosphorylation of death agonist BAD in response to survival factor results in binding to 14-3-3 not BCL-X(L). *Cell* 1996; **87:** 619-628.

112. Cardone MH, Roy N, Stennicke HR *et al.* Regulation of cell death protease caspase-9 by phosphorylation. *Science* 1998; **282:** 1318-1321.

113. Tasken K, Solberg R, Foss KB, Skalhegg BS, Hansson V, Jahnsen T. cAMP-dependent protein kinases (vertebrates). In: Hardie G, Hanks S, eds. *The Protein Kinase Factsbook I.* London: Academic Press Inc. 1995.

114. Harada H, Becknell B, Wilm M *et al.* Phosphorylation and inactivation of BAD by mitochondria-anchored protein kinase A. *Mol Cell* 1999; **3:** 413-422.

115. Datta SR, Brunet A, Greenberg ME. Cellular survival: a play in three Akts. *Genes Dev* 1999; **13:** 2905-2927.

116. Romashkova JA, Makarov SS. NF-kappaB is a target of AKT in anti-apoptotic PDGF signalling. *Nature* 1999; **401:** 86-90.

117. Zuckerman SH, Evans GF, Guthrie L. Transcriptional and post-transcriptional mechanisms involved in the differential expression of LPS-induced IL-1 and TNF mRNA. *Immunology* 1991; **73:** 460-465.

118. Faris M, Kokot N, Latinis K *et al.* The c-Jun N-terminal kinase cascade plays a role in stress-induced apoptosis in Jurkat cells by up-regulating Fas ligand expression. *J Immunol* 1998; **160:** 134-144.

119. Li-Weber M, Laur O, Hekele A, Coy J, Walczak H, Krammer PH. A regulatory element in the CD95 (APO-1/Fas) ligand promoter is essential for responsiveness to TCR-mediated activation. *Eur J Immunol* 1998; **28:** 2373-2383.

120. Miyashita T, Reed JC. Tumor suppressor p53 is a direct transcriptional activator of the human bax gene. *Cell* 1995; **80:** 293-299.

121. Zhan Q, Fan S, Bae I *et al.* Induction of bax by genotoxic stress in human cells correlates with normal p53 status and apoptosis. *Oncogene* 1994; **9:** 3743-3751.

122. Wallace-Brodeur RR, Lowe SW. Clinical implications of p53 mutations. *Cell Mol.Life Sci.* 1999; **55:** 64-75.

123. Lowe SW, Schmitt EM, Smith SW, Osborne BA, Jacks T. p53 is required for radiation-induced apoptosis in mouse thymocytes. *Nature* 1993; **362:** 847-849.

124. Clarke AR, Purdie CA, Harrison DJ *et al.* Thymocyte apoptosis induced by p53-dependent and independent pathways. *Nature* 1993; **362:** 849-852.

125. Yin C, Knudson CM, Korsmeyer SJ, Van Dyke T. Bax suppresses tumorigenesis and stimulates apoptosis in vivo. *Nature* 1997; **385:** 637-640.

126. McCurrach ME, Connor TM, Knudson CM, Korsmeyer SJ, Lowe SW. bax-deficiency promotes drug resistance and oncogenic transformation by attenuating p53-dependent apoptosis. *Proc.Natl.Acad.Sci.U.S.A* 1997; **94:** 2345-2349.

127. Soengas MS, Alarcon RM, Yoshida H *et al.* Apaf-1 and caspase-9 in p53-dependent apoptosis and tumor inhibition. *Science* 1999; **284:** 156-159.

128. Rowan S, Ludwig RL, Haupt Y *et al.* Specific loss of apoptotic but not cell-cycle arrest function in a human tumor derived p53 mutant. *EMBO J.* 1996; **15:** 827-838.

129. Friedlander P, Haupt Y, Prives C, Oren M. A mutant p53 that discriminates between p53-responsive genes cannot induce apoptosis. *Mol.Cell Biol.* 1996; **16:** 4961-4971.

130. Kerr JF, Winterford CM, Harmon BV. Apoptosis. Its significance in cancer and cancer therapy. *Cancer* 1994; **73:** 2013-2026.

131. White E. Life, death, and the pursuit of apoptosis. *Genes Dev.* 1996; **10:** 1-15.

132. Evan G, Littlewood T. A matter of life and cell death. *Science* 1998; **281:** 1317-1322.

133. Schmitt CA, Lowe SW. Apoptosis and therapy. *J.Pathol.* 1999; **187:** 127-137.

134. Hall AG. Review: The role of glutathione in the regulation of apoptosis. *Eur.J.Clin.Invest* 1999; **29:** 238-245.

135. Cantley LC, Neel BG. New insights into tumor suppression: PTEN suppresses tumor formation by restraining the phosphoinositide 3-kinase/AKT pathway. *Proc.Natl.Acad.Sci.U.S.A* 1999; **96:** 4240-4245.

136. Strasser A, Harris AW, Bath ML, Cory S. Novel primitive lymphoid tumours induced in transgenic mice by cooperation between myc and bcl-2. *Nature* 1990; **348:** 331-333.

137. Jager R, Herzer U, Schenkel J, Weiher H. Overexpression of Bcl-2 inhibits alveolar cell apoptosis during involution and accelerates c-myc-induced tumorigenesis of the mammary gland in transgenic mice. *Oncogene* 1997; **15:** 1787-1795.

138. Attardi LD, Jacks T. The role of p53 in tumour suppression: lessons from mouse models. *Cell Mol.Life Sci.* 1999; **55:** 48-63.

139. Mak TW, Yeh WC. Signaling for survival and apoptosis in the immune system. *Arthritis Res* 2002; **4 Suppl 3:** S243-S252.

140. Reed JC. Dysregulation of apoptosis in cancer. *J.Clin.Oncol.* 1999; **17:** 2941-2953.

141. Reed JC. Mechanisms of apoptosis avoidance in cancer. *Curr.Opin.Oncol.* 1999; **11:** 68-75.

142. Ziegler A, Jonason AS, Leffell DJ *et al.* Sunburn and p53 in the onset of skin cancer. *Nature* 1994; **372:** 773-776.

143. Graeber TG, Peterson JF, Tsai M, Monica K, Fornace AJ, Jr., Giaccia AJ. Hypoxia induces accumulation of p53 protein, but activation of a G1-phase checkpoint by low-oxygen conditions is independent of p53 status. *Mol.Cell Biol.* 1994; **14:** 6264-6277.

144. Graeber TG, Osmanian C, Jacks T *et al.* Hypoxia-mediated selection of cells with diminished apoptotic potential in solid tumours. *Nature* 1996; **379:** 88-91.

145. Karlseder J, Broccoli D, Dai Y, Hardy S, de Lange T. p53- and ATM-dependent apoptosis induced by telomeres lacking TRF2. *Science* 1999; **283:** 1321-1325.

146. Frisch SM, Francis H. Disruption of epithelial cell-matrix interactions induces apoptosis. *J.Cell Biol.* 1994; **124:** 619-626.

147. Parton M, Dowsett M, Smith I. Studies of apoptosis in breast cancer. *BMJ* 2001; **322:** 1528-1532.

148. Gandhi A, Holland PA, Knox WF, Potten CS, Bundred NJ. Evidence of significant apoptosis in poorly differentiated ductal carcinoma in situ of the breast. *Br.J Cancer* 1998; **78:** 788-794.

149. *Lipponen P, Aaltomaa S,* Kosma VM, Syrjanen K. Apoptosis in breast cancer as related to histopathological characteristics and *prognosis. Eur J Cancer* 1994; **30A:** 2068-2073.

150. Allan DJ, Howell A, Roberts SA *et al.* Reduction in apoptosis relative to mitosis in histologically normal epithelium accompanies fibrocystic change and carcinoma of the premenopausal human breast. *J Pathol* 1992; **167:** 25-32.

151. Berardo MD, Elledge RM, de Moor C, Clark GM, Osborne CK, Allred DC. bcl-2 and apoptosis in lymph node positive breast carcinoma. *Cancer* 1998; **82:** 1296-1302.

152. Zhang GJ, Kimijima I, Abe R *et al.* Apoptotic index correlates to bcl-2 and p53 protein expression, histological grade and prognosis in invasive breast cancers. *Anticancer Res* 1998; **18:** 1989-1998.

153. Krajewski S, Krajewska M, Turner BC *et al.* Prognostic significance of apoptosis regulators in breast cancer. *Endocr.Relat Cancer* 1999; **6:** 29-40.

154. Alsabeh R, Wilson CS, Ahn CW, Vasef MA, Battifora H. Expression of bcl-2 by breast cancer: a possible diagnostic application. *Mod.Pathol* 1996; **9:** 439-444.

155. van Slooten HJ, van de Vijver MJ, van de Velde CJ, van Dierendonck JH. Loss of Bcl-2 in invasive breast cancer is associated with high rates of cell death, but also with increased proliferative activity. *Br.J Cancer* 1998; **77:** 789-796.

156. Kumar R, Mandal M, Lipton A, Harvey H, Thompson CB. Overexpression of HER2 modulates bcl-2, bcl-XL, and tamoxifen-induced apoptosis in human MCF-7 breast cancer cells. *Clin Cancer Res* 1996; **2:** 1215-1219.

157. Weinstein EJ, Grimm S, Leder P. The oncogene heregulin induces apoptosis in breast epithelial cells and tumors. *Oncogene* 1998; **17:** 2107-2113.

158. Ricca A, Biroccio A, Del Bufalo D, Mackay AR, Santoni A, Cippitelli M. bcl-2 over-expression enhances NF-kappaB activity and induces mmp-9 transcription in human MCF7(ADR) breast-cancer cells. *Int J Cancer* 2000; **86:** 188-196.

159. Evan GI, Wyllie AH, Gilbert CS *et al.* Induction of apoptosis in fibroblasts by c-myc protein. *Cell* 1992; **69:** 119-128.

160. Harrington EA, Fanidi A, Evan GI. Oncogenes and cell death. *Curr.Opin.Genet.Dev.* 1994; **4:** 120-129.

161. Bissonnette RP, Echeverri F, Mahboubi A, Green DR. Apoptotic cell death induced by c-myc is inhibited by bcl-2. *Nature* 1992; **359:** 552-554.

162. Fanidi A, Harrington EA, Evan GI. Cooperative interaction between c-myc and bcl-2 proto-oncogenes. *Nature* 1992; **359:** 554-556.

163. Pan H, Griep AE. *Altered cell cycle regulation* in the lens of HPV-16 E6 or E7 transgenic mice: implications for tumor suppressor gene function in development. *Genes Dev. 1994; 8: 1285-1299.*

164. Howes KA, Ransom N, Papermaster DS, Lasudry JG, Albert DM, Windle JJ. Apoptosis or retinoblastoma: alternative fates of photoreceptors expressing the HPV-16 E7 gene in the presence or absence of p53. *Genes Dev.* 1994; **8:** 1300-1310.

165. Symonds H, Krall L, Remington L, Saenz RM, Jacks T, Van Dyke T. p53-dependent apoptosis in vivo: impact of p53 inactivation on tumorigenesis. *Cold Spring Harb.Symp.Quant.Biol.* 1994; **59:** 247-257.

166. Hermeking H, Eick D. Mediation of c-Myc-induced apoptosis by p53. *Science* 1994; **265:** 2091-2093.

167. Wagner AJ, Kokontis JM, Hay N. Myc-mediated apoptosis requires wild-type p53 in a manner independent of cell cycle arrest and the ability of p53 to induce p21waf1/cip1. *Genes Dev.* 1994; **8:** 2817-2830.

168. Fearnhead HO, McCurrach ME, O'Neill J, Zhang K, Lowe SW, Lazebnik YA. Oncogene-dependent apoptosis in extracts from drug-resistant cells. *Genes Dev.* 1997; **11:** 1266-1276.

169. Juin P, Hueber AO, Littlewood T, Evan G. c-Myc-induced sensitization to apoptosis is mediated through cytochrome c release. *Genes Dev.* 1999; **13:** 1367-1381.

170. Jurgensmeier JM, Xie Z, Deveraux Q, Ellerby L, Bredesen D, Reed JC. Bax directly induces release of cytochrome c from isolated mitochondria. *Proc Natl Acad Sci U S A* 1998; **95:** 4997-5002.

171. Polyak K, Xia Y, Zweier JL, Kinzler KW, Vogelstein B. A model for p53-induced apoptosis. *Nature* 1997; **389:** 300-305.

172. Bartek J, Iggo R, Gannon J, Lane DP. Genetic and immunochemical analysis of mutant p53 in human breast cancer cell lines. *Oncogene* 1990; **5:** 893-899.

173. Borresen-Dale AL. TP53 and breast cancer. *Hum.Mutat.* 2003; **21:** 292-300.

174. Schuyer M, Berns EM. Is TP53 dysfunction required for BRCA1-associated carcinogenesis? *Mol.Cell Endocrinol.* 1999; **155:** 143-152.

175. Casey G, Lo-Hsueh M, Lopez ME, Vogelstein B, Stanbridge EJ. Growth suppression of human breast cancer cells by the introduction of a wild-type p53 gene. *Oncogene* 1991; **6:** 1791-1797.

176. Hernandez-Boussard T, Rodriguez-Tome P, Montesano R, Hainaut P. IARC p53 mutation database: a relational database to compile and analyze p53 mutations in human tumors and cell lines. International Agency for Research on Cancer. *Hum.Mutat.* 1999; **14:** 1-8.

177. Patel DD, Bhatavdekar JM, Chikhlikar PR *et al.* Node negative breast carcinoma: hyperprolactinemia and/or overexpression of p53 as an independent predictor of poor prognosis compared to newer and established prognosticators. *J.Surg.Oncol.* 1996; **62:** 86-92.

178. Wang X, Gjorloff-Wingren A, Saxena M, Pathan N, Reed JC, Mustelin T. The tumor suppressor PTEN regulates T cell survival and antigen receptor signaling by acting as a phosphatidylinositol 3-phosphatase. *J.Immunol.* 2000; **164:** 1934-1939.

179. Bose S, Crane A, Hibshoosh H, Mansukhani M, Sandweis L, Parsons R. Reduced expression of PTEN correlates with breast cancer progression. *Hum.Pathol* 2002; **33:** 405-409.

180. Freihoff D, Kempe A, Beste B *et al.* Exclusion of a major role for the PTEN tumour-suppressor gene in breast carcinomas. *Br.J Cancer* 1999; **79:** 754-758.

181. FitzGerald MG, Marsh DJ, Wahrer D *et al.* Germline mutations in PTEN are an infrequent cause of genetic predisposition to breast cancer. *Oncogene* 1998; **17:** 727-731.

182. Feilotter HE, Coulon V, McVeigh JL *et al.* Analysis of the 10q23 chromosomal region and the PTEN gene in human sporadic breast carcinoma. *Br.J Cancer* 1999; **79:** 718-723.

183. Lu Y, Lin YZ, LaPushin R *et al.* The PTEN/MMAC1/TEP tumor suppressor gene decreases cell growth and induces apoptosis and anoikis in breast cancer cells. *Oncogene* 1999; **18:** 7034-7045.

184. Li J, Simpson L, Takahashi M *et al.* The PTEN/MMAC1 tumor suppressor induces cell death that is rescued by the AKT/protein kinase B oncogene. *Cancer Res* 1998; **58:** 5667-5672.

185. Tamura M, Gu J, Danen EH, Takino T, Miyamoto S, Yamada KM. PTEN interactions with focal adhesion kinase and suppression of the extracellular matrix-dependent phosphatidylinositol 3-kinase/Akt cell survival pathway. *J Biol Chem* 1999; **274:** 20693-20703.

186. Keane MM, Ettenberg SA, Lowrey GA, Russell EK, Lipkowitz S. Fas expression and function in normal and malignant breast cell lines. *Cancer Res* 1996; **56:** 4791-4798.

187. Mottolese M, Buglioni S, Bracalenti C *et al.* Prognostic relevance of altered Fas (CD95)-system in human breast cancer. *Int J Cancer* 2000; **89:** 127-132.

188. Willingham MC. Cytochemical methods for the detection of apoptosis. *J.Histochem.Cytochem.* 1999; **47:** 1101-1110.

189. Coles HS, Burne JF, Raff MC. Large-scale normal cell death in the developing rat kidney and its reduction by epidermal growth factor. *Development* 1993; **118:** 777-784.

190. Vitale M, Zamai L, Mazzotti G, Cataldi A, Falcieri E. Differential kinetics of propidium iodide uptake in apoptotic and necrotic thymocytes. *Histochemistry* 1993; **100:** 223-229.

191. Ucker DS. Death by suicide: one way to go in mammalian cellular development? *New Biol.* 1991; **3:** 103-109.

192. Koopman G, Reutelingsperger CP, Kuijten GA, Keehnen RM, Pals ST, van Oers MH. Annexin V for flow cytometric detection of phosphatidylserine expression on B cells undergoing apoptosis. *Blood* 1994; **84:** 1415-1420.

193. Emoto K, Toyama-Sorimachi N, Karasuyama H, Inoue K, Umeda M. Exposure of phosphatidylethanolamine on the surface of apoptotic cells. *Exp.Cell Res.* 1997; **232:** 430-434.

194. van Engeland M, Kuijpers HJ, Ramaekers FC, Reutelingsperger CP, Schutte B. Plasma membrane alterations and cytoskeletal changes in apoptosis. *Exp.Cell Res.* 1997; **235:** 421-430.

195. Zhang G, Gurtu V, Kain SR, Yan G. Early detection of apoptosis using a fluorescent conjugate of annexin V. *Biotechniques* 1997; **23:** 525-531.

196. van Engeland M, Nieland LJ, Ramaekers FC, Schutte B, Reutelingsperger CP. Annexin V-affinity assay: a review on an apoptosis detection system based on phosphatidylserine exposure. *Cytometry* 1998; **31:** 1-9.

197. Boersma AW, Nooter K, Oostrum RG, Stoter G. Quantification of apoptotic cells with fluorescein isothiocyanate-labeled annexin V in chinese *hamster ovary cell* cultures treated with cisplatin. *Cytometry* 1996; **24:** 123-130.

198. Gatti R, Belletti S, Orlandini G, Bussolati O, Dall'Asta V, Gazzola GC. Comparison of annexin V and calcein-AM as early vital markers of apoptosis in adherent cells by confocal laser microscopy. *J.Histochem.Cytochem.* 1998; **46:** 895-900.

199. Rimon G, Bazenet CE, Philpott KL, Rubin LL. Increased surface phosphatidylserine is an early marker of neuronal apoptosis. *J.Neurosci.Res.* 1997; **48:** 563-570.

200. Bussolati O, Belletti S, Uggeri J *et al.* Characterization of apoptotic phenomena induced by treatment with L-asparaginase in NIH3T3 cells. *Exp.Cell Res.* 1995; **220:** 283-291.

201. Schulze-Osthoff K, Walczak H, Droge W, Krammer PH. Cell nucleus and DNA fragmentation are not required for apoptosis. *J.Cell Biol.* 1994; **127:** 15-20.

202. Collins JA, Schandi CA, Young KK, Vesely J, Willingham MC. Major DNA fragmentation is a late event in apoptosis. *J.Histochem.Cytochem.* 1997; **45:** 923-934.

203. Hall PA. Assessing apoptosis: a critical survey. *Endocr.Relat Cancer* 1999; **6:** 3-8.

204. Tatton NA, Maclean-Fraser A, Tatton WG, Perl DP, Olanow CW. A fluorescent double-labeling method to detect and confirm apoptotic nuclei in Parkinson's disease. *Ann.Neurol.* 1998; **44:** S142-S148.

205. Barrett A, Morgan L, Raggatt PR, Hobbs JR. Bromocriptine in the treatment of advanced breast cancer. *Clin.Oncol.* 1976; **2:** 373-377.

206. Peyrat JP, Vennin P, Bonneterre J *et al.* Effect of bromocriptin treatment on prolactin and steroid receptor levels in human breast cancer. *Eur J Cancer Clin Oncol* 1984; **20:** 1363-1367.

207. Mandlekar S, Yu R, Tan TH *et al.* Activation of caspase-3 and c-Jun NH2-terminal kinase-1 signaling
Antiprolactinemic approach in the treatment of metastatic breast. *Cancer Res* 2000; **60:** 5995-6000.

208. Lissoni P, Vaghi M, Villa S *et al.* Antiprolactinemic approach in the treatment of metastatic breast. *Anticancer Res* 2003; **23:** 733-736.

209. Wennbo H, Kindblom J, Isaksson OG, Tornell J. Transgenic mice overexpressing the prolactin gene develop dramatic enlargement of the prostate gland. *Endocrinology* 1997; **138:** 4410-4415.

210. Vomachka AJ, Pratt SL, Lockefeer JA, Horseman ND. Prolactin gene-disruption arrests mammary gland development and retards T-antigen-induced tumor growth. *Oncogene* 2000; **19:** 1077-1084.

211. Clevenger CV, Chang W-P, Ngo W, Pasha TM, Montone KT, Tomaszewski JE. Expression of prolactin and prolactin receptor in human breast carcinoma: Evidence for an autocrine/paracrine loop. *American Journal of Pathology* 1995; **146:** 695-705.

212. Ginsburg E, Vonderhaar BK. Prolactin synthesis and secretion by human breast cancer cells. *Cancer Res* 1995; **55:** *2591-2595.*

213. Shaw-Bruha CM, Pirrucello SJ, Shull JD. Expression of the prolactin gene in *normal and neoplastic* human breast tissues and human mammary cell lines: promoter usage and alternative mRNA splicing. *Breast Cancer Res.Treat.* 1997; **44:** 243-253.

214. Touraine P, Martini JF, Zafrani B *et al.* Increased expression of prolactin receptor gene assessed by quantitative polymerase chain reaction in human breast tumors versus normal breast tissues. *J Clin Endocrinol Metab* 1998; **83:** 667-674.

215. Murphy LJ, Vrhovsek E, Sutherland RL, Lazarus L. Growth hormone binding to cultured human breast cancer cells. *J Clin Endocrinol Metab* 1984; **58:** 149-156.

216. Goffin V, Touraine P, Pichard C, Bernichtein S, Kelly, PA. Should prolactin be reconsidered as a therapeutic target in human breast cancer?. [Review] [71 refs]. *Molecular & Cellular Endocrinology* 1999; **151:** 79-87.

217. Vonderhaar BK. Prolactin involvement in breast cancer. [Review] [158 refs]. *Endocrine-Related Cancer* 1999; **6:** 389-404.

218. Wennbo H, Tornell J. The role of prolactin and growth hormone in breast cancer. *Oncogene* 2000; **19:** 1072-1076.

219. Chen WY, Ramamoorthy P, Chen N, Sticca R, Wagner TE. A human prolactin antagonist, hPRL-G129R, inhibits breast cancer cell proliferation through induction of apoptosis. *Clin Cancer Res* 1999; **5:** 3583-3593.

220. Shiu RC. Prolactin receptors in human breast cancer cells in long-term tissue culture. *Cancer Research* 1979; **39:** 4381-4386.

221. Peirce SK, Chen WY, Chen WY. Quantification of prolactin receptor mRNA in multiple human tissues and cancer cell lines by real time RT-PCR. *J Endocrinol* 2001; **171:** R1-R4.

222. Payne SG, Brindley DN, Guilbert LJ. Epidermal growth factor inhibits ceramide-induced apoptosis and lowers ceramide levels in primary placental trophoblasts. *J.Cell Physiol* 1999; **180:** 263-270.

223. Perks CM, Bowen S, Gill ZP, Newcomb PV, Holly JM. Differential IGF-independent effects of insulin-like growth factor binding proteins (1-6) on apoptosis of breast epithelial cells. *J Cell Biochem* 1999; **75:** 652-664.

224. Biswas R, Vonderhaar BK. Role of serum in the prolactin responsiveness of MCF-7 human breast cancer cells in long-term tissue culture. *Cancer Res* 1987; **47:** 3509-3514.

225. Hannun YA. Functions of ceramide in coordinating cellular responses to stress. *Science* 1996; **274:** 1855-1859.

226. Mathias S, Pena LA, Kolesnick RN. Signal transduction of stress via ceramide. *Biochem.J.* 1998; **335 (Pt 3):** 465-480.

227. Grullich C, Sullards MC, Fuks Z, Merrill AH, Jr., Kolesnick R. CD95(Fas/APO-1) signals ceramide generation independent of the effector stage of apoptosis. *Journal of Biological Chemistry* 2000; **275:** 8650-8656.

228. Tepper AD, Cock JG, de Vries E, Borst J, van Blitterswijk WJ. CD95/Fas-induced ceramide formation proceeds with slow kinetics and is not blocked by caspase-3/CPP32 inhibition. *Journal of Biological Chemistry* 1997; **272:** 24308-24312.

229. Laethem RM, Hannun YA, Jayadev S *et al.* Increases in neutral, Mg2+-dependent and acidic, Mg2+-independent sphingomyelinase activities precede commitment to apoptosis and are not a consequence of caspase 3-like activity in Molt-4 cells in response to thymidylate synthase inhibition by GW1843. *Blood* 1998; **91:** 4350-4360.

230. Chen L, Kim TJ, Pillai S. Inhibition of caspase activity prevents anti-IgM induced apoptosis but not ceramide generation in WEHI 231 B cells. *Mol.Immunol.* 1998; **35:** 195-205.

231. Yoshimura S, Banno Y, Nakashima S *et al.* Ceramide formation leads to caspase-3 activation during hypoxic PC12 cell death. Inhibitory effects of Bcl-2 on ceramide formation and caspase-3 activation. *Journal of Biological Chemistry* 1998; **273:** 6921-6927.

232. Ji L, Zhang G, Uematsu S, Akahori Y, Hirabayashi Y. Induction of apoptotic DNA fragmentation and cell death by natural ceramide. *FEBS Lett.* 1995; **358:** 211-214.

233. Hartfield PJ, Mayne GC, Murray AW. Ceramide induces apoptosis in PC12 cells. *FEBS Lett.* 1997; **401:** 148-152.

234. Saba JD, Obeid LM, Hannun YA. Ceramide: an intracellular mediator of apoptosis and growth suppression. *Philos.Trans.R.Soc.Lond B Biol.Sci.* 1996; **351:** 233-240.

235. McPherson K, Steel CM, Dixon JM. ABC of breast diseases. Breast cancer-epidemiology, risk factors, and genetics. *BMJ* 2000; **321:** 624-628.

236. Sainsbury JR, Anderson TJ, Morgan DA. ABC of breast diseases: breast cancer. *BMJ* 2000; **321:** 745-750.

237. Bole-Feysot C, Goffin V, Edery M, Binart N, Kelly PA. Prolactin (PRL) and its receptor: actions, signal transduction pathways and phenotypes observed in PRL receptor knockout mice. *Endocr Rev* 1998; **19:** 225-268.

238. Lyons WR. The hormonal control of mammary growth and lactation. *Rec Progr Horm Res* 1958; **14:** 219-248.

239. Vonderhaar BK. Prolactin: transport, function, and receptors in mammary gland development and differentiation. In: Neville M, Daniel C, eds. *The Mammary Gland*. New York: Plenum 1987: 383-438.

240. al Sakkaf KA, Dobson PR, Brown BL. Activation of phosphatidylinositol 3-kinase by prolactin in Nb2 cells. *Biochem.Biophys.Res.Commun.* 1996; **221:** 779-784.

241. Brisken C, Kaur S, Chavarria TE *et al.* Prolactin controls mammary gland development via direct and indirect mechanisms. *Dev.Biol.* 1999; **210:** 96-106.

242. Hennighausen L, Robinson GW, Wagner KU, Liu X. Developing a mammary gland is a stat affair. *J.Mammary.Gland.Biol.Neoplasia.* 1997; **2:** 365-372.

243. de Groot RP, Raaijmakers JA, Lammers JW, Jove R, Koenderman L. STAT5 activation by BCR-Abl contributes to transformation of K562 leukemia cells. *Blood* 1999; **94:** 1108-1112.

244. Demoulin JB, Uyttenhove C, Lejeune D, Mui A, Groner B, Renauld JC. STAT5 activation is required for interleukin-9-dependent growth and transformation of lymphoid cells. *Cancer Res* 2000; **60:** 3971-3977.

245. Biola A, Lefebvre P, Perrin-Wolff M, Sturm M, Bertoglio J, Pallardy M. Interleukin-2 inhibits glucocorticoid receptor transcriptional activity through a mechanism involving STAT5 (signal transducer and activator of transcription 5) but not AP-1. *Mol.Endocrinol.* 2001; **15:** 1062-1076.

246. Bittorf T, Seiler J, Ludtke B, Buchse T, Jaster R, Brock J. Activation of STAT5 during EPO-directed suppression of apoptosis. *Cell Signal.* 2000; **12:** 23-30.

247. Fuh G, Wells JA. Prolactin receptor antagonists that inhibit the growth of breast cancer cell lines. *Journal of Biological Chemistry* 1995; **270:** 13133-13137.

248. Nieves-Neira W, Pommier Y. Apoptotic response to camptothecin and 7-hydroxystaurosporine (UCN-01) in the 8 human breast cancer cell lines of the NCI Anticancer Drug Screen: multifactorial relationships with topoisomerase I, protein kinase C, Bcl-2, p53, MDM-2 and caspase pathways. *Int.J.Cancer* 1999; **82:** 396-404.

249. Janicke RU, Sprengart ML, Wati MR, Porter AG. Caspase-3 is required for DNA fragmentation and morphological changes associated with apoptosis. *Journal of Biological Chemistry* 1998; **273:** 9357-9360.

250. Gooch JL, Yee D. Strain-specific differences in formation of apoptotic DNA ladders in MCF-7 breast cancer cells. *Cancer Lett* 1999; **144:** 31-37.

251. Bowen ID, Mullarkey K, Morgan SM. Programmed cell death during metamorphosis in the blow-fly Calliphora vomitoria. *Microsc.Res.Tech.* 1996; **34:** 202-217.

252. Szende B, Keri G, Szegedi Z *et al.* Tyrphostin induces non-apoptotic programmed cell death in colon tumor cells. *Cell Biol.Int.* 1995; **19:** 903-911.

253. Lockshin RA, Zakeri Z. Caspase-independent cell deaths. *Curr Opin Cell Biol* 2002; **14:** 727-733.

254. Butt AJ, Firth SM, King MA, Baxter RC. Insulin-like growth factor-binding protein-3 modulates expression of Bax and Bcl-2 and potentiates p53-independent radiation-induced apoptosis in human breast cancer cells. *J.Biol.Chem.* 2000; **275:** 39174-39181.

255. Formby B, Wiley TS. Bcl-2, survivin and variant CD44 v7-v10 are downregulated and p53 is upregulated in breast cancer cells by progesterone: inhibition of cell growth and induction of apoptosis. *Mol Cell Biochem* 1999; **202:** 53-61.

256. Mathiasen IS, Sergeev IN, Bastholm L, Elling F, Norman AW, Jaattela M. Calcium and calpain as key mediators of apoptosis-like death induced by vitamin D compounds in breast cancer cells. *J Biol Chem* 2002; **277:** 30738-30745.

257. Fromigue O, Lagneaux L, Body JJ. Bisphosphonates induce breast cancer cell death in vitro. *J Bone Miner.Res* 2000; **15:** 2211-2221.

258. Ge X, Yannai S, Rennert G, Gruener N, Fares FA. 3,3'-Diindolylmethane induces apoptosis in human cancer cells. *Biochem Biophys Res Commun* 1996; **228:** 153-158.

259. Baj G, Arnulfo A, Deaglio S *et al.* Arsenic trioxide and breast cancer: analysis of the apoptotic, differentiative and immunomodulatory effects. *Breast Cancer Res Treat.* 2002; **73:** 61-73.

260. Pirianov G, Colston KW. Interaction of vitamin D analogs with signaling pathways leading to active cell death in breast cancer cells. *Steroids* 2001; **66:** 309-318.

261. Ginsburg E, Vonderhaar BK. Prolactin synthesis and secretion by human breast cancer cells. *Cancer Research* 1995; **55:** 2591-2595.

262. Codegone ML, Di Carlo R, Muccioli G, Bussolati G. Histology and cytometrics in human breast cancers assayed for the presence of prolactin receptors. *Tumori* 1981; **67:** 549-552.

263. Peyrat JP, Dewailly D, Djiane J *et al.* Total prolactin binding sites in human breast cancer biopsies. *Breast Cancer Res.Treat.* 1981; **1:** 369-373.

264. Ihle JN, Kerr IM. Jaks and Stats in signaling by the cytokine receptor superfamily. *Trends Genet.* 1995; **11:** 69-74.

265. Battle TE, Frank DA. The role of STATs in apoptosis. *Curr.Mol.Med.* 2002; **2:** 381-392.

266. Demoulin JB, Van Roost E, Stevens M, Groner B, Renauld JC. Distinct roles for STAT1, STAT3, and STAT5 in differentiation gene induction and apoptosis inhibition by interleukin-9. *Journal of Biological Chemistry* 1999; **274:** 25855-25861.

267. Kirito K, Watanabe T, Sawada K, Endo H, Ozawa K, Komatsu N. Thrombopoietin regulates Bcl-xL gene expression through Stat5 and phosphatidylinositol 3-kinase activation pathways. *Journal of Biological Chemistry* 2002; **277:** 8329-8337.

268. Morcinek JC, Weisser C, Geissinger E, Schartl M, Wellbrock C. Activation of STAT5 triggers proliferation and contributes to anti-apoptotic signalling mediated by the oncogenic Xmrk kinase. *Oncogene* 2002; **21:** 1668-1678.

269. Norman MR, Thompson EB. Characterization of a glucocorticoid-sensitive human lymphoid cell line. *Cancer Res* 1977; **37:** 3785-3791.

270. Gledhill RM, Gray DA, Solberg-Scott M, Norman MR. Decreased acquisition of glucocorticoid resistance in tetraploid human lymphoid cells. *Mol Cell Endocrinol* 1983; **29:** 67-77.

271. Harmon JM, Thompson EB. Isolation and characterization of dexamethasone-resistant mutants from human lymphoid cell line CEM-C7. *Mol.Cell Biol.* 1981; **1:** 512-521.

272. Ji YS, Johnson BH, Webb MS, Thompson EB. Mutational analysis of DBD*--a unique antileukemic gene sequence. *Neoplasia.* 2002; **4:** 417-423.

273. El Naghy M, Johnson BH, Chen H *et al.* The pathway of leukemic cell death caused by glucocorticoid receptor fragment 465*. *Exp.Cell Res.* 2001; **270:** 166-175.

274. Kelly PA, Djiane J, Postel-Vinay MC, Edery M. The prolactin/growth hormone receptor family. [Review] [162 refs]. *Endocrine Reviews* 1991; **12:** 235-251.

275. Kelly PA, Ali S, Rozakis M *et al.* The growth hormone/prolactin receptor family. *Recent Prog.Horm.Res.* 1993; **48:** 123-164.

276. Ali S, Pellegrini I, Kelly PA. A prolactin-dependent immune cell line (Nb2) expresses a mutant form of prolactin receptor. *Journal of Biological Chemistry* 1991; **266:** 20110-20117.

277. Lesueur L, Edery M, Ali S, Paly J, Kelly PA, Djiane J. Comparison of long and short forms of the prolactin receptor on prolactin-induced milk protein gene transcription. *Proceedings of the National Academy of Sciences of the United States of America* 1991; **88:** 824-828.

278. O'Neal KD, Yu-Lee LY. Differential signal transduction of the short, Nb2, and long prolactin receptors. Activation of interferon regulatory factor-1 and cell proliferation. *Journal of Biological Chemistry* 1994; **269:** 26076-26082.

279. Das R, Vonderhaar BK. Transduction of prolactin's (PRL) growth signal through both long and short forms of the PRL receptor. *Molecular Endocrinology* 1995; **9:** 1750-1759.

280. Darnell JE, Jr. STATs and gene regulation. *Science* 1997; **277:** 1630-1635.

281. DaSilva L, Rui H, Erwin RA *et al.* Prolactin recruits STAT1, STAT3 and STAT5 independent of conserved receptor tyrosines TYR402, TYR479, TYR515 and TYR580. *Mol.Cell Endocrinol.* 1996; **117:** 131-140.

282. Das R, Vonderhaar BK. Involvement of SHC, GRB2, SOS and RAS in prolactin signal transduction in mammary epithelial cells. *Oncogene* 1996; **13:** 1139-1145.

283. Canbay E, Norman M, Kilic E, Goffin V, Zachary I. Prolactin stimulates the JAK2 and focal adhesion kinase pathways in human breast carcinoma T47-D cells. *Biochemical Journal* 1997; **324:** 231-236.

284. David M, Petricoin EF, III, Igarashi K, Feldman GM, Finbloom DS, Larner AC. Prolactin activates the interferon-regulated p91 transcription factor and the Jak2 kinase by tyrosine phosphorylation. *Proc.Natl.Acad.Sci.U.S.A* 1994; **91:** 7174-7178.

285. Llovera M, Touraine P, Kelly PA, Goffin V. Involvement of prolactin in breast cancer: redefining the molecular targets. *Exp.Gerontol.* 2000; **35:** 41-51.

286. Rui H, Kirken RA, Farrar WL. Activation of receptor-associated tyrosine kinase JAK2 by prolactin. *Journal of Biological Chemistry* 1994; **269:** 5364-5368.

287. Chughtai N, Schimchowitsch S, Lebrun JJ, Ali S. Prolactin induces SHP-2 association with Stat5, nuclear translocation, and binding to the beta-casein gene promoter in mammary cells. *J Biol Chem* 2002; **277:** 31107-31114.

288. Liu X, Robinson GW, Gouilleux F, Groner B, Hennighausen L. Cloning and expression of Stat5 and an additional homologue (Stat5b) involved in prolactin signal transduction in mouse mammary tissue. *Proc.Natl.Acad.Sci.U.S.A* 1995; **92:** 8831-8835.

289. Liu X, Robinson GW, Hennighausen L. Activation of Stat5a and Stat5b by tyrosine phosphorylation is tightly linked to mammary gland differentiation. *Mol.Endocrinol.* 1996; **10:** 1496-1506.

290. Clevenger CV, Furth PA, Hankinson SE, Schuler LA. The role of prolactin in mammary carcinoma. *Endocr.Rev* 2003; **24:** 1-27.

291. Medh RD, Wang A, Zhou F, Thompson EB. Constitutive expression of ectopic c-Myc delays glucocorticoid-evoked apoptosis of human leukemic CEM-C7 cells. *Oncogene* 2001; **20:** 4629-4639.

292. Wojda U, Miller JL. Targeted transfer of polyethylenimine-avidin-DNA bioconjugates to hematopoietic cells using biotinylated monoclonal antibodies. *J Pharm.Sci* 2000; **89:** 674-681.

293. Guillem VM, Tormo M, Revert F *et al.* Polyethyleneimine-based immunopolyplex for targeted gene transfer in human lymphoma cell lines. *J Gene Med* 2002; **4:** 170-182.

294. Socolovsky M, Fallon AE, Wang S, Brugnara C, Lodish HF. Fetal anemia and apoptosis of red cell progenitors in Stat5a-/-5b-/- mice: a direct role for Stat5 in Bcl-X(L) induction. *Cell* 1999; **98:** 181-191.

295. Garcia R, Yu CL, Hudnall A *et al.* Constitutive activation of Stat3 in fibroblasts transformed by diverse oncoproteins and in breast carcinoma cells. *Cell Growth Differ* 1997; **8:** 1267-1276.

296. Catlett-Falcone R, Landowski TH, Oshiro MM *et al.* Constitutive activation of Stat3 signaling confers resistance to apoptosis in human U266 myeloma cells. *Immunity* 1999; **10:** 105-115.

297. Chai SK, Nichols GL, Rothman P. Constitutive activation of JAKs and STATs in BCR-Abl-expressing cell lines and peripheral blood cells derived from leukemic patients. *The Journal of Immunology* 1997; **159:** 4720-4728.

298. Rosa Santos SC, Dumon S, Mayeux P, Gisselbrecht S, Gouilleux F. Cooperation between STAT5 and phosphatidylinositol 3-kinase in the IL-3-dependent survival of a bone marrow derived cell line. *Oncogene* 2000; **19:** 1164-1172.

299. Bromberg JF, Horvath CM, Besser D, Lathem WW, Darnell JE, Jr. Stat3 activation is required for cellular transformation by v-src. *Mol Cell Biol* 1998; **18:** 2553-2558.

300. Turkson J, Bowman T, Garcia R, Caldenhoven E, De Groot RP, Jove R. Stat3 activation by Src induces specific gene regulation and is required for cell transformation. *Mol.Cell Biol.* 1998; **18:** 2545-2552.

301. Feldman GM, Rosenthal LA, Liu X *et al.* STAT5A-deficient mice demonstrate a defect in granulocyte-macrophage colony-stimulating factor-induced proliferation and gene expression. *Blood* 1997; **90:** 1768-1776.

302. Liu X, Robinson GW, Wagner KU, Garrett L, Wynshaw-Boris A, Hennighausen L. Stat5a is mandatory for adult mammary gland development and lactogenesis. *Genes Dev.* 1997; **11:** 179-186.

303. Ormandy CJ, Camus A, Barra J *et al.* Null mutation of the prolactin receptor gene produces multiple reproductive defects in the mouse. *Genes & Development* 1997; **11:** 167-178.

304. Udy GB, Towers RP, Snell RG *et al.* Requirement of STAT5b for sexual dimorphism of body growth rates and liver gene expression. *Proceedings of the National Academy of Sciences of the United States of America* 1997; **94:** 7239-7244.

305. Teglund S, McKay C, Schuetz E *et al.* Stat5a and Stat5b proteins have essential and nonessential, or redundant, roles in cytokine responses. *Cell* 1998; **93:** 841-850.

306. Matsumura I, Kitamura T, Wakao H *et al.* Transcriptional regulation of the cyclin D1 promoter by STAT5: its involvement in cytokine-dependent growth of hematopoietic cells. *EMBO Journal* 1999; **18:** 1367-1377.

307. Moriggl R, Topham DJ, Teglund S *et al.* Stat5 is required for IL-2-induced cell cycle progression of peripheral T cells. *Immunity* 1999; **10:** 249-259.

308. Smithgall TE, Briggs SD, Schreiner S, Lerner EC, Cheng H, Wilson MB. Control of myeloid differentiation and survival by Stats. *Oncogene* 2000; **19:** 2612-2618.

309. Grad JM, Zeng XR, Boise LH. Regulation of Bcl-xL: a little bit of this and a little bit of STAT. *Curr.Opin.Oncol.* 2000; **12:** 543-549.

310. Silva M, Benito A, Sanz C *et al.* Erythropoietin can induce the expression of bcl-x(L) through Stat5 in erythropoietin-dependent progenitor cell lines. *Journal of Biological Chemistry* 1999; **274:** 22165-22169.

311. Quelle FW, Wang J, Feng J *et al.* Cytokine rescue of p53-dependent apoptosis and cell cycle arrest is mediated by distinct Jak kinase signaling pathways. *Genes Dev* 1998; **12:** 1099-1107.

312. Gesbert F, Griffin JD. Bcr/Abl activates transcription of the Bcl-X gene through STAT5. *Blood* 2000; **96:** 2269-2276.

313. Carlesso N, Frank DA, Griffin JD. Tyrosyl phosphorylation and DNA binding activity of signal transducers and activators of transcription (STAT) proteins in hematopoietic cell lines transformed by Bcr/Abl. *J Exp Med* 1996; **183:** 811-820.

314. Smith PD, Crompton MR. Expression of v-src in mammary epithelial cells induces transcription via STAT3. *Biochem J* 1998; **331 (Pt 2):** 381-385.

315. Wen X, Lin HH, Shih HM, Kung HJ, Ann DK. Kinase activation of the non-receptor tyrosine kinase Etk/BMX alone is sufficient to transactivate STAT-mediated gene expression in salivary and lung epithelial cells. *J Biol Chem* 1999; **274:** 38204-38210.

316. Rosen RL, Winestock KD, Chen G, Liu X, Hennighausen L, Finbloom DS. Granulocyte-macrophage colony-stimulating factor preferentially activates the 94-kD STAT5A and an 80-kD STAT5A isoform in human peripheral blood monocytes. *Blood* 1996; **88:** 1206-1214.

317. Philp JA, Burdon TG, Watson CJ. Differential activation of STATs 3 and 5 during mammary gland development. *FEBS Lett.* 1996; **396:** 77-80.

318. Imada K, Bloom ET, Nakajima H *et al.* Stat5b is essential for natural killer cell-mediated proliferation and cytolytic activity. *J Exp Med* 1998; **188:** 2067-2074.

319. Onishi M, Nosaka T, Misawa K *et al.* Identification and characterization of a constitutively active STAT5 mutant that promotes cell proliferation. *Molecular & Cellular Biology* 1998; **18:** 3871-3879.

320. Kazansky AV, Raught B, Lindsey SM, Wang YF, Rosen JM. Regulation of mammary gland factor/Stat5a during mammary gland development. *Mol.Endocrinol.* 1995; **9:** 1598-1609.

321. Ren S, Cai HR, Li M, Furth PA. Loss of Stat5a delays mammary cancer progression in a mouse model. *Oncogene* 2002; **21:** 4335-4339.

322. Yamashita H, Iwase H. The role of stat5 in estrogen receptor-positive breast cancer [In Process Citation]. *Breast Cancer* 2002; **9:** 312-338.

323. Castro A, Buschbaum P, Nadji M, Voigt W, Ziegels-Weissman J, Morales A. Tissue immunoreactive prolactin hormone in breast cancer. *Res Commun Chem Pathol Pharmacol* 1980; **29:** 159-170.

324. Biswas R, Vonderhaar BK. Role of serum in the prolactin responsiveness of MCF-7 human breast cancer cells in long-term tissue culture. *Cancer Research* 1987; **47:** 3509-3514.

325. Oesterreich S, Lee AV, Sullivan TM, Samuel SK, Davie JR, Fuqua SA. Novel nuclear matrix protein HET binds to and influences activity of the HSP27 promoter in human breast cancer cells. *J Cell Biochem* 1997; **67:** 275-286.

326. Renz A, Fackelmayer FO. Purification and molecular cloning of the scaffold attachment factor B (SAF-B), a novel human nuclear protein that specifically binds to S/MAR-DNA. *Nucleic Acids Res* 1996; **24:** 843-849.

327. Weighardt F, Cobianchi F, Cartegni L *et al.* A novel hnRNP protein (HAP/SAF-B) enters a subset of hnRNP complexes and relocates in nuclear granules in response to heat shock. *J Cell Sci* 1999; **112 (Pt 10):** 1465-1476.

328. Kipp M, Gohring F, Ostendorp T *et al.* SAF-Box, a conserved protein domain that specifically recognizes scaffold attachment region DNA. *Mol.Cell Biol.* 2000; **20:** 7480-7489.

329. Oesterreich S, Zhang Q, Hopp T *et al.* Tamoxifen-bound estrogen receptor (ER) strongly interacts with the nuclear matrix protein HET/SAF-B, a novel inhibitor of ER-mediated transactivation. *Mol.Endocrinol.* 2000; **14:** 369-381.

330. Aravind L, Koonin EV. SAP - a putative DNA-binding motif involved in chromosomal organization. *Trends Biochem Sci* 2000; **25:** 112-114.

331. Birney E, Kumar S, Krainer AR. Analysis of the RNA-recognition motif and RS and RGG domains: conservation in metazoan pre-mRNA splicing factors. *Nucleic Acids Res* 1993; **21:** 5803-5816.

332. White R, Jobling S, Hoare SA, Sumpter JP, Parker MG. Environmentally persistent alkylphenolic compounds are estrogenic. *Endocrinology* 1994; **135:** 175-182.

333. Sesso A, Fujiwara DT, Jaeger M *et al.* Structural elements common to mitosis and apoptosis. *Tissue Cell* 1999; **31:** 357-371.

334. Negri C, Donzelli M, Bernardi R, Rossi L, Burkle A, Scovassi AI. Multiparametric staining to identify apoptotic human cells. *Exp Cell Res* 1997; **234:** 174-177.

335. Thompson JD, Higgins DG, Gibson TJ. CLUSTAL W: improving the sensitivity of progressive multiple sequence alignment through sequence weighting, position-specific gap penalties and weight matrix choice. *Nucleic Acids Res* 1994; **22:** 4673-4680.

336. DuPont BR, Garcia DK, Sullivan TM, Naylor SL, Oesterreich S. Assignment of SAFB encoding Hsp27 ERE-TATA binding protein (HET)/scaffold attachment factor B (SAF-B) to human chromosome 19 band p13. *Cytogenet.Cell Genet* 1997; **79:** 284-285.

337. Mayeda A, Munroe SH, Caceres JF, Krainer AR. Function of conserved domains of hnRNP A1 and other hnRNP A/B proteins. *EMBO J.* 1994; **13:** 5483-5495.

338. Arao Y, Kuriyama R, Kayama F, Kato S. A nuclear matrix-associated factor, SAF-B, interacts with specific isoforms of AUF1/hnRNP D. *Arch.Biochem Biophys* 2000; **380:** 228-236.

339. Nayler O, Stratling W, Bourquin JP *et al.* SAF-B protein couples transcription and pre-mRNA splicing to SAR/MAR elements. *Nucleic Acids Res* 1998; **26:** 3542-3549.

340. Huszar T, Mucsi I, Terebessy T *et al.* The use of a second reporter plasmid as an internal standard to normalize luciferase activity in transient transfection experiments may lead to a systematic error. *J Biotechnol.* 2001; **88:** 251-258.

341. Caceres JF, Kornblihtt AR. Alternative splicing: multiple control mechanisms and involvement in human disease. *Trends Genet.* 2002; **18:** 186-193.

342. Chalfant CE, Rathman K, Pinkerman RL *et al.* De novo ceramide regulates the alternative splicing of caspase 9 and Bcl-x in A549 lung adenocarcinoma cells. Dependence on protein phosphatase-1. *J.Biol.Chem.* 2002; **277:** 12587-12595.

343. Wang L, Miura M, Bergeron L, Zhu H, Yuan J. Ich-1, an Ice/ced-3-related gene, encodes both positive and negative regulators of programmed cell death. *Cell* 1994; **78:** 739-750.

344. Droin N, Rebe C, Bichat F, Hammann A, Bertrand R, Solary E. Modulation of apoptosis by procaspase-2 short isoform: selective inhibition of chromatin condensation, apoptotic body formation and phosphatidylserine externalization. *Oncogene* 2001; **20:** 260-269.

345. Benedict MA, Hu Y, Inohara N, Nunez G. Expression and functional analysis of Apaf-1 isoforms. Extra Wd-40 repeat is required for cytochrome c binding and regulated activation of procaspase-9. *J Biol Chem* 2000; **275:** 8461-8468.

346. Eckhart L, Henry M, Santos-Beneit AM *et al.* Alternative splicing of caspase-8 mRNA during differentiation of human leukocytes. *Biochem.Biophys.Res.Commun.* 2001; **289:** 777-781.

347. Caceres JF, Misteli T, Screaton GR, Spector DL, Krainer AR. Role of the modular domains of SR proteins in subnuclear localization and alternative splicing specificity. *J.Cell Biol.* 1997; **138:** 225-238.

348. George-Tellez R, Segura-Valdez ML, Gonzalez-Santos L, Jimenez-Garcia LF. Cellular organization of pre-mRNA splicing factors in several tissues. Changes in the uterus by hormone action. *Biol Cell* 2002; **94:** 99-108.

349. Zhao Y, Goto K, Saitoh M *et al.* Activation function-1 domain of androgen receptor contributes to the interaction between subnuclear splicing factor compartment and nuclear receptor compartment. Identification of the p102 U5 small nuclear ribonucleoprotein particle-binding protein as a coactivator for the receptor. *J Biol Chem* 2002; **277:** 30031-30039.

350. Jiang ZH, Wu JY. Alternative splicing and programmed cell death. *Proc.Soc.Exp.Biol.Med.* 1999; **220:** 64-72.

351. Gerbi SA, Borovjagin AV, Lange TS. The nucleolus: a site of ribonucleoprotein maturation. *Curr Opin Cell Biol* 2003; **15:** 318-325.

352. Lamond AI, Earnshaw WC. Structure and function in the nucleus. *Science* 1998; **280:** 547-553.

353. Misteli T. Cell biology of transcription and pre-mRNA splicing: nuclear architecture meets nuclear function. *J Cell Sci* 2000; **113:** 1841-1849.

354. Lewis JD, Tollervey D. Like attracts like: getting RNA processing together in the nucleus. *Science* 2000; **288:** 1385-1389.

355. Spector DL. Macromolecular domains within the cell nucleus. *Annu.Rev Cell Biol* 1993; **9:** 265-315.

356. Puvion E, Puvion-Dutilleul F. Ultrastructure of the nucleus in relation to transcription and splicing: roles of perichromatin fibrils and interchromatin granules. *Exp Cell Res* 1996; **229:** 217-225.

357. Spector DL. Nuclear organization and gene expression. *Exp Cell Res* 1996; **229:** 189-197.

358. Huang S, Spector DL. Intron-dependent recruitment of pre-mRNA splicing factors to sites of transcription. *J Cell Biol* 1996; **133:** 719-732.

359. Bourquin JP, Stagljar I, Meier P *et al.* A serine/arginine-rich nuclear matrix cyclophilin interacts with the C-terminal domain of RNA polymerase II. *Nucleic Acids Res* 1997; **25:** 2055-2061.

360. Chiodi I, Biggiogera M, Denegri M *et al.* Structure and dynamics of hnRNP-labelled nuclear bodies induced by stress treatments. *J Cell Sci* 2000; **113 (Pt 22):** 4043-4053.

361. Gentile M, Latonen L, Laiho M. Cell cycle arrest and apoptosis provoked by UV radiation-induced DNA damage are transcriptionally highly divergent responses. *Nucleic Acids Res* 2003; **31:** 4779-4790.

362. Biggiogera M, Bottone MG, Pellicciari C. Nuclear RNA is extruded from apoptotic cells. *J Histochem.Cytochem.* 1998; **46:** 999-1005.

363. Bjorling-Poulsen M, Issinger OG. cDNA array analysis of alterations in gene expression in the promyelocytic leukemia cell line, HL-60, after apoptosis induction with etoposide. *Apoptosis.* 2003; **8:** 377-388.

364. Kiechle FL, Zhang X. Apoptosis: biochemical aspects and clinical implications. *Clin Chim.Acta* 2002; **326:** 27-45.

365. Chang SH, Cvetanovic M, Harvey KJ, Komoriya A, Packard BZ, Ucker DS. The effector phase of physiological cell death relies exclusively on the posttranslational activation of resident components. *Exp Cell Res* 2002; **277:** 15-30.

366. Jiang ZH, Zhang WJ, Rao Y, Wu JY. Regulation of Ich-1 pre-mRNA alternative splicing and apoptosis by mammalian splicing factors. *Proc.Natl.Acad.Sci.U.S.A* 1998; **95:** 9155-9160.

367. Cote J, Dupuis S, Jiang Z, Wu JY. Caspase-2 pre-mRNA alternative splicing: Identification of an intronic element containing a decoy 3' acceptor site. *Proc.Natl.Acad.Sci.U.S.A* 2001; **98:** 938-943.

368. Cote J, Dupuis S, Wu JY. Polypyrimidine track-binding protein binding downstream of caspase-2 alternative exon 9 represses its inclusion. *J.Biol.Chem.* 2001; **276:** 8535-8543.

369. Tian Q, Streuli M, Saito H, Schlossman SF, Anderson P. A polyadenylate binding protein localized to the granules of cytolytic lymphocytes induces DNA fragmentation in target cells. *Cell* 1991; **67:** 629-639.

370. Forch P, Puig O, Kedersha N *et al.* The apoptosis-promoting factor TIA-1 is a regulator of alternative pre-mRNA splicing. *Mol.Cell* 2000; **6:** 1089-1098.

371. Blencowe BJ, Bowman JA, McCracken S, Rosonina E. SR-related proteins and the processing of messenger RNA precursors. *Biochem Cell Biol* 1999; **77:** 277-291.

372. Hastings ML, Krainer AR. Pre-mRNA splicing in the new millennium. *Curr Opin Cell Biol* 2001; **13:** 302-309.

373. Tacke R, Manley JL. Determinants of SR protein specificity. *Curr Opin Cell Biol* 1999; **11:** 358-362.

374. Zuo P, Maniatis T. The splicing factor U2AF35 mediates critical protein-protein interactions in constitutive and enhancer-dependent splicing. *Genes and Development* 1996; **10:** 1356-1368.

375. Brede G, Solheim J, Prydz H. PSKH1, a novel splice factor compartment-associated serine kinase. *Nucleic Acids Res* 2002; **30:** 5301-5309.

376. Cowper AE, Caceres JF, Mayeda A, Screaton GR. Serine-arginine (SR) protein-like factors that antagonize authentic SR proteins and regulate alternative splicing. *J Biol Chem* 2001; **276:** 48908-48914.

377. Chansky HA, Hu M, Hickstein DD, Yang L. Oncogenic TLS/ERG and EWS/Fli-1 fusion proteins inhibit RNA splicing mediated by YB-1 protein. *Cancer Res* 2001; **61:** 3586-3590.

378. Yang L, Embree LJ, Hickstein DD. TLS-ERG leukemia fusion protein inhibits RNA splicing mediated by serine-arginine proteins. *Mol Cell Biol* 2000; **20:** 3345-3354.

379. Ohkura N, Yaguchi H, Tsukada T, Yamaguchi K. The EWS/NOR1 fusion gene product gains a novel activity affecting pre-mRNA splicing. *J Biol Chem* 2002; **277:** 535-543.

380. Taylor JK, Zhang QQ, Wyatt JR, Dean NM. Induction of endogenous Bcl-xS through the control of Bcl-x pre-mRNA splicing by antisense oligonucleotides. *Nat.Biotechnol.* 1999; **17:** 1097-1100.

381. Scherl A, Coute Y, Deon C *et al.* Functional proteomic analysis of human nucleolus. *Mol Biol Cell* 2002; **13:** 4100-4109.

382. Gallego MI, Binart N, Robinson GW *et al.* Prolactin, growth hormone, and epidermal growth factor activate Stat5 in different compartments of mammary tissue and exert different and overlapping developmental effects. *Dev.Biol.* 2001; **229:** 163-175.

383. Bonneterre J, Peyrat JP, Vandewalle B, Beuscart R, Vie MC, Cappelaere P. Prolactin receptors in human breast cancer. *Eur.J.Cancer Clin.Oncol.* 1982; **18:** 1157-1162.

384. Favy DA, Rio P, Maurizis JC, Hizel C, Bignon YJ, Bernard-Gallon DJ. Prolactin-dependent up-regulation of BRCA1 expression in human breast cancer cell lines. *Biochem Biophys Res Commun* 1999; **258:** 284-291.

385. Ramamoorthy P, Sticca R, Wagner TE, Chen WY. In vitro studies of a prolactin antagonist, hPRL-G129R in human breast cancer cells. *Int J Oncol* 2001; **18:** 25-32.

386. Fletcher-Chiappini SE, Compton MM, La Voie HA, Day EB, Witorsch RJ, Comptom MM. Glucocorticoid-prolactin interactions in Nb2 lymphoma cells: antiproliferative versus anticytolytic effects. *Proc.Soc.Exp.Biol.Med.* 1993; **202:** 345-352.

387. Rui H, Xu J, Mehta S *et al.* Activation of the Jak2-Stat5 signaling pathway in Nb2 lymphoma cells by an anti-apoptotic agent, aurintricarboxylic acid. *Journal of Biological Chemistry* 1998; **273:** 28-32.